Terms and Conditions of Use of Digitised Theses from Trinity College Library Dublin

Copyright statement

All material supplied by Trinity College Library is protected by copyright (under the Copyright and Related Rights Act, 2000 as amended) and other relevant Intellectual Property Rights. By accessing and using a Digitised Thesis from Trinity College Library you acknowledge that all Intellectual Property Rights in any Works supplied are the sole and exclusive property of the copyright and/or other IPR holder. Specific copyright holders may not be explicitly identified. Use of materials from other sources within a thesis should not be construed as a claim over them.

A non-exclusive, non-transferable licence is hereby granted to those using or reproducing, in whole or in part, the material for valid purposes, providing the copyright owners are acknowledged using the normal conventions. Where specific permission to use material is required, this is identified and such permission must be sought from the copyright holder or agency cited.

Liability statement

By using a Digitised Thesis, I accept that Trinity College Dublin bears no legal responsibility for the accuracy, legality or comprehensiveness of materials contained within the thesis, and that Trinity College Dublin accepts no liability for indirect, consequential, or incidental, damages or losses arising from use of the thesis for whatever reason. Information located in a thesis may be subject to specific use constraints, details of which may not be explicitly described. It is the responsibility of potential and actual users to be aware of such constraints and to abide by them. By making use of material from a digitised thesis, you accept these copyright and disclaimer provisions. Where it is brought to the attention of Trinity College Library that there may be a breach of copyright or other restraint, it is the policy to withdraw or take down access to a thesis while the issue is being resolved.

Access Agreement

By using a Digitised Thesis from Trinity College Library you are bound by the following Terms & Conditions. Please read them carefully.

I have read and I understand the following statement: All material supplied via a Digitised Thesis from Trinity College Library is protected by copyright and other intellectual property rights, and duplication or sale of all or part of any of a thesis is not permitted, except that material may be duplicated by you for your research use or for educational purposes in electronic or print form providing the copyright owners are acknowledged using the normal conventions. You must obtain permission for any other use. Electronic or print copies may not be offered, whether for sale or otherwise to anyone. This copy has been supplied on the understanding that it is copyright material and that no quotation from the thesis may be published without proper acknowledgement.

Staphylococcus lugdunensis

Genome sequence, genetic systems, virulence and an amplifiable *isd* locus

A thesis submitted for the degree of Doctor in Philosophy

by

Simon Heilbronner

Moyne Institute of Preventive Medicine

Department of Microbiology

Trinity College Dublin

December 2013

Declaration

I hereby declare that this thesis has not previously been submitted for a degree at this or any other university ant that it is my own work except where it is duly acknowledged in the text.

I agree that this thesis may be lent or copied at the discretion of the Librarian, Trinity College Dublin.

Contributions of collaborators

Some experiments described within this thesis were conducted by collaborators. Our collaborators in the "Welcome Trust Sanger Institute" in Cambridge performed the full genome sequencing of *S. lugdunensis* N920143. Matthew Holden and colleagues performed the initial sequencing, the sequence alignment and the gap closing procedure. Furthermore they identified open reading frames and provided a preliminary annotation by reciprocal fasta analysis using genome sequences of other staphylococcal species as templates. The identification and annotation of genes unique for *S. lugdunensis* was performed by me, as was the evaluation of interesting genomic regions.

Ian R. Monk constructed the *E. coli* PAM strain SL01B. However, all experiments using and verifying the strains characteristics were conducted by me.

Frank Hanses conducted all *in vivo* endocarditis experiments, including the infection of the animals, description of symptoms and the determination of viable counts in the blood, kidneys and vegetations. Furthermore he chose the *S. aureus* strains used in the experiments and performed the statistical analysis. The construction of *S. lugdunensis* mutant strains, the *in vitro* description of phenotypes and the interpretation of the experimental outcome was performed by me.

Acknowledgements

I would like to acknowledge the IRCSET "Embark Initiative" for providing my scholarship to carry out the research in Trinity College.

First of all I would like to thank my supervisor Timothy J. Foster. It was a pleasure to work with you during the past years. It was a great opportunity to join your group and to work on this amazing project which lead to so many different ideas, that it was sometimes difficult to decide which lead to follow. You gave me the freedom to chase my own ideas and you always patiently dealt with my "German-English". I want to thank you for establishing great collaborations and for introducing me to so many researchers of the field.

My thanks also go to our collaborators, F. Hanses, P. Speciale, E. Skaar, E. Smeds and A. Peschel. The results you obtained with various mutants I created are amazing. Special thanks to Matt Holden and the "Pathogen Genomics" group of the Sanger Institute. You contributed to the start of this project by providing the sequence of N920143 and you offered great support with the data analysis.

I would also like to thank all members of the TJF group, past and present. Thanks Emma, Tara, Marta, Michelle, Helen and Niamh for all your support and encouragement - it was really great fun to work with you. Special thanks to our fantastic postdocs. Thanks to Joan for providing so much help and guidance through complex experimental procedures. You always had the right reference or antibody at hand to solve any problem I faced. It was a pleasure to work with you. Thank you Ian for all the inspiring ideas and methods you shared with me within the field of staphylococcal genetics. You taught me fascinating methods to genetically manipulate staphylococci and I am sure that this will be of extraordinary value for me in the future.

Finally, a very big "Thank You" to those that mean the most to me. Thank you, Katrin for spending the past years with me here in Ireland. Thanks for your never ending support, thanks for cheering me up when things went wrong and thanks for your endless efforts to correct all the weird science texts. Thank you mom and dad, Tim, Petra, Hanno, Simone, Marina, Peter and Eric. Thanks for supporting Katrin and me even though we abandoned you for almost four years. Thanks for wonderful chats using unreliable Skype connections and thanks for the constant supply with German specialties in times we needed it most.

Summary

Staphylococcus lugdunensis is a coagulase negative staphylococcus (CoNS). Infections caused by CoNS are normally less severe than infections caused by *S. aureus*. However, *S. lugdunensis* is associated with a series of severe cases of infective endocarditis displaying an aggressive course of disease akin to *S. aureus* infections.

The first complete genome sequence of *S. lugdunensis* N920143 which is reported within this thesis revealed a multitude of interesting encoded features, including multiple non-ribosomal peptide synthesis systems, a plethora of putative cell wall-anchored proteins, and an iron-dependent surface determinant locus (*isd*).

Hypothesis-driven research regarding *S. lugdunensis* has been neglected up to date and *S. lugdunensis* mutants have not been constructed before. Therefore a protocol for the transformation of *S. lugdunensis* was established, the restriction barrier was identified and techniques for the convenient transformation and the creation of mutants by allelic exchange were developed.

For the first time, *S. lugdunensis* N920143 and several isogenic mutants were investigated in a catheter-induced rat endocarditis model and compared to *S. aureus* Newman and *S. aureus* COL. *S. lugdunensis* N920143 was found to display reduced virulence compared to *S. aureus* Newman. However regarding the size and density of the vegetations, N920143 was comparable to *S. aureus* COL. A sortase A deficient strain was significantly less virulent than the wild-type in this model, confirming the importance of appropriately anchored proteins during infection.

S. lugdunensis is the only CoNS sequenced to date that encodes an *isd* locus. This system allows the acquisition of haem as a source of nutrient iron and is well described for *S. aureus*. It was found that the *S. lugdunensis* strain HKU09-01 possesses a 32 kb duplication comprising the complete *isd* operon. Duplications are known to allow high frequency RecA-dependent recombination, due to the presence of long regions of homology. This leads either to amplification of the region or to loss of the duplication. Accordingly, the duplication of the *isd* operon was found to be intrinsically unstable and could be

stabilized by the introduction of a *recA* mutation. Furthermore, subclones carrying up to seven copies of the *isd* operon could be isolated and the increase in copy number correlated with an increase in Isd protein expression. Comparison of the *isd* copy number variants revealed that one copy of *isd* is sufficient to allow optimal growth in the presence of human haemoglobin as the sole source of nutrient iron. However, Isd proteins are known to possess additional functions and the effects of the *isd* copy number are under current investigation.

Publications

Heilbronner, S., Holden, M. T., van Tonder, A., Geoghegan, J. A., Foster, T. J., Parkhill, J. & Bentley, S. D. (2011).
Genome sequence of *Staphylococcus lugdunensis* N920143 allows identification of putative colonization and virulence factors. *FEMS Microbiol Lett* **322**, 60-67.

Heilbronner, S., Hanses, F., Monk, I. R., Speziale, P. & Foster, T. J. (2013).
Sortase A promotes virulence in experimental *Staphylococcus lugdunensis* endocarditis. *Microbiology* **159**, 2141-2152.

Heilbronner, S., Monk, I. R. & Foster, T. J. (2013).
The phage integrase vector pIPI03 allows RecA-independent, site-specific labelling of *Staphylococcus lugdunensis* strains. *Plasmid* **70**, 377-384.

Haley, K. P., Janson, E. M., Heilbronner, S., Foster, T. J. & Skaar, E. P. (2011).
Staphylococcus lugdunensis IsdG Liberates Iron from Host Heme. *J Bacteriol* **193**, 4749-4757.

Zapotoczna, M., Heilbronner, S., Speziale, P. & Foster, T. J. (2012).
Iron-Regulated Surface Determinant (Isd) Proteins of *Staphylococcus lugdunensis*. *J Bacteriol* **194**, 6453-6467.

Heilbronner, S., Monk, I. R. & Foster, T. J.
Duplication and amplification of the *isd* locus in *Staphylococcus lugdunensis* HKU09-01. (Manuscript in preparation)

Table of contents

List of Tables

List of Figures

Key to abbreviations

aa	amino acid
amp	ampicillin
BSA	bovine serum albumin
bp	base pair
CC	clonal complex
CDS	(protein) coding sequence
cm	chloramphenicol
CoNS	coagulase negative staphylococci
CoPS	coagulase positive staphylococci
CWP	cell wall-anchored protein
ECM	extra cellular matrix
ery	erythromycin
Fg	fibrinogen
GDA	gene duplication and amplification
h	hours
HG	haemoglobin
IE	infective endocarditis
IPTG	isopropyl β-D-1-thiogalactopyranoside
kb	kilobase pair
kDa	kilodalton
LA/B	Luria Agar / Broth
MIC	minimal inhibitory concentration
MLST	multi locus sequence typing
min	minutes
MSCRAMM	microbial surface component recognizing adhesive matrix molecule

NGS	next generation sequencing
OD	optical density
ORF	open reading frame
PAM	plasmid artificial modification
PBS	phosphate buffered saline
PCR	polymerase chain reaction
PG	peptidoglycan
PGA	polyglutamic acid
PS	polysaccharide capsule
PSM	phenol soluble modulin
RM-system	restriction-methylation system
rpm	revolutions per minute
RPMI	Roswell Park Memorial Institute Medium
sec	second
SDS	sodium dodecyl sulfate
SDS-PAGE	sodium dodecyl sulfate polyacrylamide gel electrophoresis
SLIC	sequence and ligase independent cloning
SLUSH	*S. lugdunensis* synergistic haemolysin
SNP	single nucleotide exchange
SOE	spliced overlap extension
SSTI	skin and soft tissue infection
tet	tetracycline
TRD	target recognition domain
TSA/B	Tryptic Soy Agar / Broth
vWF	von Willebrand Factor

For Katrin

Chapter 1
Introduction

1.1 Staphylococci

Staphylococci are Gram-positive, non-motile cocci belonging to the family of *Staphylococcacea*. The cells are 0,5 – 1,5 μm in diameter and their DNA possesses a low G + C content of 30 – 39% (Hofstad, 1999). Cell division occurs in three planes, leading to grape-like cluster formation which is visible under the microscope. There are 42 species and 10 subspecies described for the genus Staphylococcus (Ghebremedhin *et al.*, 2008). All members are catalase positive, facultatively anaerobic and do not form spores. Staphylococci are divided into the coagulase positive staphylococci (CoPS) and the coagulase negative staphylococci (CoNS), depending on the presence or absence of a secreted plasma coagulase, The coagulase is a secreted, non-enzymatic activator of prothrombin that activates the blood clotting cascade (Panizzi *et al.*, 2006) thereby leading to the coagulation of blood plasma in the tube coagulase test. The only CoPS is *Staphylococcus aureus*.

1.2 *Staphylococcus aureus*

1.2.1 *S. aureus* and disease

The best studied staphylococcal species is the CoPS *S. aureus*. The characteristic golden colour of the species derives from the carotenoid pigment staphyloxanthin (Pelz *et al.*, 2005). *S. aureus* is an opportunistic pathogen that is found as a micro commensal in healthy humans. It predominantly colonizes the anterior nares of humans and about 20% of the human population carry *S. aureus* constantly while another 80 % are intermittent carriers (Kluytmans *et al.*, 1997). Colonization with *S. aureus* is recognized to be an important risk factor with infections being more frequent in carriers than non-carriers. Furthermore infections are frequently caused by a carrier's endogenous strain (von Eiff *et al.*, 2001). However, carriage of *S. aureus* appears to have an immune stimulating effect since significantly fewer fatalities are recorded if the patients are colonized with *S. aureus* (Wertheim *et al.*, 2004).

S. aureus causes wound infections and due to the frequent use of invasive procedures in modern medicine it is increasingly important in causing nosocomial infections (Kluytmans *et al.*, 1997). However, *S. aureus* is also

capable of causing invasive disease without a pre-existing breach of the outer barrier of the skin. These infections are locally confined in abscesses, furuncles or mastitis and are associated with strong pus formation. If such a focus of infection opens to the blood stream, bacteria reach all areas of the body causing life threatening infections such as endocarditis, osteomyelitis or sepsis (Lowy, 1998). An important component of modern medicine is the use of implanted medical devices such catheters, stents or artificial heart valves. Use of devices is associated with a high risk of infection with *S. aureus* and *S. epidermidis* being the two species most frequently linked to device-associated infection (Donlan, 2001).

1.2.2 The innate immune response to *S. aureus* infection

As soon as the outer physical barrier of the body is breached by *S. aureus*, the bacterium is confronted by the host immune system. The rapidly induced complement cascade is an important defence mechanism of the innate immune system. The complement is capable of detecting invading microorganisms, labelling them for destruction and attracting phagocytes to the site of infection (Moore, 2004). The complement system is composed of several serum glycoproteins. The central molecule of the cascade is the C3 protein. Upon activation of the cascade, the first C3 convertase (C4bC2a) cleaves C3 into two fragments. The small soluble C3a fragment is released and acts as a strong chemoattractant for neutrophils and macrophages. The C3b fragment becomes covalently attached to the surface of the invading pathogen. C3b is an active C3 convertase that cleaves C3 molecules into C3b and C3a, thereby amplifying the activation of the cascade. Furthermore C3b labels the pathogen for phagocytosis since it is recognised by the C3b receptor on macrophages. Additional glycoproteins are activated in the later stages of complement activation. C3b activity also results in the cleavage of C5 into C5a (chemoattractant) and C5b which becomes attached to the cell surface and possesses C5 convertase activity to amplify the loop. Finally the complement cascade activates proteins to form a membrane attack complex (MAC) which is capable of killing Gram-negative microorganisms by integration into the outer membrane.

The initial activation of the complement cascade can occur by three distinct mechanisms (Figure 1.1). The "classical pathway" uses specific antibodies bound to the surface of the invading microorganism. The complement protein C1q recognizes the Fc part of the bound immunoglobulin. Bound C1q recruits and activates the serine protease C1r which activates C1s. C1s then cleaves C2 and C4 to form the first C3 convertase C4b/C2a. The "lectin pathway" uses the mannose binding lectin (MBL) or ficolin to recognise conserved carbohydrates on the cell surface of microorganisms. Serine proteases then allow the formation of C4b/C2a and the subsequent cleavage of C3. The "alternative pathway" is initiated by free C3b that is present in low amounts within the serum. Interaction with complement regulatory factors allows the attachment of C3b to the invading pathogen and to start the endogenous loop of complement activation.

Taken together, the complement cascade is activated by the recognition of invading microorganisms and leads to the opsonisation (C3b/C5b) and to the release of chemoattractants (C3a/C5a) which stimulates phagocyte migration and induces general inflammation processes.

The immune response to *S. aureus* comprises both innate and adaptive immunity. *S. aureus* infection induces strong activation of complement, followed by the inflammation and influx of neutrophils and macrophages. These innate responses are very effective in clearing the infection.

1.2.3 *S. aureus* virulence and immune evasion factors

S. aureus is able to avoid the immune response by the production of secreted and surface-associated factors that allow the establishment of invasive disease and the evasion of host immune factors. Furthermore *S. aureus* has the ability to suppress the establishment of an effective adaptive immune response. This section will focus on the factors secreted by *S. aureus*, while cell surface-associated proteins are introduced in section 1.4. However, a comprehensive review of all immune evasion and virulence factors of *S. aureus* would go beyond the scope of this thesis. Therefore only the most important molecules are mentioned in this section.

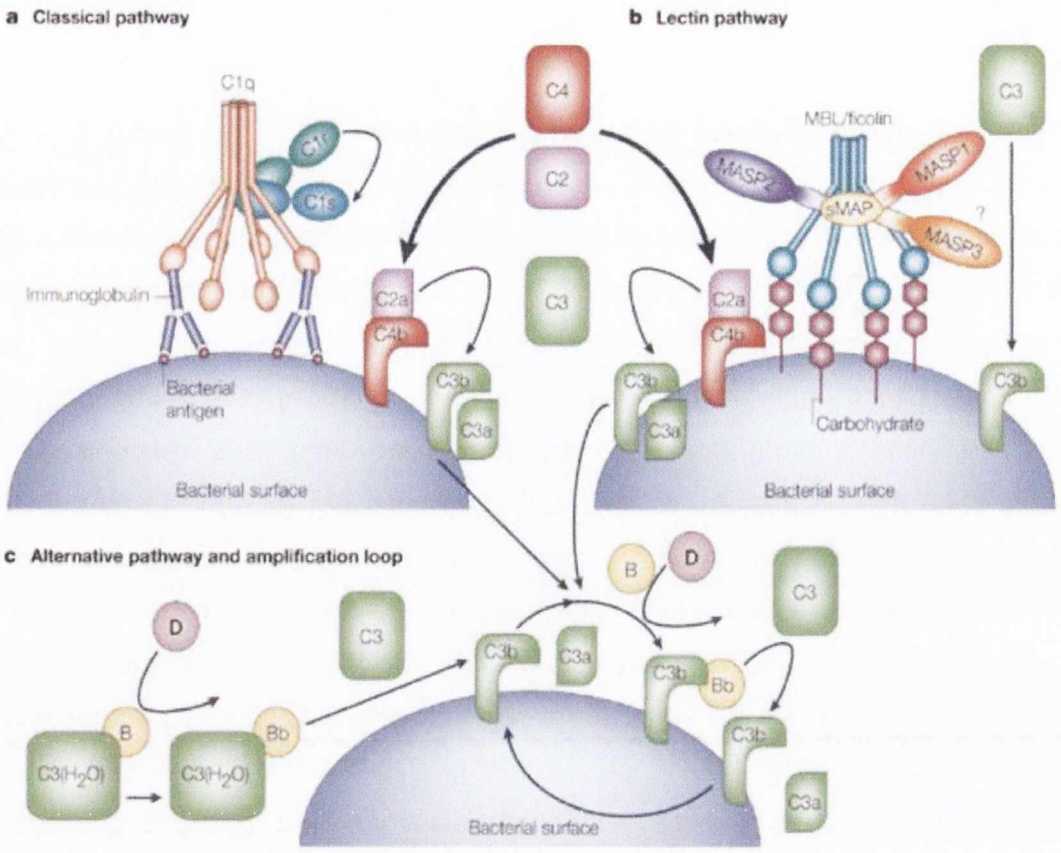

Figure 1.1 Complement activation pathways

(A) The classical pathway is initiated by the binding of the C1 complex to antibodies that are bound to antigens on the surface of bacteria. The C1 complex consists of C1q and two molecules each of C1r and C1s. The binding of the recognition subcomponent C1q to the Fc portion of immunoglobulins results in autoactivation of the serine protease C1r. C1r then cleaves and activates C1s, which translates the activation of the C1 complex into complement activation through the cleavage of C4 and C2 to form a C4bC2a enzyme complex. C4bC2a acts as a C3 convertase and cleaves C3, which results in products that bind to, and cause the destruction of, invading bacteria.

(B) The lectin pathway is initiated by the binding of either mannose-binding lectin (MBL) or ficolin - associated with MBL-associated serine protease 1 (MASP1), MASP2, MASP3 and small MBL-associated protein (sMAP) - to an array of carbohydrate groups on the surface of a bacterial cell. Similar to C1s, MASP2 is responsible for the activation of C4 and C2, which leads to the generation of the same C3 convertase (C4bC2a). As in the classical pathway, C3 convertase cleaves C3 to C3b and the chemoattractant peptide C3a. The C3b–C2a–C4b complex then cleaves C5 to C5a and the chemoattractant peptide C5b, which stimulates assembly of factors C6, C7, C8 and C9 (not shown). MASP1 is able to cleave C3 directly.

(C) The alternative pathway is initiated by the low-grade activation of C3 by hydrolysed C3 ($C3(H_2O)$) and activated factor B (Bb). The activated C3b binds factor B (B), which is then cleaved into Bb by factor D (D) to form the alternative pathway C3 convertase, C3bBb. Once C3b is attached to the cell surface, the amplification loop consisting of the alternative-pathway components is activated, and the C3-convertase enzymes cleave many molecules of C3 to C3b, which bind covalently around the site of complement activation.

Adapted from (Foster, 2005).

1.2.3.1 Inhibition of chemotaxis and opsonisation

The rapid innate immune response to infection involves the immediate chemotactic migration of phagocytes (neutrophils and macrophages) to the site of infection. Phagocytes are recruited by two independent mechanisms. Firstly the activation of the complement cascade leads to the release of the chemoattractant peptides C3a and C5a (Moore, 2004). Secondly, peptides produced by bacteria are typically formylated and are recognised by neutrophils. On neutrophils, complement fragments are recognised by the C5a receptor (Murdoch & Finn, 2000) and peptide fragments are recognized by the formylated peptide receptor (FPR) (Migeotte *et al.*, 2006). Both receptors belong to the family of G-protein coupled receptors and when activated stimulate the migration of neutrophils. Most *S. aureus* strains produce the chemotaxis inhibitor protein of staphylococci (CHIPS). CHIPS possesses two distinct binding sites. The first binds to FPR while the second binds to the C5a receptor. In both cases CHIPS prevents the cognate substrate from binding to the receptor and receptor signalling is not activated (de Haas *et al.*, 2004).

Another important step in neutrophil recruitment is the interaction of intercellular adhesion molecule-1 (ICAM-1) on the surface of endothelial cells with lymphocyte-function-associated antigen (LFA-1) on the surface of neutrophils. This interaction allows the adherence of neutrophils to blood vessels close to the site of infection and stimulates extravasation. *S. aureus* produces the extracellular adherence protein (Eap) that interacts with ICAM-1 and prevents LFA-1 mediated neutrophil extravasation (Chavakis *et al.*, 2002).

S. aureus produces the staphylococcal complement inhibitor (SCIN) which binds to and stabilises the C3 convertases C4b2a and C3bBb. Thereby SCIN inhibits convertase activity, preventing C3b and C3a production (Rooijakkers *et al.*, 2005). The extracellular fibrinogen binding protein (Efb) of *S. aureus* is a further inhibitor of C3-mediated opsonisation. Efb binds to and inhibits the deposition of C3b on the cell surface, thereby reducing opsonophagocytosis (Lee *et al.*, 2004a; Lee *et al.*, 2004b).

Opsonisation of invading bacteria can occur by the deposition of the complement factor C3b on the cell surface. Alternatively antibodies bind to specific antigens. Phagocytes recognise opsonisation by Fc-receptors and C3b receptors. In order to reduce the amount of opsonin present on the cell surface,

S. aureus uses the secreted enzyme staphylokinase (Sak) to bind to and activate host plasminogen (Chavakis *et al.*, 2002). The serine protease of activated plasmin subsequently cleaves C3b and immunoglobulin from the cell surface thereby reducing opsonin-mediated phagocytosis.

1.2.3.2 Resistance to phagocytosis and survival within neutrophils

S. aureus is known to cause abscesses where it is encapsulated in a protective layer of prothrombin and fibrin. For phagocytes this layer is difficult to penetrate. *S. aureus* secretes two proteins to enable the formation of this pseudocapsule. The secreted coagulase is a non-enzymatic activator of prothrombin that triggers the cleavage of fibrinogen to fibrin (Panizzi *et al.*, 2006). Furthermore, *S. aureus* secretes a von Willebrand Factor binding protein (vWbp), a second coagulase that also activates prothrombin in the same way as the major coagulase. Both, coagulase and vWbp are required for abscess formation by *S. aureus* (Cheng *et al.*, 2010).

Most *S. aureus* strains produce a layer of capsular polysaccharide. Most prominent are the serotypes 5 and 8 (O'Riordan & Lee, 2004; Roghmann *et al.*, 2005). The capsule is anti-opsonic and decreases the uptake of *S. aureus* by neutrophils (Thakker *et al.*, 1998). Nonetheless, if *S. aureus* is engulfed by phagocytes it possesses several factors that promote intracellular survival. Interestingly, the golden pigment staphyloxantin allows the scavenging of oxygen radicals and promotes survival within the phagolysosome (Clauditz *et al.*, 2006; Liu *et al.*, 2005). In addition *S. aureus* expresses two superoxide dismutase enzymes that remove O_2^-. Both enzymes are important for survival under oxidative stress (Karavolos *et al.*, 2003).

An additional mechanism of the innate immune system is to kill invading microorganism by the secretion of cationic antimicrobial peptides (CAMPs) such as the human defensins (Boman, 2003). The peptides possess amphiphatic properties and integrate into bacterial membranes through the interaction of the intrinsic negative charge of the prokaryotic cell envelope and the positive charge of the CAMP. *S. aureus* counteracts CAMPs by neutralizing the negative charge of the cell envelope by the addition of the positively charged amino acid alanine to wall teichoic acid (WTA) which is promoted by enzymes encoded by the *dlt* operon (Peschel *et al.*, 1999). Furthermore the multiple peptide

resistance factor (MprF) attaches lysine to the membrane lipid phosphatidyl glycerol (Peschel *et al.*, 2001). Both, Dlt and MprF confer resistance to multiple CAMPs. MprF is also implicated in resistance to the novel antibiotic daptomycin which possesses a CAMP-like mode of action (Bayer *et al.*, 2013).

1.2.3.3 Proteases and nucleases

In order to facilitate tissue destruction and to provide resistance against immune defence strategies *S. aureus* secretes several catalytic proteins. Among those are several proteases of various classes. The calcium-dependent zinc metalloprotease aureolysin is involved in the modification of *S. aureus* derived proteins, promotes the cleavage of the antimicrobial peptide cathelicidin LL-37 (Sieprawska-Lupa *et al.*, 2004) and inhibits immunoglobulin production (Prokesova *et al.*, 1988). In addition *S. aureus* secretes serine and cysteine proteases (staphopains) which are involved in tissue destruction and vascular leakage (Imamura *et al.*, 2005; Kantyka *et al.*, 2011). Besides proteases, *S. aureus* secretes at least two nucleases that degrade extracellular DNA (Beenken *et al.*, 2012). These enzymes influence biofilm formed by *S. aureus* and allow the escape from DNA released in neutrophil extracellular traps (NET) (Beenken *et al.*, 2012; Berends *et al.*, 2010).

1.2.3.4 Pore-forming toxins

A remarkable characteristic of *S. aureus* is the ability to secrete a range of pore-forming toxins. These toxins are secreted as monomers and integrate into the membrane of host cells as multimers forming a ß-barrel pore (Foster, 2005). Pore-formation leads to the leakage of cytoplasmic components and ultimately to cell death. Pore forming toxins recognize receptor molecules on the surface of target cells allowing a high degree of specificity for certain cell types. The classical example is the α-toxin which integrates into the membrane of the host cell as a heptamer. The receptor for α-toxin is the metalloprotease ADAM-10 that is expressed on epithelial cells (Wilke & Bubeck Wardenburg, 2010). Interference with receptor signalling and activation of ADAM-10 protease activity destroys the integrity of the epithelial barrier, facilitating the invasion of *S. aureus.* With ADAM-10 being highly expressed on lung epithelial cells,

α-toxin production is especially associated with staphylococcla pneumonia (Inoshima *et al.*, 2011).

S. aureus secretes up to four different bicomponent toxins, the γ-toxin (Hlg), the Panton-Valentine leukocidin (PVL), leukocidin E/D (lukE/D) and leukocidin M/F (lukM/F). These toxins comprise two subunits that are secreted separately but assemble within the membrane of the host cell to form the pore. These toxins are specific for leukocytes with the exception being Hlg which is also capable of lysing erythrocytes (Menestrina *et al.*, 2003). The receptor of lukE/D was identified as the CCR5 receptor on human T cells (Alonzo *et al.*, 2013) and the receptor of PVL was found to be the human C5a receptor (Spaan *et al.*, 2013).

1.2.3.5 Superantigens

Clinical *S. aureus* isolates often express several superantigens. These proteins have the capacity to bind to MHC class II molecules on the surface of antigen presenting cells and crosslink MHC to the T cell receptor of T-helper cells. This leads to non-specific activation, proliferation and high release of cytokines. The unspecific activation leads to T cell anergy (Lussow & MacDonald, 1994) and superantigens are therefore regarded as a strategy to suppress the initiation of an adaptive immune response (Llewelyn & Cohen, 2002; Proft & Fraser, 2003). Since each superantigen is specific for a subset of the variable Vß-chain of the T cell receptor each superantigen can only activate a subset of T cells (Choi *et al.*, 1990).

Besides the activation of T cells, many superantigens provoke an emetic response when ingested and are therefore also referred to as enterotoxins (Alber *et al.*, 1990)

1.2.3.6 Phenol soluble modulins and β-toxin

Phenol soluble modulins (PSMs) are a class of short peptide toxins that are secreted by most staphylococci (Rautenberg *et al.*, 2010) including *S. aureus* (Wang *et al.*, 2007) and *S. epidermidis* (Mehlin *et al.*, 1999). All PSMs share an amphiphatic, α-helical structure (Rautenberg *et al.*, 2010). Two classes are distinguished according to peptide mass; α-type PSMs (20-26 aa) and β-type PSMs (~44 aa) (Mehlin *et al.*, 1999; Wang *et al.*, 2007). The reported functions of these peptides are diverse. The short α-PSMs display strong

haemolytic effects (Cheung *et al.*, 2012; Wang *et al.*, 2007) and have been identified as key virulence factors of *S. aureus* in murine models (Wang *et al.*, 2007). In addition, both α- and β-PSMs have been shown to be important for biofilm development and structuring, due to their surfactant characteristics (Periasamy *et al.*, 2012; Wang *et al.*, 2011).

Bacterial proteins are typically formylated and can be recognized by the host G-protein coupled formyl peptide receptor (FPR) family (Migeotte *et al.*, 2006). The PSMs are specifically recognized by FPR2. This recognition initiates pro-inflammatory neutrophil responses and chemotactic migration (Rautenberg *et al.*, 2010; Vuong *et al.*, 2004a) and is therefore an important mechanism for the recognition of invading pathogens. Due to the conserved expression of PSMs among staphylococcal pathogens and the strong immune response induced by them, PSMs may be used by the immune system to distinguish between more aggressive staphylococci and less virulent staphylococcal commensals (Kretschmer *et al.*, 2010; Rautenberg *et al.*, 2010).

The sphingomyelinase C (also known as β-toxin) is an enzyme secreted by *S. aureus*. The toxin degrades the membrane lipid sphingomyelin (Doery *et al.*, 1963). β-toxin lyses cells containing significant amounts of the lipid in the membrane such as sheep erythrocytes, human monocytes, human granulocytes and human fibroblasts (Walev *et al.*, 1996).

1.2.3.7 Biofilm formation by *S. aureus*

Bacterial biofilms are surface-attached bacterial communities where the bacterial cells are embedded within an extracellular matrix. This form of growth has several advantages. During colonization, a biofilm protects the bacteria from being washed or scraped away and provides a protective environment during changing environmental conditions such as humidity or osmotic pressure (Otto, 2013). During infection it provides protection from host defenses such as phagocytes and antimicrobial peptides (Otto, 2006). In addition biofilms cannot be penetrated by antibiotics (Hoiby *et al.*, 2010). A major problem in modern medicine is the development of biofilms on indwelling medical devices such as catheters or implants. Most frequently the persistent bactereamia associated with device-associated biofilms can only be resolved by removing the device.

Biofilm development is generally divided in three phases, (i) attachment, (ii) maturation and (iii) detachment (Figure 1.2). If a biofilm is formed on the surface of a medical device, the interaction between the bacterial cell and the polymer surface is mediated be unspecific hydrophobic or electrostatic interactions. The staphylococcal teichoic acids (Gross *et al.*, 2001) and the autolysin AtlE (Heilmann *et al.*, 1997) are important in this process. Furthermore the lysis of a fraction of cells allows the controlled release of extracellular DNA (eDNA) which can coat the surface of devices and is involved in both biofilm attachment and maturation (Rice *et al.*, 2007). However, after the insertion of the device, the surface is rapidly coated with host matrix molecules allowing specific high affinity interactions with adhesins on the bacterial surface. Regarding *S. aureus*, cell wall-anchored proteins (CWPs) play a vital role in the interaction of *S. aureus* with host matrix proteins (section 1.4). and are therefore important for the primary adhesion and during accumulation phase (Vaudaux *et al.*, 1995).

During biofilm maturation adhesive factors are secreted that hold the bacteria together. The best studied adhesive factor is the exopolysaccharide poly-N-acetylglucosamine (PNAG) which is also known as polysaccharide intercellular adhesin (PIA) (Mack *et al.*, 1996) and its importance for biofilm formation has been demonstrated *in vitro* and *in vivo* (Heilmann *et al.*, 1996; Vuong *et al.*, 2004b). PIA is synthesized and secreted by the proteins encoded by the *icaADBC* operon and most biofilm-forming staphylococcal isolates posses this locus. It was assumed for a long time that PIA is indispensable for biofilm formation. However, biofilm-forming Isolates that do not secrete PIA have been described (Kogan *et al.*, 2006; Rohde *et al.*, 2007). Cell-cell interactions that keep PIA-independent biofilms together appear to be mediated mainly by protein-protein interactions e.g. involving the cell wall-anchored protein Aap (accumulation associated protein) and the extracellular protein Embp (extracellular matrix binding protein) (Christner *et al.*, 2010; Conrady *et al.*, 2013; Hussain *et al.*, 1997; Rohde *et al.*, 2005). Cell wall-anchored proteins of *S. aureus* are also important for cell-cell interactions, especially protein A (Merino *et al.*, 2009), SasG (Geoghegan *et al.*, 2010a) and the fibronectin binding proteins (FnBPA/B) (O'Neill *et al.*, 2008). Recent studies showed that that FnBPA promotes biofilm formation in a Zn^{2+}-dependent manner and that

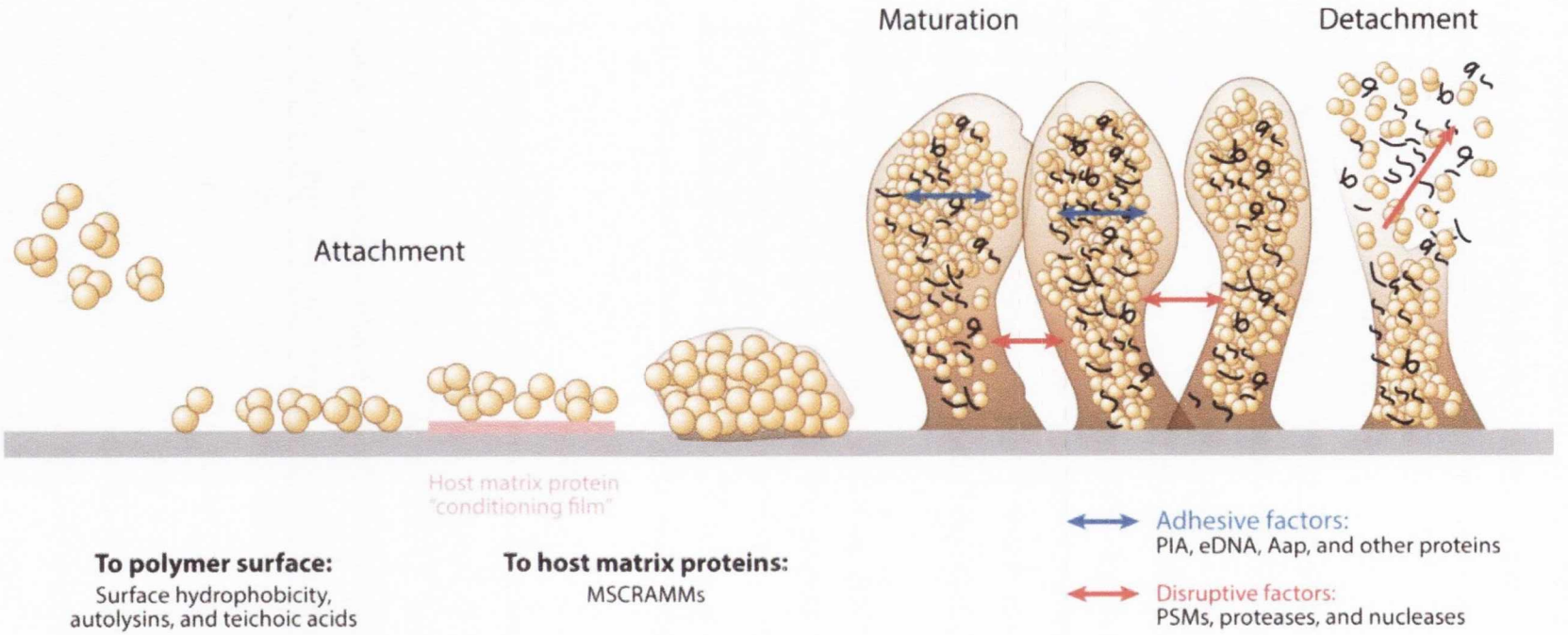

Figure 1.2 Biofilm development

Phases of biofilm development. Biofilm development includes initial attachment, maturation, and final detachment. Attachment may occur directly to a surface (such as the polymeric surface of an indwelling medical device) or to a "conditioning film" formed by host matrix molecules. Then, biofilm maturation proceeds via the agglomeration of cells, which is dependent on adhesive molecules. Formation of the characteristic channel-containing biofilm structure is dependent on disruptive factors, which also ultimately facilitate the last phase of biofilm development, detachment. Molecular determinants shown or suspected to be involved in the respective biofilm development phases in staphylococci are noted on the bottom. Abbreviations: Aap, accumulation-associated protein; eDNA, extracellular DNA; MSCRAMMs, microbial surface components recognizing adhesive matrix molecules; PIA, polysaccharide intercellular adhesin; PSMs, phenol-soluble modulins.

Adapted from (Otto, 2013)

the residues 166-498 of the protein are important (Geoghegan *et al.*, 2013). However, the precise mechanism of the interaction is not solved yet. Finally, extracellular DNA (eDNA) which is released from lysed bacteria contributes to biofilm maturation *in vitro*. The contribution of eDNA *in vivo* is questionable due to the presence of a potent DNAse in human serum (Otto, 2013).

Biofilm detachment is an important process since it allows bacteria to be released and form new colonies at different sites. To allow the detachment, several factors are produced in mature biofilms. Relevance *in vitro* has been shown for the protease aureolysin (Boles & Horswill, 2008) and the nucleases Nuc1 and Nuc2 (Beenken *et al.*, 2012; Kiedrowski *et al.*, 2011). However, relevance both *in vitro* and *in vivo* has only been demonstrated for the PSMs (see 1.2.3.6) (Periasamy *et al.*, 2012; Wang *et al.*, 2011). Synthesis of these peptides is controlled by Agr and expression increases in mature biofilms. The surfactant characteristics of PSMs allow the dispersal and structuring of biofilms.

Interestingly staphylococci do not encode an enzyme that degrades PIA to facilitate biofilm dispersal. Such an enzyme was reported for *Aggregatibacter actinomycetemcomitans* and is named dispersin B (Kaplan *et al.*, 2004). However, homologous genes could not be identified in the genomes of staphylococci.

1.2.4 Antibiotic resistance in *S. aureus*

From a clinical point of view, a major problem of *S. aureus* infection is antibiotic resistance. The first antibiotic introduced was penicillin, a ß-lactam antibiotic inhibiting the transpeptidation reaction during peptidoglycan biosynthesis. *S. aureus* developed resistance against this antibiotic within two years by the acquisition of a ß-lactamase that cleaves the ß-lactam ring of the antibiotic. Nowadays most infectious *S. aureus* isolates are resistant to penicillin (Otto, 2012). The semi-synthetic antibiotic methicillin which cannot be cleaved by

ß-lactamase was constructed to overcome this problem. However, *S. aureus* strains resistant to methicillin (MRSA) were detected only one year after its introduction (Jevons *et al.*, 1963). MRSA strains are a major problem in modern medicine and many industrialized countries report 25-50% of infectious

S. aureus isolates to be methicillin resistant (Diekema *et al.*, 2001). Resistance is caused by the acquisition of the *mecA* gene which encodes the penicillin-binding protein PBP2a. This transpeptidase possesses a low affinity for the ß-lactam ring (Hartman & Tomasz, 1981), thereby transferring resistance against the entire class of ß-lactam antibiotics including penicillin, methicillin, cephalosporins and carbapenems. The *mecA* gene is located on the staphylococcal cassette chromosome *mec* (SCC*mec*) (Katayama *et al.*, 2000), a mobile genetic element that can be acquired by lateral gene transfer. Eleven types of SCC*mec* have been described, ranging in size from 21 – 67 kb (Hiramatsu *et al.*, 2001). All SCC*mec* elements carry the *mecA* gene and *ccr* genes for the integration of the element into and its excision from the chromosome. Depending on the type of the element addition antibiotic resistance determinants (Hiramatsu *et al.*, 2001) or virulence factors can be encoded within SCC*mec* (Queck *et al.*, 2009).

S. aureus strains have also acquired resistances to antibiotics of other classes such as erythromycin, clindamycin, ciprofloxacin, tetracycline, etc (Shorr, 2007). Alarmingly, multidrug resistant strains are occurring that can only be treated with vancomycin and rare cases of vancomycin resistant MRSA isolates have been reported (CDC, 2002).

1.3 *Staphylococcus lugdunensis*

The species *Staphylococcus lugdunensis* was first described by Freney *et al.* in 1988 in Lyon, France (Freney *et al.*, 1988). It is a Gram-positive, catalase negative and non-motile coccus. The species displays colony morphology and colony sizes ranging from 1-4 mm are reported (Freney *et al.*, 1988). Also the pigmentation of isolates is known to vary and the described colours vary from cream to a yellow/golden (Freney *et al.*, 1988). Most strains display a haemolytic phenotype on agar plates containing rabbit or sheep erythrocytes (Freney *et al.*, 1988).

S. lugdunensis does not produce a secreted plasma coagulase and is therefore a member of the CoNS. Phylogenetic analysis of 16S rDNA (Takahashi *et al.*, 1999) and *dnaJ* (Shah *et al.*, 2007) gene sequences places *S. lugdunensis* in a clade that includes *S. epidermidis, S. aureus* and *S. haemolyticus.*

S. lugdunensis is a constituent of the normal human skin flora and is predominantly isolated from the moist areas of the skin such as the groin, the axilla and the perineum (Bieber & Kahlmeter, 2010). In contrast to *S. aureus*, *S. lugdunensis* is only infrequently isolated from the nasal cavity and about 90% of all healthy individuals carry *S. lugdunensis* on either one or multiple sites of the body (Bieber & Kahlmeter, 2010).

S. lugdunensis can be easily misidentified as *S. aureus* due to their similar colony morphology, haemolytic activity and the ability to agglutinate latex particles coated with fibrinogen (Zbinden *et al.*, 1997). Yet, a tube coagulase test clearly identifies *S. lugdunensis* as a CoNS and a positive pyrrolidonylarylamidase (PYR) reaction along with positive ornithine decarboxylase activity distinguishes *S. lugdunensis* from the other CoNS (De Paulis *et al.*, 2003).

1.3.1 *S. lugdunensis* and disease

Compared to *S. aureus*, diseases caused by CoNS are normally sub-acute, less severe and rarely associated with mortality (Frank *et al.*, 2008). However, described as a "wolf in sheep's clothing" (Frank *et al.*, 2008), *S. lugdunensis* behaves in many ways more like the coagulase positive *S. aureus* than the other CoNS including having an apparently elevated degree of virulence. *S. lugdunensis* is known to cause a wide range of diseases including superficial skin and soft tissue infections (SSTI) (Arias *et al.*, 2010; Bocher *et al.*, 2009; Papapetropoulos *et al.*, 2013), ocular infections (Chiquet *et al.*, 2007; Pinna *et al.*, 1999), peritonitis (Ludlam & Phillips, 1989; Schnitzler *et al.*, 1998) and urinary tract infections (Casanova-Roman *et al.*, 2004; Haile *et al.*, 2002). In diagnostic microbiology SSTIs caused by CoNS are rarely identified to species level (Bocher *et al.*, 2009). This makes a reliable estimation of the frequency of *S. lugdunensis* infections impossible. However, a study focusing on *S. lugdunensis* infections in one Swedish county showed that accurate species identification of CoNS infections increased the reported *S. lugdunensis* isolations eleven times from 5 to 53 infections per 100.000 inhabitants per year (Bocher *et al.*, 2009). *S. lugdunensis* was predominantly found to cause abscesses. In abscesses *S. aureus* (86%) and *S. lugdunensis*

(70%) are most frequently isolated in monoculture which is significantly higher than the rate of all the other CoNSs which are predominantly isolated as mixed cultures (Bocher *et al.*, 2009).

S. lugdunensis is also able to cause severe invasive infections such as septic arthritis (Grupper *et al.*, 2010), osteomyelitis (Vigna *et al.*, 2007) or necrotizing fasciitis (Hung *et al.*, 2012). Most importantly, *S. lugdunensis* is associated with an aggressive form of infective endocarditis (IE). Around 1% of IE cases are reported to be caused by *S. lugdunensis* (Anguera *et al.*, 2005) with mortality rates ranging from 38% (Liu *et al.*, 2010) to 42% (Anguera *et al.*, 2005). *S. lugdunensis* most frequently causes left sided native valve endocarditis involving mitral and/or aortic valves (Frank *et al.*, 2008; Liu *et al.*, 2010). Also, *S. lugdunensis* IE shows a very aggressive course of disease with 70% of the patients requiring surgery compared to 37% of patients suffering from *S. aureus* IE (Liu *et al.*, 2010).

1.3.2 *S. lugdunensis* pathogenicity and virulence factors

Although *S. lugdunensis* is now recognized as an important pathogen there is still remarkably little information regarding virulence factors and the molecular mechanisms of pathogenicity. Previous research failed to identify genes encoding toxins (superantigens, pore-forming toxins) with similarity to toxins of *S. aureus* (Fleurette *et al.*, 1989). Furthermore, no IgG binding molecule could be detected. However, *S. lugdunensis* possesses a regulatory *agr* locus 63% identical to that encoded by *S. aureus* with the apparent difference that the *S. lugdunensis* locus does not encode a δ-haemolysin (Vandenesch *et al.*, 1993). Neither α- nor β-toxin activity was reported for *S. lugdunensis* but three short peptides combine to generate delta-like haemolysis. The three peptides A/B/C have a length of 43 aa and are named *S. lugdunensis* synergistic haemolysin (SLUSH). These peptides are encoded within an operon upstream of the *agr* locus together with a fourth peptide (OrfX) for which no function is yet described (Donvito *et al.*, 1997). The expression of the peptides is dependent on *agr* activity (Donvito *et al.*, 1997). The SLUSH peptides have been recognized to belong to the group of ß-PSMs (Rautenberg *et al.*, 2010).

S. lugdunensis is capable of forming biofilm (Fleurette *et al.*, 1989) and the organism carries the *icaADBC* operon (Cramton et al., 1999; Frank & Patel, 2007) suggesting it is able to produce PIA. However, PIA was shown not to be a major component of *S. lugdunensis* biofilms. In contrast, microscopy of "SYPRO Ruby" stained *S. lugdunensis* biofilms showed vast amounts of extracellular proteins and the addition of proteases lead to biofilm dispersal (Frank & Patel, 2007). This suggests that cell-cell adherence is mediated mainly by protein interactions. The identities of the proteins contributing to biofilm formation in *S. lugdunensis* have yet to be identified.

1.3.3 Antibiotic resistance in *S. lugdunensis*

In contrast to *S. aureus, S. lugdunensis* has remained remarkably sensitive to the antibiotics used in modern medicine. Only sporadic isolates were reported to be resistant against single antibiotics and no accumulation of multiple resistances has been observed (Frank *et al.*, 2008). Interestingly, compared to *S. aureus* most *S. lugdunensis* isolates have an increased tolerance towards glycopeptide antibiotics such as vancomycin or teicoplanin (Bourgeois *et al.*, 2007; Frank *et al.*, 2007). The reasons for this are unknown.

Only 20 to 40% of *S. lugdunensis* isolates produce β-lactamase (Frank *et al.*, 2008). Methicillin resistant clinical isolates that have acquired SCC*mec* have been reported (MRSL) (Becker *et al.*, 2006; Nakamura *et al.*, 2012; Pereira *et al.*, 2010; Tee *et al.*, 2003) and account for ca. 5% of all isolates (Tan *et al.*, 2008). MRSL does not yet pose a significant problem for the treatment of infections.

1.4 Cell surface-associated proteins

Staphylococci express a variable number of cell surface-displayed proteins that are covalently anchored to the cell wall peptidoglycan (PG). These proteins form the interface between the bacterial cell and the environment. Consequently the proteins fulfil important functions for the colonization of the host and for the establishment of invasive diseases.

1.4.1 Sortase mediated attachment to the peptidoglycan

The precursors of cell wall-anchored proteins (CWPs) are produced with an N-terminal signal sequence and are secreted using the universal Sec pathway. Additionally, the proteins possess a sortase cleavage motif at the C-terminal end which is followed by a membrane-spanning hydrophobic helix and several positively charged amino acids (Figure 1.3). This ensures that the precursor remains attached to the cell membrane until the transpeptidase sortase connects the CWP to the PG. Sortase genes have been identified in all Gram-positive genomes and in most cases more than one sortase is encoded (Pallen *et al.*, 2001). *S. aureus* encodes two distinct sortase enzymes. Sortase A (SrtA) anchors CWPs possessing an LPXTG motif at the C-terminal end. The amino acid sequence is highly stringent and exchanges at position 1, 2, 4 and 5 are not tolerated (Schneewind *et al.*, 1992). In *S. aureus* SrtA anchors 23 of 24 CWPs to the PG. The three dimensional structure of SrtA is described as an 8 stranded β-barrel in which a hydrophobic depression is present between β7 and β8. This depression contains the active site of the enzyme (Ilangovan *et al.*, 2001). The active site is composed of Cys^{184} and His^{120}. These residues are absolutely conserved among sortases (Zong *et al.*, 2004). The *S. aureus* sortase B (SrtB) recognizes the NPQTN motif of IsdC and no other substrates for this enzyme occur in *S. aureus*. The three dimensional structure of SrtB is similar to the structure of SrtA including the cysteine-histidine pair within the active site. However SrtB possess three α-helixes that are not present in SrtA explaining the different substrate specificity (Marraffini *et al.*, 2006).

Sortases represent a class of transpeptidases that attach CWPs to PG-building blocks during cell wall-biosynthesis. The synthesis of PG starts in the cytoplasm where *N*-acetylmuramic acid (MurNAc) attached to the pentapepide [L-Ala-D-iGlu-L-Lys-D-Ala-D-Ala] is synthesized and coupled to the cyotoplasmic side of the membrane using the lipid carrier undecaprenol (lipid I) (Figure 1.4). Subsequently *N*-acetylglucosamine (GlcNAc) is attached to the MurNAc and the pentaglycine bridge is attached to the L-Lys in the middle of the stempentapeptide (lipid II) (Figure 1.4). This PG building block is flipped to the extracellular side of the membrane and incorporated into the growing PG by

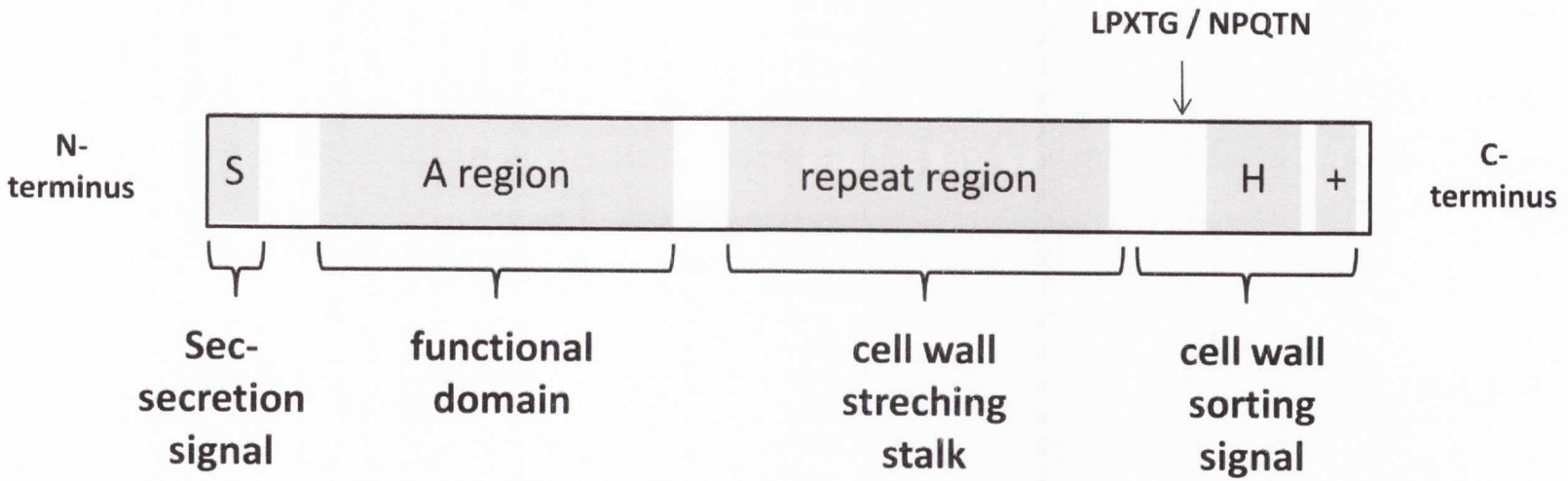

Figure 1.3 Schematic diagram of a CWP precursor
Regions with different functions are denoted by grey boxes. S - Sec secretion signal; H - hydrophobic region; + - positively charged region. Cleavage motifs for sortase A (LPXTG) and sortase B (NPQTS) are indicated.

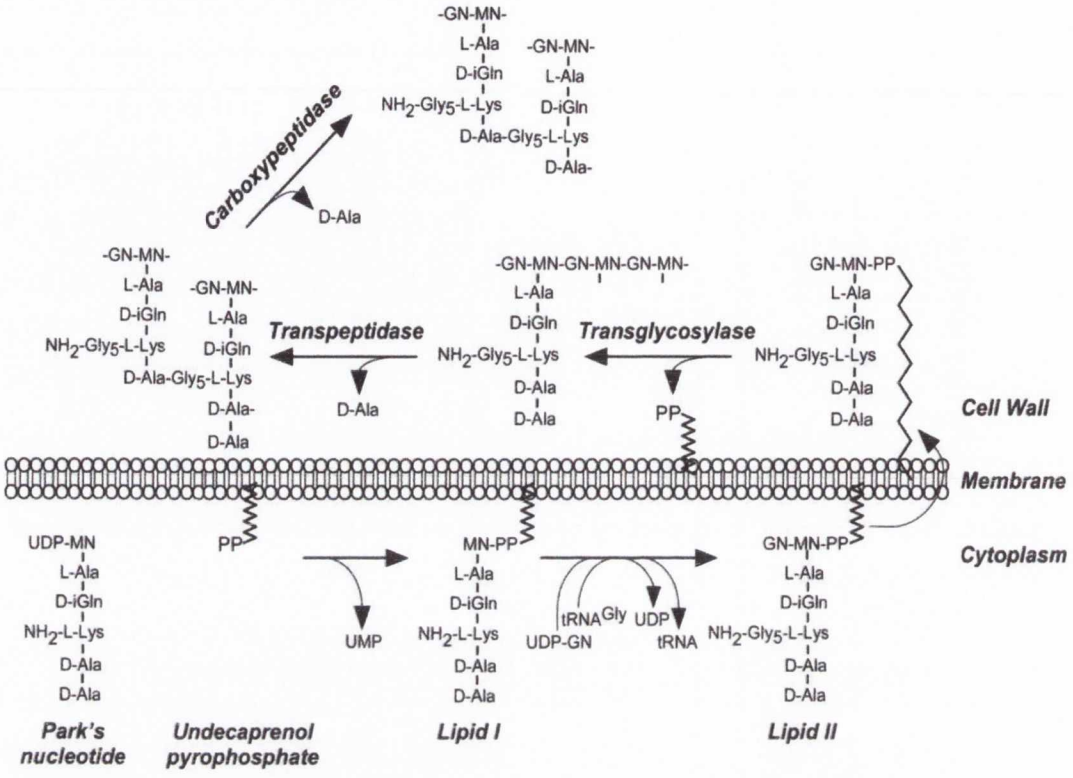

Figure 1.4 Peptidoglycan synthesis in *S. aureus*

Park's nucleotide, a soluble nucleotide precursor, originates in the bacterial cytoplasm by successive addition of l-stereoisomer amino acids (l-Ala and l-Lys) as well as d-stereoisomer amino acids (d-isoglutamine [d-iGln] and d-Ala) to UDP-*N*-acetylmuramic acid (UDP-NM). Precursor transfer to undecaprenol pyrophosphate, a bacterial membrane carrier, generates lipid I and removes UMP nucleotide. Lipid I modification with *N*-acetylglucosamine (GN) and pentaglycine cross bridge formation at the ε-amino of l-Lys with $tRNA^{Gly}$ substrate generates lipid II. Following translocation across the cytoplasmic membrane, lipid II serves as substrate for PBPs that catalyze three reactions: transglycosylation, transpeptidation, and carboxypeptidation. Transglycosylases polymerize MN-GN subunits into repeating disaccharide chains, the glycan strands. Transpeptidases cleave the amide bond of the terminal d-Ala in pentapeptide precursors and generate an amide bond between the carboxyl group of d-Ala at position four and the amino group of pentaglycine cross bridges in wall peptides. Carboxypeptidases hydrolyze the C-terminal d-Ala of most non-cross-linked pentapeptides to yield mature peptidoglycan.

Adapted from (Marraffini *et al.*, 2006)

transglycosylation and transpeptidation (Marraffini *et al.*, 2006; Ton-That *et al.*, 2004).

Sortase-mediated incorporation of CWPs into the cell wall occurs before transglycosylation and transpeptidation. CWP precursors are secreted by the Sec pathway and remain attached to the membrane by the C-terminal hydrophobic region. Sortase A recognises the LPXTG motif, cleaves between the threonine and the glycine residues and captures the polypeptide as a thioester-linked acyl enzyme at its active site cysteine residue (Ton-That *et al.*, 1999; Ton-That *et al.*, 2000). The subsequent nucleophilic attack of the amino group of the cross-bridge in the PG-precursor completes the anchoring of the CWP (Ton-That *et al.*, 1999). The building block is subsequently incorporated into the PG by transglycosylation and transpeptidation. The steps for correct display of a CWP are shown in Figure 1.5.

Sortase B recognizes the NPQTN motif of IsdC and cleaves the substrate between the threonine and the asparagine residues and connects it to the penta glycine bridge of the PG (Marraffini & Schneewind, 2005; Mazmanian *et al.*, 2002). Interestingly, it seems to link IsdC to a different location within the PG scaffold, at sites showing a low level of cross linking. However, the precise mechanism of this mechanism and its implications are not completely understood (Marraffini et al., 2006).

1.4.2 Functions of cell wall-anchored proteins

Classically, CWPs were referred to as microbial surface component recognizing adhesive matrix molecules (MSCRAMMs) since the first proteins described promoted adhesion to molecules of the extracellular matrix (ECM). Recently a new classification system was proposed since the structural organizations of many CWPs have been described, revealing different tertiary structures and domains. Additionally, several functions other than ligand binding have been uncovered and many CWPs do not promote adhesion to ECM. Thus, CWPs should be classified according to structural similarities and the term MSCRAMM was proposed to be used for one class of CWPs that show two independent IgG-like folds and promote binding to their ligand by the "dock, lock and latch" mechanism (described in 1.4.3.1) (Foster *et al.*, 2013).

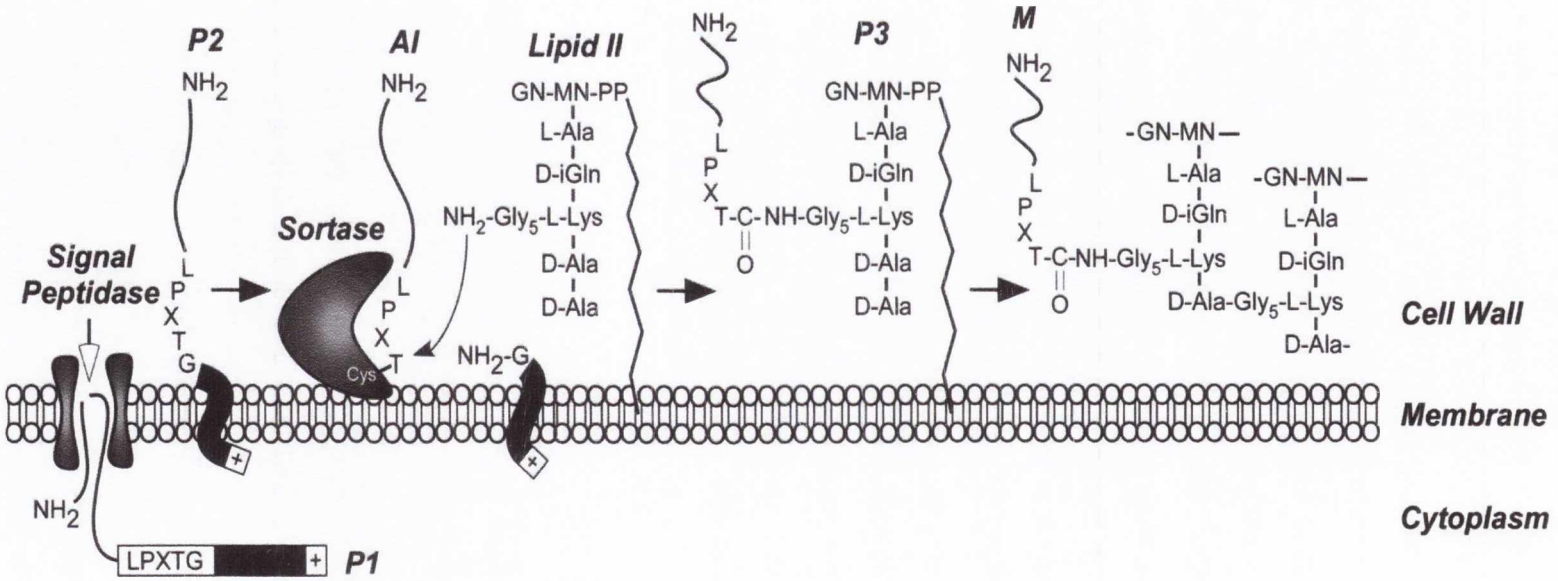

Figure 1. 5 Cell wall sorting pathway of surface proteins in Gram-positive bacteria

Surface proteins are first synthesized in the bacterial cytoplasm as full-length precursors (P1) containing an N-terminal signal sequence and a C-terminal sorting signal. The signal sequence directs the cellular export of the polypeptide through the Sec system and, upon translocation, is cleaved by signal peptidase. The product of this reaction, the P2 precursor harboring only the C-terminal sorting signal, is retained within the secretory pathway via its C-terminal hydrophobic domain (black box) and positively charged tail (+). Sortase, a membrane-anchored transpeptidase with active-site cysteine, cleaves the peptide bond between the threonine (T) and the glycine (G) of the LPXTG motif, generating an acyl intermediate (AI). Lipid II, the peptidoglycan biosynthesis precursor, and its pentaglycine cross bridge (Gly_5) amino group attack the acyl intermediate, linking the C-terminal threonine of the surface protein to lipid II (P3 precursor) and regenerating the active site of sortase. The P3 precursor functions as a substrate for penicillin binding proteins and is incorporated into the cell wall envelope to generate mature anchored surface protein (M), which is also displayed on the bacterial surface. This pathway is universal in many Gram-positive bacteria, and the functional elements of cell wall cross bridges, LPXTG motif, sortase, and penicillin binding proteins are conserved.

Adapted form (Marraffini *et al.,* 2006)

All CWPs possess a distinct N-terminal region (A domain) and in most cases a C-terminal stalk region consisting of a varying number of repeated domains or amino acid motifs (see Figure 1.3). The stalk region is needed to span the cell wall and to enable the display of the A domain some distance away from the cell surface. It was shown that 60-110 residues are needed between the cell wall anchor and the A region for functional expression (Hartford *et al.*, 1997; Strauss & Götz, 1996). However, in some CWPs the repeat region also binds ligands (e.g. the fibronectin binding proteins of *S. aureus* that are described in section 1.4.3.3). *S. aureus* has the potential to express 24 different CWPs that promote binding to the most prominent proteins of the ECM and blood plasma, such as fibrinogen (Fg), fibronectin (Fn), keratins and collagens (Speziale *et al.*, 2009) and many surface proteins have been shown to represent virulence factors (Cheng *et al.*, 2009; Gomez *et al.*, 2004; Moreillon *et al.*, 1995; Que *et al.*, 2005). Cell wall-anchored proteins were also shown to play a role in *S. aureus* nasal colonization. The MSCRAMM clumping factor B (ClfB) and its interaction with the envelope protein loricrin of squamous epithelial cells was shown to be an important factor in nasal colonization by *S. aureus* (Mulcahy *et al.*, 2012). In addition to their role as adhesins, CWPs possess additional functions. As described in detail in section 1.5, the iron-regulated proteins IsdA, IsdB, IsdC and IsdH possess haem binding NEAT domains and are important for the extraction of haem from haemoproteins and its transport into the cytoplasm (Grigg *et al.*, 2007; Grigg *et al.*, 2010; Mazmanian *et al.*, 2003; Pishchany *et al.*, 2010; Torres *et al.*, 2006). Furthermore, CWPs are important immune evasion factors. The *S. aureus* protein A (Spa) binds to the Fc-region of IgG thereby preventing opsonisation (Cedergren *et al.*, 1993; Deisenhofer, 1981). Furthermore Spa acts as a B cell mitogen by binding to the heavy-chain variable domain 3 (VH3) of IgM. This induces unspecific proliferation and thereby anergy and immune suppression (Graille *et al.*, 2000; Silverman & Goodyear, 2006). ClfA promotes adhesion to Fg but possesses also antiphagocytic characteristics (Higgins *et al.*, 2006) and interacts with regulatory complement factors to prevent complement-mediated killing and opsonisation (Hair *et al.*, 2008).

A high degree of functional redundancy is observed between different CWPs. Thus, ClfA, ClfB, FnBPA and FnBPB all bind to Fg, which might

underline the importance of this interaction for *S. aureus*. Furthermore, many CWPs possess multiple functions. As an example, IsdA is important for haem uptake and the resistance to host immune defences and FnBPs bind both Fg and Fn. Thus, a limited set of CWPs possess a multitude of functions. A summary of the *S. aureus* CWPs and their described functions in adhesion and immune evasion are summarized in Table 1.1.

1.4.3 Ligand binding mechanisms of CWPs

1.4.3.1 Fibrinogen binding by the "dock, lock and latch" mechanism

The archetypes of Fg binding MSCRAMMs are clumping factor A (ClfA) of *S. aureus* and SdrG of *S. epidermidis*. The molecular mechanism of the interaction between SdrG and fibrinogen has been characterized in great detail (Bowden *et al.*, 2008; Ponnuraj *et al.*, 2003). Fg is a soluble plasma protein and consists of three pairs of non-identical chains (Aα, Bβ and γ) as shown in Figure 1.6 A. The A region of SdrG consists of three independently folded domains (N1/N2/N3). The role of the N1 domain has still to be characterized in detail, but was shown to be important for the functional secretion and surface display of the homologue ClfA in *S. aureus* (McCormack *et al.*, 2013). The minimal Fg binding region of SdrG consists of two domains N2/N3 comprising IgG-like folds and consisting predominantly of β-strands (Ponnuraj *et al.*, 2003). Without bound peptides (apo form) a hydrophobic trench is present between the N2 and N3 domains (Figure 1.7). The docking of the fibrinogen Bβ-chain into this trench leads to a change in conformation, allowing the C-terminal extension of N3 to interact with the peptide within the cleft, locking the peptide in place. Further changes in the conformation allow the C-terminal extension of the N3 domain to be inserted into a trench within the N2 domain by β-strand complementation. By this latch, the fibrinogen peptide is tightly locked within the cleft (Bowden *et al.*, 2008; Ponnuraj *et al.*, 2003). A model of SdrG binding to fibrinogen is shown in Figure 1.7.

Various cell wall-anchored proteins share the structural organization of N1/N2/N3 domains at their N-terminal end and are therefore also classified as MSCRAMMs. Among them are ClfA, ClfB, FnBPA and FnBPB of *S. aureus*. The N2/N3 domains of each protein can bind to human Fg, although different parts

Table 1.1 *S. aureus* CWPs and their ligands

CWP	Ligands / Functions	Reference
Bone sialoprotein binding protein (SdrE)	bone sialoprotein fibrinogen	(Tung *et al.*, 2000; Vazquez *et al.*, 2011)
Clumping factor A (ClfA)	fibrinogen complement factor I	(Ganesh *et al.*, 2008; Hair *et al.*, 2008; McDevitt *et al.*, 1994)
Clumping factor B (ClfB)	fibrinogen cytokeratin 10 loricrin	(Mulcahy *et al.*, 2012; Ni Eidhin *et al.*, 1998; Walsh *et al.*, 2004)
Collagen binding protein (Cna)	collagen complement protein C1q	(Kang *et al.*, 2013; Patti *et al.*, 1993)
Fibronectin binding protein A (FnBPA)	fibronectin fibrinogen elastin tropoelastin	(Keane *et al.*, 2007a; Keane *et al.*, 2007b; Meenan *et al.*, 2007; Wann *et al.*, 2000)
Fibronectin binding protein B (FnBPB)	fibronectin, fibrinogen elastin	(Roche *et al.*, 2004)
Iron-regulated surface determinant A (IsdA)	heam, fibronectin, fibrinogen, lactoferrin, transferrin, involucrin, loricrin, cytokeratin 10	(Clarke *et al.*, 2004; Clarke & Foster, 2008; Clarke *et al.*, 2009; Hammer & Skaar, 2011)
Iron-regulated surface determinant B (IsdB)	haemoglobin, haem GPIIb/IIIa receptor on platelets, β3 integrins on epithelia cells	(Hammer & Skaar, 2011; Miajlovic *et al.*, 2010; Zapotoczna *et al.*, 2012)
Iron-regulated surface determinant C (IsdC)	Haem	(Hammer & Skaar, 2011)
Iron-regulated surface determinant H (IsdH)	haemoglobin-haptoglobin complex, haem	(Hammer & Skaar, 2011)
Protein A	IgG, IgM, von Willebrand factor, TNFR-1	(Gomez *et al.*, 2004; Moks *et al.*, 1986; O'Seaghdha *et al.*, 2006)
SdrC	β-neurexin desquamated epithelial cells – no known ligand	(Barbu *et al.*, 2010; Corrigan *et al.*, 2009)

Table 1.1 *S. aureus* CWPs and their ligands, continued

CWP	Ligands / Functions	Reference
SdrD	desquamated epithelial cells – no known ligand	(Corrigan *et al.*, 2009)
SdrE	complement regulation factor H	(Sharp *et al.*, 2012)
SasG	No known ligand. The A domain masks ligands for other CWPs, the B repeats induce biofilm formation. Promotes adherence to desquamated epithelial cells.	(Corrigan *et al.*, 2007; Corrigan *et al.*, 2009)
Adenosine synthase A (AdsA)	Promotes survival within neutrophils.	(Thammavongsa *et al.*, 2009; Thammavongsa *et al.*, 2011)
SasA (SraP)	salivary agglutinin, gp340, platelets – no known ligand	(Kukita *et al.*, 2013; Siboo *et al.*, 2005)
staphylococcus aureus surface protein X (SasX)	No known ligand, involved in biofilm formation and cell aggregation.	(Li *et al.*, 2012)
SasC, SasB, SasD, SasF, SasJ, SasK, SasL.	No known ligands or functions.	

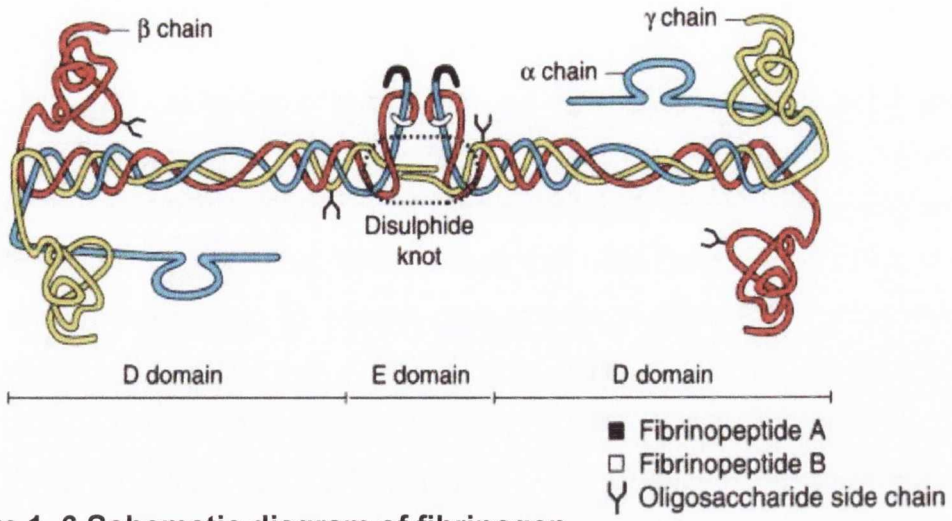

Figure 1. 6 Schematic diagram of fibrinogen
There are three sets of non-identical chains which are bound by disulphide bonds at the amino-terminal end. Removal of fibrinopeptides A and B in the E domain via the action of thrombin, leads to cross-linking and the formation of the fibrin clot.
Adapted from (Herrick *et al.* 1999.)

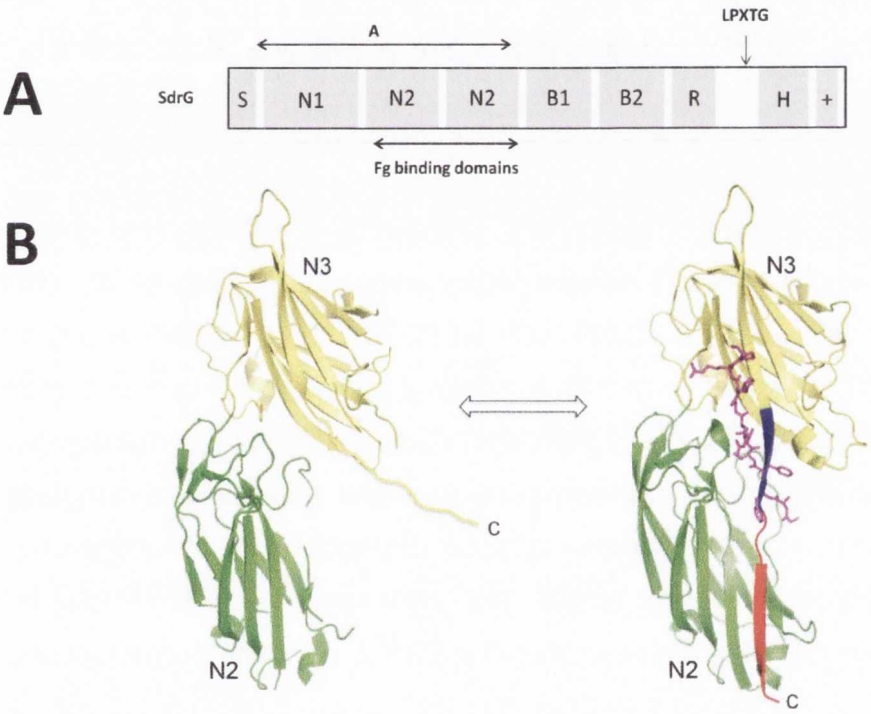

Figure 1.7 SdrG binding to fibrinogen by "dock, lock and latch"
(A) Schematic representation of the SdrG molecule: A - N-terminal region; N2-N3 - subdomains with IgG-like folds binding to Fg; B1-B2 - repeats of unknown function; R - serine-aspartate repeat region; H - hydrophobic region; + -positively charged region;.
(B) SdrG N2/N3 bind Fg by the "dock, lock and latch" mechanism. SdrG in its open apo form has a wide trench between the N2 and N3 subdomains. The ligand inserts into this trench and SdrG undergoes conformational changes to a closed form and locks the ligand in place. In the apo form the disordered C-terminal extension of the N3 subdomain is not part of the crystal structure. After "Dock Lock and Latch" this region forms the lock (blue) and the latch (red).
Adapted from (Foster *et al.* 2013).

of the various fibrinogen chains are recognized. SdrG binds to the N-terminal segment of the β-chain. In contrast ClfA interacts with the extreme C-terminus of the fibrinogen γ-chain (Deivanayagam *et al.*, 2002; McDevitt *et al.*, 1994). In addition the Fg peptide bound to the cleft in the opposite orientation. ClfB binds to the α-chain of fibrinogen and to loop regions of cytokeratin 10 and loricrin (Mulcahy *et al.*, 2012; Walsh *et al.*, 2004; Walsh *et al.*, 2008; Xiang *et al.*, 2012). All ligands are bound by the "dock, lock and latch" mechanism.

The same mechanism of binding to Fg was shown for FnBPA and FnBPB (Burke *et al.*, 2011; Wann *et al.*, 2000). However, the N2/N3 domains of FnBPA/B also bind to elastin and tropoelastin (Keane *et al.*, 2007; Roche *et al.*, 2004). Thus the "dock, lock and latch" mechanism is quite promiscuous in the ligands that can be accepted into the binding trench and phage display has recently been used to identify β-neurexin as a ligand for the MSCRAMM SdrC (Barbu *et al.*, 2010). However some MSCRAMMs (e.g. SdrE or SdrD) have no known ligand.

1.4.3.2 The collagen hug

The collagen binding protein (CNA) of *S. aureus* binds to collagens in a variation of the "dock, lock and latch" mechanism (Zong *et al.*, 2005). The protein possesses an A domain with N1/N2/N3 domain organisation and a stalk region of B-repeats (Figure 1.8). In contrast to the mechanism described above, the ligand binding domain of CNA comprises the N1/N2 IgG-like domains rather than the N2/N3 domains. However, the general interaction is comparable. The N1/N2 domains are organized to allow the docking of a collagen triple helix within the trench between N1/N2. The linker region between N1/N2 in CNA is longer than the linker between N2/N3 in ClfA to allow the accommodation of the triple helix within the cleft. In CNA the C-terminal extension of N2 serves as lock and latch to tighten the interaction (Zong *et al.*, 2005).

1.4.3.3 The β zipper mechanism of fibronectin binding

The *S. aureus* fibronectin binding proteins A/B FnBPs possess a N1/N2/N3 domain organisation at the N-terminal end which binds to fibrinogen. However, the IgG-like domains are followed by a series of Fn binding motifs (Figure1.8). Fibronectin is a homodimer composed of two splice variant protein

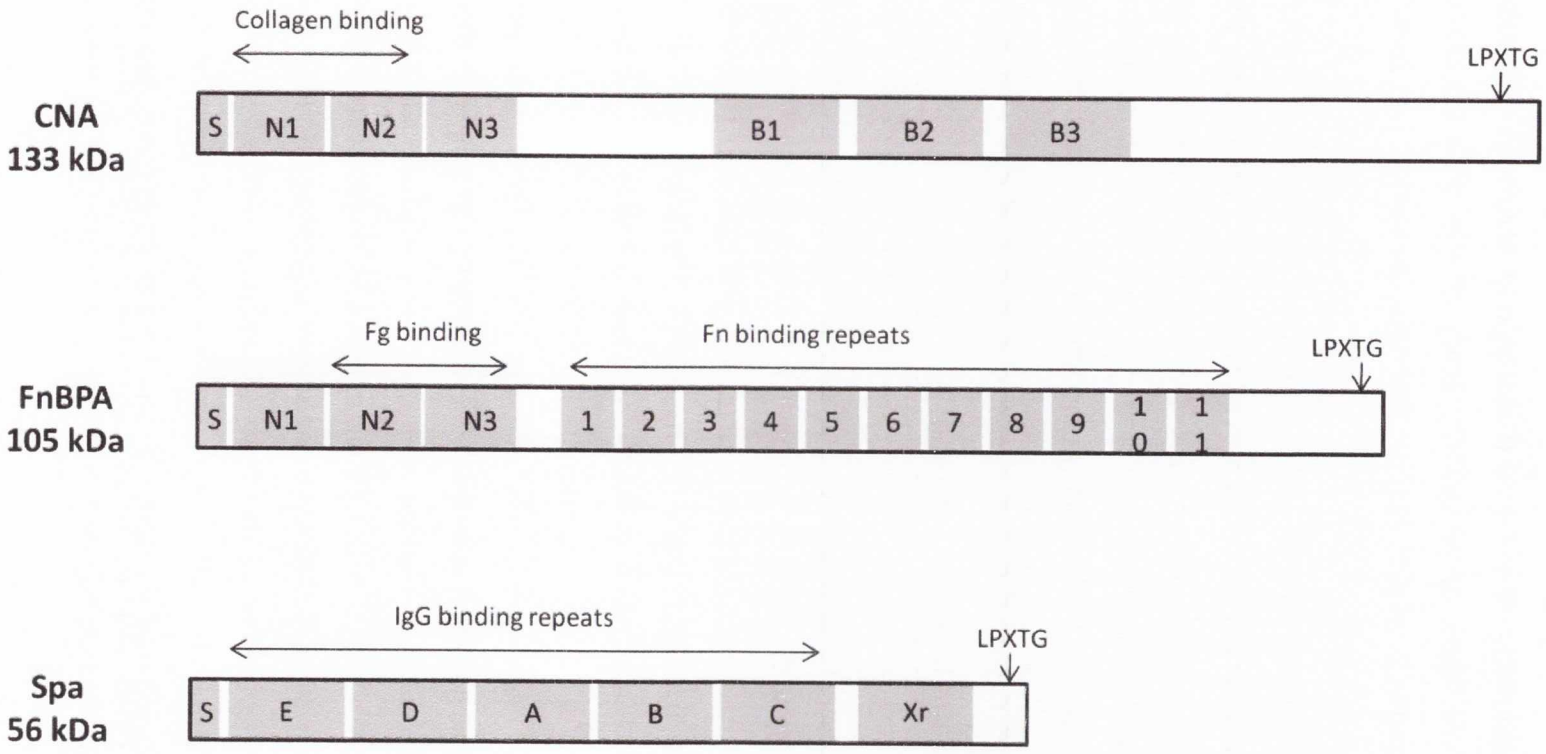

Figure 1.8 *S. aureus* cell wall-anchored proteins
Schematic representation of the *S. aureus* cell wall-anchored proteins CNA, FnBPA and Spa. The molecular weights of the proteins from MRSA252 are given. Grey boxes denote individual domains. Ligand binding regions are indicted by biheaded arrows. S – signal sequence; Fg – fibrinogen; Fn – fibronectin.

chains of between 230 and 270 kDa in size. The two chains are linked by disulfide bonds near their C-termini. Each chain is composed of an array of repeated modules designated type I, type II and type III which are separated by connecting sequences (Bork *et al.*, 1996). Each of the type I modules is composed of a β-sandwich of anti parallel β-sheets containing two and three strands.

The Fn binding motif bind to the type 1 modules of Fn by short anti-parallel β-strand complementation (Schwarz-Linek *et al.*, 2003) and the Fn binding domains vary in their affinity for Fn. The mechanism allows low affinity interaction of a single binding motif with a single type one module but a high affinity interaction when the Fn binding region interacts with an array of type I modules.

1.4.3.4 Immunoglobulin binding by protein A

The *Staphylococcus aureus* protein A (Spa) is composed of an A domain consisting of five domains designated E, D, A, B, C followed by a repeat region consisting of an octapeptide motif (Xr) (Figure 1.8) (Moks *et al.*, 1986). Each of the five N-terminal domains consists of three anti-parallel α-helixes (10 residues) separated by short loops (5 residues) (Cedergren *et al.*, 1993; Deisenhofer, 1981). The bundles possess the ability to bind the Fc region of IgG. The binding site is located between the C_H2 and the C_H3 domains of IgG. Spa is an important virulence factor (Palmqvist *et al.*, 2002) that prevents opsonisation and complement activation by displaying IgG in the incorrect orientation on the cell surface. Furthermore the bundle domains of Spa bind to the Fab region of IgM (Graille *et al.*, 2000). Since IgM molecule represent the B cell receptor on immature B cells, Spa dependent activation can lead to B cell anergy and immune suppression (Silverman & Goodyear, 2006).

Spa also binds to von Willebrand factor thereby promoting interactions with platelets (O'Seaghdha *et al.*, 2006). Finally Spa binds to the ectodomain of tumor necrosis factor receptor-1 thereby inducing inflammation (Gomez *et al.*, 2004; Gomez *et al.*, 2006).

1.5 Iron acquisition by *S. aureus*

1.5.1 Characteristics and importance of iron

Iron is an important molecule for the host and the pathogen, since it is required as prosthetic group or cofactor for many enzymes in essential processes such as DNA replication and aerobic respiration (Schaible & Kaufmann, 2004; Weinberg, 2000). This is attributed to the chemical characteristics of this metal. It readily engages in one electron oxidation/reduction reactions between the ferric (Fe^{3+}) and ferrous (Fe^{2+}) state which makes it valuable for enzymatic reactions. However, "free" reactive ferrous iron in the cytoplasm can engage in Fenton type reactions, thereby creating ferric iron and various radicals, damaging membrane lipids and ultimately leading to cell death (Hentze *et al.*, 2004). Due to the toxicity of free iron, its concentration is strongly limited within mammalian cells and in the extracellular milieu. Greater than 90% of the iron in mammals is located intracellularly and is therefore not accessible for extracellular pathogens unless it can be liberated from the cells (Drabkin, 1951). Intracellular iron is either engaged as a cofactor or prosthetic group into biochemical reactions or complexed to the tetrapyrrole ring of haem and stored by haemoproteins such as haemoglobin, myoglobin or haemopexin (Hentze *et al.*, 2004). Extracellular iron is bound by high affinity iron chelating proteins such as lactoferrin and transferrin found in lymph and mucosal secretions or within the serum, respectively. The process of iron sequestration is also referred to as "nutritional immunity" (Cassat & Skaar, 2013; Hood & Skaar, 2012) and poses a significant problem for any invading microorganism. The importance of strictly controlled iron metabolism was heightened by several experimental and descriptive studies, linking an increased level of free iron to an increased severity of bacterial infections (Gladstone & Walton, 1971; Schaible & Kaufmann, 2004; Singh & Sun, 2008).

Due to the importance of iron for biochemical reactions, bacteria deposit intracellular reserves of iron within iron storage proteins. These internal stores can be used to enhance growth when external iron is restricted. Three different forms of iron storage proteins are described: ferritins, bacterioferritins and Dps

proteins (Andrews *et al.*, 2003). All proteins show a modular structure composed of identical subunits consisting of a four α-helix-bundle. Ferritin (Bou-Abdallah, 2010) and bacterioferritin are composed of 24 subunits while the smaller Dps proteins are composed of 12 subunits. The architecture of the protein complexes allows the formation of a central cavity where the ferric form of iron is stored. Bacterioferritin is more common in bacteria then ferritins (Andrews *et al.*, 2003). In contrast to Dps proteins and ferritins, bacterioferritins contain haem which is used to coordinate the iron molecule in the central cavity.

1.5.2 The *S. aureus* Fur protein

S. aureus reacts to iron shortage with a dramatic change in its gene expression profile (Friedman *et al.*, 2006). This is due to the iron-dependent regulator Fur (ferric uptake regulator). Under iron-rich conditions, the conformation of the regulator allows the binding of Fur to the consensus sequence in the DNA (*fur* boxes) upstream of iron regulated genes. Fur acts as a repressor, preventing the transcription of these genes. It was shown for the Fur protein of *Pseudomonas aeroginosa* that under iron starvation conditions Fe dissociates from Fur, leading to a subtle change in conformation and allowing the repressor to drop off the operator sequence (Pohl *et al.*, 2003). Subsequently the RNA polymerase can access the operator sequence and transcribe the genes. In *S. aureus*, Fur is known to negatively regulate at least 20 different genes (Friedman *et al.*, 2006). Among these are genes involved in iron acquisition such as the *sfn/sbn* genes and the *isd* locus described below. Furthermore up-regulation of fermentative enzymes is observed. This results in the increased production of lactate which results in a decrease of the local pH. Since host proteins such as transferrin possess a lower affinity for iron at low pH (Friedman *et al.*, 2006), the secretion of lactate is believed to stimulate the release of iron from these proteins to make it accessible for *S. aureus* (Hammer & Skaar, 2011). Additionally, several staphylococcal virulence factors are Fur regulated (Torres *et al.*, 2010). Among those are proteins involved in, biofilm formation (Hussain *et al.*, 2001; Johnson *et al.*, 2008) in delayed wound healing (Athanasopoulos *et al.*, 2006) and secreted cyotolytic and immunostimulatory toxins (Nizet, 2007). A functional *fur* gene is important for full virulence of *S. aureus* (Horsburgh *et al.*, 2001; Torres *et al.*, 2010). Taken together, Fur

represents an important sensor for *S. aureus*, specifically recognizing the environment during invasive infection and adapting bacterial physiology for survival within the host.

1.5.3 *S. aureus* siderophores

Iron-scavenging siderophores are small secreted molecules that show an exceptionally high affinity for iron, thereby outcompeting host proteins such as transferrin and lactoferrin. Secretion and reuptake of siderophores by membrane transporter systems allows *S. aureus* to steal iron from host proteins. At least two different siderophores are produced by *S. aureus*, staphyloferrin A (Beasley *et al.*, 2009; Cotton *et al.*, 2009) and staphyloferrin B (Cheung *et al.*, 2009). Both belong to the carboxylate family of siderophores (Figure 1.9). A third siderophore (aureochelin) has been proposed, but has not been characterized (Courcol *et al.*, 1997). The 479 Da molecule staphyloferrin A is produced by four proteins (SfnABCD). The haem transporter HtsABC was shown to be responsible for the reuptake of staphyloferrin A (Beasley *et al.*, 2009). Staphyloferrin B is synthesized by SbnABCDEFGHI and its reuptake is mediated by the staphylococcal iron regulated transporter SirABC. Inactivation of *sbnE* lead to a reduced bacterial load within the kidneys of systemically infected mice, underlining the importance of the molecule during pathogenesis (Dale *et al.*, 2004a).

The active transport of substrates is typically associated with ATP usage. Interestingly, neither the *hts* locus nor the *sir* locus encodes an ATPse. It was shown that both systems are energised by the ATPase FhuC of the ferric hydroximate uptake operon (*fhuCBG*) (Beasley *et al.*, 2009; Speziali *et al.*, 2006). The xeno-siderophores are a further class of iron scavenging molecules. Although *S. aureus* does not produce this class of siderophore, it is capable of using them as a source of iron (Sebulsky *et al.*, 2000). The uptake is FhuCBG dependent and is proposed to allow *S. aureus* to establish itself within the microbiome by stealing siderophores produced by other bacteria within the community (Hammer & Skaar, 2011). A schematic diagram of the siderophore mediated iron acquisition is shown in Figure 1.9

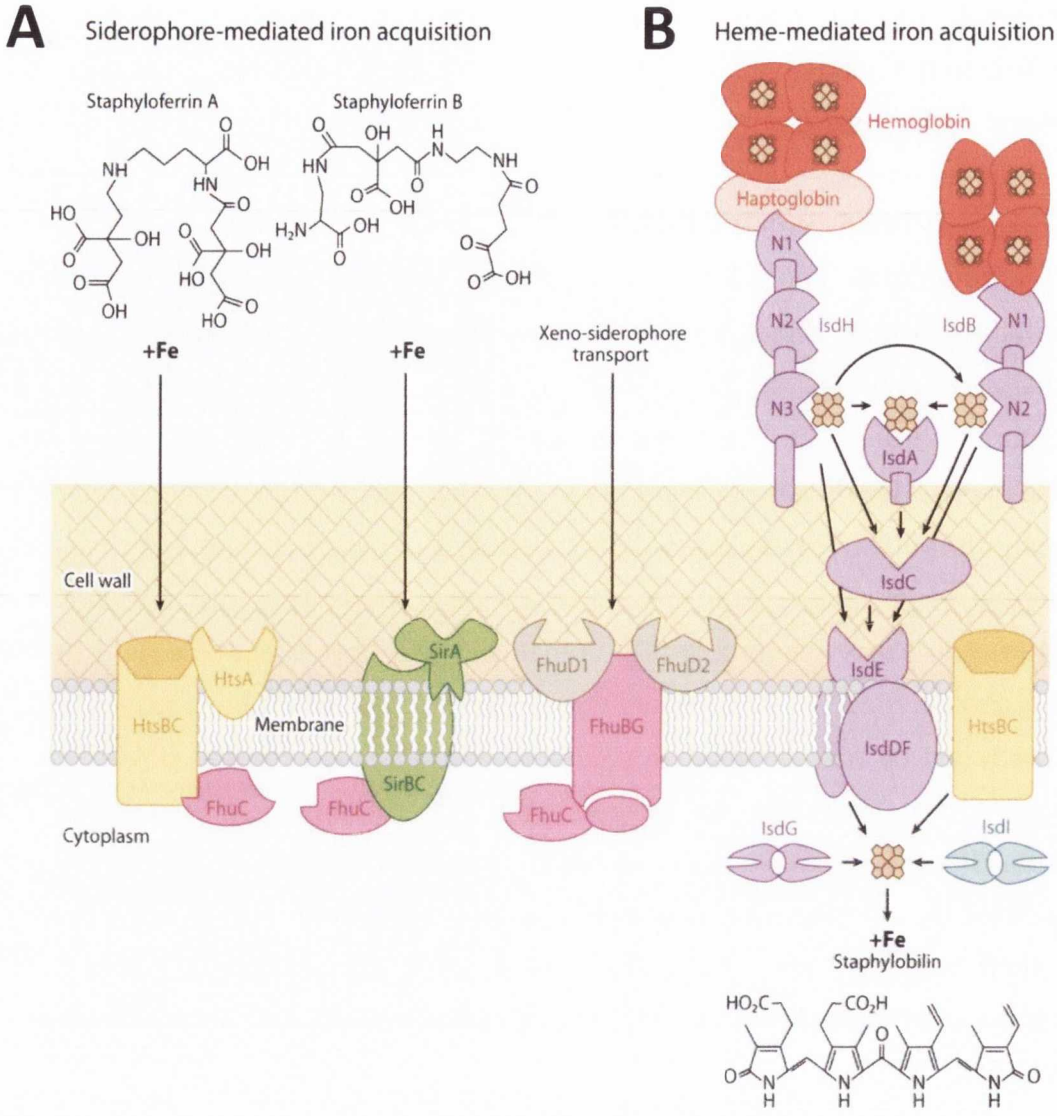

Figure 1.9 A model of the *Staphylococcus aureus* iron acquisition pathways

(A) *S. aureus* produces two siderophores, staphyloferrin A and staphyloferrin B. Staphyloferrin A import is mediated by the HtsA lipoprotein and HtsBC permease. The SirA lipoprotein is the receptor for staphyloferrin B, and the SirBC permease mediates the translocation of staphyloferrin B across the membrane. *S. aureus* imports xenosiderophores produced by other bacteria through the binding activity of FhuD1 and FhuD2 receptor lipoproteins and the FhuBG permease. The energy needed for siderophore uptake is provided by the FhuC ATPase.

(*B*) Haem acquisition is mediated by the Isd system. IsdH binds the haemoglobin-haptoglobin complex and IsdB binds haemoglobin. Haem is passed through the NEAr iron Transporter (NEAT) domains of IsdH (N1-N3), IsdB (N1-N2), IsdA, and IsdC. Haem can also be passed from IsdH or IsdB directly to the IsdE haem-receptor lipoprotein. Haem transport across the membrane occurs through either the IsdDF or the HtsBC permeases. Once in the cytoplasm haem is a substrate for the haem-degrading enzymes IsdG and IsdI. *S. aureus* degradation of haem leads to the release of iron and the production of staphylobilin.

Adapted from (Hammer & Skaar, 2011).

1.5.4 The *S. aureus isd* locus

With about 80% of host iron bound to haem, this protein represents the most abundant iron source within the host and was shown to be the preferred source of nutrient iron for *S. aureus* (Skaar *et al.*, 2004). Four haem molecules are bound by the protein haemoglobin which is enclosed within erythrocytes. In order to make this rich source available, *S. aureus* produces several haemolytic toxins that lyse erythrocytes and release the haemoglobin. Several host molecules reduce the concentration of free haemoglobin and haem within the blood plasma and lymph. The protein haptoglobin is a high affinity haemoglobin binding protein and is present in high amounts within serum (Hwang & Greer, 1980; Oliviero *et al.*, 1987). Haemopexin (Tolosano & Altruda, 2002) binds to free haem. Both haemoglobin-haptoglobin complexes and haemopexin-haem complexes are rapidly recycled by hepatocytes within the liver. This rapid clearance of haemoproteins is thought to have two distinct advantages for the host. Firstly, it reduces the toxic effects associated with the presence of free iron/haem. Secondly it reduces the amount of iron available for invading microorganism (nutritional immunity). *S. aureus* is capable of using free haem, haemoglobin, myoglobin and the haemoglobin-haptoglobin complex as a source for nutrient iron. However, the bacterium is not able to use the haemopexin-haem complex (Torres *et al.*, 2006).

The *S. aureus isd* operon (iron regulated surface determinant) represents an efficient haem uptake and degradation system. Protein expression is controlled by Fur. Therefore the proteins are only expressed under iron limiting conditions (Mazmanian *et al.*, 2002). The system allows the extraction of haem from haemoproteins, its transport through the cell wall and the cell membrane and its subsequent degradation in the cytoplasm (Hammer & Skaar, 2011).

The *S. aureus isd* locus contains two cytosolic haem-degrading monooxygenases (IsdG, IsdI), three membrane transport proteins (IsdE, IsdF, IsdD) and four cell wall-anchored proteins (IsdA, IsdB, IsdC, IsdH). IsdC contains the alternative sorting signal NPQTN at its C-terminal end. This signal is recognized by sortase B (SrtB) which is also encoded within the operon (Mazmanian *et al.*, 2002). All cell wall-anchored proteins contain NEAT (near iron transporter) domains. These 125 aa domains bind one haem molecule

within a groove possessing a conserved tyrosine residue (Grigg *et al.*, 2007). The cell wall-anchored proteins IsdH, IsdB and IsdC are cell surface exposed proteins and possess three, two and one NEAT domain, respectively (Hammer & Skaar, 2011; Mazmanian *et al.*, 2003). IsdB is a haemoglobin receptor, while IsdH was found to bind the haemoglobin-haptoglobin complex (Torres *et al.*, 2006). The transfer of haem has been described with *in vitro* experiments. Haem is transferred unidirectionally from IsdB NEAT2 to the NEAT motif of IsdA or IsdC. Additionally, the NEAT motif of IsdA can transfer haem to IsdC (Liu *et al.*, 2008). The NEAT domain of IsdC can transfer haem to IsdE within the membrane. No transfer occurs directly between IsdA and IsdE (Muryoi *et al.*, 2008). The NEAT1 domain of IsdH binds to haemoglobin-haptoglobin, NEAT2 binds to haemoglobin and NEAT3 binds to haem. The IsdH NEAT3 domain can receive and transfer haem from/to IsdB NEAT2. Furthermore it can transfer haem to IsdA, IsdC or directly to IsdE (Dryla *et al.*, 2007; Pilpa *et al.*, 2009). Haem transfer between the NEAT domains is indicated in Figure 1.9. IsdB and IsdH represent the haemoglobin receptors on the cell surface. However only the deletion of *isdB* prevented the utilization of haemoglobin as a source of nutrient iron (Torres *et al.*, 2006). Furthermore, deletion of *isdB* led to a decrease in bacterial burden in murine models of systemic infection with special importance for the colonization of the heart (Pishchany *et al.*, 2009). This implicates IsdB as an important factor for haemoglobin binding and haem uptake.

Taken together, haemoproteins are captured at the cell surface by the receptors IsdH and IsdB. Haem is extracted and transferred to IsdA which is also surface exposed. Subsequently haem is transferred to IsdC which is buried within the cell wall and passed on to IsdE in the membrane. It is transported into the cytoplasm where IsdG/I degrade the haem and release the iron. Figure 1.9 shows a diagram of the haem transfer through the *S. aureus* cell envelope.

It was shown, that *S. aureus* Isd proteins recognize human haemoglobin more efficiently than the murine molecule (Pishchany *et al.*, 2010). This underlines the adaption of *S. aureus* to humans and shows the limitations of standard mouse models. However, transgenic mice (expressing human haemoglobin) are more susceptible to *S. aureus* strains expressing IsdB than to the Δ*isdB* mutant (Pishchany *et al.*, 2010). Thus, transgenic mice represent the best model currently available to study effects of Isd proteins *in vivo.*

1.1.5 Haem mediated toxicity

Haem is an indispensable element in many physiological processes, and most bacteria dedicate significant efforts to acquire haem from extracellular sources or to synthesise it endogenously. However, the high reactivity of haem that makes it important for physiological reactions are inseparable from toxic side effects. This poses a problem for all bacteria that take up extracellular haem. In general Gram-positive bacteria seem to be more susceptible to haem mediated toxicity than Gram-negative organisms (Nitzan *et al.*, 1994). The mechanism of toxicity is not completely understood, but haem possesses potent monooxygenase-like and peroxidise-like activity, thereby it might damage multiple cellular constituents including the DNA (Anzaldi & Skaar, 2010).

S. aureus uses extracellular haem as a source of nutrient iron. Subsequently haem toxicity is a problem for the pathogen if too much haem is taken up. *S. aureus* encodes a haem regulated transporter (HrtAB) in order to avoid accumulation of excess haem within the cytoplasm (Torres *et al.*, 2007). The system is upregulated in the presence of haem and confers tolerance to high extracellular concentrations. The exact mechanism is unknown but HrtA is an ATPase that energises the system and HrtB is a membrane located porin. It is assumed that the system allows the efflux of haem. HrtAB expression is regulated by the two component system HssRS (haem sensor system). HssS is a membrane located histidine kinase that senses the presence of haem by an unknown mechanism. Haem sensing leads to autophosphorylation of HssS. The phosphorylation is transferred to the response regulator HssR which subsequently binds to the HrtAB promoter region and allows the expression of the system (Stauff *et al.*, 2007).

1.5.6 Additional functions of Isd proteins

Besides their importance for haem uptake, several additional functions have been described for the Isd proteins of *S. aureus*. Under iron limited conditions, IsdA is the predominant covalently attached surface protein of *S. aureus* and its expression leads to a significant reduction in the hydrophobicity of the bacterial cell (Clarke *et al.*, 2007). This effect was shown to be conferred by the C-terminal domain of IsdA and not by the N-terminal

NEAT domain, which is involved in haem uptake (Clarke *et al.*, 2007). Several host defence molecules use hydrophobic interactions to damage bacterial membranes. For this reason, the decrease in the hydrophobicity conferred by IsdA confers resistance to antimicrobial fatty acids, antibacterial peptides and lantibiotics (Clarke *et al.*, 2007). Furthermore it reduces biofilm formation, protects *S. aureus* from protease activity of apolactoferrin and increases survival on the human skin (Clarke *et al.*, 2007; Clarke & Foster, 2008). Thus IsdA represents an important molecule for *S. aureus* to circumvent the host immune defence. In addition IsdA is a broad spectrum adhesin. It mediates adherence to Fg, Fn, fetuin, asialofetuin (Clarke *et al.*, 2004), involucrin, loricrin and cytokeratin 10 and is important for nasal colonization (Clarke *et al.*, 2009). A murine model confirmed the importance of IsdA for abscess formation (Cheng *et al.*, 2009).

IsdB was shown to mediate the adherence to platelets by the direct interaction with the integrin receptor GPIIb/IIa (Miajlovic *et al.*, 2010). Furthermore, the interaction with β3 interaction allows the invasion of human non-phagocytotic cells to evade the host immune response (Zapotoczna *et al.*, 2012b).

1.6 Allelic exchange in staphylococci

In order to gain an in depth understanding of bacterial pathogen biology, the ability to create specific mutations is of crucial importance. Targeted mutations preventing normal protein expression allow the investigation of the importance of single proteins in physiology and pathogenicity.

Several methods have been established for the creation of mutations in *S. aureus*. Most of them function by the introduction of a genetic element into the target gene thereby disrupting the open reading frame of the protein. Examples for this type of system are transposon mutagenesis (Foster, 1998) or the use of type II introns in the targetron system (Sigma Aldrich) (Chen *et al.*, 2005; Yao *et al.*, 2006). However, these systems have a number of disadvantages including the insertion of antibiotic resistances and the possibility of polar effects on the expression of downstream genes.

1.6.1 Mutagenesis using allelic exchange

In contrast to insertions, allelic exchange allows the construction of deletion mutations in order to avoid polar effects. It also allows the creation of chromosomal point mutations and the targeted insertion of antibiotic resistances and is therefore the preferable method for many applications. On the downside, it is a more time consuming procedure. The allelic exchange methodology uses the ability of bacteria to integrate DNA into and to excise DNA from the chromosome if homologous regions are present. This RecA-dependent process is known as homologous recombination and happens with different frequencies, depending on the length of the homologous regions (Alberts & Lewis, 2002).

For the construction of a deletion mutation by allelic exchange, a deletion cassette consisting of a short DNA fragment upstream and downstream of the gene of interest is constructed and cloned onto a thermosensitive plasmid (Figure 1.10). The use of thermosensitive plasmids provides a convenient method to select for plasmid integration since a temperature shift from low temperatures (allowing plasmid replication) to a restrictive temperature allows only cells with integrated plasmid to grow and form colonies. Subsequent growth at a low temperature without antibiotic pressure promotes plasmid replication, its excision and subsequent loss. The process of integration and excision will delete the target gene from the chromosome, if one of the recombination events (integration or excision) occurs at the upstream sequence while the other event occurs at the downstream sequence (Figure 1.10).

1.6.2 Thermosensitive plasmids for the use in *S. aureus*

The first highly efficient thermosensitive plasmid constructed specifically for *S. aureus* is pKOR1 (Bae & Schneewind, 2006). The pE194ts replicon of this plasmid requires 43°C for the selection of integrants. It has been reported that mutations in the genes encoding the two component system *sae* can be selected at high temperatures in the presence of antibiotics (Sun *et al.*, 2010). To avoid the risk of acquiring secondary mutations, novel thermosensitive plasmids have been constructed. pIMAY (Monk *et al.*, 2012) and pIMAYZ (Monk et al. unpublished) are plasmids with the improved thermosensitivity conferred by the pWV01ts replicon (Maguin *et al.*, 1992) which allows the selection of

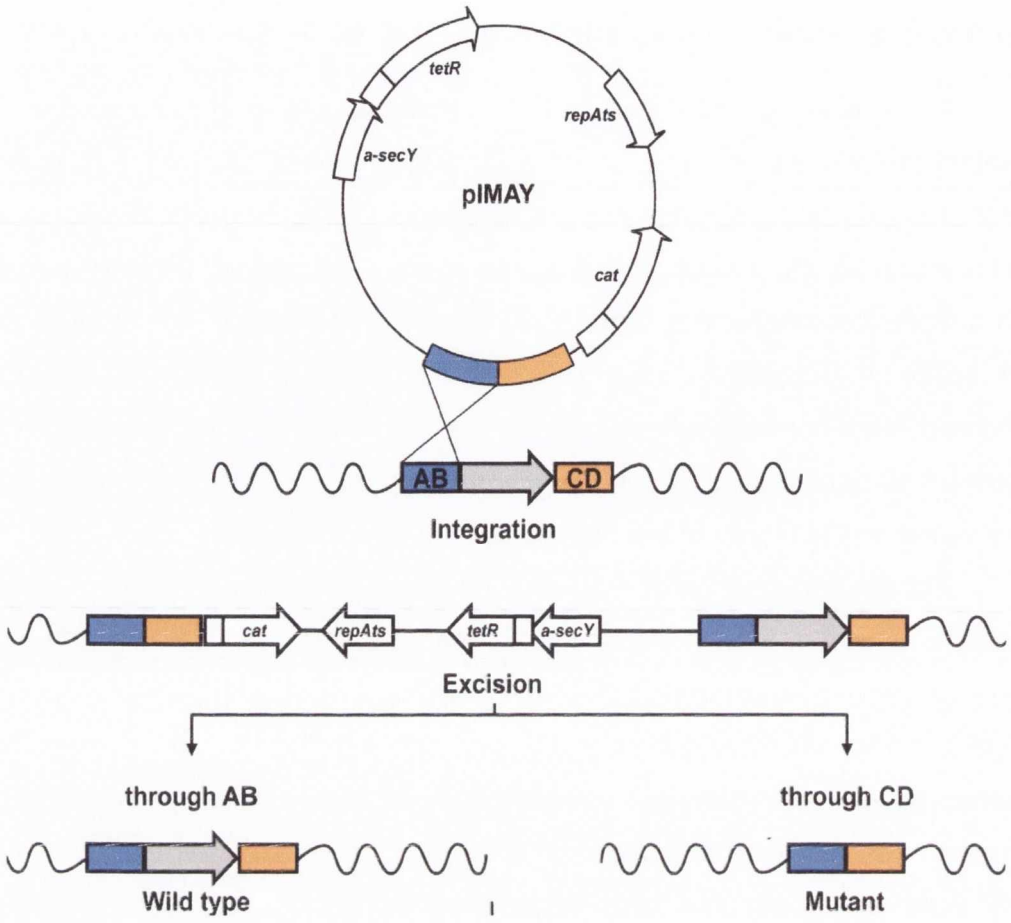

Figure 1.10 Schematic of allelic exchange in *S. aureus* using pIMAY
pIMAY is transformed into staphylococci at 28°C, and single-crossover integration is stimulated by growth at 37°C. The diagram details an integration event through the AB side. A clone from either AB or CD integration event is grown at 28°C without antibiotic selection to stimulate plasmid excision and loss. Plasmid excision through the AB side recreates the wild-type locus, while CD excision yields a mutated gene.
Adapted from (Monk *et al.*, 2012)

integrants at 37°C. This decreases the risk of stress-induced secondary mutations.

1.6.3 Counter selection to identify plasmid loss

A long standing problem for targeted mutagenesis by allelic exchange is the identification of clones that have lost the plasmid after integration in the chromosome. In times when antibiotic resistance was the only marker associated with the thermosensitive plasmid, this process used to be work intensive and time consuming since single colonies had to be picked and patched on different plates for the identification of plasmid loss. Both pKOR1 and pIMAY/pIMAYZ carry a coding sequence for *secY*-antisense RNA to simplify this process. Protein secretion is an essential capability and bacteria without a functional Sec-system are not viable (Ji *et al.*, 2001). Thus the induction of plasmid-encoded *secY* antisense RNA can be used to suppress growth of bacteria harbouring the plasmid (Bae & Schneewind, 2006). In pKOR1 and pIMAY the *secY* antisense RNA is under tight control of the TetR repressor. After induction with anhydrotetracycline, only cells without integrated or replicating plasmid are able to grow allowing the easy identification of putative mutants.

pIMAYZ (Monk *et al.*, unpublished) represents the next generation of thermosensitive plasmids. In addition to the inducible *secY* antisense RNA, the plasmid encodes the *lacZ* gene in a transcriptional fusion with the constitutively expressed *cat* gene (chlormaphenicol resistance). By using the chromogenic substrate X-Gal, pIMAYZ allows a simple identification of clones without the plasmid by the colour of the colony. Clones carrying the plasmid are able to degrade X-Gal and possess a blue colour, while colonies without the plasmid fail to degrade X-Gal and exhibit a white colour.

1.7 Rationale of this study

S. lugdunensis is more and more recognized to be an important pathogen and seems to be unusually virulent for a coagulase negative staphylococcus. However, hypothesis-driven research regarding *S. lugdunensis* has not been performed prior to this study and very little was known about the virulence factors that account for the apparent *S. aureus*-like behaviour.

A *S. lugdunensis* genome sequence was not available prior to this study. Therefore the chromosome of the clinical isolate N920143 was sequenced and analysed to identify any putative virulence and colonisation factors. Furthermore *S. lugdunensis* had not been transformed prior to this study and mutant strains had not been created.

This project was therefore aiming for a detailed investigation of the *S. lugdunensis* genome sequence, the establishment of a genetic system and the investigation of any apparent virulence factors that might account for its aggressive behaviour.

Chapter 2
Material and Methods

Remark

Unless stated otherwise, materials and reagents were obtained from Sigma Aldrich.

2.1 Genome sequencing and analysis

2.1.1 Genome sequencing

The genome of the *S. lugdunensis* strain N920143 was sequenced by collaborators of the Welcome Trust Sanger Institute, using both reversible terminator sequencing (on Illumina Genome Analysers (GAII)) and pyrosequencing (on 454 instruments; subsidiary of Roche Diagnostics Corporation, Branford, Connecticut, US). A total of 40.1 Mb of Illumina sequence was produced from a 200 bp standard paired-end library run in one lane of a flow cell with 54 bp reads representing approximately 850-fold coverage. The 454 sequencing produced 0.23 Mb sequence with an average length of 250 bp. The assembly of the Illumina reads using Velvet 0.7.62 gave 142 contigs of > 1 kb with a contig N50 of 22 kb.

A combined assembly of the 454 reads using Newbler 2.1 and the Illumina consensus sequences from the Velvet assembly produced 69 contigs > 500 bp with an N50 of 72 kb. The length of the combined assembly was 2,588,004 bp in 9 scaffolds. IMAGE (Tsai *et al.*, 2010) and ICORN (Otto *et al.*, 2010), along with a further 1070 high quality reads, were used to close gaps and to improve the quality of the sequence to the standard of improved high quality draft (Chain *et al.*, 2009).

2.1.2 Bioinformatic analysis

The sequence and annotation of the *S. lugdunensis* strain N920143 genome has been deposited in the EMBL database under accession number FR821777. The sequence was finished and annotated as described previously using Artemis software (Holden *et al.*, 2009). Comparison of the genome sequences was facilitated by using the Artemis Comparison Tool (ACT) (Carver *et al.*, 2005). Orthologous proteins were identified as reciprocal best matches using FASTA (Pearson & Lipman, 1988) with subsequent manual curation. Circular diagrams were created using the program DNAPlotter (Carver *et al.*, 2009). Protein domains were predicted using the Pfam database (Finn *et al.*,

2010) and repeat-regions were identified using the web based radar program [www.ebi.ac.uk/Tools/Radar].

2.2 Bacterial culture conditions

S. lugdunensis strains were grown at 37°C in Tryptic Soy Broth (TSB) or on Tryptic Soy Agar (TSA) with 200 rpm shaking for liquid cultures. To represent iron-limited conditions, *S. lugdunensis* was grown in RPMI medium containing 1% casamino acids (Difco). *E. coli* strains were grown at 37°C Luria Bertani Broth (LB) or on Luria Bertani Agar (LA) (Difco) with 200 rpm shaking for liquid cultures. *Lactococcus lactis* strains were grown in GM17 (M17 medium (Difco), 200 mM sucrose, 25 mM glucose). *L. lactis* was grown on plates and in broth without agitation at 30°C.

For strains carrying chromosomal or plasmid-encoded antibiotic resistance, the appropriate antibiotic was added to the medium. Stock concentrations and final concentrations are summarized in Table 2.1.

Strains were kept for up to four weeks on agar plates. For long term storage, 0.5 ml of freezing solution (65% glycerol, 0.1 M $MgSO_4$, 25 mM Tris-HCl, pH 8) was added to 0.5 ml of a fresh overnight culture and the strain was stored at -80°C.

2.3 Molecular Biology

2.3.1 Isolation for DNA

For isolation of plasmid DNA the Wizard® *Plus* SV Miniprep kit (Promega) was used according to the manufacturers protocol. The only additional step required when isolating plasmid from *S. lugdunensis* was the incubation of the resuspended cells of 5 ml overnight culture for 15 min with 5 µl lysostaphin (Ambi Products LLC, 10 mg/ml) prior to lysis. For the purification of higher amounts of pRMC2 for comparative transformation experiments, the Qiagen® Plasmid *Plus* Midi Kit was used.

The PureElute Bacterial Genomic kit (Edge Biosystems) was used for the isolation of chromosomal DNA from *S. lugdunensis* with an additional incubation step with lysostaphin 10 µl (10 mg/ml) at 37°C for 20 min prior to lysis. For

Table 2.1 Antibiotics and medium supplements

Antibiotic/Supplement	Solvent	Stock concentration	Final concentration
Ampicillin	dH_2O	100 mg/ml	100 µg/ml
Chloramphenicol	100% EtOH	10 mg/ml	10 µg/ml (5 µg/ml for *L. lactis*)
Erythromycin	100% EtOH	10 mg/ml	10 µg/ml
Kanamycin	dH_2O	25 mg/ml	50 µg/ml
Tetracycline	50% EtOH	7.5 mg/ml	2-40 µg/ml (strain dependent)
IPTG	dH_2O	1 M	1 mM
X-GAL	Dimethylformamide	50 mg/ml	100 µg/ml

purification of DNA from PCR reactions, agarose gels or enzymatic reactions, the Wizard® *Plus* SV PCR purification kit (Promega) was used.

2.3.2 Polymerase chain reaction (PCR)

PCR reactions were carried out using thermal cyclers (Finnzymes/Techne). 10 ng plasmid DNA or 100 ng chromosomal DNA was used in a 50 µl PCR reaction. For cloning purposes the Phusion polymerase (Finnzymes) was used with a final primer (MWG-Biotech / IDT) concentration of 0.5 µM and 200 µM of each dNTP (Bioline). Cycling conditions were chosen according the requirements of for the polymerase and the melting temperature of the primers. 30-35 cycles of amplification were carried out.

2.3.3 Colony PCR

One bacterial colony (*E. coli* / *S. lugdunensis*) was resuspended in 20 µl TE Buffer (10 mM Tris-HCl, 1 mM EDTA, pH 8), boiled for 10 min and centrifuged (5 min at 10000 x g). 0.5 µl of the supernatant was used for a 25 µl PCR reaction using Phire hot start polymerase (Finnzymes). Cycling conditions were chosen according to the requirements of the polymerase and the melting temperature of the primers. 30-35 cycles of amplification were carried out.

2.3.4 Restriction and ligation

DNA manipulations were carried out using standard restriction enzymes (Roche) and fast restriction enzymes (Fermentas). The enzymes were used with concentrations and incubation conditions as specified by the supplier. The T4 fast ligase (Promega) was used for the ligation of DNA fragments according to the manufacturers' protocol.

2.3.5 Subcloning of DNA fragments

For rapid high efficiency blunt end subcloning of DNA fragments the "Zero Blunt® pCR cloning kit" (Invitrogen) was used according to the recommended protocol.

2.3.6 Sequence and ligase independent cloning

Some of the DNA constructs described within this thesis were cloned into the plasmids pIMAY, pIMAYZ, or pRMC2 using sequence and ligase independent cloning (SLIC) (Li & Elledge, 2007; Li & Elledge, 2012). This

method is based on the PCR amplification of the vector backbone and of the insert. Amplification of the vector backbone has the advantage that the resulting product is open-linear with blunt ends at the site required for the cloning. Primer synthesis allows the integration of short identical DNA sequences in vector and insert. Treatment of both PCR products with T4 polymerase (3'-5' exonuclease activity) creates single stranded, 5'-overhangs in both vector and insert. The DNA fragments are assembled *in vitro* (without a ligation step) and used to transform *E. coli*. SLIC provides a high efficiency cloning method that is independent of available restriction sites.

Primers used for the amplification of the pIMAY/pIMAYZ/pRMC2 backbones are summarized in Table 2.2. Identical sequences (20-25 nucleotides) were integrated in the primers for the amplification of the insert (indicated in Table 2.2). 10 ng of plasmid DNA was used as template for the amplification of the plasmid backbone with Phusion polymerase (Finnzymes). The PCR products were purified and the vector product was digested with DpnI in order to remove the methylated template DNA. 1 µg of vector and insert DNA was treated with T4 polymerase in a final volume of 40 µl. The reaction contained NEB Buffer 2 (New England Biolabs), molecular grade BSA (New England Biolabs), 5 mM Dithiothreitol (DTT), 200 mM urea and 3 units T4 DNA polymerase (New England Biolabs). The reaction was incubated for 20 min at 23°C and stopped by the addition of 25 mM EDTA and subsequent incubation for 20 min at 73°C.

5 µl of vector DNA and 5 µl of insert DNA were mixed and the single-stranded overhangs were allowed to anneal. For this the reaction was placed in a PCR machine for 10 min at 65°C followed by a slow decrease in temperature from 65 – 25°C with 1 min hold for each degree. 2.5 µl – 5 µl of the reaction was subsequently used for the transformation of *E. coli*.

2.4 Transformation

2.4.1 Transformation of *E. coli*

E. coli cells were made chemically competent using the rubidium chloride method. 100 ml prewarmed LB-broth was inoculated with a 1 : 100 dilution of fresh overnight culture and grown shaking at 37°C to an OD_{578} = 0.5. Cells were

Table 2.2 Oligonucleotides used in this thesis

Name	5' – 3' sequence	Purpose
SlsD-F	GATTTAGATGGATCCATTGTGGCAGAAGC	Cloning of *slsD* N2/N3 domains (amino acids 230-610) into pQE30
SlsD-R	GTCTCGAGCTCTAATTCCAGACAATGTC	Cloning of *slsD* N2/N3 domains (amino acids 230-610) into pQE30
SlsE-F	GAAGCAGGATCCCAAAGCAATAGTTCAGC	Cloning of *slsE* (amino acids 46-800) into pQE30
SlsE-R	CCAGTTGTCGACTAAGCATAGCGTTTTGT	Cloning of *slsE* (A amino acids 46-800) into pQE30
SlsF-F	AATGTTGGATCCGAAACCGCAGAAAATC	Cloning of *slsF* (amino acids 42-578) into pQE30
SlsF-R	CCAGAGGAAGCTTATGATAGCGAGCC	Cloning of *slsF* (amino acids 42-578) into pQE30
SlsG-R	GACCTGTAGTCGACTAAGATTTCTGTTCA	Cloning of *slsG* (amino acids 48-921) into pQE30
vWbl-F	CTAATTCTAGATCTCATACTGCAGAGATA	Cloning of *vWbl* (amino acids 46-1200) into pQE30
vWbl-R	ATTAAGTCGACCTATTTAGTTTGACCTTT	Cloning of *vWbl* (amino acids 46-1200) into pQE30
Construction of chromosomal deletion and reversion cassettes		
ΔhsdR-A	TGTTGAGCTCTTATTAAAGATCAAAAATTATGAAATTCCG	Cloning of the *hsdR* deletion cassette into pIMAY
ΔhsdR-B	CATCAAATCACCCAAAAATTAGTAGTTTCTTTAAATATAGCAC	Cloning of the *hsdR* deletion cassette into pIMAY
ΔhsdR-C	CTAATTTTTGGGTGATTTGATGTAAATAAGTTAGGCGGCATACC	Cloning of the *hsdR* deletion cassette into pIMAY
ΔhsdR-D	GAATGAATTCATCTTCACTGTCATGGCCTCGGG	Cloning of the *hsdR* deletion cassette into pIMAY
ΔhsdR-Sc. F	GAACTTGTCGTAAAGATATAGAAGATTTGAATAG	Screening for the *hsdR* deletion
ΔhsdR-Sc. R	ATTAAATATTCATACGCATCGCCTAACATATC	Screening for the *hsdR* deletion
Δfbl-A	CAATTGAAGGAGCTCTTGGAGGATTATTTAGC	Cloning of the *fbl* deletion cassette into pIMAY
Δfbl-B	CATTTAATCTCTCCTTTGATTGATATGATTATGCCC	Cloning of the *fbl* deletion cassette into pIMAY

Table 2.2 Oligonucleotides used in this thesis, continued

Δfbl-C	CAATCAAAGGAGAGATTAAATGTAAAAGATAGTAAGATG GAAATGTTC	Cloning of the *fbl* deletion cassette into pIMAY
Δfbl-D	CACCTCTATAATTTATTTGAATTCATGCTGAAAATC	Cloning of the *fbl* deletion cassette into pIMAY
Δfbl-Sc. F	TACAGATACAGGTGCATATATTTTTGGG	Screening for the *fbl* deletion
Δfbl-Sc. R	CTCCAAATACGATAGCAAATGATACAACTG	Screening for the *fbl* deletion
ΔvWbl-A	CTGTAATGAGCTCATTAAGAAAATTAGCACC	Cloning of the *vWbl* deletion cassette into pIMAY
ΔvWbl-B	CAATGGGTTCTCTCTCCTTAATTGAAATTATTAAG	Cloning of the *vWbl* deletion cassette into pIMAY
ΔvWbl-C	AAGGAGAGAGAACCCATTGTAATATAGCAATACACGTC GAG	Cloning of the *vWbl* deletion cassette into pIMAY
ΔvWbl-D	GTAAAATGAATTCAATAGCAAATTGATTATATACTAAAAC C	Cloning of the *vWbl* deletion cassette into pIMAY
ΔvWbl-Sc. F	AATACATATCTCTATGTTCATGAATTGAGG	Screening for the *vWbl* deletion
ΔvWbl-Sc. R	CAAAATCTATCTCAACTAATTCAACAATACC	Screening for the *vWbl* deletion
ΔisdG-A	GTATTGCGAGCTCAAGATAATAAGACTTATTTAC	Cloning of the *isdG* deletion cassette into pIMAY
ΔisdG-B	CATTGCTACATGCTCCTTTTCTATTTTAATTC	Cloning of the *isdG* deletion cassette into pIMAY
ΔisdG-C	AGGAGCATGTAGCAATGTAAAGTGAATCAGATTGCTTT GAAATTTA	Cloning of the *isdG* deletion cassette into pIMAY
ΔisdG-D	GGATTGTTAACTTGCTGAATTCGTGCCTTAGAC	Cloning of the *isdG* deletion cassette into pIMAY
ΔisdG-Sc. F	GAGGCGGACACAACAAATGAAATTAG	Screening for the *isdG* deletion
ΔIsdG-Sc. R	AAATGCTGCAGTTGTTTGATACATTTTACC	Screening for the *isdG* deletion
ΔSLUSH-A	ACTGAGCTCTGCTGGCAATGCATTAAC	Cloning of the *slush* locus deletion cassette into pIMAY
ΔSLUSH-B	CATTGTAGTTACCTCCTTTATTGTGTGCCTC	Cloning of the *slush* locus deletion cassette into pIMAY
ΔSLUSH-C	TAAAGGAGGTAACTACAATGTAATATAATGTTCTAAATC TTTGAAAGACC	Cloning of the *slush* locus deletion cassette into pIMAY
ΔSLUSH-D	GATGAATTCATACAGACTGGCAACGTTCC	Cloning of the *slush* locus deletion cassette into pIMAY
ΔSLUSH-Sc. F	CTGAATTTCAAATGATTCAATTTATTCC	Screening for the *slush* locus deletion
ΔSLUSH-Sc. R	GATGACATACGCTATGAAATATGATGC	Screening for the *slush* locus deletion

Table 2.2 Oligonucleotides used in this thesis, continued

SLUSH-Rev.-E	CGCTCCTTTTTAGGATCCTTGTTAAAGTCTC	Construction of the *slush* locus reversion cassette with a novel BamHI restriction site
SLUSH-Rev.-F	GAGACTTTAACAAGGATCCTAAAAAGGAGCG	Construction of the *slush* locus reversion cassette with a novel BamHI restriction site
ΔatlI-A	CGTTATCGAGCTCTGAAGATGCGTATAG	Cloning of the *atlI* deletion cassette into pIMAY
ΔatlI-B	CACTTATTTACCTCCATCAATTCTCTATTCC	Cloning of the *atlI* deletion cassette into pIMAY
ΔatlI-C	TGATGGAGGTAAATAAGTGTAAGAAGCATTGTGAATGC	Cloning of the *atlI* deletion cassette into pIMAY
ΔatlI-D	CGATTGAATTCGACGTACCTTATTTCTTC	Cloning of the *atlI* autolysin deletion cassette into pIMAY
ΔatlI-Sc. F	CTATGACAAATTTTTAAAAGAAACGATGC	Screening for the *atlI* deletion
ΔatlI-Sc. R	ATTAGTCTAGTGGGAAATATTAGCTTCG	Screening for the *atl* deletion
Δisd-loc.-A	TTCAGGATTGGAGCTCGATATTACCGTTAAG	Cloning of the deletion cassette for the complete *isd* locus into pIMAY
Δisd-loc.-B	TAAATAAAGCACTGAAAGATACCACCGC	Cloning of the deletion cassette for the complete *isd* locus into pIMAY
Δisd-loc.-C	GGTATCTTTCAGTGCTTTATTTATAAGAAGCATTGTGAATGCAAG	Cloning of the deletion cassette for the complete *isd* locus into pIMAY
Δisd-loc.-D	CGATTGAATTCGACGTACCTTATTTCTTC	Cloning of the deletion cassette for the complete *isd* locus into pIMAY
Δisd-loc.-Sc. F	GGCAATAGTAATCCTAAATTGAAGC	Screening for the *isd* locus deletion
Δisd-loc.-Sc. R	ATTAGTCTAGTGGGAAATATTAGCTTCG	Screening for the *isd* locus deletion
ΔisdJ-A	AACTGAGCTCACCACATTAGCAATTAAA	Cloning of the *isdJ* deletion cassette into pIMAY
ΔisdJ-B	TACATGTGTTTGTCTCCTTGTATCAATAT	Cloning of the *isdJ* deletion cassette into pIMAY
ΔisdJ-C	CAAGGAGACAAACACATGTAATATCGCCCAAATAATTAAA	Cloning of the *isdJ* deletion cassette into pIMAY
ΔisdJ-D	AAGAAGAATTCCGCTTAAGTGACGAG	Cloning of the *isdJ* deletion cassette into pIMAY
ΔisdJ-Sc. F	AAATTTTTTCTTAATTTTTTAAGGC	Screening for the *isdJ* deletion
ΔisdJ-Sc. R	TCAGTTATTTGCTGAAGATTTAGAAGA	Screening for the *isdJ* deletion
ΔisdB-A	TTTTTGAGCTCTAGCAATTAACAACATAATTG	Cloning of the *isdB* deletion cassette into pIMAY
ΔisdB-B	TACATGGTTTTAACAACTCCCAATTTATTT	Cloning of the *isdB* deletion cassette into pIMAY

Table 2.2 Oligonucleotides used in this thesis, continued

ΔisdB-C	GAGTTGTTAAAACCATGTAAATAAAGCACTGAAAGATACC	Cloning of the *isdB* deletion cassette into pIMAY
ΔisdB-D	GATGAGAATTCTGTCAATGTTTTAAAGATG	Cloning of the *isdB* deletion cassette into pIMAY
ΔisdB-Sc. F	TAATAAGACATAAAATAGTTAGCGCTC	Screening for the *isdB*-deletion
ΔisdB-Sc. R	TAAAAAATCTTTGCCTATGGC	Screening for the *isdB*-deletion
ΔisdC-A	AGGGAACAAAAGCTGGGTACCCCATGTCATTTTACAACAAGG	SLIC cloning of the *isdC* deletion cassette into pIMAY
ΔisdC-B	CACGCTTATTTTGCCTCCTT	SLIC cloning of the *isdC* deletion cassette into pIMAY
ΔisdC-C	GCAAAATAAGCGTGTAATAATGTCTAAGCGTTTG	SLIC cloning of the *isdC* deletion cassette into pIMAY
ΔisdC-D	**CACTATAGGGCGAATTGGAGCTC**CTGTTGATGGTGTAATATTG	SLIC cloning of the *isdC* deletion cassette into pIMAY
isdC-Rev.-E	GATTTATTTATTCCCGGGGTTGCTGC	Construction of the *isdC* reversion cassette with a novel SmaI restriction site
isdC-Rev.-F	GCAGCAACCCCGGGAATAAATAAATC	Construction of the *isdC* reversion cassette with a novel SmaI restriction site
ΔisdC Sc. F	GAGTAGTGTGTAAGTCATGTGG	Screening for the *isdC*-deletion
ΔisdC Sc. R	TTTACGTACATAAAAATTAACTGC	Screening for the *isdC*-deletion
ΔrecA-A	ATTTTGAGCTCTAACATGAAATTAATATAAGTTTACC	Cloning of the *recA* deletion cassette into pIMAY
ΔrecA-B	CCTAAAGCATTATCTAATGTCACTGATCC	Cloning of the *recA* deletion cassette into pIMAY
ΔrecA-C	CATTAGATAATGCTTTAGGCTAAAAGAAAATCCAGAAGTAAGAG	Cloning of the *recA* deletion cassette into pIMAY
ΔrecA-D	ACAAACGAATTCTACTTTTTTAGTTGTGT	Cloning of the *recA* deletion cassette into pIMAY
ΔrecA-Sc. F	GGTTCTGATGATATTCTTATAGAAGAAGC	Screening for the *recA* deletion
ΔrecA-Sc. R	ATCTAAATTTTCCTCTTTTTGAAGAAGTC	Screening for the *recA* deletion
ΔsrtA-A	**CTAAAGGGAACAAAAGCTGGGTACC**TCATCTTTAGCAATTTGCATTAG	SLIC cloning of the *srtA* deletion cassette into pIMAY
ΔsrtA-B	CATGCAGTATTTCTCCTTTAAACCGTAAAA	SLIC cloning of the *srtA* deletion cassette into pIMAY

Table 2.2 Oligonucleotides used in this thesis, continued

ΔsrtA-C	AAAGGAGAAATACTGCATGTAATTGTAGAACACTTTGATCCG	SLIC cloning of the *srtA* deletion cassette into pIMAY
ΔsrtA-D	**CACTATAGGGCGAATTGGAGCTC**CTTTATCTTGCTCAGGTGCAG	SLIC cloning of the *srtA* deletion cassette into pIMAY
srtA Rev.-E	GGTGTTGCTGGTCCCGGGTAAACAGGTTC	SLIC cloning of the *srtA* reversion cassette with novel SmaI site into pIMAY
srtA Rev.-F	GAACCTGTTTACCCGGGACCAGCAACACC	SLIC cloning of the *srtA* reversion cassette with novel SmaI site into pIMAY
ΔsrtA-Sc.-F	CCTGCATGAATAAAACCAATTTTTTCGTG	Screening for the *srtA* deletion
ΔsrtA-Sc.-R	GATTTTGCTCTTTCTGTGGTGCTACGTGC	Screening for the *srtA* deletion
ΔsrtB-A	**AGGGAACAAAAGCTGGGTACC**GCAAAGATAGTGTCGTGAA	SLIC cloning of the *srtB* deletion cassette into pIMAY
ΔsrtB-B	CATTTGTTGTGTCCGCCTCG	SLIC cloning of the *srtB* deletion cassette into pIMAY
ΔsrtB-C	GCGGACACAACAAATGTAGAAAAGGAGCATGTAGC	SLIC cloning of the *srtB* deletion cassette into pIMAY
ΔsrtB-D	**ATAGGGCGAATTGGAGCTC**CATCGCATAGGAACTTAGTGG	SLIC cloning of the *srtB* deletion cassette into pIMAY
ΔsrtB Sc.-F	GTCGCTAATCGCTGAGCTAACGC	Screening for the *srtB* deletion
ΔsrtB Sc.-R	ATCCTCATCTTGCTTATGTACC	Screening for the *srtB* deletion
ΔdltA-A	**AGGGAACAAAAGCTGGGTACC**TAGCCATTAAATTATGATAC	SLIC cloning of the *dltA* deletion cassette into pIMAY
ΔdltA-B	CATATGTTATATTCTCCCTCATT	SLIC cloning of the *dltA* deletion cassette into pIMAY
ΔdltA-C	GGGAGAATATAACATATGTGATTCCATATGGTACGTTTAC	SLIC cloning of the *dltA* deletion cassette into pIMAY
ΔdltA-D	**ATAGGGCGAATTGGAGCTC**GAAATAAATTGCATTAACTTG	SLIC cloning of the *dltA* deletion cassette into pIMAY
ΔdltA Sc.-F	CGTTGATAATATCGTGGCTG	Screening for the *dltA* deletion
ΔdltA Sc.-R	GTCGATTGGACCAGATGATAC	Screening for the *dltA* deletion

Table 2.2 Oligonucleotides used in this thesis, continued

ΔtagO-A	**AGGGAACAAAAGCTGGGTACC**AAAATTCATCGTTATATGATG	SLIC cloning of the *tagO* deletion cassette into pIMAY
ΔtagO-B	CATCCGTTCACCTTCAATAGAT	SLIC cloning of the *tagO* deletion cassette into pIMAY
ΔtagO-C	CTATTGAAGGTGAACGGATGTAAAAAATAAGCTATTCAGCC	SLIC cloning of the *tagO* deletion cassette into pIMAY
ΔtagO-D	**ATAGGGCGAATTGGAGCTC**TCAAAAAGCAAATGATGATG	SLIC cloning of the *tagO* deletion cassette into pIMAY
ΔtagO Sc.-F	ACGTCCTAAAAACAACAATGG	Screening for the *tagO* deletion
ΔtagO Sc.-R	CACATCATTGTTCTGCCTATACA	Screening for the *tagO* deletion
ΔtagE1-A	**AGGGAACAAAAGCTGGGTACC**CGTACAACGATTGTAATCGCTC	SLIC cloning of the *tagE1* deletion cassette into pIMAY
ΔtagE1-B	CACATAATCTCCTCCAATATATC	SLIC cloning of the *tagE1* deletion cassette into pIMAY
ΔtagE1-C	ATATTGGAGGAGATTATGTGTAAAGTAAAATGGAGCGAAACA	SLIC cloning of the *tagE1* deletion cassette into pIMAY
ΔtagE1-D	**ATAGGGCGAATTGGAGCTC**TTAATAATAGCTGTTCTGAAT	SLIC cloning of the *tagE1* deletion cassette into pIMAY
ΔtagE1 Sc.-F	ACGAAGCCACAGCAAATCTA	Screening for the *tagE1* deletion
ΔtagE1 Sc.-R	AACTTTCATTGAATCTAATGTGATG	Screening for the *tagE1* deletion
ΔtagN-A	**AGGGAACAAAAGCTGGGTACC**ACGCATCAAGAACGTAATATAG	SLIC cloning of the *tagN* deletion cassette into pIMAY
ΔtagN-B	CATATTAATTTTTCCTTTCTAAGTTG	SLIC cloning of the *tagN* deletion cassette into pIMAY
ΔtagN-C	AGAAAGGAAAAATTAATATGTAGTTGAAGAGAGATCTGAG	SLIC cloning of the *tagN* deletion cassette into pIMAY
ΔtagN-D	**ATAGGGCGAATTGGAGCTC**CTATAATGTGCCAACGTCTTG	SLIC cloning of the *tagN* deletion cassette into pIMAY
ΔtagN Sc.-F	TCTTTATAGGACCATCGTGTGG	Screening for the *tagN* deletion
ΔtagN Sc.-R	CCATTGTCTCCATATGCTATTCAAA	Screening for the *tagN* deletion

Table 2.2 Oligonucleotides used in this thesis, continued

slsD-A	AAAGGAGCTCCCAGGTCAACAGCCTAAA	Reversion of the nonsense mutation in N920143
slsD-B	CATCTTTTATAGGCGTTTGTTGGATTGATGG	Reversion of the nonsense mutation in N920143
slsD-C	CCATCAATCCAACAAACGCCTATAAAAGATG	Reversion of the nonsense mutation in N920143
slsD-D	CATTTAAAGAATTCTCTTTACTAACGACGTTCCC	Reversion of the nonsense mutation in N920143
Investigation of the *isd* duplication		
Isd_dupl.-F	GGATAAGTACCCAAATACTAACACTGTTGAC	Screening primer directed against the boundaries of the duplication
Isd_dupl.-R	TACAATGCTTAACTGTAAAATAATTGGAATATACC	Screening primer directed against the boundaries of the duplication
Prb-F.	AATATCTTCCACATAACAACCTCC	Amplification of the probe for Southern blotting
Prb-R.	TTTTAGAAGGTGAAGGTGCC	Amplification of the probe for Southern blotting
tet-int.A	ATTTTTTCAGAGCTCATGGCTTTCGTTAAGATG	Cloning of the *tet* integration cassette
tet-int.B	AAGCTTATTGAAAACCCCGTTGACACTCATC	Cloning of the *tet* integration cassette
tet-int.C	ACGGGGTTTTCAATAAGCTTATGTTTTGTTAGTGTTATG TG	Cloning of the *tet* integration cassette
tet-int.D	ATATAACGGGTACCTTTGAAACACCATTGC	Cloning of the *tet* integration cassette
tet-F.	GTCAACGGGGTTTTCAATGGGGAAAGCTTCACAGAA	Amplification of *tet* from pT181
tet-R.	CATAACACTAACAAAACATCGCTGTTAAAGCTTTTTTATT AC	Amplification of *tet* from pT181
tet-int Sc.-F	CCCATTCATCATGCTTAGTATTGCTG	Screening for *tet*-integration
tet-int Sc.-R	CGTATTCCTTTTTATGAATGCCG	Screening for *tet*-integration
qPCR primers for determination of the *isd* copy number		
IsdJ-F	CGGCTTCAATTATCGTTGGT	Determination of *isd* copy number
IsdJ-R	TGTGGCAGCTTGATTTTGAG	Determination of *isd* copy number
Ori-F	TCCCGTAACTGTTATCGTCAAA	Determination of *isd* copy number
Ori-R	TCGAGCAACTTATCCACACAA	Determination of *isd* copy number

Table 2.2 Oligonucleotides used in this thesis, continued

Construction of the phage integrase vector pIPI03		
ccrB-F	**GATAGGCCTAATGACTGGCTTTTATAA**AGGAGGTGAAACAATGAAAGTAG	SLIC cloning of the ϕSL01 integrase and *attP* in pIMAY downstream of *cat*
attP-R	**AAAAAGTACAGTCGGCATTATCTCATA**GCATGCATATAATTTTTTAAATG	SLIC cloning of the ϕSL01 integrase and *attP* in pIMAY downstream of *cat*
pSL1 attB Sc.-F (scr.F)	CCCTTTATCTGCAGTTATCTTAATTTTATATGGC	Screening for pIPI03 integration into the chromosome of HKU09-01
pSL1 attB Sc.-R (scr. R)	GACCAAAAAGCAAAACCGGTACCC	Screening for pIPI03 integration into the chromosome of HKU09-01
Miscellaneous purposes		
SlsD stop-F	ATTAGAATCTATGAGGTCAATCCAGATGG	Investigation of the conserved nonsense mutation in *slsD*
SlsD stop-R	ACAGATGTTCCATTTTGGCCATCTTTACC	Investigation of the conserved nonsense mutation in *slsD*
atlI_pR-F	**ATTAAAATAAGCTTGATGGTACC**AGGAGGTAAATAAGTGAGCAGAAAT	SLIC cloning of the Isd autolysine *atlI* in pRMC2
atlI_pR-R	**GACGTTGTAAAACGACGGCCAGTGAATTC**TTAAGGTTGAATATATTGTAATG	SLIC cloning of the Isd autolysine *atlI* in pRMC2
Amplification of the plasmid backbone for SLIC cloning purposes		
pRMC2-SLIC-F	GGTACCATCAAGCTTATTTTAATTATACT	Amplification of the pRMC2 backbone for cloning into the MCS between KpnI and EcoRI
pRMC2-SLIC-R	GAATTCACTGGCCGTCGTTTTACAACGTC	Amplification of the pRMC2 backbone for cloning into the MCS between KpnI and EcoRI
pIMAY-SLIC-F	GGTACCCAGCTTTTGTTCCCTTTAGTGAGG	Amplification of the pIMAY/pIMAYZ backbone for cloning into the MCS between KpnI and SacI
pIMAY-SLIC-R	GAGCTCCAATTCGCCCTATAGTGAGTCG	Amplification of the pIMAY/pIMAYZ backbone for cloning into the MCS between KpnI and SacI

Table 2.2 Oligonucleotides used in this thesis, continued

pIMAY-SLICcat-F	TTATAAAAGCCAGTCATTAGGCCTATCTGAC	Amplification of the pIMAY/pIMAYZ backbone for cloning downstream of the chloramphenicol resistance gene
pIMAY-SLICcat-R	TATGAGATAATGCCGACTGTACTTTTTACAG	Amplification of the pIMAY/pIMAYZ backbone for cloning downstream of the chloramphenicol resistance gene

* Restriction sites are underlined
** Sequences with homology to vector sequences for SLIC purposes are shown in bold

harvested by centrifugation (5 min, 4000 x g at 4°C) resuspended in 4 ml ice-cold TFB1 (100 mM RbCl, 50 mM $MnCl_2$, 30 mM potassium acetate, 10 mM $CaCl_2$, 15% glycerol, pH 5.8) and incubated on ice for 90 min. The cells were collected by centrifugation (5 min, 4000 x g at 4°C), resuspended in 4 ml ice-cold TFB2 (10 mM MOPS, 10 mM RbCl, 75 mM $CaCl_2$, 15% glycerol, adjusted to pH 6.8 with KOH) and 200 µl aliquots were stored at -80°C. Prior to use an aliquot of cells was thawed on ice for 10 min. Depending on the DNA concentration, 1-20 µl of the ligation mixture was added to 50 µl of competent cells and the mixture was incubated for 15 min on ice. Afterwards the cells were heat-shocked for 90 sec at 42°C. 950 µl of LB was added and the cells were incubated for 30 min at 37°C with agitation to allow the expression of the plasmid-encoded antibiotic resistance. Afterwards cells were plated on agar plates containing the appropriate antibiotic.

2.4.2 Transformation of *S. lugdunensis*

Electrocompetent *S. lugdunensis* cells were prepared according to a protocol described for *S. carnosus* (Löfblom *et al.*, 2007) with only minor differences. In brief, 50 ml TSB was inoculated with a fresh overnight culture to an OD_{578} = 0.5 and incubated with agitation at 37°C for 1 h. Cells were harvested (10 min at 4000 x g at 4°C), washed twice with 50 ml of ice-cold distilled H_2O and finally with 50 ml ice-cold 10% glycerol (adjusted to pH 7). Cells were taken up in 250 µl 10% glycerol (pH 7) and 70 µl aliquots were stored at -80°C or used directly. Prior to transformation an aliquot was thawed on ice and centrifuged for 10 min at 9000 x g. The pellet was taken up in 60 µl of 0.5 M sucrose, 10% glycerol (no pH adjustment). 1-5 µg of DNA was added (in up to 10 µl H_2O) and the mixture was incubated for 10 min at room temperature. The electroporation was carried out in 0.1 cm cuvettes (Bio-Rad) at 2.1 kV, 100 Ω and 25 µF. Immediately after electroporation 950 µl TSB with 0.5 M sucrose was added and the cells were incubated with shaking for 2 h before plating on TSA containing the appropriate antibiotic.

2.4.3 Transformation of *Lactococcus lactis*

L. lactis competent cells were prepared as described previously (Monk *et al.*, 2010). The method uses medium containing glycine to weaken the cell wall of *L. lactis*. In brief, an overnight culture of *L. lactis* NZ9000 was grown statically

at 30°C in GM17 (M17-medium, 200 mM sucrose, 25 mM glucose) and used to inoculate (1:100) a second GS-GM17 (M17 medium, 200 mM sucrose, 25 mM glucose, 300 mM glycine) overnight culture. 5 ml of the second culture was used to inoculate the third overnight culture of 50 ml GS-GM17. After incubation overnight at 30°C, 400 ml GS-GM17 were inoculated with 50 ml of the third overnight culture and grown for 3 h statically at 30°C. The cells were harvested (4000 x g for 20 min at 4°C) The pellet was washed with 200 ml, 100 ml and 50 ml ice-cold SGWB (0.5 M sucrose, 10% glycerol) with 15 min incubation on ice between every washing step. The cells were resuspended in 2 ml SGWB and 40 µl aliquots were stored at - 80°C.

Electroporation was carried out using 0.1 cm cuvettes (Bio-Rad) at 2.0 kV, 200 Ω and 25 µF. Cells were regenerated in 1 ml GM17 containing 20 mM $MgCl_2$ and 2 mM $CaCl_2$ for 2 h at 30°C. Dilutions were plated on GM17 agar containing the appropriate antibiotic.

2.5 Vector construction

2.5.1 Construction of pIMAY deletion cassettes

Construction of cassettes for the generation of deletion mutations was carried out as described previously (Monk *et al.*, 2012). In brief, A and B primer combinations (Table 2.2) were used for each construct to amplify a 500 bp fragment located upstream of the target gene sequence (including the start codon). Primers C and D were used to amplify a 500 bp fragment downstream from the target gene (including the stop codon). The PCR products were used as templates for spliced overlap extension (SOE) PCR using primers A and D. SOE PCRs use ~15 nucleotide identity between the primers B and C to allow the fusion and amplification of the AB and CD templates, resulting 1 kb deletion fragment. The fragment was gel-purified, cleaved at endonuclease cleavage sites introduced in forward and reverse primers (A and D) and cloned into pIMAY treated with the same endonucleases. Successful cloning was confirmed by restriction digest and DNA sequencing. This method was used for the construction of all deletion plasmids which are summarised later in this chapter in Table 2.3.

2.5.2 Construction of pIMAY variants for the reversion of deletion mutations

The program SILENT [emboss.bioinformatics.nl/cgi-bin/emboss/silent] was used to identify single nucleotides within the target gene that can be mutated to create novel restriction sites without causing translational changes in the protein. For the reversion of *srtA* primers E and F were synthesized, exchanging nucleotide 252 of *srtA* (T to G) thereby creating a novel SmaI restriction site. For the complementation of the *slush* locus, primers E and F were designed to create a novel BamHI site in the non-coding region between *slush-A* and *slush-B2.* For the complementation of the *isdC* mutation primers E and F exchanged nucleotide 459 of *isdC* (A to C) creating a novel SmaI site.

Primer A and E were used to amplify the upstream sequence and the 5'-fragment of the gene to be complemented, and primers F and D were used to amplify the downstream region together with 3'-fragment of the gene to be complemented. PCR products were gel-purified and used for the SOE PCR using primers A and D. The complementation cassette was gel-purified, cleaved at endonuclease cleavage sites introduced in primers A and D and cloned into pIMAY treated with the same endonucleases. The success of the cloning was confirmed by restriction digests and DNA sequencing.

2.5.3 Construction of pIMAY cassette to reverse the nonsense mutation in *slsD* of N920143

For the construction of the *slsD*-reversion plasmid, AB and CD primer combinations were used to amplify a 500 bp fragment upstream and a 500 bp fragment downstream of the nonsense mutation in *slsD.* Primers B and C covered the sequence of the nonsense mutation and possessed a single nucleotide exchange (taa-caa) to change the ochre stop codon to a glutamine codon as found in related strains expressing surface-anchored SlsD. The AB and CD fragments were gel-purified and used for SOE PCR using primers A and D. The resulting 1 kb fragment was gel-purified, cleaved at endonuclease cleavage sites (introduced in primers A and D) and cloned into pIMAY treated with the same endonucleases. The success of the cloning was confirmed by restriction digests and DNA sequencing.

2.5.4 Construction of the pIMAY:*tet* integration cassette

Two 500 bp fragments, one upstream and one downstream of the chosen insertion site were PCR-amplified using the primer combinations tet-int.A / tet-int.B and tet-int.C / tet-int.D, respectively (Table 2.2). The two fragments were fused together using SOE PCR resulting in a single 1 kb fragment. A novel HindIII restriction site (inserted in primers B and C) was thereby introduced between the fragments AB and CD. The recombinant fragment was cloned into the SacI / KpnI sites of the multiple cloning site (MCS) of pBluescript. The 2.3 kb *tet* fragment of pT181 was PCR-amplified (primers tet-F. / tet-R.) harbouring a HindIII site at both ends. The fragment was subsequently cloned into HindIII cleaved pBluscript:AB/CD. The resulting integration cassette AB-*tet*-CD was excised from pBluescript using the restriction endonucleases NotI and AatLI and cloned into pIMAY treated with the same endonucleases.

2.5.5 Construction of pRMC2:*atlI*

The DNA fragment encoding *atlI* was amplified from *S. lugdunensis* N920143 chromosomal DNA using the primers atlI_pR-F and atlI_pR-R (Table 2.2). The PCR product was purified and SLIC-cloned into pRMC2. The vector was amplified as described in paragraph 2.3.6. The success of the cloning was confirmed by restriction digestion and DNA sequencing.

2.6 Allelic exchange in *S. lugdunensis*

The protocol described by Monk *et. al.* (Monk *et al.*, 2012) was used successfully in *S. lugdunensis*. *S. lugdunensis* was transformed with recombinant plasmids, plated on TSA containing 10 µg/ml chloramphenicol (TSA_{cm10}) and incubated at 28°C. Clones with integrated plasmids were selected by growth on TSA_{cm10} at 37°C and loss of replicating plasmid and was confirmed by PCR as described (Monk *et al.*, 2012). Although the *secY* genes of *S. aureus* and *S. lugdunensis* are similar (the 561 nucleotide *secY* antisense fragment derived from *S. aureus* RN4220 in pIMAY shares 81.3% identity with the *S. lugdunensis* N920143 *secY*), anhydrotetracycline-induction of *secY* antisense RNA did not result in selection of colonies lacking the plasmid. In order to detect plasmid loss, clones with an integrated plasmid were grown for

18 h in TSB at 28°C, sub-cultured (1 : 1000) in fresh TSB and grown at 28°C for 18 h. The culture was plated out on TSA and incubated at 37°C. Colonies were patched on TSA and TSA_{cm10} and Cm^S clones were screened by colony PCR for the presence of the mutant allele.

The plasmid pIMAYZ carries a constitutively expressed *lacZ* gene (encoding β-galactosidase) and allows a more efficient way to screen for the loss of plasmid (Monk *et al.*, unpublished). Several mutants created in this thesis were created using this novel plasmid. The transformation procedure and integration of plasmid into chromosome did not differ between pIMAY and pIMAYZ. However, using pIMAYZ, clones with an integrated plasmid were grown for 18 h in TSB at 28°C and subsequently dilutions were plated on TSA containing 100 µg/ml 5-Brom-4-chlor-3-indoxyl-β-D-galactopyranosid (X-GAL) (Melford Laboratories Ltd). Blue and white colonies could be identified after 24 h of incubation at 37°C. White colonies (indicating loss of pIMAYZ) were screened for the mutant allele and plasmid loss was confirmed by verifying chloramphenicol sensitivity.

Allelic change allows the exchange of plasmid- and chromosome-based genetic elements. This technique was used for all genetic manipulations described within this thesis. The protocol was used for the creation of the all deletion mutations, for the chromosomal reversion of deletion mutations, for the integration of *tet* into the duplicated region of HKU09-01 and for the reversion of the nonsense mutation in *slsD* of N920143. The strains are summarized in Table 2.3.

2.7 The phage integrase vector pIPI03

2.7.1 Construction of pIPI03

The integrase gene *ccrB* of phage ϕSL01 (see Chapter 3) together with the corresponding attachment site could only be amplified from the circular phage genome and not from the linearized genome of the lysogenic phage. For amplification of *ccrB* and the corresponding attachment site (*attB*) *S. lugdunensis* N920143 was grown to exponential phase and induced for 1 h with 1 µg/ml mitomycin C. Cells were harvested, chromosomal DNA was extracted and used as template for the PCR using the primers ccrB-F / attP-R

Table 2.3 Bacterial strains and plasmids

Strain / Plasmid	Description	Reference
Staphylococci		
S. lugdunensis N920143	Human clinical isolate, genome sequenced, CC1	NRC[a], this study
S. lugdunensis N920143 Δ*hsdR*	Deletion of *hsdR* encoding the SluI restriction subunit HsdR	This study
S. lugdunensis N920143 Δ*fbl*	Deletion of *fbl*	This study
S. lugdunensis N920143 Δ*fbl* / *slsD*+	Deletion of *fbl,* nonsense mutation in *slsD* was restored to a sense codon (TAA-CAA)	This study
S. lugdunensis N920143 Δ*vWbl*	Deletion of *vWbl*	This study
S. lugdunensis N920143 Δ*srtA*	Deletion of *srtA*	This study
S. lugdunensis N920143 Δ*srtA-R*	Reverted *srtA* deletion with novel SmaI site	This study
S. lugdunensis N920143 Δ*isdG*	Deletion of *isdG*	This study
S. lugdunensis N920143 Δ*atlI*	Deletion of the *isd* autolysin *atlI*	This study
S. lugdunensis N920143 Δ*srtB*	Deletion of *srtB*	This study
S. lugdunensis N920143 Δ*isdC-R*	Reverted *srtA* deletion with novel SmaI site	This study
S. lugdunensis N920143 Δ*isdB*	Deletion of *isdB*	This study
S. lugdunensis N920143 Δ*isdJ*	Deletion of *isdJ*	This study
S. lugdunensis N920143 Δ*tagO*	Deletion of *tagO*	This study
S. lugdunensis N920143 Δ*tagN*	Deletion of *tagN*	This study
S. lugdunensis N920143 Δ*tagE1*	Deletion of *tagE1*	This study
S. lugdunensis N920143 Δ*dltA*	Deletion of *dltA*	This study
S. lugdunensis N920143 Δ*tagN* / Δ*tagE1*	Double mutant of Δ*tagN and* Δ*tagE1*	This study
S. lugdunensis N920143 Δ*tagN* / Δ*tagE1* / Δ*dltA*	Triple mutant of Δ*tagN,* Δ*tagE1and dltA*	This study
S. lugdunensis HKU09-01[b]	Clinical isolate, genome sequenced to completion, CC1, duplication of the *isd* locus	(Tse *et al.*, 2010)
S. lugdunensis HKU09-01 Δ*recA*[b]	Deletion of *recA*	This study

Table 2.3 Bacterial strains and plasmids

Strain / Plasmid	Description	Reference
S. lugdunensis HKU09-01 Δ*slush*	Deletion of the entire *slush* locus	This study
S. lugdunensis HKU09-01 Δ*slush-R*	Reverted *slush* deletion with novel BamHI site	This study
S. lugdunensis HKU:tet	Tetracycline resistance determinant integrated into the duplicated region	This study
S. lugdunensis HKU(R)-Δisd[b]	Tetracycline resistance determinant integrated, no duplication of the *isd* region, deletion of the entire *isd* locus, deletion of *recA*	This study
S. lugdunensis HKU(R)-Δdup[b]	Tetracycline resistance determinant integrated, no duplication of the *isd* region, deletion of *recA*	This study
S. lugdunensis HKU(R)-WT[b]	Tetracycline resistance determinant integrated, duplication of the *isd* locus, deletion of *recA*	This study
S. lugdunensis HKU(R)-Y1	Tetracycline resistance determinant integrated, amplification of the *isd* locus (5 copies), deletion of *recA*	This study
S. lugdunensis HKU(R)-X1[b]	Tetracycline resistance determinant integrated, amplification of the *isd* locus (5 copies), deletion of *recA*	This study
S. lugdunensis HKU(R)-Z1	Tetracycline resistance determinant integrated, amplification of the *isd* locus (5 copies), deletion of *recA*	This study
S. lugdunensis HKU(R)-K4	Tetracycline resistance determinant integrated, amplification of the *isd* locus (5 copies), deletion of *recA*	This study
S. lugdunensis HKU(R)-K4-2	Tetracycline resistance determinant integrated, amplification of the *isd* locus (4 copies), deletion of *recA*	This study
S. lugdunensis N910319	Clinical isolate	NRC[a]
S. lugdunensis N910320	Clinical isolate	NRC[a]
S. lugdunensis N930432	Clinical isolate	NRC[a]
S. lugdunensis N930432 Δ*fbl*	Deletion of *fbl*	This study
S. lugdunensis N940025	Clinical isolate	NRC[a]

Table 2.3 Bacterial strains and plasmids

Strain / Plasmid	Description	Reference
S. lugdunensis N940025 Δ*isd*	Deletion of the entire *isd* locus	This study
S. lugdunensis N940025 Δ*srtA*	Deletion of *srtA*	This study
S. lugdunensis N940084	Clinical isolate	NRC[a]
S. lugdunensis N940113	Clinical isolate	NRC[a]
S. lugdunensis N940113 Δ*isdC*	Deletion of *isdC*	This study
S. lugdunensis N940135	Clinical isolate	NRC[a]
S. lugdunensis N940164	Clinical isolate	NRC[a]
S. lugdunensis N950646	Clinical isolate	NRC[a]
S. lugdunensis SL2	Clinical isolate CC2	(Chassaîn *et al.*, 2012)
S. lugdunensis SL9	Clinical isolate CC5	(Chassaîn *et al.*, 2012)
S. lugdunensis SL13	Clinical isolate CC1	(Chassaîn *et al.*, 2012)
S. lugdunensis SL27	Clinical isolate CC4	(Chassaîn *et al.*, 2012)
S. lugdunensis SL37	Clinical isolate CC3	(Chassaîn *et al.*, 2012)
S. lugdunensis SL57	Clinical isolate CC3	(Chassaîn *et al.*, 2012)
S. lugdunensis SL62	Clinical isolate CC4	(Chassaîn *et al.*, 2012)
S. lugdunensis SL71	Clinical isolate CC2	(Chassaîn *et al.*, 2012)
S. lugdunensis SL72	Clinical isolate CC1	(Chassaîn *et al.*, 2012)
S. lugdunensis SL81	Clinical isolate CC5	(Chassaîn *et al.*, 2012)
S. aureus Newman	Human clinical isolate, MSSA, genome sequenced	(Baba *et al.*, 2008)
S. aureus COL	Human clinical isolate, MRSA, genome sequenced	(Gill *et al.*, 2005)
E. coli		
DH10B	*dam* $^{+}$ *dcm* $^{+}$ Δ*hsdRMS endA1 recA1 high efficiency cloning strain*	Invitrogen
Topp3	Non K-12 strain for protein expression	Stratagene
XL1-blue	*dam* $^{+}$ *dcm*$^{+}$ *cloning strain*	Stratagene
DC10B	*dcm* $^{-}$ in the DH10B background	(Monk *et al.*, 2012)

Table 2.3 Bacterial strains and plasmids

Strain / Plasmid	Description	Reference
SL01B	*S. lugdunensis* (CC1) *hsdM/S* genes expressed in the DC10B background	This study, constructed by I. Monk
L. lactis		
NZ9000	Nisin responsive *L. lactis* MG1363 derivative	(Mierau & Kleerebezem, 2005)
Deletion and reversion plasmids		
pIMAY	Thermosensitive vector for allelic exchange	(Monk *et al.*, 2012)
pIMAYZ	pIMAY encoding *lacZ* in a transcriptional fusion with the *cat* gene	(Monk *et. al* unpublished)
pIMAY:Δ*hsdR*	A deletion encompassing the entire *fbl* gene (from ATG to TAA codons) amplified from N920143	This study
pIMAY:Δ*fbl*	A deletion encompassing the entire *fbl* gene (from ATG to TAA codons) amplified from N920143	This study
pIMAY:Δ*vWbl*	A deletion encompassing the entire *vwbl* gene (from ATG to TAA codons) amplified from N920143	This study
pIMAY:Δ*srtA*	A deletion encompassing the entire *srtA* gene (from ATG to TAA codons) amplified from N920143	This study
pIMAY:*srtA-R*	A reversion fragment containing the entire *srtA* gene with a novel SmaI restriction site amplified from N920143	This study
pIMAY;Δ*srtB*	A deletion encompassing the entire *srtB* gene (from ATG to TAA codons) amplified from N920143	This study
pIMAY:Δ*slush*	A deletion encompassing the entire *slush* operon (from ATG of *orfX* to TAA of *slushC*) amplified from N920143	This study
pIMAY:Δ*slush-R*	A reversion fragment encompassing the entire *slush* operon (from ATG of *orfX* to TAA of *slushB2*) amplified from HKU09-01 with a novel BamHI site	This study

Table 2.3 Bacterial strains and plasmids

Strain / Plasmid	Description	Reference
pIMAY:*tet*	Fragment to insert the tetracycline resistance determinant into the duplicated region in HKU09-01	This study
pIMAY:Δ*isd*	A deletion encompassing the entire *isd* operon (from TAA of *atlI* to TAA of *isdB*) amplified from N920143	This study
pIMAY:Δ*isdB*	A deletion encompassing the entire *isdB* gene (from ATG to TAA codons) amplified from N920143	This study
pIMAY:Δ*isdC*	A deletion encompassing the entire *isdC* gene (from ATG to TAA codons) amplified from N920143	This study
pIMAY:Δ*isdC-R*	A reversion fragment containing the entire *isdC* gene with a novel SmaI restriction site amplified from N920143	This study
pIMAY:Δ*atlI*	A deletion encompassing the entire *atlI* gene (from ATG to TAA codons) amplified from N920143	This study
pIMAY:*slsD*$^{+}$	Fragment to restore the nonsense mutation in *slsD* of N920143 to a sense codon (TAA-CAA)	This study
pIMAYZ:Δ*recA*	A deletion encompassing a 700 bp internal fragment of *recA* amplified from HKU09-01	This study
pIMAYZ:Δ*tagO*	A deletion encompassing the entire *tagO* gene (from ATG to TAA codons) amplified from N920143	This study
pIMAYZ:Δ*tagN*	A deletion encompassing the entire *tagN* gene (from ATG to TAA codons) amplified from N920143	This study
pIMAYZ:Δ*tagE1*	A deletion encompassing the entire *tagE1* gene (from ATG to TAA codons) amplified from N920143	This study
pIMAYZ:Δ*dltA*	A deletion encompassing the entire *dltA* gene (from ATG to TAA codons) amplified from N920143	This study
Expression and cloning plasmids		
pQE30	Protein expression vector N-terminal His tag	Qiagen

Table 2.3 Bacterial strains and plasmids

Strain / Plasmid	Description	Reference
pQE30:*vWbl*t	Expression of the N-terminal amino acids 46 – 1200 of vWbl with a hexa histidine tag	This study
pQE30:*slsD* (N2/N3)	Expression of the N-terminal amino acids 230 – 610 of SlsD with a hexa histidine tag	This study
pQE30:*slsE*	Expression of the N-terminal amino acids 46 – 800 of SlsE with a hexa histidine tag	This study
pQE30:*slsF*	Expression of the N-terminal amino acids 42 – 778 of SlsF with a hexa histidine tag	This study
pQE30:*slsG*	Expression of the N-terminal amino acids 48 – 920 of SlsG with a hexa histidine tag	This study
pRMC2	*E. coli, S. aureus* shuttle plasmid	(Corrigan & Foster, 2009)
pRMC2:*atlI*	Expression plasmid for the *isd* autolysin AtlI	This study
pBluescript	cloning vector	(Short *et al.*, 1988)
pCR-Blunt	cloning vector	Invitrogen
pT181	Staphylococcal plasmid conferring tetracycline resistance	(Khan & Novick, 1983)
Phage integrase vectors		
pIPI03	Site-specific integration vector for HKU09-01	This study
pIPI03:*ery*	pIPI03 carrying IPTG-inducible *ermAM* genes from pIMC*ery* within the MCS	This study
pIPI03:*kan*	pIPI03 carrying the IPTG-inducible *aphA3* gene from pIMC*kan* within the MCS	This study
pIMC*ery*	Site-specific integration vector for *L. monocytogenes*	(Monk *et al.*, 2008)
pIMC*kan*	Site-specific integration vector for *L. monocytogenes*	(Monk *et al.*, 2008)

[a] NRC – National Reference Centre for Staphylococci, Lyon, France.

[b] the strains were also created with pIPI03:*ery* and pIPI03:*kan* integrated in the chromosome.

(Table 2.2). The primers maintained overlapping ends to the pIMAY sequence downstream from the *cat* gene. The pIMAY backbone was amplified using the primers pIMAY – SLICcat-F and pIMAY – SLICcat-R, allowing the insertion of *ccrB* downstream of the *cat* gene. The two fragments were assembled *in vitro* using the SLIC cloning method described above.

Isopropyl-β-D-thiogalactopyranosid (IPTG)-inducible kanamycin and erythromycin resistance cassettes (Monk *et al.*, 2008) were excised from pIMC*kan* and pIMC*ery* using the restriction endonucleases KpnI and SacI. The fragments were gel-purified and cloned into the MCS of pIPI03 treated with the same endonucleases.

2.7.2 Integration of pIPI03

pIPI03 was used to transform *S. lugdunensis* HKU09-01 strains as described above. Due to the thermosensitive character of the plasmid (pIMAY *repA*) transformants were selected at 28°C on TSA_{cm10}. To select clones with an integrated plasmid, one colony grown at 28°C (replicating plasmid) was resuspended in TSB, dilutions were plated out on TSA_{cm10} and incubated at 37°C. Colonies were screened by PCR to confirm site-specific integration.

To determine the frequency of pIPI03 integration, a HKU09-01 (pIPI03) colony was resuspended in TSB, dilutions were plated on TSA_{cm10} and incubated at 28°C to determine the total number of CFUs or at 37°C to determine the number of CFUs carrying the integrated plasmid.

To test the stability of the integration, HKU09-01::pIPI03 was grown for four consecutive cultures at 37°C or 28°C without antibiotic selection. Dilutions were plated out and 50 colonies were screened for chloramphenicol resistance.

2.8 Recombinant proteins

2.8.1 Expression and purification of recombinant proteins

For purification and subsequent antibody production, recombinant proteins were expressed with N-terminal histidine-tag in *E. coli* using the IPTG-inducible expression vector pQE30. Molecular cloning was carried out using the *E. coli* strain XL1-blue. The plasmids constructed for the expression of the *S. lugdunensis* LPXTG proteins SlsD, SlsE, SlsF, SlsG and vWbl are summarised in Table 2.3. To facilitate protein purification, the protease-deficient

E. coli strain Topp3 was used. Cultures were grown at 37°C to an OD_{578} = 0.5-0.6 and induced for 3 h with 1 mM IPTG. The cells were harvested and resuspended in 30 ml Buffer A (4 mM Tris-HCl, 100 mM NaCl, pH 7.9) with one EDTA-free protease inhibitor tablet (Roche) added. Cells were lysed using a French Press and the lysate was centrifuged for 20 min (17000 x g). 150 µl of DNase (1 mg/ml) was added to the supernatant. After 20 min incubation on ice, the supernatant was filtered through a 0.45 µm Seratorius filter and applied to a HiTrap™ Chelating HP column (5 ml, Amersham Pharmacia) charged with nickel. The column was washed with 50 ml of Buffer A and the protein was subsequently eluted by applying increasing concentrations (5-100% v/v) of Buffer B (4 mM Tris, 100 mM NaCl, 200 mM imadizole pH 7.9) in Buffer A to the column. 10 ml fractions of each Buffer B concentration were collected and screened by SDS-PAGE and Coomassie staining for the presence of the recombinant protein. Positive fractions were pooled and dialysed against PBS for 16 h at 4°C. If needed, the protein was concentrated using appropriately sized filters (Amicon Ultra, Millipore) and the concentration was measured using the BCA assay kit (Pierce).

2.8.2 Antibody production

Antibodies against the recombinant proteins SlsD, SlsE, SlsF, SlsG and vWbl were raised in mice by P. Speziale, University of Pavia, Italy. Pooled serum of immunized mice was used for immunoblotting.

2.8.3 Solid phase binding assays using recombinant protein

Wells of a 96 well plate were coated in triplicates with 100 µl fibrinogen (Calbichem) (10 µg/ml), human serum albumin (40 µg/ml) or bovine serum albumin (40 µg/ml) at 4°C overnight. Wells were washed 3 times with 200 µl PBS, blocked for 2 h at 37°C with 5% (w/v) milk powder (Marvel) in PBS and washed again 3 times with PBS. Subsequently 100 µl of different concentrations of recombinant protein (8/4/2/1/0.5/0.25/0.125 µM) in sodium carbonate buffer were added to the wells and incubated at 37°C for 2 h. Wells were washed 3 times with PBS, 100 µl of anti-His6-HRP antibody (Roche) (1 : 500) in 1% (w/v) milk powder in PBS were added to the wells and the plates were incubated for 1 h at 37°C. Binding was detected using the tetramethylbenzidine reaction. One tetramethylbenzidine tablet and 2 µl of 30% (w/v) hydrogen peroxide were

added to 10 ml of phosphate citrate buffer (1 tablet dissolved in 100 ml ddH_2O). 100 µl of this solution were added to each well. The reaction was stopped after 10 min by the addition of 50 µl 2 M sulphuric acid and the absorbance at 450 nm was measured using an ELISA plate reader.

2.9 Immunoblotting

2.9.1 Whole cell immunoblotting

Cells were either grown to stationary or to early exponential phase (OD_{578} = 0.8). For exponential growth, cultures were inoculated to an OD_{578} = 0.075 with overnight cultures washed once with TSB. For growth under iron limited conditions, the strains were grown in RPMI with 1% casamino acids (CA, Difco). Cells were harvested, washed once with PBS and adjusted to OD_{578} = 1. 5 µl of the cell suspension was applied to a nitrocellulose membrane (Roche) and allowed to air dry. The membrane was subsequently blocked for 1 h with 10% (w/v) milk powder (Marvel) in TS buffer (10 mM Tris-HCl, 150 mM NaCl, pH 7.4). Membranes were washed 3 times for 10 min with TS buffer, and stained with primary antibodies for 1 h in 10% (w/v) milk powder in TS buffer. The antibodies and the dilutions used are summarized in Table 2.4. The antibodies α-SlsD, α-SlsE, α-SlsF, α-SlsG and α-vWbl were shown to bind their ligands with high specificity and titres were comparable (data not shown). Membranes were washed 3 times with TS buffer and stained with polyclonal HRP-conjugated rabbit α-mouse or goat α-rabbit antibodies (Roche). The secondary antibodies were applied in 10% (w/v) milk powder in TS buffer. Finally the membranes were washed 3 times with TS buffer and the chemiluminesent substrate LumiGlo (Cell Signaling Technology) was used according to the manufacturers recommendation. The blots were exposed to X-Omat autoradiographic film (Kodak) for 1-5 min and developed manually. Alternatively, the blots were analysed using the the "ImageQuant Las 4000" system and the corresponding "ImageQuant TL" software.

2.9.2 Western immunoblotting

Western immunoblotting was carried out using standard procedures. Protein samples were diluted 1 : 2 in protein sample buffer containing β-mercaptoethanol and separated by sodium dodecyl sulphate-polyacrylamide

Table 2.4 Antibodies used in this study

Antibody	Dilution used	Source / Reference
Goat α-Rabbit-HRP	1 : 3000	Dako
Rabbit α-Mouse-HRP	1 : 3000	Dako
Rabbit α-SrtA*	1 : 2000	Abcam
Rabbit α-IsdJ	1 : 5000	(Zapotoczna *et al.*, 2012)
Rabbit α-IsdB	1 : 5000	(Zapotoczna *et al.*, 2012)
Rabbit α-IsdC	1 : 5000	(Zapotoczna *et al.*, 2012)
Rabbit α-IsdK	1 : 5000	(Zapotoczna *et al.*, 2012)
Rabbit α-FbI	1 : 2000	(Mitchell *et al.*, 2004)
Mouse α-SlsA	1 : 4000	This study
Mouse α-SlsD	1 : 4000	This study
Mouse α-SlsG	1 : 4000	This study
Mouse α-SlsF	1 : 4000	This study

* directed against *S. aureus* SrtA

gelelectrophoresis (SDS-PAGE). The acrylamide gels used for the separation contained a 4.5% stacking gel and a 7.5% separating gel. Prestained molecular weight markers were supplied by Fermentas. The proteins were separated at 130 V and visualized on the gel using Coomassie blue strain. Alternatively the proteins were .electroblotted onto PVDF membranes (Roche) for 1.5 h at 100 V using a wet transfer cell (BioRad). Nonspecific binding to the membrane was blocked using 10% milk powder (Marvel) in TS buffer (10 mM Tris-HCl, 0.9% NaCl, pH 7.4) for 2-18 h. Primary antibodies were applied to membrane in 10% milk powder (Marvel) in TS buffer and incubated for 2 h with gentle agitation (dilutions used for the antibodies are summarized in Table 2.4). The membrane was washed three times with 20 ml TS buffer and the secondary antibody (conjugated to horse radish peroxidase) was applied in 10% milk powder and incubated for 2 h. The membrane was washed three times with TS buffer. LumiGLO reagent (Cell Signaling Technology) was added to the membrane for the detection of immune reactive bands. The blots were exposed to X-Omat autoradiographic film (Kodak) for 1-5 min and developed manually or bands were detected with the "ImageQuant Las 4000" system and the corresponding "ImageQuant TL" software.

2.9.3 Southern immunoblotting

Digoxigenin (Dig) labelled molecular weight markers were supplied by Roche. 3 µg genomic DNA was cleaved for 18 h using ApaLI (Fermentas) and separated by electrophoresis through an 0.8% agarose gel (40 V for 22 h). The DNA was denatured by submerging the gel for 45 min in DN buffer (1.5 M NaCl, 0.5 M NaOH). The gel was rinsed with ddH_2O, and neutralized for 45 min in NE buffer (1.5 M NaCl, 1 M Tris-HCl pH 7.4). The DNA fragments were transferred to a nylon membrane (Roche) using overnight capillary transfer with 20 x SCC buffer (3 M NaCl, 0.3 M Na_3Citrate). After transfer the DNA was heat-fixed (80°C for 2 h) to the membrane. Nonspecific binding was blocked for 4 h at 70°C using 30 ml of BL buffer (5 x SCC buffer, 0.1% N-lauroylsarcosine, 0.02% SDS, 1 x blocking reagent (Roche).

The 600 bp DNA probe was amplified by PCR using primers Prb-F / Prb-R and labelled with Digoxygenin (Roche) according to the supplier's recommendation. The probe was denatured by boiling for 10 min. Hybridization

was carried out overnight at 70°C using 30 ml BL buffer containing 15 ng/ml probe.

The membrane was washed twice for 10 min with 50 ml W1 (5 x SSC, 0.1% SCC) at room temperature and twice for 20 min with 50 ml W2 (0.5 x SCC, 0.1% SDS) at 68°C. Additional washing was performed at room temperature with Buffer-1 (0.1 M maleic acid, 0.15 M NaCl, pH 7.5). The membrane was washed for 5 min with 50 ml Buffer-1 (with 0.3% Tween 20) and 30 min with 50 ml Buffer-1 (containing 1 x blocking reagent). Anti-Dig-AP-Fab fragments (Roche) were diluted 1 : 10000 in Buffer-1 (containing 1 x blocking Reagent) and 40 ml were added to the membrane and incubated 30 min at room temperature. The membrane was washed twice with 50 ml Buffer-1 (with 0.3% Tween 20). The membrane was equilibrated for 5 min in 30 ml EB (100 mM Tris-HCl, 100 mM NaCl, pH 9.5), CSPD substrate solution (Roche) was diluted 1 : 100 in EB and 5 ml were added to the membrane and incubated for 5 min. The solution was poured off the membrane and the membrane was sealed in a hybridization bag (Roche). Immunoreactive bands were detected with the "ImageQuant Las 4000" system and the corresponding "ImageQuant TL" software.

2.10 *S. lugdunensis* cell fractionation

Fractionation was carried out as described earlier (Monk *et al.*, 2004) with minor modifications. Cells were grown in TSB or RPMI to stationary phase and washed once with buffer WB (10 mM Tris-HCl pH 7, 10 mM MgCl). A 1 ml aliquot OD_{578} = 5 was centrifuged (18000 x g) and resuspended in 100 µl buffer DB (10 mM Tris-HCl pH 7, 10 mM MgCl, 500 mM sucrose, 0.3 mg/ml lysostaphin (Ambi Products LLC), 250 U/ml mutanolysin, 30 µl protease inhibitor cocktail (Roche - 1 complete mini tablet dissolved in 200 µl H_2O), 1 mM phenyl-methanesulfonylfluoride (PSMF)). The digestion of the cell wall was carried out at 37°C for 1.5 h followed by centrifugation (18,000 x g, 10 min and 4°C). The supernatant was designated the cell wall fraction. The pellet containing the protoplasts was washed with 1 ml WB (with 500 mM sucrose) and centrifuged again as above. The protoplasts were resuspended in 200 µl buffer LB (100 mM Tris-HCl pH 7, 10 mM MgCl, 100 mM NaCl, 10 µg/ml DNaseI, 100 µg/ml RNaseA). The suspension was frozen and thawed three times to ensure

protoplast lysis and centrifuged for 30 min (4°C, 18,000 x g). The pellet (designated the membrane fraction) was washed with 1 ml of buffer LB and resuspended in 100 µl TE buffer (100 mM Tris-HCl pH 8, 1 mM EDTA).

5-15 µl of the fractions were used for analysis by protein electrophoresis and Western immunoblotting.

2.11 Determination of the minimal inhibitory concentration to tetracycline (MIC)

Bacterial strains carrying various copies of the *tet* gene were grown overnight in TSB containing 2 µg/ml tetracycline. 10^{-6} dilutions were prepared in PBS and 10 µl were dotted on TSA plates containing increasing concentrations of tetracycline. The lowest concentration of tetracycline inhibiting the growth of single colonies was designated as the MIC of the respective strain.

2.12 Quantitative PCR to determine the *isd* copy number

Quantitative PCR (qPCR) experiments are used for the accurate quantification of the relative amount of template within a PCR reaction. The method uses the fact that under optimal conditions (after the first cycles of the PCR with sufficient dNTP and polymerase) the PCR product doubles with every additional cycle. Thus, the relative amount of template within the reaction can be determined by measuring DNA synthesis and comparison to a standard curve.

Primers used for the experiments are summarized in Table 2.2. Primers OriF/R amplified a 100 bp fragment at the origin of the chromosome. The amplification of *ori* served as a standard for these experiments since there is only one copy per chromosome. Primers IsdJ F/R amplified a 100 bp internal fragment of *isdJ*. Thus relative template amount of *isdJ* compared to *ori* can be determined, allowing an estimation of the *isdJ* copy number.

Chromosomal DNA of N920143 was isolated and 10-fold dilutions (10^{-2} to 10^{-6}) were used to generate the standard curves for *ori* and *isdJ*. Chromosomal DNA of the sample strains was isolated and the 10^{-4} dilution was used as template. Each reaction was carried out in a 20 µl volume containing 2 µl template, 150 nM of primer F and R and 10 µl Power SYBR Green PCR Master Mix (Applied Biosystems). Each reaction was performed in duplicates.

The RT-PCR Cycler "StepOnePlus" with the appropriate equipment (96 well plates, adhesive covers) was used for the experiments (Applied Biosystems). Cycling was performed as follows: 2 min at 50°C followed by 10 min at 95°C followed by 40 cycles of 15 s at 95°C and 1 min at 60°C.

A melt curve analysis was performed, confirming that only a specific product was generated by the primers used. StepOne software Version 2.1 was used for data analysis.

2.13 PCR colony screen to determine the stability of the duplication in HKU09-01

Single colonies of HKU09-01 wild-type or the isogenic Δ*recA* mutant were used to inoculate TSB cultures. The cultures were grown at 37°C with agitation to stationary phase and dilutions were plated on TSA and incubated overnight at 37°C. 22 colonies were screened by colony PCR (paragraph 2.3.3) for the presence of the duplication using the primers Isd_dupl-F and Isd_dupl-R (Table 2.2). All clones that did not allow the amplification of a PCR product were screened a second time to ensure loss of the duplication. Only clones that did not allow the amplification of a product in both PCR screens were regarded as strains without the duplication.

2.14 Growth curves

The growth of different strains was assessed using the SynergyH1 Hybrid reader (BioTek) in 96 well plates (NUNC). Triplicate wells were filled with 200 µl TSB inoculated to an OD_{578} = 0.05 with a fresh overnight culture. The optical density at 578 nm was measured every 45 min with 10 min of shaking prior to each read. The mean of the triplicate wells at each time point was used to represent a single growth curve. The temperature was set as indicated to 28°C or 37°C. Each growth curve was performed three times using independent overnight starter cultures.

2.15 Bacterial adhesion assay

Ligands were diluted to appropriate concentrations in sodium carbonate buffer (0.1 M $NaHCO_3$, 33 mM Na_2CO_3, pH 9.6) and 100 µl were applied in triplicates to wells of a 96 well plate. Human fibrinogen (Calbiochem) – 5 µg/ml, fibronectin (kindly supplied by P. Speziale University of Pavia, Italy) – 5 µg/ml,

human / bovine serum albumin – 40 µg/ml, cytokeratin 10 (kindly supplied by H. Miajlovic (Walsh *et al.*, 2004)) – 5 µg/ml, human loricrin subdomain 2 (kindly supplied by M. Mulcahy (Mulcahy *et al.*, 2012) – 30 µg/ml. The plates were incubated for 12 h at 4°C. Plates were washed three times with 200 µl PBS, blocked with 100 µl 10% (w/v) milk powder (Marvel) in PBS for 2 h at 37°C and washed three times with 200 µl PBS. *S. lugdunensis* cultures were either grown to stationary or to early exponential phase (OD_{578} = 0.9). For exponential growth cultures were inoculated to an OD_{578} = 0.075 with overnight cultures washed once with TSB. Cells were harvested, washed with PBS and adjusted to OD_{578} = 1. 100 µl of the cells were added to the wells and incubated for 2 h at 37°C. Wells were washed (3 times with 200 µl PBS) and adherent cells were fixed by the addition of 100 µl 25% formaldehyde and incubated for 20 min at room temperature. Subsequently the wells were washed three times with 200 µl PBS, stained for 1 min with crystal violet and washed again 4-5 times with 200 µl PBS. 100 µl 5% acetic acid was added to the wells and absorbance 570 nm was measured using a plate reader.

2.16 UV sensitivity

Colonies were picked from a fresh plate and streaked in a sinuous line on a new TSA plate. Plates were exposed for indicated times to short wave UV light using the "Mineralight Lamp" Model CC10 (UVP) and the Chomato-VUE Cabinet. Plates were incubated for 24 h at 37°C and growth was evaluated qualitatively.

2.17 Single culture growth with haemoglobin as the sole source of nutrient iron

The experiment was carried out as describe previously (Pishchany *et al.*, 2010; Zapotoczna *et al.*, 2012a), with minor modifications. Completely iron-deficient medium was obtained by treating RPMI + 1% casamino acids with Chelex100 according to the supplier's instructions. The resulting medium was filter sterilized and designated D-RPMI. For growth analysis the medium was supplemented with 25 µM $ZnCl_2$, 25 µM $MnCl_2$, 100 µM $CaCl_2$, 1 µM $MgCl_2$ and 25 µM ethylenediamine-di(o-hydroxyphenylacetic acid) (EDDHA, LGC Standards GmbH). The medium was designated DD-RPMI.

Bacterial overnight cultures were grown in RPMI to represent iron-limited growth. The bacteria were sedimented (10 min at 9000 x g), washed once with D-RPMI and adjusted to OD_{578} = 3. 50 µl of the suspensions were used to inoculate 5 ml of DD-RPMI supplemented with 10 µg/ml human haemoglobin (Pointe Scientific Inc.). The experiment was carried out in 50 ml conical tubes incubated at 37°C with shaking at 150 rpm. Bacterial growth was measured by reading the OD_{578} over a 48 h period.

2.18 Competitive growth experiments

2.18.1 Competitive growth in TSB

For the comparison of the HKU09-01 wild type and the isogenic Δ*recA* mutant, the two strains (labelled with pIPI03*kan* or pIPI03*ery*) were grown overnight in TSB_{cm10}. Cells were harvested (10 min at 9000 x g), washed with TSB and adjusted to an OD_{578} = 3. 50 µl of each strain was used to inoculate 10 ml TSB_{cm10}. Dilutions were plated out on $TSA_{IPTG/kan}$ (1 mM IPTG + 50 µg/ml kanamycin) and $TSA_{IPTG/ery}$ (1 mM IPTG + 10 µg/ml erythromycin) to determine the ratio of cells at the start of the experiment (C0). The culture was incubated for 24 h with shaking (200 rpm) at 37°C. The OD_{578} of the overnight culture was read to determine the number of generations, and dilutions were plated on $TSA_{IPTG/kan}$ and $TSA_{IPTG/ery}$ to determine the ratio of the strains after 24 h growth (C1). A new TSB culture was inoculated to an OD_{578} = 0.01 with the previous culture and incubated at 37°C for another 24 h. The process was repeated four times and the ratio of strains in the consecutive cultures was determined for every overnight culture.

2.18.2 Competitive growth in iron deficient medium

For the comparison of the HKU(R) strains with different *isd* copy numbers, two strains (labelled with pIPI03*kan* or pIPI03*ery*) were grown overnight in TSB_{cm10}. Cells were harvested (10 min at 9000 x g), washed with D-RPMI and adjusted to an OD_{578} = 3. 50 µl of each strain were used to inoculate 5 ml $DD\text{-}RPMI_{cm10}$, containing 4 µg/ml haemoglobin or 0.5 mM $FeCl_3$. Dilutions were plated out on $TSA_{IPTG/kan}$ and $TSA_{IPTG/ery}$ to determine the ratio of cells at the start of the experiment (C0). The culture was incubated for 24 h with shaking (150 rpm.) at 37°C. The OD_{578} of the overnight culture was read to

determine the number of generations, and dilutions were plated on $TSA_{IPTG/kan}$ and $TSA_{IPTG/ery}$ to determine the ratio of the strains after 24 h growth (C1). Fresh DD-RPMI cultures were inoculated to an OD_{578} = 0.01 with the previous cultures and incubated at 37°C for 24 h. The process was repeated four times and the ratio of strains in the consecutive cultures was determined for every overnight culture.

2.19 Autolysin activity

2.19.1 Zymogram analysis

S. lugdunensis cell wall fractions were separated using an SDS-PAGE containing 0.2% lyophilized *Micrococcus lysodeikticus* cells. After electrophoresis the gel was washed 3 times for 30 min with 50 ml renaturation buffer (10 mM Tris-HCl, 1 mM DTT, pH 7.6) to allow the proteins to refold. The gel was sealed in plastic foil together with renaturation buffer and incubated overnight at 37°C. Zones of hydrolysis were assed using the "ImageQuant Las 4000" system and the corresponding "ImageQuant TL" software.

2.19.2 Autolysis assay

Autolysis assays were carried out as described earlier (Schlag *et al.*, 2010) with minor modifications. Bacterial cultures were grown to exponential phase in TSB (iron-rich) or RPMI 1% CA (iron-limited). HKU09-01 strains expressing *atlI* from pRMC2 were grown in TSB and induced in early exponential phase for 1.5 h with 1.2 µg/ml anhydrotetracycline.

The cells were harvested (10 min 9000 x g), washed twice with PBS and adjusted to OD_{578} = 0.7 in PBS containing 0.05% Triton-X100. The decrease of the optical density over time was measured in triplicate wells using the SynergyH1 Hybrid reader (BioTek).

2.20 Catheter induced-rat endocarditis model

Animal experiments were performed by F. Hanses, Department of Internal Medicine I, University Hospital Regensburg, Germany

Experiments were approved by the local animal protection committee at the University of Regensburg and the responsible state authorities. Male Sprague-Dawley rats (~200 g) were obtained from Charles River Laboratories,

Sulzfeld, Germany. Rats were maintained under standard housing conditions and given food and water *ad libitum*. A model of catheter-induced staphylococcal endocarditis was described previously (Lee *et al.*, 1997). Rats were anesthetized with a mixture of ketamine and xylazine, and a polyethylene catheter (Becton Dickinson, Heidelberg, Germany) was passed through the right carotid artery and the aortic valve into the left ventricle. Vigorous pulsation of blood within the catheter indicated correct positioning of the device. The catheter was sealed and tied in place with sterile suturing material, and the incision was closed. The rats were challenged intravenously with $3x10^4$ to $1x10^5$ *S. lugdunensis* or *S. aureus* as indicated 48 h after surgery. Heparinized blood was collected from each animal by tail vein puncture 24, 48, 72 h and 96 h (for *S. lugdunensis* infections) after inoculation and plated on agar. Surviving rats were euthanized 72-96 h after challenge, and their hearts and kidneys were removed. The position of the catheter within the heart and the presence or absence of vegetations was noted. The kidneys and aortic valve vegetations were weighed and homogenized in PBS or TSB, respectively. Quantitative plate counts were performed on serial dilutions of the homogenates, and the CFU per g of tissue was calculated.

Chapter 3

The *S. lugdunensis* genome

Introduction

The rapidly increasing amount of genomic sequence information that is publicly available has enabled comparative genomic analysis to become an important tool in understanding complex diseases, pathogenicity, evolution and individuality (Bentley, 2006). The recent development of sequencing technologies and the associated bioinformatic analysis tools allow the *de novo* sequencing and annotation of a bacterial chromosome within moderate time (weeks-months) with constantly decreasing costs (Loman *et al.*, 2012; Metzker, 2010). Due to their haploid genome and the absence of introns the identification of open reading frames (ORFs) is especially efficient for prokaryotes and strongly facilitated by bioinformatic software (Delcher *et al.*, 1999; Frishman *et al.*, 1998). The database "GenBank®" facilitates the process of annotation. "GenBank®" is a multinational project which comprises the DNA DataBank of Japan (DDBJ), the European Molecular Biology Laboratory (EMBL), and GenBank at NCBI (Benson *et al.*, 2013). The database merges publicly available DNA sequence data of almost 260.000 species along with corresponding amino acid sequences of the encoded proteins (Benson *et al.*, 2013).

The amount of wet-biology based experimental evidence on protein structure and function increases steadily and is included in the database. This allows a prediction of structures and functions for unknown proteins identified from novel sequence data. Additional databases such as PFAM (Finn *et al.*, 2010; Sammut *et al.*, 2008) are available to facilitate the identification of conserved domain structures in predicted proteins and help to suggest protein functions.

The vast amount of sequence information available allows an efficient investigation of the distribution of genes among individuals of the same species, genus or family. Taking this into account, investigation of novel genome sequences can help to identify special genomic regions, mobile genetic elements or mutations that might account for a certain phenotype of an individual or a bacterial strain. Additionally, it can give insight into the niche adaption of a species.

Next generation sequencing (NGS) technology has greatly improved the amount of sequence data gathered in recent years (Liu *et al.*, 2012; Mardis, 2008). The first generation of sequencing technology used the chain termination technique (Sanger sequencing). This method is time consuming, but allows long reads of up to 900 nucleotides in length (Liu *et al.*, 2012). Current NGS platforms such as 454 or Illumina technology produce shorter, random reads of 30 – 150 nucleotides. However, they produce up to 6 billion reads in a single run thereby greatly reducing the costs of full genome sequencing (Liu *et al.*, 2012). NGS is especially powerful if a reference genome is already available. Single nucleotide exchanges (SNPs) and the insertion / deletion of nucleotides or of genetic elements can be identified by mapping the short reads to the reference. NGS technology can also be used for the *de novo* sequencing of genomes without a reference. In this case a combination of different techniques is necessary to generate reads of different lengths which allows the assembly to longer alignments (Aury *et al.*, 2008). The biggest problem of *de novo* genome sequencing is caused by repetitive DNA sequences (Treangen & Salzberg, 2012). Repetitive sequences are present in all genomes, from bacteria to mammals and cause problems in alignments as the short reads match to different regions equally well (Treangen & Salzberg, 2012). In bacterial genomes repetitive sequences are found especially in regions encoding ribosomal RNAs (Klappenbach *et al.*, 2001) or the stalk regions of cell wall-anchored proteins (Speziale *et al.*, 2009). Even if state of the art technology is used, it remains difficult to determine the exact number of repeats in these areas and the gap closing process is time consuming and costly.

The first *S. aureus* genome sequences were published in 2001 (Kuroda *et al.*, 2001). Due to the availability of NGS technology the amount of sequence information increased rapidly within the last decade. Seven complete *S. aureus* sequences were available in 2004 (Lindsay & Holden, 2004) and there are currently 44 complete genome sequences available in the public domain (NCBI, 2013). The collection contains strains of different regional and temporal isolation and represents MSSA, community and hospital-acquired MRSA as well as both, human and bovine isolates. However, the given number does only include genome sequences that have been sequenced to completion and are lacking gaps in the sequence alignment. Recent studies regarding *S. aureus* used the

enormous potential of NGS technology to sequence hundreds of closely related *S. aureus* isolates. The studies used one reference genome which was sequenced to completion, whereas all the others were sequenced without gap closing. The reference genome enables the arrangement of the contigs in the correct order and allows an estimation of gap size and the features encoded within the gap. Full genome comparison of this kind allows a high quality insight into the transfer of mobile genetic elements and phages and enables the mapping of single nucleotide exchanges (SNPs) between closely related strains. This allows the creation of phylogenetic trees of strains that are too closely related to be distinguished by conventional methods such as MLST or PFGE. One of these studies provided insight into the global geographic structure of MRSA (ST239) and traced its global spread and transmission within a hospital (Harris *et al.*, 2010). Another study identified MRSA transmission events in a special care baby unit (Harris *et al.*, 2013). Similarly, the transmission of CC30 strains between hospitals within the UK (McAdam *et al.*, 2012) and the emergence and global spread of the EMRSA15 strains was assessed (Holden *et al.*, 2013) using full genome sequencing.

The classical approach to comparative genomics uses full genome sequences to explain differences between strains with interesting phenotypic characteristics rather than focusing on an evolutionary aspect. *S. aureus* is known be an important pathogen in modern medicine and experimental research (*in vitro* and *in vivo*) has identified a multitude of toxins, virulence and immune evasion factors that contribute to its fitness and pathogenesis. *In silico* analysis of genome sequences can therefore help to understand clinically important phenotypic differences between strains. The genomic comparison of two *S. aureus* strains (MRSA252 and MSSA476) identified interesting differences mainly in the accessory genome of the strains including different patterns of inserted genomic islands, lysogenic phages, transposons, SCC-elements and plasmids. The different mobile genetic elements encoded different virulence factors and resistance determinants responsible for the observed phenotypic differences (Holden *et al.*, 2004). Including additional genome sequences into the evaluation identified that the core genome of *S. aureus* is conserved between all lineages (Lindsay & Holden, 2004). In contrast the accessory genome is highly variable between the strains. Different

virulence factors are encoded in the accessory genome indicating differences in the virulence potential of the strains (Lindsay & Holden, 2004).

However, comparative genomic analysis is not limited to strains of the same species. Knowledge gained about *S. aureus* virulence factors and genomics can give important insights into the biology and niche adaption of other staphylococcal species. Thus genome sequencing of many staphylococcal species has been performed and their genomic characteristics have been investigated. The comparison of *S. aureus* to *S. epidermidis* confirmed many previously known phenotypic differences. Most factors of *S. aureus* involved in pathogenesis including superantigens, leukocidins and staphylokinase are absent in *S. epidermidis* underlining that the species can in general be regarded as less virulent (Gill *et al.*, 2005; Lindsay & Holden, 2004; Zhang *et al.*, 2003) The genome sequence of *S. haemolyticus* revealed an apparent high frequency of recombination events and a lower number of putative virulence factors compared to *S. aureus* (Takeuchi *et al.*, 2005). Analysis of the *S. carnosus* genome (a staphylococcal species used in food processing and known to be avirulent) showed a remarkable lack of mobile genetic elements and an accumulation of mutations with the potential to inactivate regulatory systems such as *agr* and *sae* (Rosenstein *et al.*, 2009; Rosenstein & Götz, 2010). Additionally, genome sequencing has been performed for the *S. intermedius* group (Ben Zakour *et al.*, 2012), *S. simiae* (Suzuki *et al.*, 2012) and *S. suis* (Holden *et al.*, 2009) all representing animal pathogens.

S. saprophyticus is a staphylococcal pathogen known to be associated with uncomplicated urinary tract infections of young females (Schito *et al.*, 2009). Unlike most of the other staphylococcal species, *S. saprophyticus* is not a commensal of the human skin. Comparative genomic analysis gave remarkable insight into the specific niche adaption of this pathogen. The sequence revealed the absence of most *S. aureus* specific toxins and secreted proteases. Interestingly, the genome encodes only a single cell wall-anchored protein (Kuroda *et al.*, 2005) which was shown to be involved in the initiation of adherence to the human bladder cells and to promote haemagglutination (Kuroda *et al.*, 2005; Sakinc *et al.*, 2006). This protein is not present in any other staphylococcal species. Furthermore, the species shows a paralogous

expansion of ion transport systems which is thought to be associated with the variable ion content in the urinary tract environment (Kuroda *et al.*, 2005). Thus the genome sequence allowed an in-depth understanding of the adaption of *S. saprophyticus* to the specific environment within the human bladder.

In clinical microbiology it is more and more recognized that the pathogen *S. lugdunensis* represents an unusually virulent coagulase negative species that is especially associated with invasive diseases such as infective endocarditis. Prior to this study a completed genome sequence was not available and the virulence potential of the species had not been assessed.

This chapter reports the analysis of the genome sequence of the breast abscess isolate N920143 (National Reference Centre of Staphylococci, Lyon, France), a strain that has been investigated previously due to his strong fibrinogen binding properties (Geoghegan *et al.*, 2010b; Mitchell *et al.*, 2004). Comparative genomic analysis was performed, comparing *S. lugdunensis* to *S. aureus* and all the CoNS genome sequences within the public domain at the time. The recently announced sequence of the *S. lugdunensis* clinical isolate HKU09-01 (Tse *et al.*, 2010) was included in the evaluation.

Results

3.1 The genome sequence of *S. lugdunensis* N920143

Genome sequencing was performed by collaborators of the Welcome Trust Sanger Institute. The final sequence gained consisted of 6 contigs and accordingly 6 gaps of approximately 1,5 kb to 4 kb which occurred in repetitive DNA stretches like ribosomal RNA and the repeat region of a surface-anchored protein. The contigs were aligned according to their order in HKU09-01. Gap closing was not completed since no important features are encoded within these regions in HKU09-01. The genome of *S. lugdunensis* N920143 comprises an approximately 2.6 Mbp chromosome with a GC-content of 33.8 %. In total there are 2452 protein-encoding sequences (CDS) present, of which 27 appear to be pseudogenes. The genome contains a single prophage named ϕSL01 and 14 insertion sequences. It does not carry any integrated or replicating plasmids. Furthermore there were no pathogenicity islands, transposons or

staphylococcal chromosomal cassettes detectable within the N920143 chromosome.

3.2 Comparison of the *S. lugdunensis* genome to the genomes of other staphylococci

Phylogenetic analysis of 16S rDNA (Takahashi *et al.*, 1999) and *dnaJ* (Shah *et al.*, 2007) gene sequences places *S. lugdunensis* in a clade that includes *S. epidermidis, S. aureus and S. haemolyticus*. Comparative genomic analysis revealed that a large proportion of the *S. lugdunensis* N920143 genome is shared with these related pathogenic staphylococci. Of the 2447 CDSs in the N920143 genome, 77.8% have reciprocal FASTA matches to *S. aureus* MRSA252, 74.7% to *S. epidermidis* RP62a, and 78.3% to *S. haemolyticus*. In comparison to the more distantly related staphylococci, 71.4% of all CDSs have matches to *S. saprophyticus*, 71.3% to *S. carnosus* and 54.4% to *M. caseolyticus* (Figure 3.1).

Compared to all other staphylococci there is an inversion of 60,375 bp located between nucleotide 1,457,500 and nucleotide 1,518,000 in a conserved region of the *S. lugdunensis* chromosome. Analysis of the boundaries of the inversion in N920143 has failed to identify flanking repeat sequences that could account for the inversion via recombination.

3.3 Comparison to the *S. lugdunensis* HKU09-01 genome

A pair wise comparison between N920143 and HKU09-01 identified that 95.4% of the chromosome is conserved (including the inversion), and that there are 125 unique CDSs in N920143. The major differences between *S. lugdunensis* N920143 and HKU09-01 are the following. Firstly, two identical putative transposons are present in HKU09-01 encoding a β-lactamase (*bla*) and

β-lactamase regulatory proteins. Secondly, HKU09-01 possesses a putative genomic island encoding resistance to cadmium but lacking identifiable virulence factors. Thirdly, the SLUSH locus of HKU09-01 underwent recombination between two of the peptide coding sequences. Only two peptides are encoded, SLUSH-A and SLUSH-B2 (this recombination is discussed in

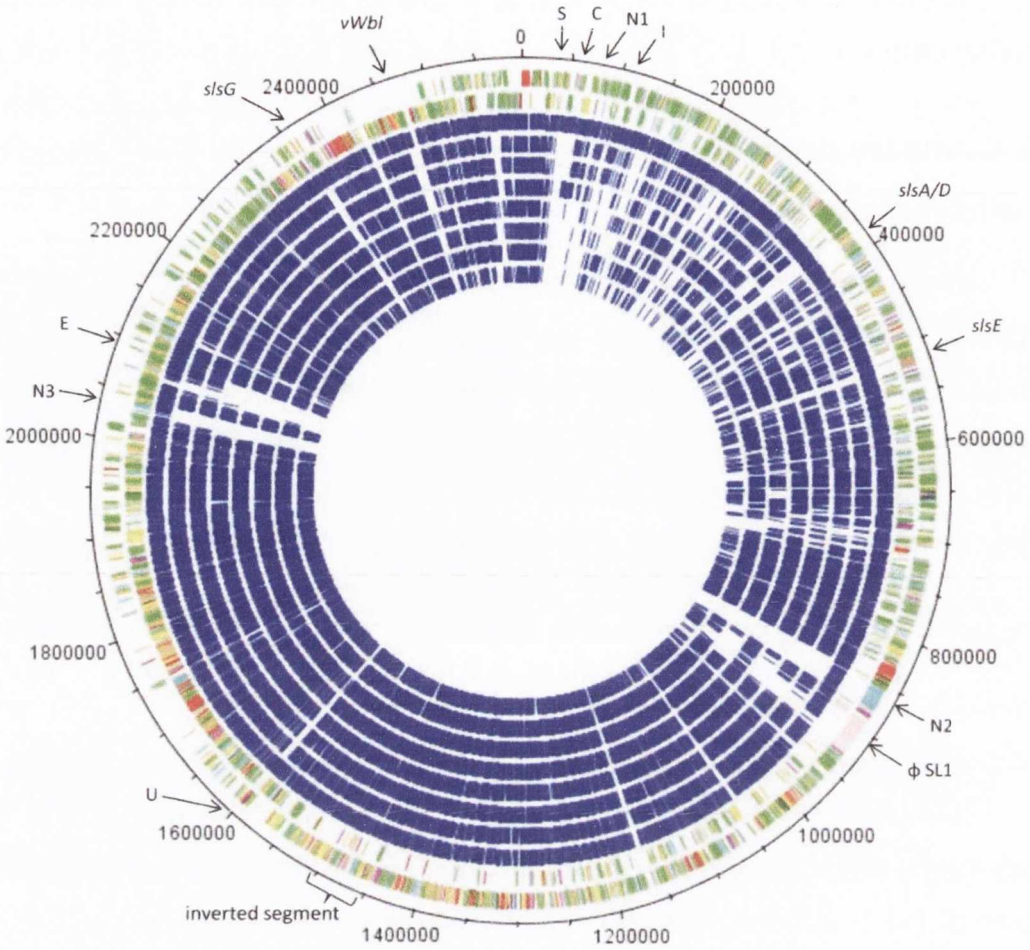

Figure 3.1 Schematic circular diagram of the *S. lugdunensis* N920143 chromosome

Key for the circular diagram (outer to inner): annotated CDSs colored according to predicted function are shown on a pair of concentric circles, representing both coding strands; blue circles show *S. lugdunensis* N920143 reciprocal Fasta matches shared with *S. lugdunensis* HKU09-01; MRSA252; MSSA476; *S. epidermidis*; *S. haemolyticus*; *S. saprophyticus*; *S. carnosus*; *M. caseolyticus*. Colour coding for *S. lugdunensis* CDS functions: neon green – pathogenicity/adaptation; dark gray – energy metabolism; red – information transfer; dark green – surface associated; sky blue – degradation of large molecules; dark pink – degradation of small molecules; yellow – central/intermediary metabolism; pale green – unknown; pale blue – regulators; orange – conserved hypothetical; brown – pseudogenes; pink – phage and IS elements; gray – miscellaneous. Arrows indicate regions of interest: C – CRISPR region; E – ESAT 6 toxin and secretion; I – Isd operon; N1 – Nonribosomal peptide synthetase 1; N2 – Nonribosomal peptide synthetase 2; N3 – Nonribosomal peptide synthetase 3; ϕSL1 – prophage; S – Streptolysin S-like toxin; U – Gene cluster for sugar uptake and degradation.

detail in Chapter 4). Fourthly, there is a 32 kb tandem repeat duplication comprising the region encoding the iron responsive surface determinant locus (*isd*) and the siderophore uptake system *sir* in HKU09-01 (this duplication is discussed in detail in Chapter 6).

3.4 Important features conserved among staphylococci

Several genes and loci were identified in the *S. lugdunensis* genome which might be of relevance to skin survival and virulence. A summary of these features and their presence in different staphylococcal species is shown in (Table 3.1). All staphylococci carry genes that encode a single iron-regulated ferric siderophore uptake system (*sst*) (Morrissey *et al.*, 2000) which is duplicated in both *S. lugdunensis* strains. All species encode an accessory gene regulator (Agr) system (Otto, 2001) and systems for neutralizing the negatively charged cell envelope by adding D-alanine to teichoic acid (Dlt) (Peschel *et al.*, 1999) and L-lysine to phosphatidyl glycerol (MrpF) (Peschel *et al.*, 2001). *M. caseolyticus* and all sequenced staphylococci except *S. haemolyticus* and *S. carnosus* have the capacity to express poly-N-acetyl glucosamine encoded by the *ica* operon, important for biofilm formation (Götz, 2002).

Along with *S. haemolyticus* and *S. saprophyticus*, *S. lugdunensis* has the potential to express a polysaccharide (O'Riordan & Lee, 2004) and a polyglutamic acid capsule (Kocianova *et al.*, 2005). All other staphylococci encode only one of the two capsule types. Only *S. epidermidis* and *S. lugdunensis* share a 12.5 kb CRISPR region, which is known to limit horizontal gene transfer (Marraffini & Sontheimer, 2008). Only *S. lugdunensis* and *S. aureus* encode the siderophore uptake system *sir* responsible for iron acquisition (Dale *et al.*, 2004b). The system is located directly upstream of the *S. lugdunensis isd* locus and is therefore duplicated in HKU09-01.

3.5 Putative virulence factors

Because *S. lugdunensis* displays a *S. aureus*-like phenotype in its ability to cause skin and soft tissue infections (SSTIs) and infectious endocarditis (IE) it is worthwhile to examine the differences in the repertoires of virulence factors.

Table 3.1 Summary of notable *S. lugdunensis* features and distribution of orthologues in other staphylococci

	S. lugdunensis N920143	S. lugdunensis HK09-01	S. aureus MRSA252	S. epidermidis RP62a	S. haemolyticus	S. saprophyticus	S. carnosus	M. caseolyticus
NRPS 1 (SLUG_00630)	+	+	+	+	-	-	-	-
NRPS 2 (SLUG_08100 to SLUG_08130)	+	+	-	-	-	-	-	-
NRPS 3 (SLUG_19080 to SLUG_19260)	+	+	-	-	-	-	-	-
isd locus (SLUG_00890 to SLUG_01010)	+	duplicated	+	-	-	-	-	-
sst locus (SLUG_20640 to SLUG_20710)	duplicated	duplicated	+	+	+	+	+	+
cap locus (PS capsule) (SLUG_03200 to SLUG_03350)	+	+	+	-	+	+	+	+
cap locus (PGA capsule) (SLUG_04590 to SLUG_04630)	+	+	-	+	+	+	-	-
esx locus (SLUG_19650 to SLUG_19700)	+ one gene FS	+ one gene FS	+	-	-	-	-	-
Streptolysin S - like toxin (SLUG_00380 to SLUG_0045	+ one gene FS	+ one gene FS	- (RF122)	-	-	-	-	-
Lantibiotic resistance locus (SLUG_05880 to SLUG_05910)	+	+	-	-	-	-	-	-
agr locus (SLUG_10210 to SLUG_10240)	+	+	+	+	+	+	+	-
ica locus (SLUG_00210 to SLUG_00240)	+	+	+	+	-	+	-	+
mprF / dlt (SLUG_15410 / SLUG_19300 to SLUG_19330)	+	+	+	+	+	+	+	+
CRISPR region (SLUG_00510 to SLUG_00590)	+	+	-	+	-	-	-	-

FS – frameshift; NRPS – nonribosomal peptide synthetase; PGA – polyglutamic acid; FS – polysaccharide ;
RF122 – sequenced *S. aureus* bovine isolate. Systematic IDs in the genome sequence of *S. lugdunensis* N920143 are given.

The *S. aureus* sphingomyelinase β-toxin (*hlb*) is conserved in *S. lugdunensis* and a putative haemolysin III is encoded as well. Furthermore, *S. lugdunensis* possesses a gene cluster encoding a streptolysin S-like toxin. The locus maintains genes encoding the toxin precursor, putative toxin modifying enzymes and the secretion system. Similar gene clusters are described for many Gram-positive pathogens but among the staphylococci only the bovine *S. aureus* isolate RF122 possesses a similar system (Lee *et al.*, 2008). Only *S. lugdunensis* and *S. aureus* encode ESAT-6 like toxin and secretion systems (*ess*) with homology to ESAT-6 proteins of *Mycobacterium tuberculosis* (Burts *et al.*, 2005). The *ess* loci of *S. aureus* MRSA252 and *S. lugdunensis* lack the genes encoding the cytoplasmic protein EsaC and the effector EsxB but only *S. lugdunensis* N920143 contains a frameshift in the gene encoding the membrane-associated protein EssC. Finally, the already described SLUSH-toxin locus (Donvito *et al.*, 1997) is present in *S. lugdunensis*, encoding short haemolytic peptides.

However, *S. lugdunensis* does not have genes encoding any other virulence factors known from *S. aureus*. There are no genes encoding coagulase, protein A, staphylokinase, superantigens, exfoliatins, β-barrel pore forming toxins (*hly, luk, hlg*), or small secreted proteins involved in immune evasion viz *map, efb, chp, scn, sak, ssl.*

S. aureus is known to produce two different iron chelating siderophores to allow the efficient uptake of iron during infection. The proteins encoded by the genes *sfnABCD* and *sbnABCDEFGHI* produce staphyloferrin A and staphyloferrin B, respectively. The reuptake of staphyloferrin A is mediated by HtsABC while the import of staphyloferrin B is mediated by the SirABC transporter. Both uptake systems were shown to be driven by the ATPase FhuC. *S. lugdunensis* encodes neither the *sfn* nor the *sbn* locus. In addition neither the *hstABC* nor *fhuCBGD1D2* genes are present in the *S. lugdunensis* genome. However, the SirABC transporter is conserved in *S. lugdunensis*.

3.6 Putative colonization factors

S. lugdunensis encodes several genes linking it to the lifestyle of a skin commensal. Most strikingly, it possesses three non-ribosomal peptide synthesis

systems (NRPS). One of the systems (NRPS1) consists of only one enzyme (273.4 kDa) and is conserved in *S. aureus* and *S. epidermidis* (Wyatt *et al.*, 2010). The second system (NRPS2) is encoded on a 20 kb genomic region and consists of four genes encoding proteins that are predicted to be 277.2, 14.8, 143.3 and 341.4 kDa in size. Whether these proteins produce one nonribosomal peptide each, or whether they catalyze different modifications of the same peptide is not possible to decide without experimental evidence. The third synthetase system (NRPS3) stretches over a 16.3 kb genomic region and encodes nine proteins with sizes ranging from 21 to 232 kDa. One of these shows homology to *pchD* of *Pseudomonas fluorescence*. The PchD synthetase is involved in siderophore biosynthesis, thus it might be speculated that the *S. lugdunensis* synthetase also produces a siderophore.

S. lugdunensis carries a locus of four genes encoding Lantibiotic resistance proteins similar to GdmG/E/F/H of *S. gallinarum* (Siezen *et al.*, 1996). Interestingly, no lantibiotic biosynthesis proteins are encoded within the locus.

3.7 The *S. lugdunensis isd* locus

S. lugdunensis is unique among CoNS in having a locus encoding iron regulated surface determinant (Isd) proteins. *S. aureus* Isd proteins can extract haem from haemoglobin and transport it across the cell wall using a series of wall-anchored proteins bearing NEAT motifs and into the cytoplasm using an ABC transporter. There, heam monooxygenases cleave the porphyrin ring to release the Fe^{2+} (Hammer & Skaar, 2011). *S. aureus* specifies three surface-exposed proteins that are anchored to peptidoglycan by processing at the C-terminal LPXTG-motif by sortase A. The IsdH, IsdB and IsdA proteins have three, two and one NEAT domains, respectively. *S. lugdunensis* has two putative LPXTG-anchored proteins, both with two NEAT motifs. One is an orthologue of IsdB with the sequence similarity to IsdB NEAT motifs being particularly high (50 and 55% identities). The second LPXTG-anchored protein named IsdJ has two NEAT motifs with 50 and 54 % identity to the single NEAT motif of IsdA whereas the IsdJ NEAT2 and C-terminal residues 457 to 646 have 39% identities to IsdA 63-350. Thus, *S. lugdunensis* IsdJ apperes to be an

enlarged version of the *S. aureus* IsdA having the NEAT domain duplicated while the N-terminal end is conserved. (Figure 3.2 shows the *isd* loci of *S. aureus* and *S. lugdunensis* in comparison, Figure 3.3 shows schematic diagrams of the surface-anchored proteins). The *S. aureus isd* locus includes a sortase B (SrtB) that recognizes the C-terminal NPQTN motif in IsdC when anchoring the protein to the peptidoglycan. *S. lugdunensis* has SrtB and IsdC orthologues and encodes a second putative SrtB substrate (IsdK) carrying a NKQPN motif in a gene located between *isdC* and *isdE* that replaces *isdD* in the *S. aureus* locus. In contrast to IsdD the *S. lugdunensis* IsdK protein has a NEAT motif. Another major difference between *S. aureus* and *S. lugdunensis* Isd is the absence of the IsdI haem oxygenase and the cell wall-anchored protein IsdH. Finally, a putative autolysin (*atlI*) is encoded downstream of *isdG* in the *S. lugdunensis* operon. No orthologous gene is present in *S. aureus*. Otherwise the overall gene organization is very similar apart from the presence of an insertion of genes encoding a membrane transporter located between the *isdA*-like gene and the *isdB* orthologue. Also a gene encoding an ABC transporter subunit is located between *isdF* and *srtB*.

Due to the high redox potential of haem, haem mediated toxicity is a problem for bacteria that acquire haem as a source of nutrient iron (Anzaldi & Skaar, 2010). *S. aureus* encodes the haem sensing two component system HssRS and the haem efflux ABC transporter HrtAB to allow the export of excess haem (Torres *et al.*, 2007). Interestingly this system is not conserved in *S. lugdunensis*.

Of special interest is the location of the *isd* locus with respect to the replication origin of the chromosome. The *S. aureus* MRSA252 locus is located in the middle of the chromosome (nucleotide 1146876-1155059). In contrast, the *S. lugdunensis* locus (nucleotide 96442-111616) is located in a different genomic context, close to the origin of replication.

3.8 Cell wall-anchored proteins

Proteins that are covalently anchored to the cell wall by sortase A-mediated processing of LPXTG are of particular interest because of their possible roles in adhesion to skin and host tissue, immune evasion and biofilm

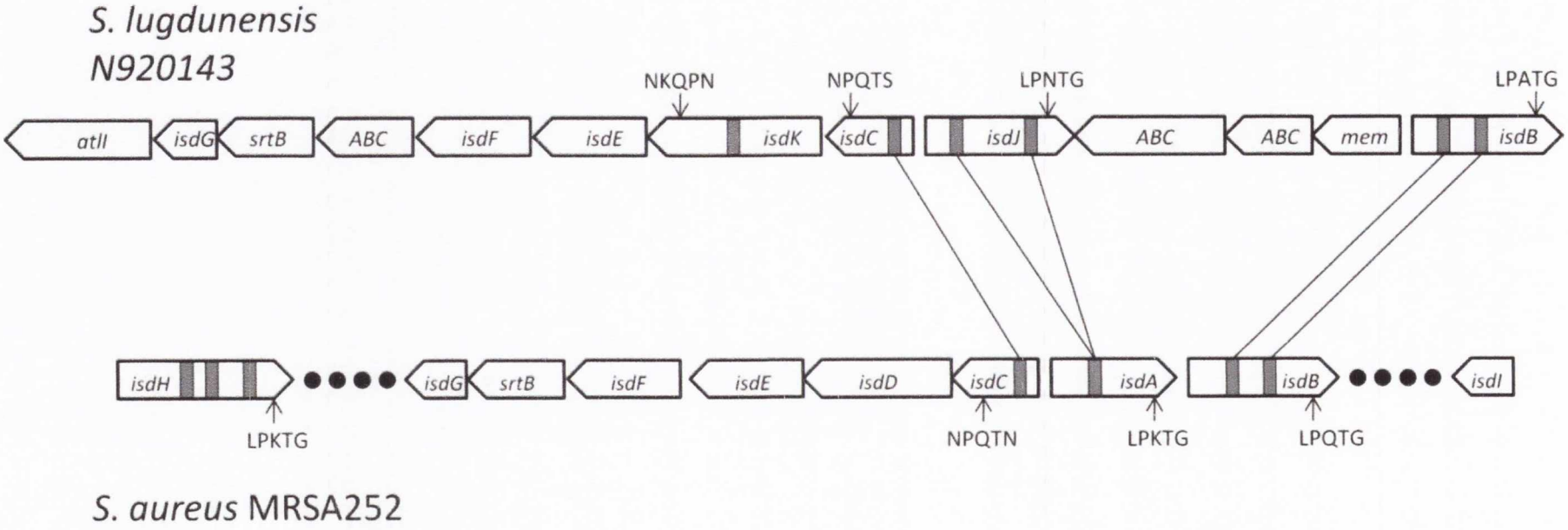

Figure 3.2 Comparison of the *isd* loci of *S. aureus* and *S. lugdunensis*
A schematic diagram of the *isd* loci is shown. The open boxes denote individual genes and the arrows the direction of their transcription. Encoded NEAT motifs are shown as small black boxes. Orthologous NEAT motifs are linked by black lines. The % identities between the encoded proteins are as follows: IsdB 36.8%, IsdC 57.6%, IsdE, 74.7%, IsdF 57.7%, SrtB 58.2%, IsdG 68.2%. Cell wall sorting signals are indicated. The *isdH* and *isdI* genes of *S. aureus* are located outside the locus as indicated by black circles.

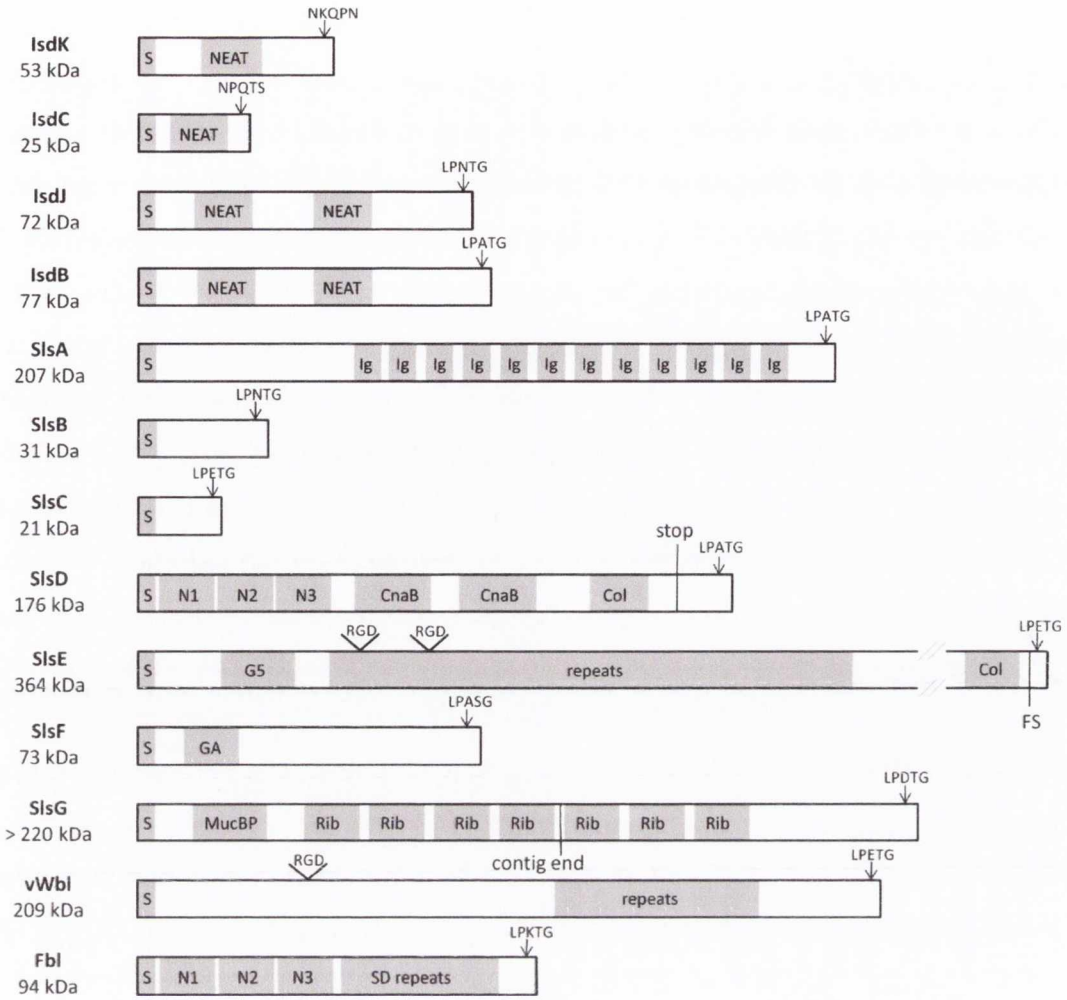

Figure 3.3 Schematic diagrams of the *S. lugdunensis* surface proteins

Predicted domains are indicated as grey boxes. NEAT – NEAT domain; GA – GA module; Ig – IgG-like fold; N1 domain of unknown function; N2/N3 – fibrinogen binding IgG-like folds of MSCRAMMs; CnaB – B-repeat found in the Collagen binding protein (CNA) of *S. aureus*; RGD – Argenine-Glycine-Asparagine; Col – Collagen triple helix repeat; G5 – G5 domain; MucBP – mucin binding domain; Rib – Rib-like repeat; SD – Serine-Aspartate; FS – frame shift; See text for predicted functions of the various domains. S-labelled boxes indicate the putative signal sequences.

formation. Apart from the two Isd proteins described above, the previously described fibrinogen binding protein Fbl that is related to ClfA of *S. aureus* (Geoghegan *et al.*, 2010b) and the von Willebrand factor binding protein vWbl (Nilsson *et al.*, 2004b), *S. lugdunensis* has seven genes with potential to encode wall-anchored proteins ranging in size from 20.8 kDa to 380 kDa. These proteins have been named *S. lugdunensis* surface proteins (Sls). Figure 3.3 shows schematic diagrams of these proteins. Analysis using the Pfam database (Sammut *et al.*, 2008) has revealed several interesting features. (i) The 1930 residue SlsA protein has twelve non-identical repeats of an IgG-like fold located between the LPXTG sequence and the 734 residue N-terminal domain. (ii) SlsE (3459 residues) has an 1240 residue N-terminal domain containing a 78 residue G5 motif (Ruggiero *et al.*, 2009) followed by a collagen-like sequence (24 residues), 46 repeats of a 31 residue motif and a C-terminal collagen-like sequence (50 residues). SlsE contains two RGD motifs at the N-terminal end of the repeat region. The *slsE* gene of N920143 has a frameshift between the region encoding the collagen-like domain and the LPXTG sequence while that of HKU09-01 is intact. (iii) SlsG has a 874 residue N-terminal domain with a 125 residue MucBP domain which is described for a mucin binding protein of *Streptococcus pneumonia* (Du *et al.*, 2011). The domain is followed by repeats of a Rib-like domain (Wastfelt *et al.*, 1996) seen in group B streptococci surface-anchored proteins. There are 18 Rib repeats in the HKU09-01 protein whereas in the N920143 protein the number of repeats is uncertain since the gene is located on two contigs in our sequence. (iv) The SlsD protein has a 575 residue N-terminal domain that has sequence and putative structural similarity to the fibrinogen-binding domain of SdrG of *S. epidermidis* (Ponnuraj *et al.*, 2003). Located C-terminally to this are two repeats with similarity to the B repeats of the collagen binding protein Cna of *S. aureus* and a 45 residue collagen-like domain. The *slsD* gene contains a nonsense codon located just 5' to the region encoding LPXTG so it is unlikely that the protein would remain anchored to the cell wall. (v) The 659 residue SlsF protein has a 41 residue GA domain described for an albumin binding protein of *Peptostreptococcus magnus* (Johansson *et al.*, 1997).

All putative surface proteins are conserved in the strain HKU09-01 with only minor differences in the number of repeats within the stalk regions. The

only major difference is that *slsE* does not contain a frameshift in HKU09-01. Although both strains represent isolates form distant geographical origins, the nonsense mutation in *slsD* is present in both strains.

Discussion

The first in depth analysis of a *S. lugdunensis* genome sequence and the comparison with several other staphylococci revealed a multitude of interesting characteristics, making *S. lugdunensis* an outstanding member of the staphylococci. The core genome of all species included in the evaluation is highly conserved and encodes housekeeping functions like DNA replication, RNA synthesis, sugar and amino acid degradation/biosynthesis and metabolite transport. However, several features are apparent in *S. lugdunensis* that make it unique and place it in between *S. aureus* and the other CoNS. The presence of three non-ribosomal peptide synthetases is remarkable, knowing that most staphylococci do not encode a single one. One can only speculate about the products but they might support *S. lugdunensis* while colonizing the human skin by inhibiting other skin commensals or by facilitating the uptake of rare ions or other substrates. Interestingly, *S. lugdunensis* does not encoded genes for the production of the iron chelating siderophores staphyloferrin A and B (Cheung *et al.*, 2009; Cotton *et al.*, 2009). In addition the staphyloferrin A transporter HstABC is not encoded by *S. lugdunensis* and the required ATPase FhuC is absent. These systems are known to be important for *S. aureus* pathogenicity (Dale *et al.*, 2004a). One might speculate that *S. lugdunensis* uses the putative siderophores produced by the NRPS to compete for free iron during infection. This seems a likely possibility since NRPSs are well known to produce iron chelating siderophores like enterobactin or vibriobactin (Crosa & Walsh, 2002). The staphyloferrin B transporter SirABC is encoded by *S. lugdunensis* and is duplicated in HKU09-01. This should allow the theft of this molecule produced by other bacteria in the microbiome or during mixed infection.

S. lugdunensis is known to be an important pathogen although it causes invasive infections only infrequently. Paradoxically, once *S. lugdunensis* gets established in a thrombus on a heart valve or is encased in an abscess it appears to be as virulent as *S. aureus* (Frank *et al.*, 2008). The genome sequence revealed only very few putative virulence factors, verifying earlier

reports about the absence of many typical *S. aureus* toxins in *S. lugdunensis* (Fleurette *et al.*, 1989). This might explain the low infectivity of the organism. However, *S. lugdunensis* has the potential to encode a streptolysin S-like toxin and secretion system, which is well described for different bacterial species but amongst the staphylococci it is only found in the bovine *S. aureus* isolate RF122 (Lee *et al.*, 2008). Further, *S. lugdunensis* is the only CoNS carrying an ESAT-6-like secretion system similar to that encoded by *S. aureus*. A striking difference between *S. lugdunensis* and *S. aureus* is the absence of any obvious immune evasion molecules. In *S. aureus*, immune evasion molecules and virulence factors are frequently located on mobile genetic elements, pathogenicity islands or prophages. The lack of these elements seems to be a characteristic of *S. lugdunensis* and might in part explain its low infectivity.

The most interesting linkage between *S. aureus* and *S. lugdunensis* is the presence of an *isd* locus. In *S. aureus* the locus has been shown to be important for pathogenicity. Isd proteins of *S. aureus* are not only involved in the acquisition of iron. In particular, IsdA is an important virulence factor because its C-terminal part confers resistance to antimicrobial fatty acids and lantibiotics (Clarke *et al.*, 2007). Furthermore IsdA binds to fibronectin, fibrinogen, lactoferrin, transferrin, feutin, involucrin, loricrin and cytokeratin 10 and is important for nasal colonization (Clarke *et al.*, 2004; Clarke & Foster, 2008; Clarke *et al.*, 2009). IsdB promotes binding to and activation of platelets (Miajlovic *et al.*, 2010). In addition it allows the invasion of epithelia cells by the interaction with ß3-integrins (Zapotoczna *et al.*, 2012b). Interestingly, IsdB and the N-terminal domain of IsdA are conserved in *S. lugdunensis*, perhaps suggesting similar functions of the proteins. In addition, the duplication of the locus in HKU09-01 strengthens the hypothesis of an important function of the locus. The ability of the bacterium to adhere to certain ligands or to resist antimicrobial agents might be enhanced by a gene dosage effect.

In *S. lugdunensis* and *S. aureus* the *isd* loci are located in different chromosomal contexts, suggesting that they were acquired independently from different sources. This explains the apparent differences between the loci including the absence of *isdI* and *isdH* in *S. lugdunensis*. In *S. aureus* these genes are located outside the *isd* operon and must have been acquired independently of the other genes to support the function of the operon. The

functions of these proteins are probably dispensable in *S. lugdunensis*. However, the presence of an independently acquired *isd* operon in *S. lugdunensis* and *S. aureus* suggests convergent evolution towards invasive behaviour that has not been described for any other CoNS. In conclusion, the genome analysis gives a picture showing *S. lugdunensis* to be an extraordinary skin commensal that is well equipped for the survival and competition on human skin. Nevertheless, provided with capsules, different toxins, putative haemolysins and a plethora of surface anchored proteins, the aggressive, *S. aureus*-like behaviour of *S. lugdunensis* that distinguishes it from the other CoNS might be explained. The properly annotated sequence provides the starting point for projects to investigate the mechanistic basis of skin colonization and pathogenesis by facilitating cloning and expression of genes.

Chapter 4

Genetic manipulation of *S. lugdunensis*

Introduction

S. lugdunensis is an opportunistic pathogen that is particularly associated with infectious endocarditis (IE). Although infections frequently show a devastating outcome and the organism appears to be exceptionally virulent for a coagulase negative staphylococcus (CoNS), hypothesis-driven research to identify virulence factors has not previously been conducted. Prior to this study a convenient genetic system for *S. lugdunensis* was not available. Mutations in the *fbl* gene of *S. lugdunensis* have been reported (Marlinghaus *et al.*, 2012). However, the methodology used for the creation of the mutations involved protoplast transformation and the insertion of an antibiotic resistance determinant into the *fbl* gene. This made the method time-consuming and infeasible for the creation of multiple mutations in the same genetic background. Furthermore, polar effects might make it difficult to interpret experimental results. For a comprehensive investigation of putative virulence factors of *S. lugdunensis*, a more convenient genetic system is required. Generally, the transformation of Gram-positive bacteria is often difficult. This is likely to be caused by two independent factors. Firstly, the Gram-positive bacterial cell envelope consists of a single membrane and a thick layer of peptidoglycan (PG) that acts as a physical barrier. Compared to the transformation of Gram-negative bacteria it is more difficult to force DNA across the envelope into the cytoplasm (Löfblom *et al.*, 2007). Thus, the precise protocol used for the preparation of electrocompetent cells is known to have a great impact on the level of bacterial competence and has to be optimized for each bacterial species or even strain (Löfblom *et al.*, 2007; Monk *et al.*, 2012). Secondly, bacteria express different restriction-modification systems (RM). As a result, foreign DNA is degraded in heterologous hosts. RM systems function as a barrier against the uptake of foreign DNA, thereby conferring resistance to infection with bacteriophages, preventing the transfer of conjugative plasmids and the uptake of extracellular DNA through natural competence (Tock & Dryden, 2005).

All RM systems recognize methylation of specific target patterns in the DNA thereby allowing the cleavage of foreign DNA molecules while cellular DNA remains unharmed. Depending on the methylation status of the DNA

different reactions are carried out by the RM enzyme complex. Unmethylated DNA is target of restriction, hemimethylated DNA is a substrate for methylation and fully methylated DNA is immune to cleavage (Vovis *et al.*, 1974). Four different types of RM restriction systems (Types I-IV) are distinguished (Tock & Dryden, 2005). Type I systems are named "host specificity for DNA (*hsd*)" and comprise three genes encoding the restriction subunit (R), the methylation subunit (M) and the specificity subunit (S). The S subunit of the enzyme complex is of special interest. The protein possesses two target recognition domains (TRD). Each of the TRDs binds to one part of the recognition sequence. Thus, identical sequences in the TRDs of S subunits occurring in different lineages indicate that the RM systems recognize the same target sequences (Corvaglia *et al.*, 2010; Roberts *et al.*, 2013). The functional Type I enzyme complex consists of two R, two M and one S subunit. Cleavage of unmethyleted DNA occurs at a site distant from the recognition site (Janscak *et al.*, 1999). Type II RM systems are a diverse, expanding collection. The enzyme complex typically consists of two subunits (M and R) and the enzyme is functional in a R_2M_1 complex. Several conserved amino acids in the M subunit allow the classification of Type II enzymes. The R subunits are not conserved and the enzymes show different recognition and restriction characteristics, yet they all cleave the DNA directly at their recognition site and typically recognize palindromic sequences (Tock & Dryden, 2005). Type III systems are similar to Type I RM systems but substrate recognition and modification are mediated by a single subunit (named mod). The restriction subunit of Type III is named res. The restriction complex is a heterooligomer and is functional in a mod_2res_2 complex (Janscak *et al.*, 2001). Type IV systems normally consist of two subunits forming an enzyme complex. In contrast to those systems described above, the Type IV complex recognizes and degrades DNA with foreign methylation patterns rather than unmethylated DNA and the cleavage site is unspecific. Importantly, a Type IV system does not confer methylation but cleaves methylated DNA with a foreign profile (Tock & Dryden, 2005).

S. aureus possesses a strong restriction barrier that prevents the uptake of foreign DNA. This barrier confronted research using genetic manipulation of *S. aureus* with significant problems. Two steps were required in order to transform wild-type *S. aureus* strains with plasmids isolated from *E. coli*. Firstly,

plasmid DNA was isolated from *E. coli* and used to transform the restriction deficient / methylation proficient *S. aureus* mutant RN4220 which was isolated following heavy chemical mutagenesis (Kreiswirth *et al.*, 1983). This strain readily accepts *E. coli*-derived DNA. Secondly, the plasmid was isolated from RN4220 and used to transform *S. aureus* wild-type strains. Not all *S. aureus* strains can be transformed using this method due to lineage-specific differences between the RM systems (Monk *et al.*, 2012; Roberts *et al.*, 2013).

Recently, new knowledge was gained about the RM systems of *S. aureus*. It was found that *S. aureus* possesses two distinct systems conserved between the different clonal complexes (CCs) (Corvaglia *et al.*, 2010; Veiga & Pinho, 2009). It possesses a Type I restriction system (SauI) conferring and recognizing *S. aureus*-specific methylation (Veiga & Pinho, 2009; Waldron & Lindsay, 2006). Most strains possess a single *hsdR* gene but two operons encoding distinct HsdS and HsdM subunits (Corvaglia *et al.*, 2010; Roberts *et al.*, 2013). Although Type I systems are conserved among *S. aureus* lineages, the nucleotide sequences of the *hsdS* genes differ significantly between the lineages, especially within their TRDs (Roberts *et al.*, 2013). This indicates different sequence specificities and explains the observation that DNA isolated from *S. aureus* is only accepted by closely related isolates (Corvaglia *et al.*, 2010; Roberts *et al.*, 2013; Waldron & Lindsay, 2006).

In addition to the Type I system, a Type IV modification-dependent restriction endonuclease named SauUSI is encoded by *S. aureus* (Corvaglia *et al.*, 2010). The endonuclease is encoded by a single gene and recognizes cytosine methylation of DNA (5mC methylation), thereby preventing the uptake of DNA from wild-type *E. coli* K12 (dcm^+) where Dcm confers this methylation (Xu *et al.*, 2011). The system is conserved in all *S. aureus* lineages and homologues are found in other staphylococci such as *S. epidermidis* and *S. carnosus*. This system is the major factor preventing uptake of *E. coli*-derived plasmid DNA (Corvaglia *et al.*, 2010; Monk *et al.*, 2012).

The restriction-deficient *S. aureus* host RN4220 contains premature stop codons in both, the gene encoding the restriction subunit of SauI (*hsdR*) and in the gene encoding SauUSI (Corvaglia *et al.*, 2010; Waldron & Lindsay, 2006). This allows a high frequency of transformation of DNA from dcm^+ *E. coli* strains. However, the genes encoding the specificity and methylation subunits of Hsd

are intact. Therefore *S. aureus* lineage-specific methylation will occur in RN4220 and subsequent transformation of wild-type *S. aureus* strains (from the same lineage) is possible (Corvaglia *et al.*, 2010; Monk *et al.*, 2012).

E. coli K12 strains that are widely used for cloning purposes such as XL1-blue or DH10B produce 5mC methylated DNA. A high efficiency *E. coli* cloning strain (named DC10B) was constructed recently in the DH10B background. This strain is deficient in *dcm* and produces unmethylated DNA (Monk *et al.*, 2012). This prevents recognition of DC10B-derived plasmid DNA by SauUSI and allows direct transformation of many *S. aureus* strains from different CCs (Monk *et al.*, 2012). The Type IV system is conserved in *S. epidermidis* RP62a and DNA isolated from *E. coli* DC10B was also able to transform this strain (Monk *et al.*, 2012). This indicates that the *S. epidermidis* system also recognizes the cystosine methylation conferred by Dcm of *E. coli*.

To improve the transformation frequency the DC10B strain was manipulated genetically so that plasmid DNA could circumvent Type I restriction systems in different *S. aureus* lineages. The method used was firstly applied to *Bifidobacterium breve* (O'Connell Motherway *et al.*, 2009) and *Bifidobacterium adolescentis* (Yasui *et al.*, 2009) and is called plasmid artificial modification (PAM). Monk *et. al.* (unpublished) described the construction of DC10B strains that expressed different *hsdMS* genes of several *S. aureus* CCs and from *S. epidermidis* RP62a. The genes were expressed from a constitutive promoter and were integrated into the *E. coli* DC10B chromosome. Plasmid isolated from the PAM strains improved the transformation frequency of the target strains ~100 fold allowing direct high frequency transformation of *S. aureus* / *S. epidermidis* with *E. coli*-derived plasmid (Monk *et al.* unpublished).

Prior to this study plasmid transformation by electroporation had not been described for *S. lugdunensis*. The establishment of an efficient electroporation protocol and its application to various CCs of *S. lugdunensis* is described within this chapter. Further, the restriction barrier of *S. lugdunensis* was identified and methods for efficient transformation were developed. The isolation of markerless deletion mutations has not been described for *S. lugdunensis*. Thus, a protocol for allelic exchange using pIMAY was established and is also reported within this chapter. The new protocol was used

for the construction of various deletion mutants to enable collaborators all over the world to study specific areas of *S. lugdunensis* biology and pathogenicity.

Results

4.1 Establishment of a genetic system for *S. lugdunensis*

4.1.1 Transformation of *S. lugdunensis*

Several different protocols to render the strain N920143 electrocompetent were attempted using the shuttle plasmid pRMC2 (Corrigan & Foster, 2009) isolated from *E. coli* XL1-blue. The protocol of Augustin and Götz (Augustin & Götz, 1990) did not yield any transformants. However, a modified procedure based on the protocol originally optimized for *S. carnosus* (Löfblom *et al.*, 2007) did allow the transformation of *S. lugdunensis* N920143 with a low frequency of ca 0.6 x 10^1 (Figure 4.1 B). A detailed description of the optimized protocol for the preparation of electrocompetent *S. lugdunensis* cells is given in Chapter 2.

Although the frequency of transformation of *S. lugdunensis* was low, it was sufficient to establish genetic manipulation procedures using the thermosensitive plasmids pIMAY (Monk *et al.*, 2012) or pIMAYZ (Monk *et al.*, unpublished) and allelic exchange (the optimized protocol is described in Chapter 2). The *secY* genes of *S. aureus* and *S. lugdunensis* are similar. The 561 nucleotide *secY* antisense fragment in pIMAY is derived from *S. aureus* RN4220 (Bae & Schneewind, 2006) and shares 81.3% identity with *S. lugdunensis* N920143 *secY*. However, anhydrotetracycline induction of *secY* antisense RNA did not result in selection of colonies lacking the plasmid in *S. lugdunensis* (data not shown). pIMAYZ allowed the detection of plasmid loss during allelic exchange by the colour of colonies. Colonies that had lost pIMAYZ failed to cleave the chromogenic β-galactosidase substrate X-Gal and displayed white instead of blue colour on agar plates containing X-Gal. Thus pIMAYZ allowed monitoring of the presence or absence of the plasmid during the allelic exchange procedure. This method proved to be efficient in *S. lugdunensis* which is naturally non-lactose fermenting.

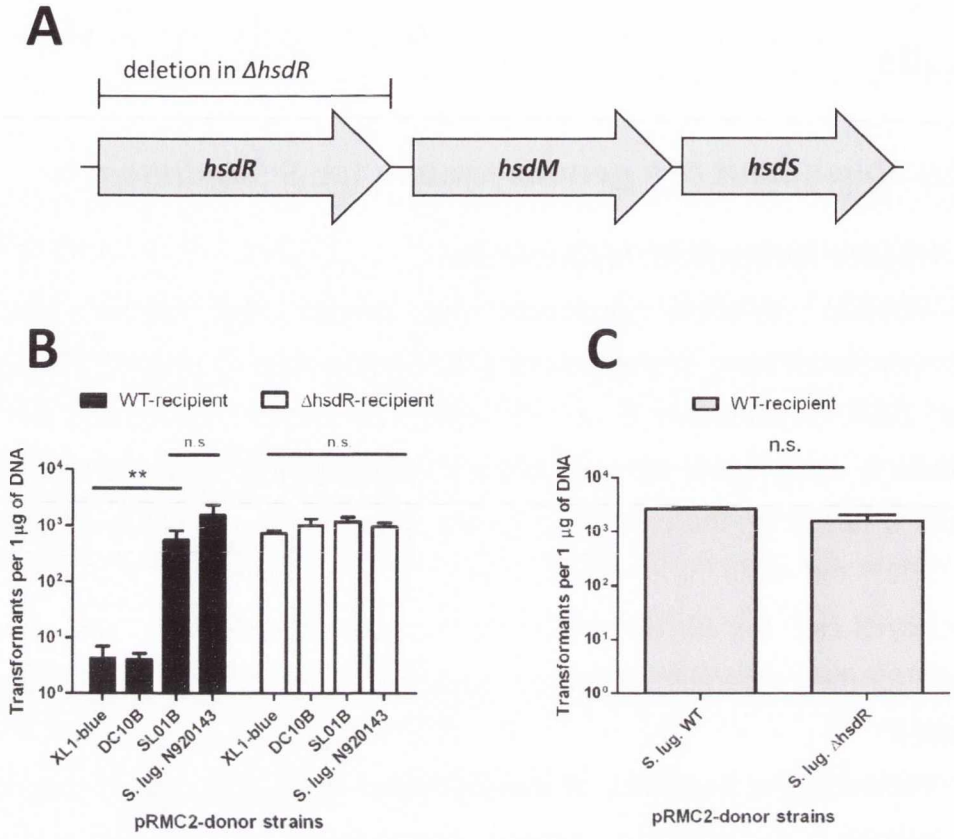

Figure 4.1 Transformation frequency of *S. lugdunensis*

(A) Schematic diagram of the SluI operon in N920143. The deletion in the Δ*hsdR strain* is indicated.

(B) Recipient strains N920143 and the isogenic Δ*hsdR* mutant were transformed with plasmid from various sources. XL1-blue - *dcm*$^+$; DC10B - *dcm*$^-$; SL01B - *dcm*$^-$, *hsdMS*$^+$: *S. lugdunensis* N920143. The absolute number of transformants achieved per µg plasmid is shown. The mean and SEM of three independent experiments is shown.

(C) *S. lugdunensis* N920143 wild-type was transformed with plasmid DNA isolated from the wild-type itself or from the isogenic Δ*hsdR* mutant. The absolute number of transformants achieved per µg plasmid is shown. The mean and SEM of three independent experiments is shown.

Statistical evaluation was performed using an unpaired two tailed t-test. P-values <0.05 were regarded as significant and are indicated by *. ** indicate P-values <0.005.

4.1.2 Bypassing the restriction barrier in *S. lugdunensis* N920143

As described above *S. lugdunensis* could be transformed at a low frequency with plasmid DNA (pRMC2) isolated from *E. coli* XL1-blue. The frequency of transformation increased ~90 fold when plasmid DNA that was isolated from the transformed *S. lugdunensis* (N920143) was used (Figure 4.1 B). This suggests that the protocol for the induction of electrocompetence was quite efficient. However, a restriction system appeared to prevent the efficient uptake of DNA from *E. coli*, and reduced the frequency of transformation.

The *S. lugdunensis* (N920143) genome sequence was searched for the presence of genes similar to RM systems of *S. aureus* and other Gram-positive bacteria. Interestingly, *S. lugdunensis* does not harbour a gene with the potential to encode a Type IV restriction system similar to SauUSI of *S. aureus*. (Corvaglia *et al.*, 2010; Monk *et al.*, 2012) that recognizes and cleaves cytosine methylated DNA (Xu *et al.*, 2011). DNA isolated from Dcm^+ (XL1-blue) or Dcm^- (DC10B) strains of *E. coli* transformed *S. lugdunensis* N920143 at the same frequency (Figure 4.1 B) confirming that the strain failed to recognise the pattern of cytosine methylation expressed by *E. coli* K12.

However, *S. lugdunensis* was found to possess three genes with the potential to encode a Type I restriction system. The system was dedicated SluI. The *hsdS*, *hsdM* and *hsdR* genes are closely linked and are likely to represent a single operon (Figure 4.1 A). Only a single set of *hsdM* and *hsdS* genes is present in *S. lugdunensis* N920143 and HKU09-01. Most likely, this system represents the major barrier to transfer of DNA from other bacterial species. In order to investigate this hypothesis, a mutant deficient in *hsdR* (encoding the restriction subunit) was constructed using pIMAY. Deletion of *hsdR* increased the transformation with *E. coli* K12-derived DNA (XL1-blue and DC10B) ~90 fold (Figure 4.1 B). In fact, the transformation frequency of the Δ*hsdR* strain was the same with plasmid from *E. coli* K12 or *S. lugdunensis*, suggesting that SluI is the only restriction system recognizing foreign DNA in *S. lugdunensis*. Plasmid isolated from the Δ*hsdR* strain transformed the wild-type strain with the same efficiency as DNA isolated from the wild-type strain itself (Figure 4.1 C), confirming that DNA modification occurs in the mutant strain. Thus, Δ*hsdR* can be used as an intermediate host for the efficient transfer of DNA from *E. coli* into *S. lugdunensis* N920143.

E. coli PAM strains that modify plasmid DNA with methylation patterns specified by Type I RM systems allow highly efficient transfer of plasmid from *E. coli* into the target strain. A *S. lugdunensis* N920143-specific PAM strain of *E. coli* DC10B (SL01B) was constructed by I. Monk (the construction of the strain is not described within this thesis). The strain constitutively expressed the *hsdMS* genes from *S. lugdunensis* N920143 to create a SluI-specific pattern of methylation. Plasmid DNA isolated from SL01B improved the transformation frequency of *S. lugdunensis* N920143 ~90 fold compared to the level achieved with XL1-blue or DC10B-derived DNA to the same level achieved with *S. lugdunensis* N920143-derived DNA (Figure 4.1 B). Furthermore SL01B-derived plasmid DNA did not improve the transformation frequency of the Δ*hsdR* strain. These results indicate that SluI represents the single barrier to the uptake of DNA in *S. lugdunensis* N920143 and is efficiently bypassed with the appropriately methylated DNA produced by the PAM strain SL01B.

4.1.3 Transformation of *S. lugdunensis* strains from different CCs

In *S. aureus,* strains from different lineages exhibit differences in transformation frequency depending on the source of the transforming plasmid. This is determined by variations in the specificity of HsdS (Monk *et al.*, 2012; Roberts *et al.*, 2013). It was investigated whether the same is true for *S. lugdunensis*. Recently, multilocus sequence typing (MLST) was established for *S. lugdunensis* (Chassaîn *et al.*, 2012). The 87 isolates investigated clustered in five CCs with 20 different sequence types (ST). CC1 formed the biggest complex with 33% of all isolates. CC2, CC3, CC4 and CC5 contained 20%, 21%, 4.5% and 5.8% of the isolates, respectively. The two sequenced strains HKU09-01 and N920143 belong to CC1. In addition to N920143 and HKU09-01 two isolates from each CC were chosen as recipients for comparative transformation experiments using pRMC2 plasmid DNA derived from XL1-blue and SL01B (Figure 4.2). Each strain from CC1 and CC2 exhibited increased (10-90 fold) transformation efficiency with pRMC2 plasmid DNA isolated from the PAM strain SL01B compared to XL1-blue. These data suggest that CC1 and CC2 strains express the same RM system which allows SL01B-derived plasmid to be readily accepted. Compared to the transformation frequency of N920143, strain SL13 from CC1 was transformed with ca 30-fold

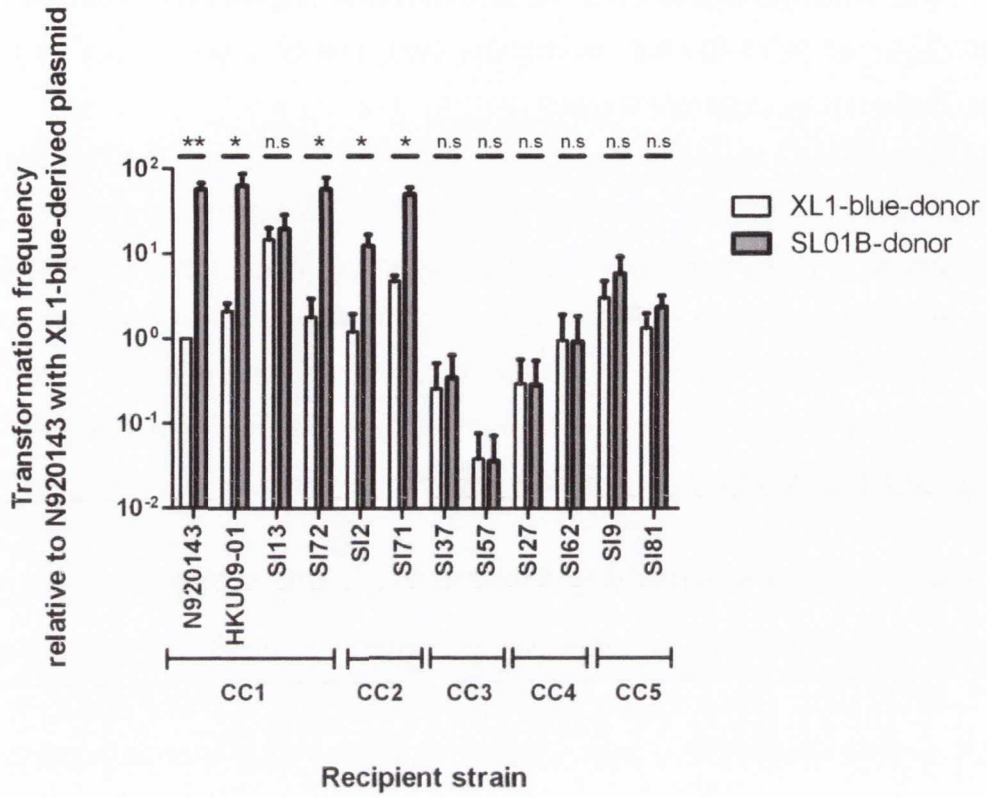

Figure 4.2 Transformation frequency of *S. lugdunensis* strains from various clonal complexes

S. lugdunensis strains were transformed with 5 µg plasmid isolated from different *E. coli* strains. XL1-blue - *dcm*$^+$; SL01B - *dcm*$^-$, *hsdMS*$^+$. CC - clonal complex.

The number of transformants achieved using N920143 and pRMC2 isolated form XL1-blue in each experiment is set to 1. The number of transformants achieved with different strains and DNA is expressed in relation to this value. The mean and SEM of four independent experiments is shown.

Statistical evaluation was performed using an unpaired two tailed t-test. P-values <0.05 were regarded as significant and are indicated by *.
** indicate P-values <0.005.

higher frequency with XL1-blue-derived DNA and the frequency did not increase when SL01B-derived plasmid was used (Figure 4.2).These data suggest that no Type I RM system is functional in SL13. However, sequencing of the *hsdR* and *hsdS* genes of SL13 did not identify the presence of a deleterious mutation within these genes (data not shown).

Interestingly isolation of plasmid DNA from SL01B did not improve the transformation frequency of CC3, CC4 and CC5 isolates above the level achieved with XL1-blue-derived DNA suggesting that different methylation patterns are recognized. In general strains from CC3 and CC4 were more difficult to transform than the other strains. Compared to the transformation of N920143 (CC1) with XL1-blue-derived DNA, 5- to 50-fold fewer transformants were obtained with strains from CC3 and CC4.

4.2 Genetically manipulated strains of *S. lugdunensis*

The availability of two complete genome sequences of *S. lugdunensis* (Heilbronner *et al.*, 2011; Tse *et al.*, 2010) allowed the identification of several loci that might influence virulence. In order to provide experimental evidence for any putative virulence factor, Koch's Postulates need to be fulfilled at the molecular level. Specific mutants created by allelic exchange are a prerequisite for testing phenotypes *in vitro* and *in vivo*.

Several collaborations were established where mutations in a multitude of potentially important loci were created. The mutants were sent to our collaborators for detailed phenotypic analysis. The construction of these mutations and the preliminary characterization of mutants and corresponding revertants are reported in the following section of this Chapter.

4.2.1 The *slush* locus in HKU09-01

S. lugdunensis encodes three haemolytic peptides (Donvito *et al.*, 1997). These peptides display synergistic properties similar to the *S. aureus* δ-toxin and were therefore named *Staphylococcus lugdunensis* synergistic haemolysin (SLUSH). Analysis of the *S. lugdunensis* genome sequences identified only three loci with the potential to encode putative toxins (SLUSH, streptolysin S-like toxin, haemolysin III-domain protein). However, only the SLUSH peptides are known to be expressed and the haemolytic properties were confirmed. The

SLUSH peptides belong to the PSM class of toxins. As described in Chapter 1, the recognition of PSMs plays an important role in the host immune response against staphylococcal pathogens and a plethora of further functions has been described. This makes the SLUSH peptides interesting targets for further examination. Collaborations were established with E. Smeds (Texas A & M University, Houston, Texas, USA) and A. Peschel (Institut für Medizinische Mikrobiologie, Eberhard Karls Universität Tübingen, Germany) aiming for a closer characterization of the *S. lugdunensis* SLUSH peptides.

In order to identify SLUSH peptide secreting strains, eleven *S. lugdunensis* isolates were screened for their haemolytic activity. Eight out of eleven strains (72%) produced distinct zones of haemolysis after 48h on Columbia agar with 5% sheep blood (data not shown). The complete genome sequences were available for the haemolytic HKU09-01 strain and the non-haemolytic N920143 strain. Consequently, HKU09-01 was chosen for further investigation. Analysis of the *slush* locus of HKU09-01 revealed that it had undergone genetic rearrangement. Figure 4.3 A shows a diagram of the *slush* locus of N920143 which is 99.3% identical to that previously described (Donvito *et al.*, 1997). The locus comprises *orfX* and the SLUSH peptide-encoding genes *slush-A*, *slush-B* and *slush-C*. A stretch of 29 nucleotides is shared between *slush-B* and *slush-C*. At this short stretch of homology, recombination has taken place in HKU09-01, deleting 193 nucleotides comprising the 3' end of *slush-B* and the 5' end of *slush-C*. A new gene was created by this rearrangement consisting of the 5' end of *slush-B* and the 3' end of *slush-C*. Here the new gene and the encoded peptide are called *slush-B2* and SLUSH-B2, respectively. Thus, the *slush* locus of HKU09-01 encodes only three peptides: OrfX, SLUSH-A and SLUSH-B2. The difference in the loci was investigated by PCR using primers binding upstream and downstream of the *slush* locus (Figure 4.3 B). The fragment amplified from N920143 was ~200 bp larger than that amplified from HKU09-01 chromosomal DNA which is consistent with the observed deletion.

In order to investigate the importance of the SLUSH peptides, a deletion mutation removing *orfX*, *slush-A* and *slush-B2* in HKU09-01 was isolated using pIMAY and allelic exchange (Monk *et al.*, 2012). Allelic exchange was also used to revert the mutation in the Δ*slush* strain. The wild-type *slush* locus from

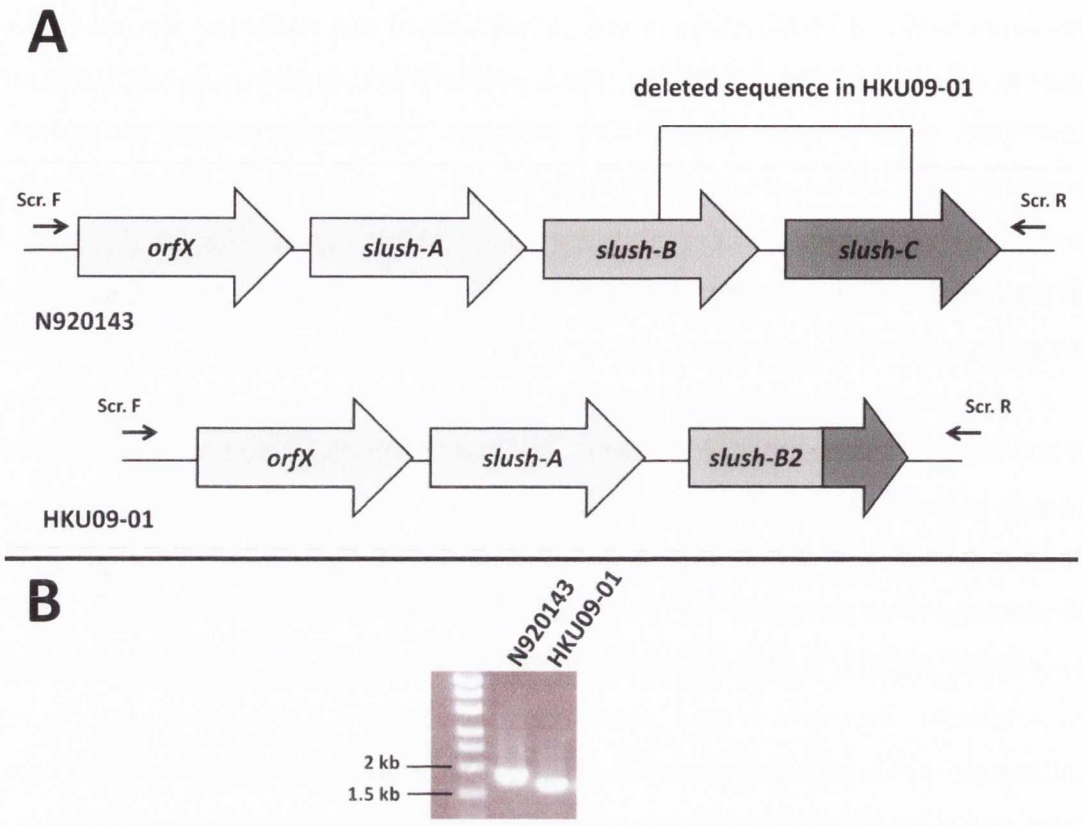

Figure 4.3 Comparison of the *slush* loci of N920143 and HKU09-01
(A) Schematic diagram of the *slush* loci of *S. lugdunensis* N920143 (top) and HKU09-01 (bottom). Recombination leading to the expression of only two peptides in HKU09-01 is indicated. Binding sites for primers are indicated by small horizontal arrows.
(B) PCR using the primers indicated in (A).

HKU09-01 was reinserted at its original site in the chromosome. The created strain was designated *slush-R*. PCR was used to integrate a nucleotide exchange between *slush-A* and *slush-B2* creating a novel BamHI site to distinguish between wild-type and revertant. A schematic diagram of deletion and reversion constructs is shown in Figure 4.4 A. PCR experiments using SLUSH screening primers (Figure 4.4 B) resulted in the amplification of a ~1.7 kb fragment from the wild-type and the *slush-R* strains confirming the presence of the *slush* locus. The amplification of a ~1 kb fragment confirmed the deletion of the *slush* locus in the *Δslush* strain. Only the fragment amplified from the *slush-R* strain was cleaved by BamHI confirming the introduction of the restriction site during the reversion procedure.

As reported earlier, the *slush* locus could not be cloned in *E. coli*, most likely due to toxicity of the peptides (Donvito *et al.*, 1997). To overcome this problem, the Gram-positive bacterium *Lactococcus lactis* was used as the host for cloning of the *slush* locus. Positive clones could be identified when *L. lactis* was used, indicating that the SLUSH peptides expressed from the reversion cassette did not have toxic effects on this Gram-positive bacterium.

As shown in Figure 4.5, deletion of the *slush* locus abrogated the haemolytic phenotype displayed by *S. lugdunensis* HKU09-01, indicating that the SLUSH peptides are the only haemolysins secreted by this strain under the growth conditions used. Reversion of the deletion restored the haemolytic phenotype. The virulence of the strains is currently being tested in a mouse sepsis model and their ability to stimulate human immune cells is under current investigation by collaborators.

4.2.2 Mutations of *isd* genes

S. lugdunensis is unique among the CoNS in that it is the only species identified up to date that carries an iron responsive surface determinant locus (Isd). In *S. aureus* the locus represents a haem uptake system and studies have been begun by E. Skaar and his group (Vanderbilt University Medical Center, Nashville, Tennessee, USA). In order to gain insight into *S. lugdunensis* haem utilization, a mutant deficient in the haem degrading monooxygenase IsdG was constructed in N920143. The studies showed that IsdG functions as a haem degrading monoxygenase to liberate iron from haem (Haley *et al.*, 2011).

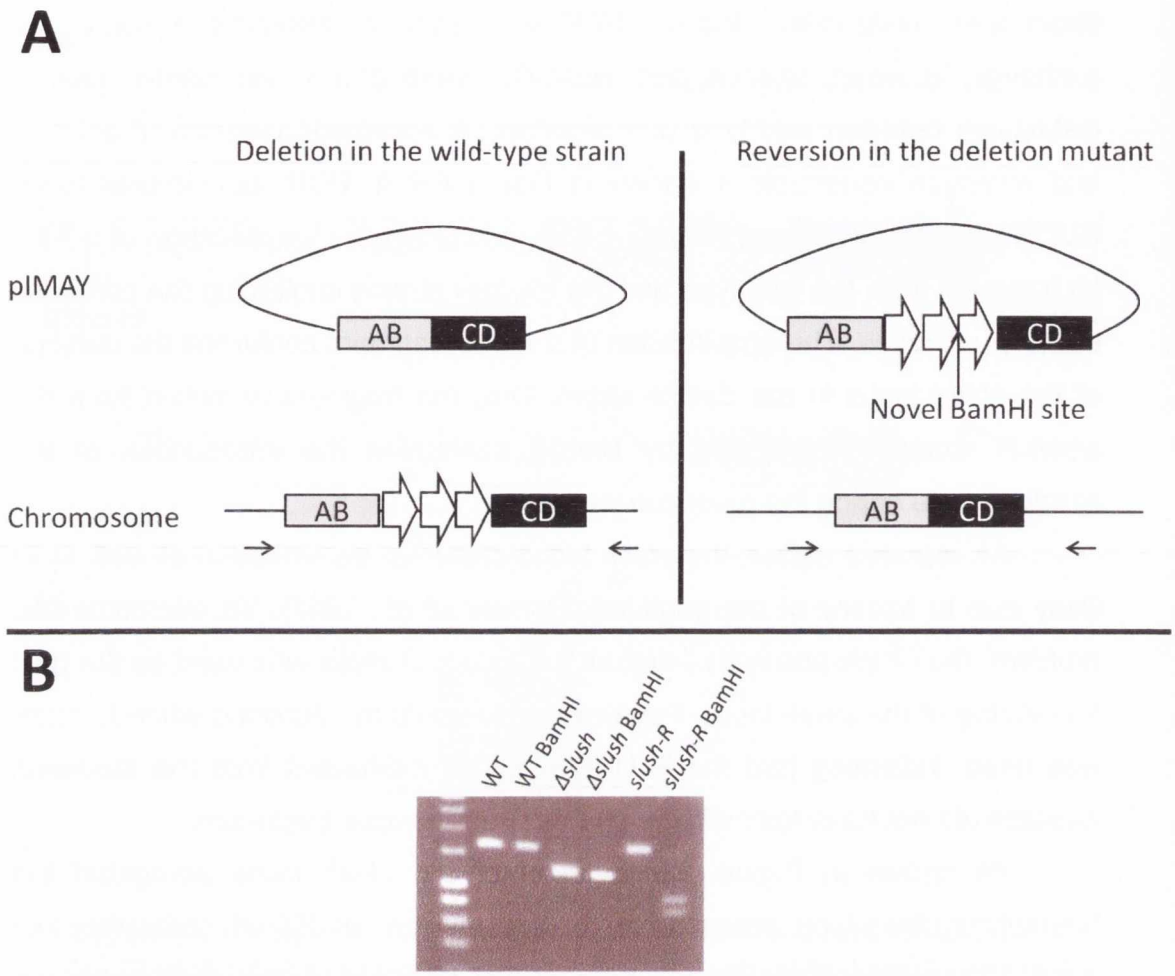

Figure 4.4 Deletion and reversion of the *slush* locus
(A) Schematic diagrams of the constructed deletion and reversion cassettes in pIMAY. Coding sequences for OrfX, SLUSH-A and SLUSH-B2 are indicated as white arrows. Integration and subsequent excision of the thermosensitive plasmid over the homologous sites AB and CD, respectively, allows the exchange of the chromosomal and plasmid based elements. Arrows indicate the location of screening primers to confirm the successful exchange of cassettes after excision. The novel restriction site in the reversion constructs allows discrimination of wild-type and reversion strains when the locus was deleted and subsequently restored. (B) Confirmation of SLUSH wild-type, deletion mutant and reversion strains. PCR products of wild-type, Δ*slush* and *slush*-reversion (*slush-R*) strains using screening primers as indicated in (A) were digested with BamHI as indicated on the lanes.

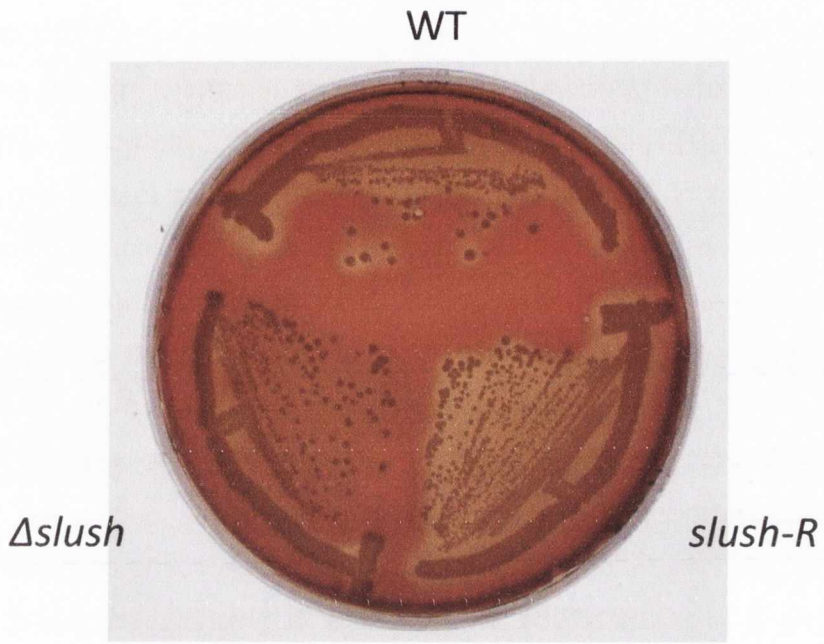

Figure 4.5 Haemolytic activity of *S. lugdunensis*
HKU09-01 wild-type, Δ*slush* and the chromosomal reversion *slush-R* were streaked on Columbia agar with 5% sheep erythrocytes and incubated for 48 h at 37°C.

Furthermore, the presence of the *atlI* gene (encoding a putative autolysin) within the locus is of special interest. The enzyme is suspected to influence the SrtB-dependent sorting of IsdC. To investigate this hypothesis, deletion mutants of *atlI* and *srtB* were constructed.

Here in TCD studies regarding localization and function of Isd proteins were performed by M. Zapotoczna. In order to investigate expression and cell surface-localization of *S. lugdunensis* Isd proteins, isogenic mutants of *isdB*, *isdJ* and *isdC* in N920143 were isolated. Studies by M. Zapotoczna confirmed that the *isd* locus of *S. lugdunensis* functions in a similar fashion to that of *S. aureus*. The Isd proteins were only expressed under iron-limited conditions. IsdB represents the single haemoglobin receptor of *S. lugdunensis* and transfers haem to IsdC. IsdB and IsdC were shown to be cell wall-anchored, while IsdJ and IsdK were located in the cytoplasmic membrane. The locus allowed growth of *S. lugdunensis* with haemoglobin as the sole source of nutrient iron. Furthermore the proteins were found to be specific for human haemoglobin and did not bind to the murine protein (Zapotoczna *et al.*, 2012a).

Experiments conducted by P. Speziale (University of Pavia, Italy) indicated a role for Isd proteins in *S. lugdunensis* biofilm formation, in particular IsdC. An *isdC* mutant of N920143 showed a significant reduction in biofilm formation. To verify this observation, a chromosomal reversion of *isdC* in the Δ*isdC* strain was constructed. *S. lugdunensis* strains N940113 and N940025 form high levels of biofilm. Deletion mutants were isolated to investigate the role of the different cell wall-anchored proteins in this process. The hypothesis that IsdC is of particular importance for biofilm formation will be tested using isogenic *ΔisdC* mutants of these two strains. Furthermore, strains deficient in all Isd proteins (*Δisd*) or Δ*srtA* were constructed to investigate the role Isd proteins and other cell wall-anchored molecules in biofilm formation.

All strains with mutations within *isd* genes created for collaborations are shown in Figure 4.6.

4.2.3 Mutants with defects within the wall teichoic acid glycosilation

A. Peschel (Tübingen, Germany) identified several unusual genes clustered with genes encoding the wall teichoic acid (WTA) biosynthesis enzymes. The genes encode putative glycosyltransferases that are presumably

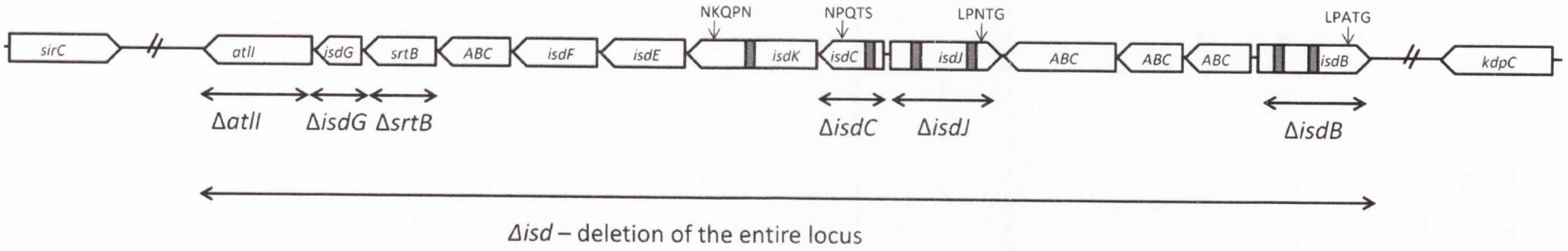

Figure 4.6 Mutations within the *isd* operon created for collaborations
A schematic diagram of the *isd* loci is shown. The open boxes denote individual genes and the arrows the direction of their transcription. Encoded NEAT motifs are shown as small black boxes. Angled dashes indicate the beginning and the end of the *isd* locus. Mutations created in individual strains are indicated by horizontal biheaded arrows.

involved in the glycosylation of WTA. WTA is known to be important for the nasal colonization of *S. aureus* (Weidenmaier *et al.*, 2004), for the coordination of autolysins during cell division (Biswas *et al.*, 2012), the resistance against antibacterial host defences (Kohler *et al.*, 2009; Peschel, 2002) and ß-lactam antibiotics (Brown *et al.*, 2012). Furthermore, WTA and its glycosilation are important for the recognition of *S. aureus* by bacteriophages (Xia *et al.*, 2011). In order to investigate phenotypes that are associated with the glycosylation of the *S. lugdunensis* WTA, deletion mutants were constructed in *tagO*, *tagN*, *tagEI* or *dltA* of N920143. Furthermore a Δ*tagN* Δ*tagE1* double mutant and a Δ*tagN* Δ*tagEI* Δ*dltA* triple mutant were constructed.

Discussion

Although *S. lugdunensis* is recognized as an important pathogen, hypothesis-driven research to identify virulence factors has been neglected and an efficient system for the transformation and genetic manipulation of this bacterium has not been available prior to this study. The comparison of different methods for the transformation of *S. lugdunensis* revealed that classical protocols used for the transformation of *S. aureus* (Augustin & Götz, 1990) did not allow the transformation of strain N920143. However, the method developed in this study which is based on the protocol established for *S. carnosus* did allow transformation. It has to be mentioned that a similar protocol used for the transformation of *S. aureus* and *S. epidermidis*, also allowed an improved transformation frequency (Monk *et al.*, 2012). Another advantage is that the preparation of cells is less time consuming and work intensive.

It was possible to transform *S. lugdunensis* strains from CC1, CC2 and CC5 with DNA derived from commonly used *E. coli* strains. CC3 and CC4 isolates were found to be more difficult to transform. Nevertheless sporadic transformants could be isolated even from these strains. The only restriction barrier in *S. lugdunensis* N920143 appears to be the Type I RM system SluI that was identified in this study. Deletion of the gene encoding the restriction endonuclease HsdR improved the efficiency of transformation with DNA derived from XL1-blue ~90-fold to the same frequency achieved with DNA derived from *S. lugdunensis.* This suggests that SluI is the only RM system in N920143.

I. Monk constructed the *E. coli* PAM strain SL01B which expresses the *hsdM/S* genes of N920143. The plasmid DNA isolated from this strain improved the transformation frequency of N920143 to the same level achieved with *S. lugdunensis* derived plasmid, confirming that SluI-mediated restriction was avoided.

Plasmid DNA isolated from SL01B allowed 10-90 fold higher transformation efficiency with CC1 and CC2 strains. This indicates that SluI is conserved among these isolates and represents the single restriction barrier. However, the investigation of additional strains would be needed to confirm that this is a general characteristic of all CC1 and CC2 isolates. For the CC1 and CC2 strains tested SL01B allowed streamlining of the transformation process by making the passage through the restriction-deficient Δ*hsdR* mutant obsolete. This will simplify future manipulation of these CCs.

Strain SL13 represented the only CC1 strain that could not be transformed with a higher frequency with SL01B-derived DNA compared to XL1-blue-derived DNA. The frequency of transformation with DNA isolated from XL1-blue was found to be 30-50 higher for SL13 than for the other strains of CC1, CC2. This suggests that no functional Type I RM is present in this isolates. SluI genes could be detected in SL13 and deleterious mutations could not be identified, suggesting that the genes are not expressed under the conditions used. However additional experiments are needed to verify this hypothesis.

Compared to the transformation frequency with XL1-blue-derived plasmid DNA, *S. lugdunensis* isolates from CC3, CC4 and CC5 could not be transformed with a higher frequency when SL01B-derived plasmid was used. This suggests that the specificity determinant of CC3, CC4 and CC5 recognizes a different sequence to that of CC1. The nature of the recognized pattern has yet to be determined. Differences in the specificity subunit of the Type I RM system appear to be the most likely explanation since such variations occur in different lineages of *S. aureus* (Corvaglia *et al.*, 2010; Roberts *et al.*, 2013; Waldron & Lindsay, 2006). Furthermore most *S. aureus* strains carry two different Type I RM systems (Corvaglia *et al.*, 2010; Holden *et al.*, 2004; Roberts *et al.*, 2013). Neither N920143 nor HKU09-01 encode two distinct Type I alleles but this possibility has to be considered for the CC5, CC3 and CC4

strains. Also, additional restriction systems of Type II-IV might be present in these CCs. Interestingly, plasmid DNA isolated from the *E. coli* cloning strain DC10B (*dcm*$^-$) did not improve transformation efficiency of any strain tested, indicating that the cytosine methylation pattern recognised by SauUSI is not relevant to this species. This distinguishes *S. lugdunensis* from *S. aureus* and *S. epidermidis* (Monk *et al.*, 2012).

Strains from CC3 and CC4 have proven to be difficult to transform. On average 10 - 100 times fewer transformants were obtained with CC3 and CC4 strains compared to CC1, CC2 and CC5 strains, suggesting the existence of a problem with the induction of competence. Strain-specific differences in the cell wall characteristics and in the expression of capsules (*S. lugdunensis* has the potential to produce polyglutamic acid and polysaccharide capsules) might impede the transfer of DNA by electroporation. In combination with a RM system this might reduce the transformation frequency.

The thermosensitive plasmid pIMAY (Monk *et al.*, 2012) has been constructed to create deletion mutations in *S. aureus* using allelic exchange. The protocol has now been optimized for use in *S. lugdunensis*. A particular advantage of pIMAY is the possibility to select plasmid integration at the optimal growth temperature of 37°C rather than the stress-inducing 42°C - 44°C needed for earlier vectors (Bae & Schneewind, 2006). This decreases the risk of selecting secondary mutations. The inducible counter selection (mediated by induction of anti-secY RNA) has been developed for *S. aureus* to simplify the selection of clones without plasmid (Bae & Schneewind, 2006; Monk *et al.*, 2012). It was found that the induction of *S. aureus* anti-secY did not result in selection of plasmid loss in *S. lugdunensis*, which is probably caused by the divergence within the *secY* genes. Therefore plasmid loss had to be screened manually when pIMAY was used. This process was simplified by use of the *lacZ*-encoding plasmid pIMAYZ. Observation of white colonies on X-Gal-agar was a reliable method for identifying plasmid-free colonies during the allelic exchange procedure.

The deletion constructs used in for the creation of mutations consisted of a 500 bp fragment upstream of the target gene and a 500 bp fragment downstream of the target gene. This size of homology was found to be sufficient for high frequency integration/excision of the plasmid into/from the bacterial

chromosome. In the deletion construct the start codon was fused to stop codon of the target gene. This approach promises minimal polar side effects after mutagenesis since the mutation does not interfere with promoter activity or translation of polycistronic transcripts, making the method favorable over the creation of mutations by insertion of genetic elements. The reinsertion of the target gene into the chromosome of a deletion mutant (reversion) represents a novel approach for the complementation of mutations. This method allows the expression of the target gene from its native promoter, thereby allowing a wild-type gene expression profile.

. Standard methods to complement mutations frequently involve plasmid-based gene expression. However, multicopy plasmids place a high physiological burden on the bacterial cells and antibiotic selection is necessary to maintain the plasmid over the course of an experiment. This entails problems in animal models where antibiotic selection is difficult. Furthermore, the presence of multiple plasmids within one cell creates a high dosage of the gene to be complemented, making the expression level difficult to control. Reversion of a chromosomal mutation overcomes these problems by the stable integration of the gene into the original chromosomal context. This allows wild-type level of expression and makes antibiotic selection redundant.

S. lugdunensis is increasingly recognized to be an important pathogen with interesting characteristics. The new genetic system described here has allowed genetic manipulation of several strains. Several mutations as well as reversal of mutations have been constructed for collaborators to facilitate projects investigating several *S. lugdunensis* potential virulence factors.

The *slush* locus of *S. lugdunensis* is of special interest. The deletion mutation showed that these peptides represent the only haemolytic toxins secreted by HKU09-01 under standard laboratory conditions. The locus has undergone genetic rearrangement in HKU09-01 resulting in the production of only two instead of three SLUSH peptides. Nonetheless, the locus in HKU09-01 has proven to be sufficient to create a haemolytic phenotype. It is suspected that these peptides fulfil important functions during infection and the Δ*slush* mutation and its reversion will allow a detailed characterization of the importance of the peptides *in vitro* and *in vivo.*

Chapter 5

S. lugdunensis cell wall-anchored proteins and their role in infective endocarditis

Introduction

Cell wall-anchored proteins (CWPs) of *S. aureus* are known to be important molecules in staphylococcal colonization and disease (Foster *et al.*, 2013). This has been demonstrated for several CWPs of *S. aureus* using various animal models of colonization and infection. The general approach of *in vivo* studies is the use of mutants deficient in a single protein. The comparison of mutant and wild-type allows determination of the importance of a single factor during infection. If possible the experiment should include the appropriate complementation. Such experiments identified the *S. aureus* MSCRAMM ClfA to be an important virulence factor in the development of endocarditis in a rat model (Moreillon *et al.*, 1995). Furthermore, a mouse systemic infection model showed that mutants deficient in SdrD, IsdB, ClfB, IsdA, IsdC, ClfA, Spa or SasG caused a tenfold reduced bacterial burden within the kidneys and mutants deficient in SdrD, IsdB, IsdA and Spa caused a smaller number of abscesses in this model (Cheng *et al.*, 2009). These experiments underline the importance of CWPs during infection. However, due to the functional redundancy the use of single mutants is not always applicable when *S. aureus* CWPs are studied. As an example, *S. aureus* encodes four fibrinogen (Fg) binding proteins (ClfA / ClfB / FnBPA / FnBPB). Consequently a single deletion of one of the genes does not result in the abrogation of Fg binding by *S. aureus*. To bypass this problem, CWPs were expressed on the surrogate non-virulent host *Lactococcus lactis*. The change in the phenotypic characteristics of *L. lactis* can subsequently be attributed to the single factor. This experimental setup identified the importance of FnBPA in experimental endocarditis (Que *et al.*, 2001; Que *et al.*, 2005) and highlighted the role of ClfB and its interaction with loricrin in nasal colonization (Mulcahy *et al.*, 2012).

In order to establish if CWPs are involved in infection, a mutant defective in sortase A can be used before attempts are undertaken to discover individual factors. The transpeptidase Sortase A catalyses the anchoring of CWPs to the bacterial cell wall. It recognizes the conserved LPXTG motif at the C-terminal end of the CWPs and attaches the proteins covalently to the peptidoglycan (PG). Accordingly, a deletion of *srtA* results in the abrogation of cell wall-sorting of all expressed CWPs (harbouring a LPXTG motif) simultaneously. Murine

infection models showed a strong decrease in virulence when *S. aureus* Newman (wild-type) was compared to the *srtA* deletion mutant. This included strongly decreased mortality in a systemic infection model and less severe disease in an experimental arthritis model (Jonsson *et al.*, 2002; Weiss *et al.*, 2004). Furthermore, *srtA* mutants were less virulent in experimental models of murine kidney infection and in an experimental, catheter-induced rat endocarditis model (Weiss *et al.*, 2004). These findings highlight the importance of correctly displayed CWPs for the establishment of infections. CWPs possess multiple functions ranging from adherence to host tissue (e.g. ClfA/B, FnBPA/B) to iron acquisition (IsdA/B/H) to immune evasion (e.g. Spa, ClfA). A mutation in sortase A impairs the combined functions of the CWPs, explaining the strong effect on virulence.

A mutation of *srtB* had little effect in the *S. aureus* infection models described above (Weiss *et al.*, 2004). This might be not surprising, since SrtB is only responsible for the cell wall-sorting of IsdC. Therefore the deletion of *srtB* is expected only to interfere with haem acquisition. Recent studies showed that the *S. aureus* Isd proteins specifically recognize human haemoglobin and bind poorly to the murine version (Pishchany *et al.*, 2010). This might explain why a *srtB* mutant did not display a defect in virulence in the murine models.

Earlier studies identified surface-anchored proteins of *S. lugdunensis*. Phage display experiments resulted in the identification of the fibrinogen binding protein of *S. lugdunensis* (Fbl – 94,7 kDa) (Nilsson *et al.*, 2004a). Fbl possesses just like ClfA of *S. aureus* and SdrG of *S. epidermidis* an N-terminal A region consisting of three independently folded subdomains (N1/N2/N3). The N2/N3 subdomains are predicted to comprise IgG-like folds. The A domain is followed by a stalk region. In ClfA and SdrG this consists of serine-aspartate (SD) repeats whereas in Fbl the repeats contain an alanine (SDSDSA) (Nilsson *et al.*, 2004a). Fbl promotes adherence to immobilized fibrinogen (Fg) and the N2/N3 domains were shown to be sufficient for Fg binding (Geoghegan *et al.*, 2010b). ClfA and Fbl show similar binding affinities to Fg and bind the ligand by the "dock, lock and latch" mechanism. Furthermore both MSCRAMMs bind to the C-terminal end of the fibrinogen γ-chain (Geoghegan *et al.*, 2010b). A schematic diagram of Fbl is shown in Figure 5.1.

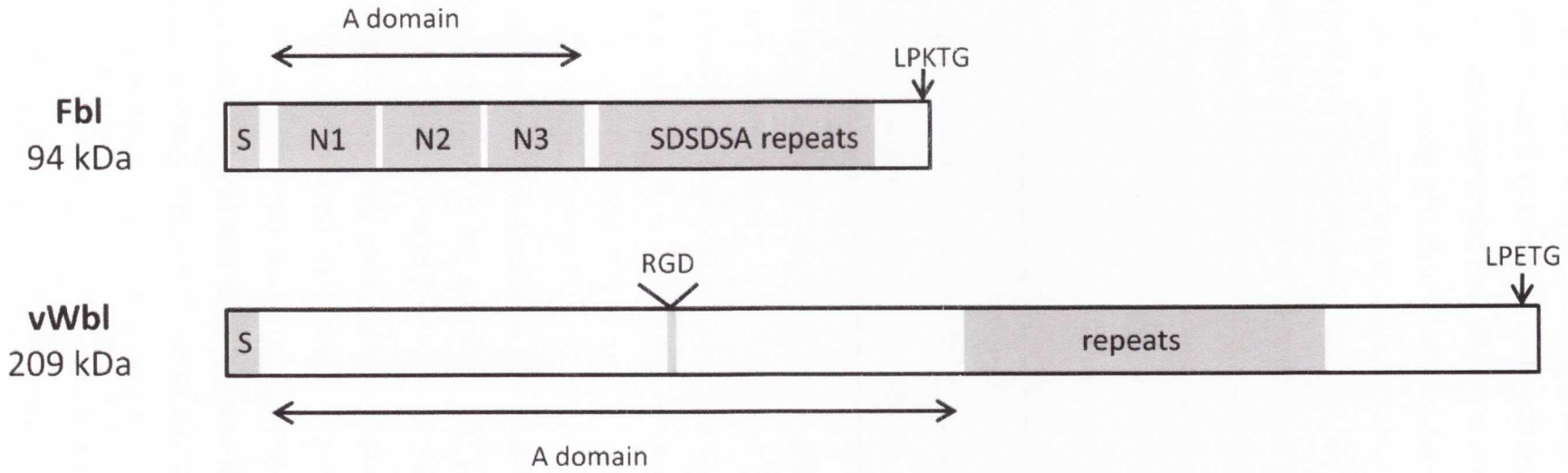

Figure 5.1 Schematic diagrams Fbl and vWbl
Predicted domains are indicated as grey boxes. N1 – domain of uncertain function; N2/N3 – fibrinogen binding IgG-like folds typical of MSCRAMMs; SDSDSA – repeats consisting of serine-aspartate-alanine; S-labelled boxes indicate the putative signal sequences.
A domains are indicated by biheaded arrows. Antibodies were produced against the recombinant A domain of $vWbl_{aa46\text{-}1200}$.

A von Willebrand factor-binding protein of *S. lugdunensis* (vWbl) has also been described (Nilsson *et al.*, 2004b). This 226 kDa LPXTG-anchored protein possesses a 1300 aa N-terminal A domain with an Arg-Gly-Asp (RGD) motif, followed by 10 highly similar repeats of 67 residues (Figure 5.1). The binding of vWbl to von Willebrand Factor (vWF) occurs at the C-terminal repeat region (Nilsson *et al.*, 2004b) although no detailed molecular model for the interaction is available. Furthermore only phage particles displaying parts of the vWbl on the surface bound to vWF. *S. lugdunensis* adherence to immobilized vWF was not tested and solid phase binding assays using recombinant vWbl were not carried out. A ligand for the A domain of vWbl has not been described but the presence of an RGD motive, which is found in several integrin-binding proteins such as fibronectin laminin or vWF (Ruoslahti & Pierschbacher, 1986), suggests the possibility that the A domain might promote adherence to eukaryotic cells (Nilsson *et al.*, 2004b). A schematic diagram of vWbl is shown in Figure 5.1.

Very little is known about the ability of *S. lugdunensis* to bind to human extra cellular matrix (ECM) proteins. Using iodine labelled protein binding assays, it was shown that most *S. lugdunensis* stains bound strongly to collagens type I and IV, with a lower affinity to laminin and vibronectin and weakly to fibronectin, thrombospondin, plasminogen and IgG (Paulsson *et al.*, 1993). The evaluation of the genome sequences of *S. lugdunensis* N920143 and HKU09-01 identified several putative cell surface-anchored proteins, possessing domain organizations that are unusual for staphylococci (Chapter 3). These proteins might promote adhesion to several ECM molecules.

Very little is known about the behaviour of *S. lugdunensis* in *in vivo* models. A mouse foreign-body abscess model (Ferguson *et al.*, 1991; Lambe *et al.*, 1990) and an implant associated foreign-body peritoneal infection model (Rozalska & Ljungh, 1995) have been used to investigate the pathogenicity of *S. lugdunensis*. Both models confirmed the virulence potential of the species. However, *S. lugdunensis* mutants have not been investigated and little is known about virulence factors and the molecular mechanisms of pathogenicity.

This chapter describes the characteristics of *S. lugdunensis* N920143 and of three isogenic mutants deficient in Fbl, vWbl or SrtA in a catheter-induced rat endocarditis model. Furthermore, the expression of various cell

surface-anchored proteins by different clinical *S. lugdunensis* isolates is described.

Results

5.1 Virulence of *S. lugdunensis* N920143 in a rat endocarditis model

Clinical reports suggest that *S. lugdunensis* is a virulent pathogen causing both native and prosthetic valve endocarditis (Frank *et al.*, 2008; Liu *et al.*, 2010). An animal model of *S. lugdunensis* endocarditis has not been reported previously. Therefore a rat model of catheter-induced endocarditis that is well established for *S. aureus* was used to compare the virulence of *S. lugdunensis* strain N920143 to *S. aureus* strains Newman (MSSA) and COL (MRSA). These experiments were carried out in collaboration with F. Hanses (Department of Internal Medicine I, University Hospital Regensburg, Germany). *S. lugdunensis* N920143 was chosen because the complete genome sequence is available (Heilbronner *et al.*, 2011) and it expresses Fbl (Mitchell *et al.*, 2004, Geoghegan *et al.*, 2010b). Fbl is related to ClfA of *S. aureus*, a known virulence factor in rat endocarditis caused by this organism (Moreillon *et al.*, 1995).

S. lugdunensis N920143 was capable of causing invective endocarditis in the rat model and all infected rats developed infected vegetations on the heart valves (Figure 5.2). Infection caused by *S. lugdunensis* N920143 seemed to be less severe than that caused by both *S. aureus* strains. Rats infected with N920143 displayed weaker symptoms than *S. aureus*-infected rats and most *S. lugdunensis*-infected animals were still alive at day 4 post infection. *S. aureus*-infected rats were either dead or had to be euthanized at day 3 post infection. Animals infected with N920143 consistently showed lower levels of bactereamia compared to both *S. aureus* strains (Figure 5.2 A). This might explain the milder course of disease and could be due to a more effective clearance of *S. lugdunensis* from the bloodstream as well as to less severe endocarditis.

Rats infected with *S. lugdunensis* N920143 had significantly fewer viable bacteria in their kidneys than animals infected with *S. aureus* strain Newman

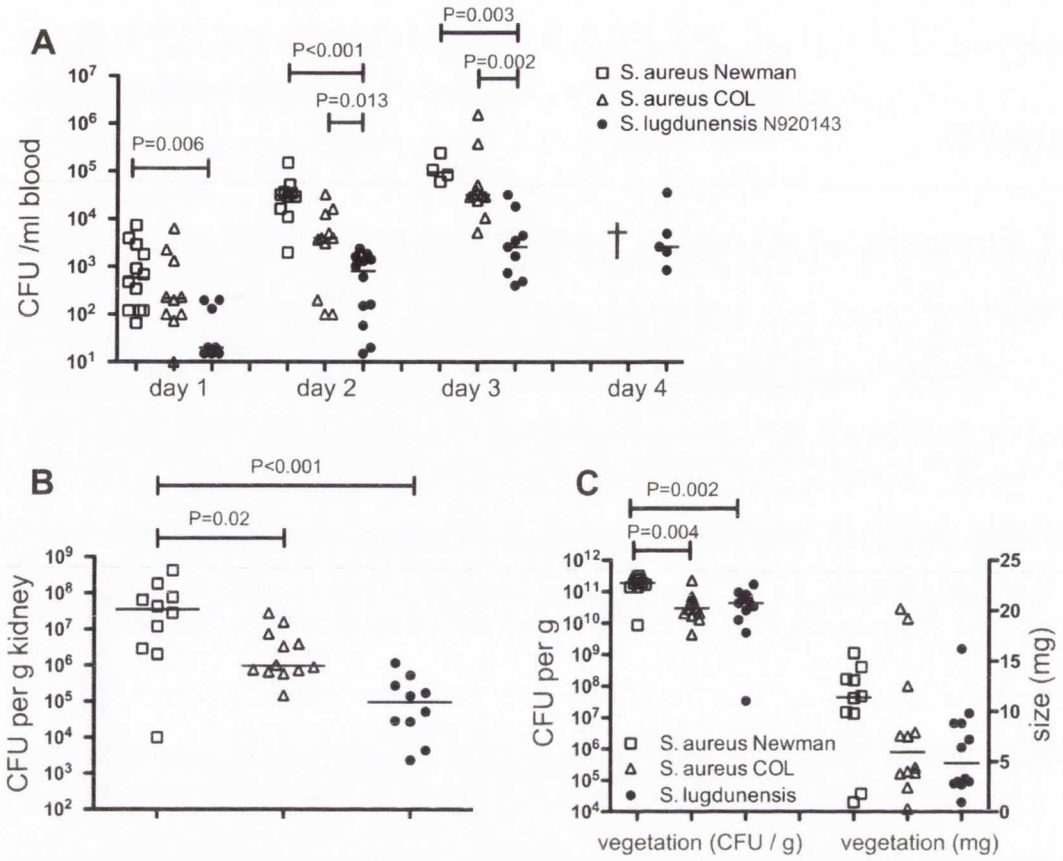

Figure 5.2 Virulence of *S. lugdunensis* compared to *S. aureus* in the catheter-induced rat endocarditis model

After placement of the catheter, rats were challenged with *S. aureus* or *S. lugdunensis*. The level of bactereamia was monitored every day. Rats were sacrificed after 3 days (*S. aureus*) or 4 days (*S. lugdunensis*) and the CFU in endocardial vegetations and kidneys were determined.

(A) CFU per ml blood up to day 4 after infection.

(B) CFU in kidneys at the end of the experiment (*S. aureus* - 3 days after infection; *S. lugdunensis* 4 days after infection)

(C) CFU in endocardial vegetations (*S. aureus* - 3 days after infection; *S. lugdunensis* 4 days after infection) Bacterial densities (CFU/g) and size of vegetations (mg) were compared to *S. aureus* Newman and to *S. aureus* COL.

The experiments were conducted by F. Hanses.

Number of infected animals were 10 for *S. aureus* Newman, 12 for *S. aureus* COL and 10 for *S. lugdunensis* N920143.

Statistical evaluation was performed using the Mann–Whitney U-test.

P-values <0.05 were regarded as significant and are indicated.

(Figure 5.2 B). Furthermore, the endocardial vegetations were smaller and bacterial densities in vegetations were lower (Figure 5.2 C). Interestingly, vegetations caused by *S. lugdunensis* N920143 and *S. aureus* strain COL were similar in size and bacterial density. Furthermore spreading of the bacteria to the kidneys was comparable between N920143 and *S. aureus* COL. In summary, *S. lugdunensis* N920143 was less virulent than either *S. aureus* strain with regard to the levels of bactereamia but formed comparable endocardial vegetations to *S. aureus* strain COL.

5.2 Importance of cell wall-anchored proteins during infective endocarditis

5.2.1 Deletion mutations in *fbl*, *vWbl* and *srtA*

In order to investigate the role of *S. lugdunensis* CWPs in the development of infective endocarditis (IE), pIMAY was used for the creation of deletion mutations in the genes encoding Fbl, vWbl and sortase A. In order to revert the mutation in *srtA* to wild-type, the allele exchange procedure was employed a second time. Using pIMAY, the *srtA* gene was reinserted at its original location in the chromosome (see the diagram in Chapter 4, Figure 4.4 for the reversion of the *slush* locus). A novel SmaI restriction site was introduced in *srtA* to distinguish between wild-type and revertant (*srtA-R*). Figure 5.3 shows SmaI-treated PCR products amplified from chromosomal DNA of the wild-type, the Δ*srtA* and the *srtA-R* strains. A 1.7 kb fragment was amplified from the wild-type strain containing the *srtA* coding sequence (0.7 kb) plus 0.5 kb flanking sequence on either side of the gene. A SmaI site was not present in the wild-type fragment. A 1 kb fragment (containing the flanking sequences only) without a SmaI site was amplified from the Δ*srtA* mutant, confirming the successful deletion of the gene. A 1.7 kb fragment (*srtA-R* plus flanking sequences) was amplified from the revertant, confirming the introduction *srtA-R*. The introduction of the silent mutation allowed SmaI digestion of this fragment.

5.2.2 Effects of the *srtA* deletion on CWP sorting

In order to test the veracity of the Δ*srtA* mutant, cell fractionation was performed. This method used lysostaphin and mutanolysin to degrade the cell wall in order to release CWPs into the supernatant. The resulting protoplasts were lysed to gain membrane and cytoplasmic fractions. The collected cell wall and membrane fractions were probed with antibodies to IsdB, a protein that is known to harbour an LPXTG motif and which is known be detectable in the cell wall fraction of iron-starved bacteria (Zapotoczna *et al.*, 2012a). Furthermore the fractions were probed for SrtA. In the wild-type sample an immunoreactive band of 70 kDa corresponding to IsdB was found exclusively in the wall fraction consistent with proper sorting and a protein of 27 kDa corresponding to SrtA was detected in the membrane fraction (Figure 5.4). This band was missing in the Δ*srtA* mutant and the IsdB protein was mis-localised in the membrane fraction. The IsdB protein in the Δ*srtA* mutant was slightly larger, most likely due to retention of residues C-terminal to the LPXTG sorting signal. In the reverted *srtA-R* strain IsdB and SrtA expression was the same as wild-type (Figure 5.4).

5.2.3 Validation of the *fbl* mutation

In order to validate the *fbl* deletion mutation, the expression of Fbl on the surface of the wild-type and mutant bacteria was assessed by whole cell immunoblotting using anti-Fbl serum (Mitchell *et al.*, 2004) (Figure 5.5 A). Fbl was detected on the surface of wild-type *S. lugdunensis* N920143 but was absent from the Δ*fbl* mutant. Fbl is known to promote adherence to Fg (Geoghegan *et al.*, 2010b; Mitchell *et al.*, 2004). Therefore whole cell adherence assays were carried out, using immobilized Fg (Figure 5.5 B). While the wild-type showed strong adherence to the immobilized ligand, the Δ*fbl* mutant was unable to adhere to Fg. This result validated the mutation in *fbl* and indicated that Fbl is the only CWP of *S. lugdunensis* N920143 that recognizes Fg under the conditions used.

However, all attempts to detect Fbl in membrane or cell wall fractions generated by the formation of protoplasts were unsuccessful, most likely due to proteolytic degradation (unpublished results and J. Geoghegan, personal communication).

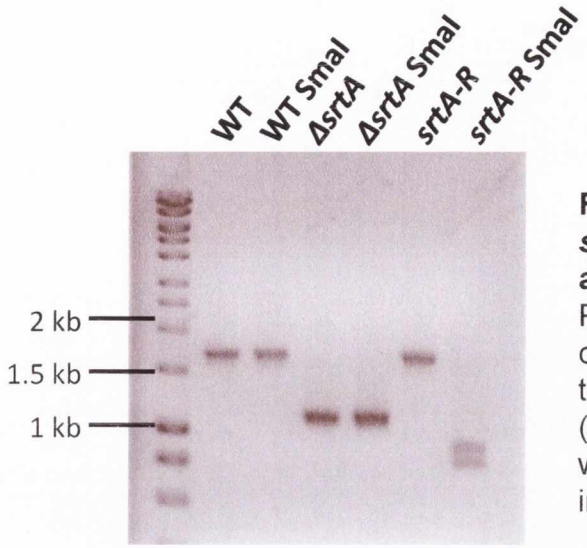

Figure 5.3 Confirmation of *srtA* wild-type, *ΔsrtA* mutant and *srtA-R* strains
PCR products of the *srtA* coding region using the wild-type, Δ*srtA* and *srtA*-reversion (*srtA-R*) strains. PCR products were SmaI-digested as indicated in the lanes.

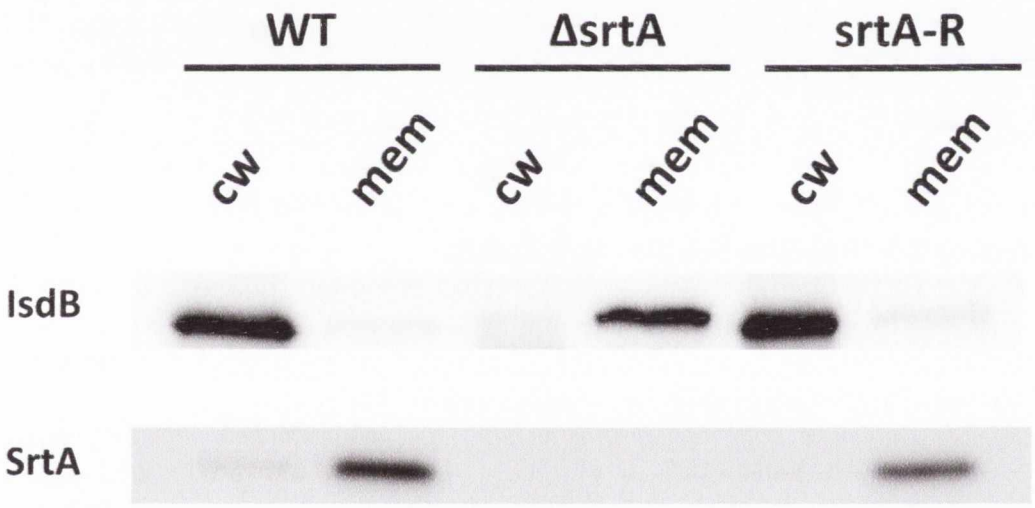

Figure 5.4 Western immunoblotting to confirm the SrtA mutation
Strains were grown to stationary phase, adjusted to OD_{578}= 5 and the cell wall was digested with lysostaphin in the presence of 0.5 M sucrose to stabilize the protoplasts. Cell wall and membrane fractions were formed, separated by SDS-PAGE and blotted onto a PVDF membrane. CW – cell wall fraction, mem – membrane fraction.
(A) Detection of IsdB using rabbit anti-IsdB IgG in cell fractions of *S. lugdunensis* N920143 grown in RPMI.
(B) Detection of SrtA using rabbit anti-SrtA in cell fractions of *S. lugdunensis* grown in TSB. Binding of primary antibodies was detected using goat anti-rabbit IgG-HRP.

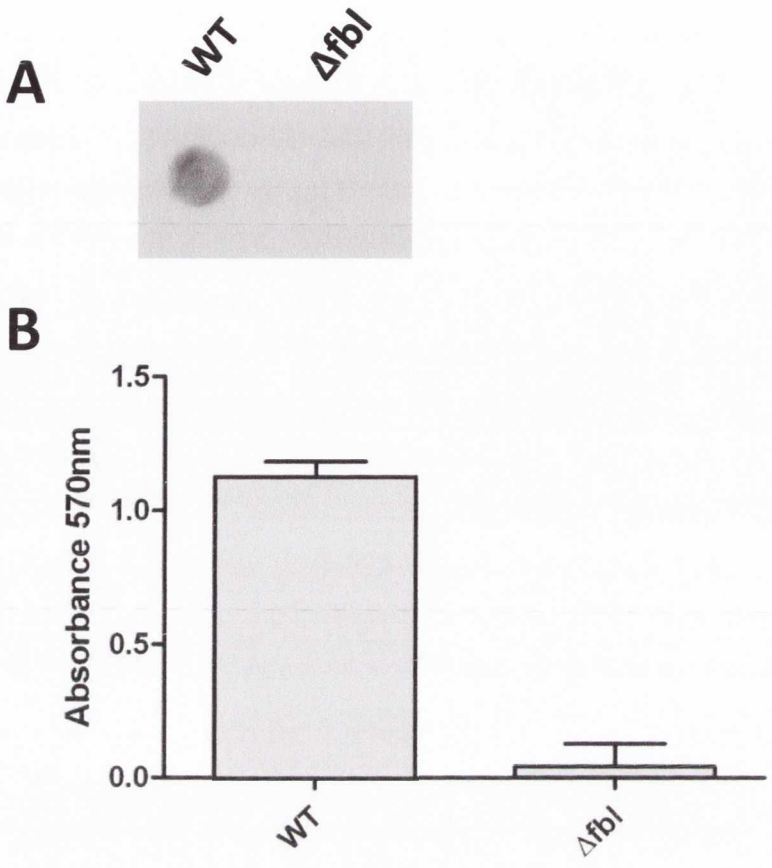

Figure 5.5 Validation of the *fbl* mutation

(A) Whole cell immunoblot. *S. lugdunensis* stationary phase cells were adjusted to OD_{578} = 1 and 5 µl of the suspension was dotted on a nitrocellulose membrane. Fbl was detected with rabbit anti-Fbl serum followed by goat anti-rabbit-IgG conjugated to HRP.

(B) Adherence of *S. lugdunensis* to immobilized fibrinogen. *S. lugdunensis* cells (100 µl of OD_{578} = 1) were added to wells of microtiter plates coated with human fibrinogen. Adhering cells were stained with crystal violet and the absorbance was measured in an ELISA plate reader at 570 nm. Values represent the mean and SEM of triplicate wells. The experiment was carried out three times with similar results.

5.2.4 vWbl expression

Antibodies were raised against the A domain of the vWbl (amino acids (aa) 46-1200, see Figure 5.1) and were used to probe *S. lugdunensis* for expression of the protein on the bacterial cell surface. Expression of the protein by strain N920143 could not be detected by whole cell immunoblotting or cell fractionation and Western immunoblotting. Neither a change in growth phase (stationary or exponential) nor culture medium (TSB or RPMI) led to detectable vWbl expression *in vitro* (data not shown). To investigate whether this is a common feature among *S. lugdunensis* strains, or whether it is a characteristic of strain N920143, eleven *S. lugdunensis* clinical isolates were chosen for examination of vWbl expression using whole cell immunoblotting. Only two of the strains displayed detectable protein on the cell surface (Figure 5.6). However, none of the strains adhered to immobilized human vWF (data not shown). This leaves the N920143 Δ*vWbl* mutant without a detectable phenotype in *in vitro* experiments and raises the question whether vWbl is indeed a vWF binding protein when displayed on the cell surface of *S. lugdunensis*.

5.3 *S. lugdunensis* mutants in the rat endocarditis model

To assess the relative contribution of Fbl, vWbl and SrtA in *S. lugdunensis* endocarditis, the isogenic mutants were tested in the rat endocarditis model. A trend towards a reduced virulence was observed for each of the mutants compared to the parental strain. However, differences reached the level of significance only for the Δ*srtA* strain (Figure 5.7 and Figure 5.8).

The *srtA* mutant of *S. lugdunensis* showed significant defects in virulence including reduced bactereamia (Figure 5.7 A), reduced bacterial spreading to the kidneys (Figure 5.7 B) and reduced size / density of endocardial vegetations (Figure 5.7 C). This highlights the importance of LPXTG-anchored proteins in pathogenesis.

Mutants defective in individual surface proteins Fbl and vWbl were not significantly different from the wild-type (Figure 5.8). However there were trends towards reduced virulence observed for both mutants. An interesting observation is that the development of endocardial vegetations appears to be an all-or-nothing phenomenon. Either the infected rats developed vegetations of

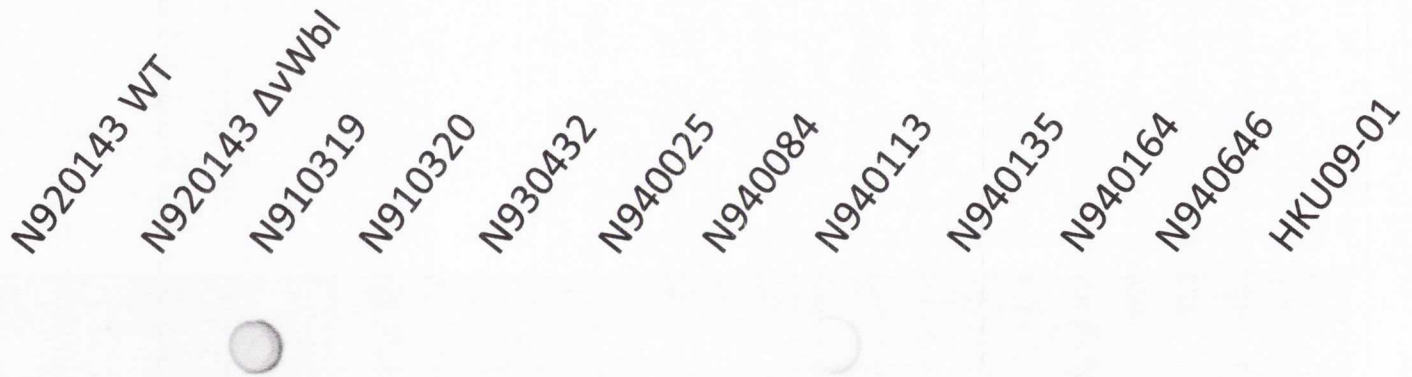

Figure 5.6 vWbl expression of *S. lugdunensis* clinical isolates
Whole-cell immunoblotting. *S. lugdunensis* stationary phase cells were adjusted to OD_{578} = 1 and 5 µl of the suspension was dotted on a nitrocellulose membrane. vWbl was detected with mouse anti-vWbl serum followed by rabbit anti-mouse-IgG conjugated to HRP.
Expression in exponential phase did not change and is not shown.

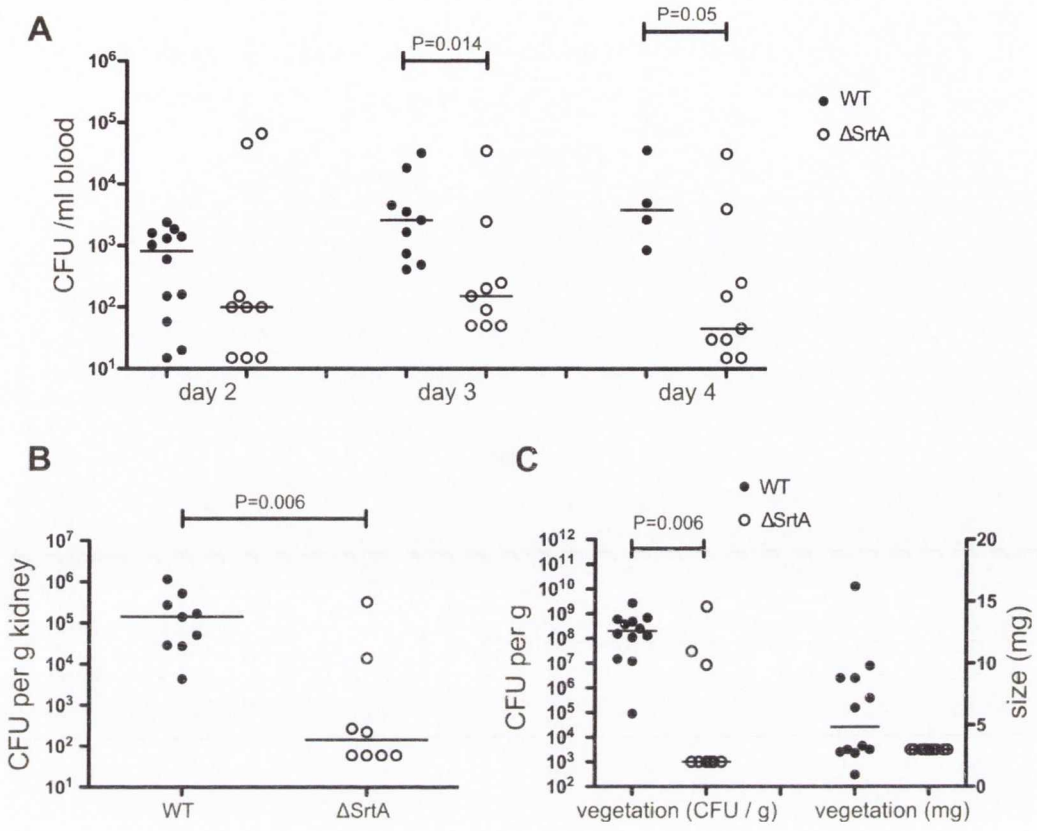

Figure 5.7 Virulence of *S. lugdunensis* Δ*srtA* in the catheter-induced rat endocarditis model

After placement of the catheter, rats were challenged with *S. lugdunensis*. The level of bactereamia was monitored every day. Rats were sacrificed after 4 days and the CFU in endocardial vegetations and kidneys were determined.

(A) CFU per ml blood up to day 4 after infection.

(B) CFU in kidneys.

(C) CFU in endocardial vegetations. Bacterial densities (CFU/g) and size of vegetations (mg) formed by N920143 wild-type and Δ*srtA* mutant.

The experiments were conducted by F. Hanses.

Nine animals were infected with each *S. lugdunensis* strain.

Statistical evaluation was performed using the Mann–Whitney U-test.

P-values <0.05 were regarded as significant and are indicated.

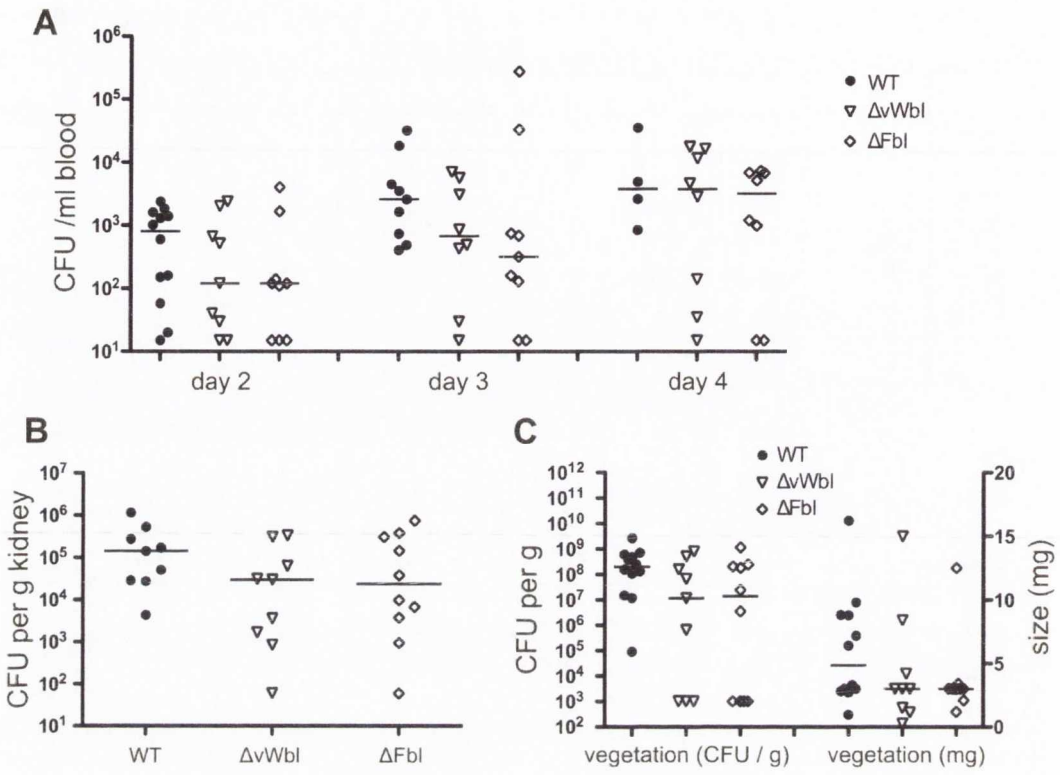

Figure 5.8 Virulence of *S. lugdunensis* Δ*vWbl* and Δ*fbl* mutants in the catheter-induced rat endocarditis model

After placement of the catheter, rats were challenged with *S. lugdunensis*. The level of bactereamia was monitored every day. Rats were sacrificed after 4 days and the CFU in endocardial vegetations and kidneys were determined.

(A) CFU per ml blood up to day 4 after infection.

(B) CFU in kidneys.

(C) CFU in endocardial vegetations. Bacterial densities (CFU/g) and size of vegetations (mg) formed by N920143 wild-type, Δ*vWbl* and Δ*fbl*.

The experiments were conducted by F. Hanses.

Nine animals were infected with each *S. lugdunensis* strain.

Statistical evaluation was performed using the Mann–Whitney U-test.

P-values <0.05 were regarded as significant.

similar size and density to the wild-type, or they did not infect heart valve detectably. This was particularly noticeable with the Δ*srtA* mutant where 66% of rats did not develop detectable endocardial vegetations. In comparison 33% of rats infected with Δ*vWbl* and Δ*fbl* failed to establish a thrombus on the heart valve while not a single rat maintained sterile vegetations ($<10^{-3}$ CFU) when infected with the wild-type strain.

5.4 Expression of *S. lugdunensis* cell wall-anchored proteins and adherence to various ligands

5.4.1 Expression of *S. lugdunensis* cell wall-anchored proteins

As described in Chapter 3, *S. lugdunensis* N920143 and HKU09-01 harbour eleven genes with the potential to encode SrtA-anchored, cell surface-exposed proteins. The A regions (Figure 5.9) of the proteins SlsD (aa 230-610), SlsE (aa 46-800), SlsF (aa 42-778) and SlsG (aa 48-920) were expressed using the expression plasmid pQE30. The vector added an N-terminal hexa-histidine tag to the recombinant protein to aid purification. The recombinant proteins $rSlsD_{230-610}$, $rSlsE_{46-800}$, $rSlsF_{42-778}$ and $rSlsG_{48-920}$ were purified and used for antibody production.

Eleven *S. lugdunensis* clinical isolates from the TCD collection were investigated for the expression of the CWPs. The strains were grown to either stationary or exponential phase and the expression of CWPs was investigated using whole cell immunoblotting. The levels of expression of SlsE, SlsF and SlsG differed strongly between the strains (Figure 5.10), suggesting a strain-dependent regulation of expression. The general expression level seemed to be higher in exponential phase. However, quantification of the expression levels was not performed. N940164 was the only strain that expressed SlsF on the cell surface in these experiments.

5.4.2 Adherence of *S. lugdunensis* strains to various ECM molecules

In order to Identify ECM molecules that might serve as ligands for *S. lugdunensis*, a range of different molecules (cytokeratin 10, fibronectin, fibrinogen, loricrin, vWF, human/bovine albumin) were used in bacterial adherence assays. Surprisingly, with the exception of fibrinogen, none of the

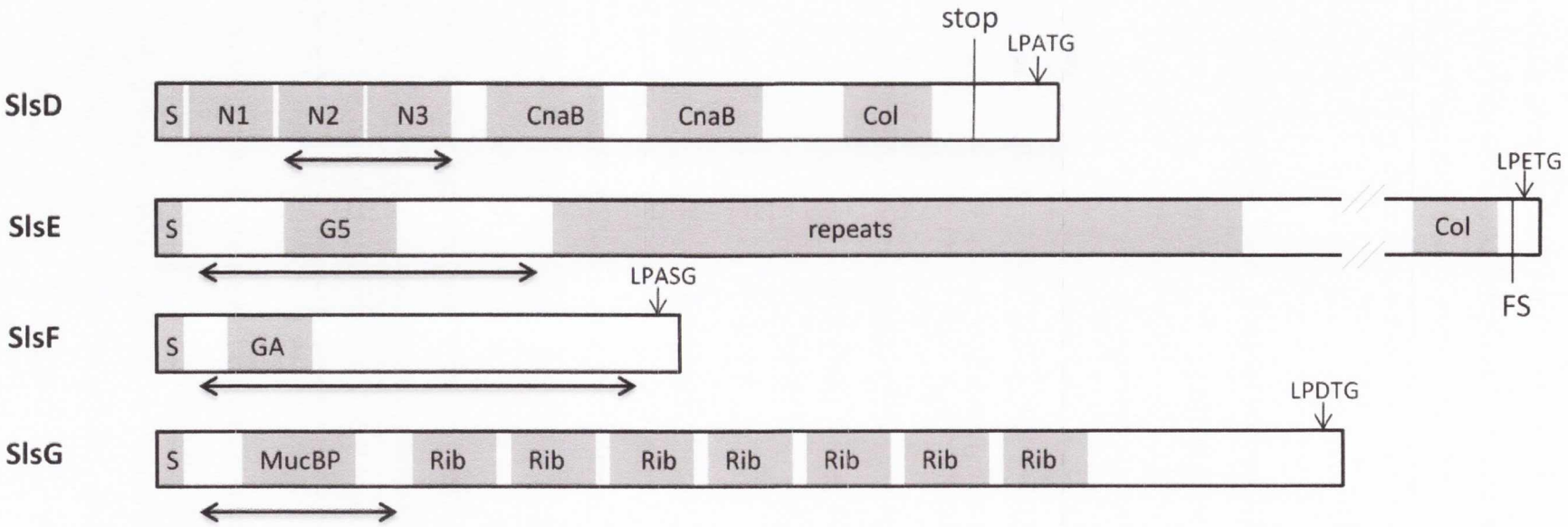

Figure 5.9 Schematic diagrams of *S. lugdunensis* CWPs used for antibody production
Predicted domains are indicated as grey boxes. N1 – domain of uncertain function; N2/N3 – fibrinogen binding IgG-like folds of MSCRAMMs; CnaB – B-repeat of Cna; GA – GA module; Ig – IgG-like fold; Col – Collagen triple helix repeat; G5 – G5 domain; MucBP – mucin binding domain; Rib – Rib like repeat; FS – frameshift; See Chapter 3 for predicted functions of the various domains. S-labeled boxes indicate the putative signal sequences. Biheaded arrows indicated the A domains used for the expression of recombinant protein.

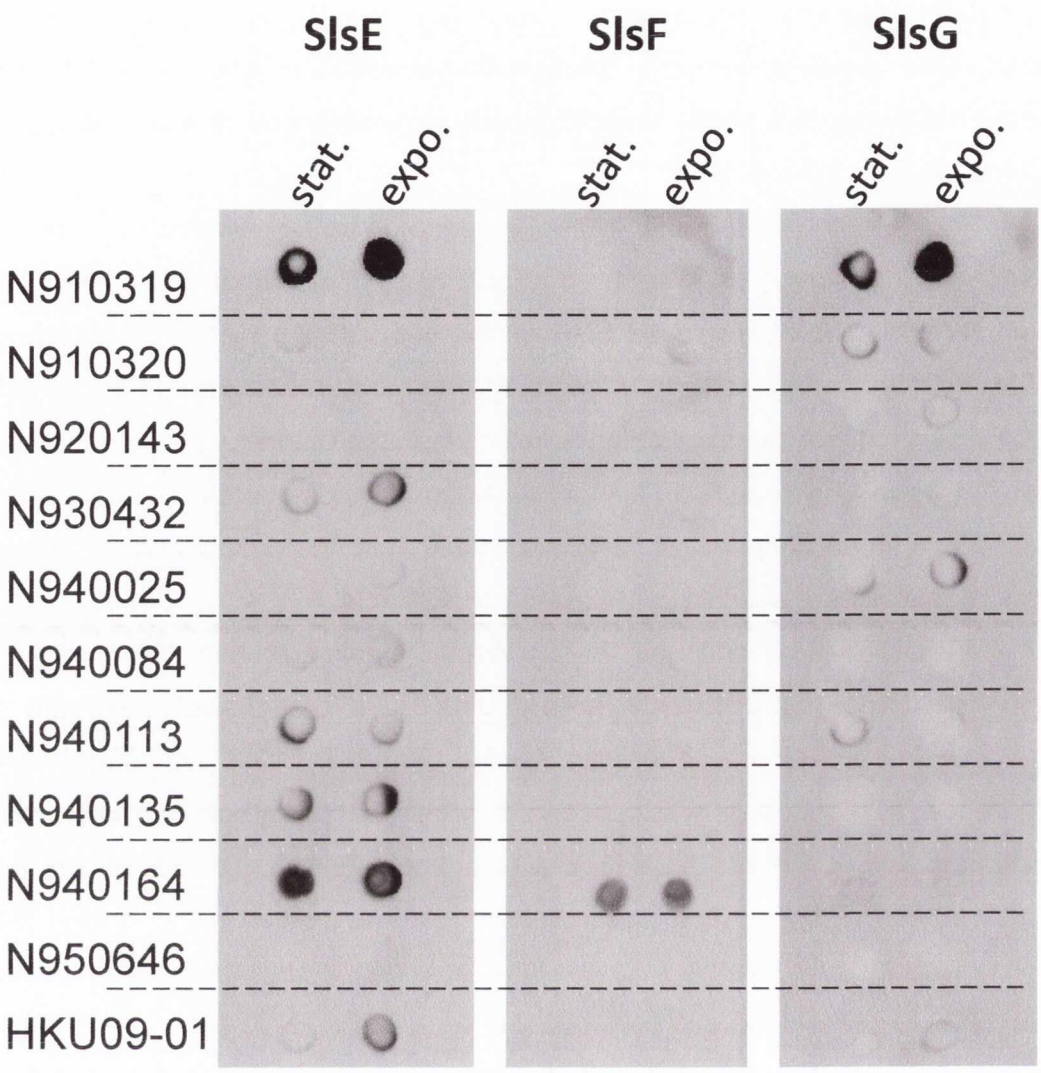

Figure 5.10 Whole cell immunoblot to detect CWP expression of various *S. lugdunensis* strains

S. lugdunensis cells were adjusted to OD_{578} = 1 and 5 µl of the suspension was dotted on a nitrocellulose membrane. SlsE, SlsF and SlsD were detected with specific mouse serum followed by rabbit anti-mouse-IgG conjugated to HRP.

stat. – stationary phase cells; expo. – exponential phase cells.

S. lugdunensis strains displayed adherence to any of the ligands used in these experiments (data not shown). Effective immobilization was confirmed by the use of the *S. aureus* strain SH1000 which adhered to all ligands except for albumin (data not shown).

The GA domain of SlsF was suggested to be an albumin binding domain, yet none of the strains used adhered to albumin (either human or bovine). The strain N940164 which displayed SlsF on the cell surface (Figure 5.10) did not adhere to albumin in these experiments. Furthermore, recombinant SlsF protein ($rSlsF_{42-778}$) did not bind to albumin in solid phase binding assays (data not shown) suggesting that SlsF is not an albumin binding protein. Importantly, successful immobilisation of albumin could not be confirmed in these experiments since a positive control was not available.

S. lugdunensis encodes the fibrinogen binding protein Fbl. However, apart from strain N920143 only three strains (27,2 %) adhered detectably to fibrinogen in solid phase adherence assays (Figure 5.11 A). No difference in adherence to fibrinogen was observed when stationary phase cells were compared to exponential phase cells (data not shown). To investigate this phenomenon, Fbl surface expression was assessed by whole cell immunoblotting. Interestingly Fbl was detectable on the cell surface of all strains tested and in general the expression levels seemed higher in exponential phase (Figure 5.11 B). This suggested that the failure to adhere to fibrinogen is rather caused by properties of the encoded Fbl than by strain-specific differences in expression. The nucleotide sequences of two *fbl* alleles are available. N920143, a strain which displays strong Fbl-dependent adherence to fibrinogen (see Figure 5.5) and HKU09-01, a strain which expresses Fbl but does not display detectable fibrinogen binding (Figure 5.10). A comparison of Fbl of the two strains revealed that the entire N-terminal regions encompassing the fibrinogen binding N2/N3 domains (Geoghegan *et al.*, 2010b) are 100% identical. This suggests that both encoded proteins could bind to fibrinogen by the same mechanism. However, a major difference was observed in the putative stalk regions of the proteins. Fbl of N920143 possesses 14 perfect DSDSDADSDSDADSDS repeats (224 residues) while Fbl of HKU09-01 possesses only 5 imperfect repeats (74 residues) which would result in a significantly smaller protein. The size of the stalk region is known to be

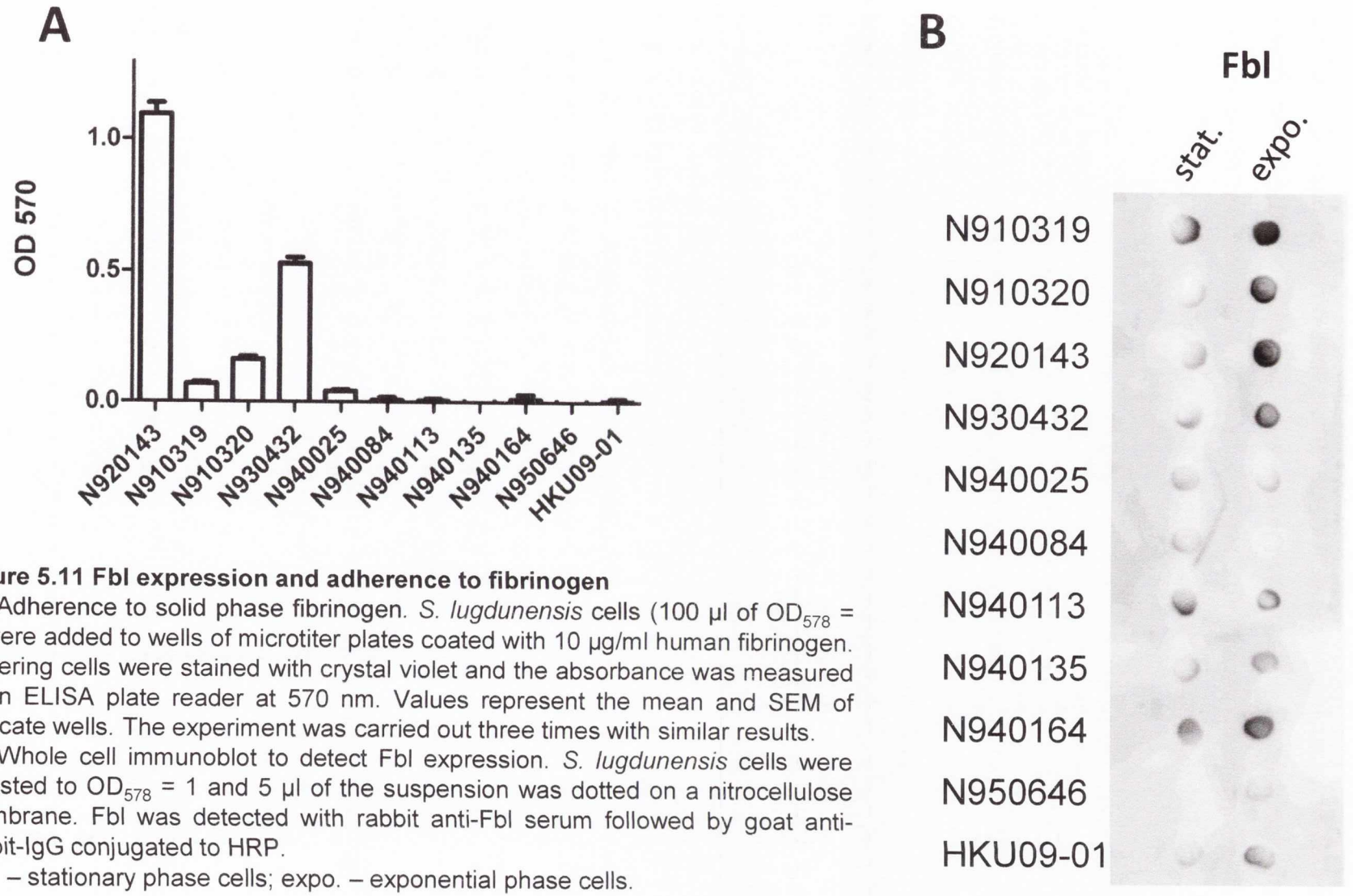

Figure 5.11 FbI expression and adherence to fibrinogen

(A) Adherence to solid phase fibrinogen. *S. lugdunensis* cells (100 µl of OD_{578} = 1) were added to wells of microtiter plates coated with 10 µg/ml human fibrinogen. Adhering cells were stained with crystal violet and the absorbance was measured in an ELISA plate reader at 570 nm. Values represent the mean and SEM of triplicate wells. The experiment was carried out three times with similar results.

(B) Whole cell immunoblot to detect FbI expression. *S. lugdunensis* cells were adjusted to OD_{578} = 1 and 5 µl of the suspension was dotted on a nitrocellulose membrane. FbI was detected with rabbit anti-FbI serum followed by goat anti-rabbit-IgG conjugated to HRP.

stat. – stationary phase cells; expo. – exponential phase cells.

important for the functional surface display of cell wall-anchored proteins (Hartford *et al.*, 1997; Strauss & Götz, 1996). Thus it can be proposed that the short stalk region of Fbl is in part a reason for the failure of HKU09-01 to adhere to fibrinogen. However, experiments with different strains expressing various length Fbl proteins are needed to verify this hypothesis.

5.4.3 Investigation of SlsD

As described in Chapter 3, *slsD* of *S. lugdunensis* encodes a second putative fibrinogen binding protein. The amino acid sequence of the N-terminal A domain (aa 50 – 612) shares homology with Fbl (23 % identity / 40% similar) and analysis of the putative three dimensional structure predicted N2/N3 domain organization. The *slsD* coding sequence possesses a conserved nonsense mutation upstream of the region encoding the LPXTG anchoring motif in both N920143 and HKU09-01. This should prevent the anchoring of the protein to the peptidoglycan.

In order to investigate whether SlsD is indeed a fibrinogen binding protein, Surface expression of SlsD was investigated using whole cell immunoblotting (Figure 5.12). Two out of eleven strains (N930432 and N940164) expressed SlsD detectably on the cell surface. Sequencing of the location where the nonsense mutation is present in N920143 and HKU09-01 revealed that the mutation was conserved in all isolates except for the two strains showing SlsD surface-expression (N930432 and N940164) along with N950646 (Figure 5.13). The latter strain did not express SlsD although the nonsense mutation was not present. This might be explained by a different regulation of SlsD expression or by the presence of nonsense / frame-shift mutation at a different location, but was not further investigated.

As described above, most *S. lugdunensis* strains expressed Fbl on the cell surface but only a few were able to adhere to solid phase Fg. Strain N930432 was the only strain of the TCD collection which displayed adherence to fibrinogen and expressed both Fbl and SlsD on the cell surface. To examine whether the adherence of this strain was dependent on Fbl or SlsD, a Δ*fbl* mutant was constructed in N930432 using pIMAY. Fbl was not detectable on the cell surface of the mutant strain, while SlsD was still expressed (Figure 5.14 A). However, deletion of Fbl abrogated adherence to fibrinogen, suggesting that

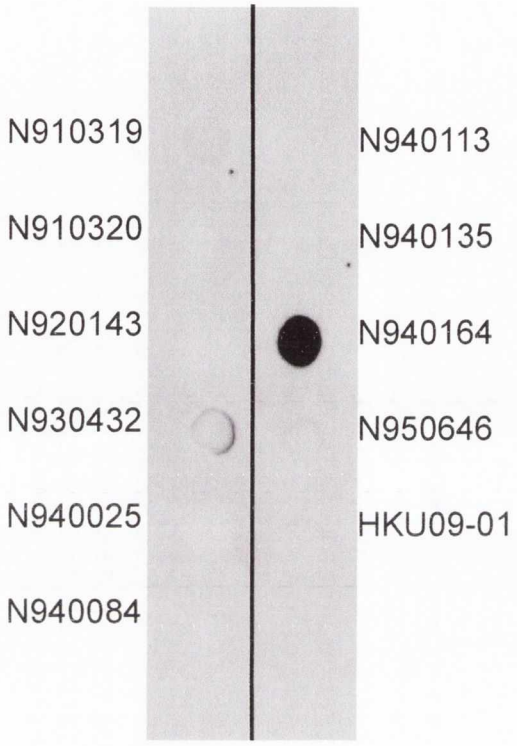

5.12 Whole cell immuno dot blotting for SlsD expression

S. lugdunensis stationary phase cells were adjusted to OD_{578} = 1 and 5 µl of the suspension was dotted on a nitrocellulose membrane. SlsD was detected with mouse anti-SlsD serum, followed by rabbit anti-mouse-IgG conjugated to HRP.

Expression in exponential phase did not change and is not shown.

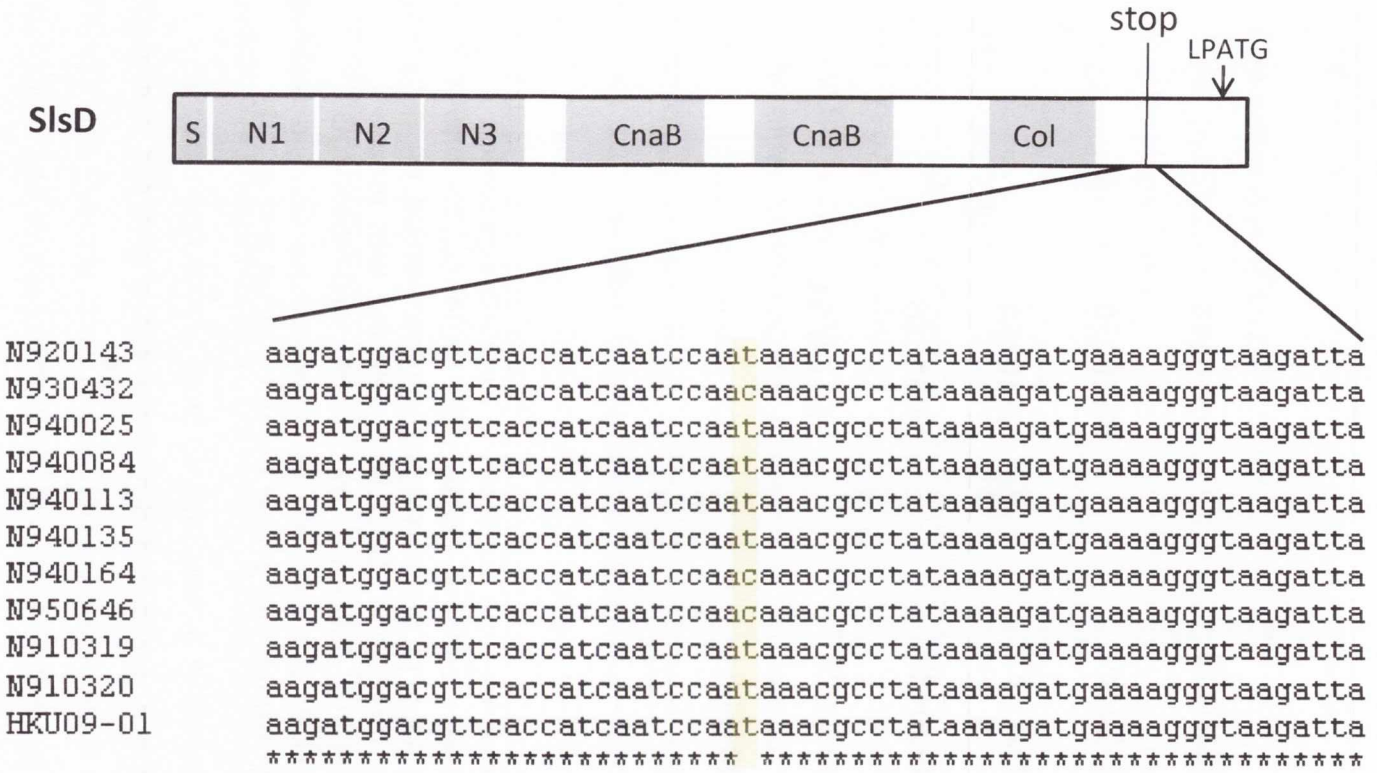

5.13 Detection of the nonsense mutation in various *S. lugdunensis* strains
The upper part shows a schematic diagram of SlsD. The lower part shows the *slsD* sequences of *S. lugdunensis* strains. Only the region containing the nonsense mutation is shown. The location of the nonsense mutation is highlighted.

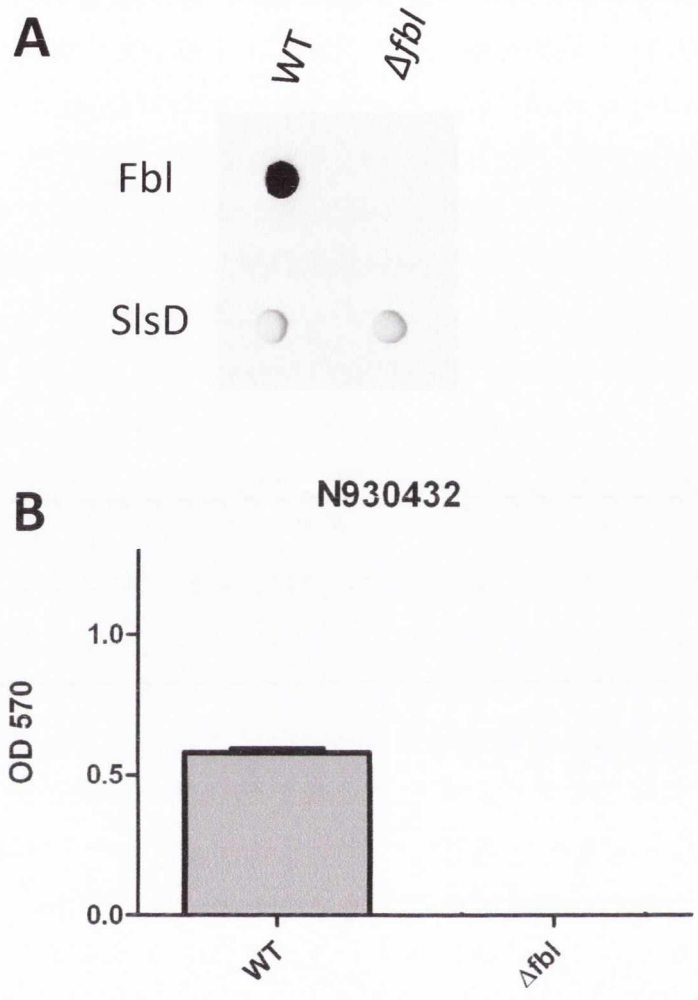

5.14 Expression of SlsD by strain N930432

(A) Whole cell immunoblot for SlsD and Fbl expression. *S. lugdunensis* stationary phase cells were adjusted to OD_{578} = 1 and 5 µl of the suspension was dotted on a nitrocellulose membrane. SlsD was detected with mouse anti-SlsD serum, Fbl was detected with rabbit anti-Fbl serum. Primary antibodies were detected by rabbit anti-mouse-IgG conjugated to HRP or goat anti-rabbit-IgG conjugated to HRP, respectively.

(B) Adherence to immobilized fibrinogen. *S. lugdunensis* cells (100 µl of OD_{578} = 1) were added to wells of microtiter plates coated with 10 µg/ml human Fg. Adhering cells were stained with crystal violet and the absorbance was measured in an ELISA plate reader at 570 nm. Values represent the mean and SEM of triplicate wells. The experiment was carried out three times with similar results.

Fbl and not SlsD was responsible for the adherence to fibrinogen by N930432 (Figure 5.14 B).

The *slsD* gene of N920143 possesses a nonsense mutation that is likely to prevent cell wall-anchoring of the protein. However, the truncated protein could be detected in N920143 culture supernatants (Figure 5.15 A). To assess, whether SlsD of N920143 possesses the capacity to promote adherence to fibrinogen, the nonsense mutation was reverted to wild-type in the Δ*fbl* strain of N920143. Plasmid pIMAY was used to replace the single nucleotide (TAA-CAA) within the *slsD* gene of N920143 Δ*fbl* by allelic exchange. The N920143 wild-type strain expressed Fbl but not SlsD on the cell surface. The Δ*fbl* strain expressed neither of the proteins while the Δ*fbl* *slsD*$^+$ strain expressed only SlsD on the cell surface (Figure 5.15 B). Furthermore the truncated SlsD protein disappeared from the culture supernatant in the Δ*fbl* *slsD*$^+$ strain (Figure 5.15 A). However, expression of surface associated SlsD had no impact on adherence of bacteria to fibrinogen. The deletion of Fbl abolished adherence to Fg and this was not restored by surface expression of SlsD (Figure 5.15 C). The experiments suggest that SlsD does not possess the capacity to bind fibrinogen. These results were supported by solid phase fibrinogen binding assays using recombinant SlsD. The rSlsD$_{230\text{-}610}$ protein contained the N2/N3 domain which corresponds to be the minimum Fg binding domain of SdrG. However, rSlsD$_{230\text{-}610}$ did not bind to fibrinogen in these assays (data not shown). The N2/N3 domains of Fbl bind strongly to Fg (Geoghegan *et al.*, 2010b). Recombinant Fbl (rFbl$_{205\text{-}533}$) was kindly provided by J. Geoghegan and served as a positive control to confirm the functionality of the assay.

Discussion

Several case studies described *S. lugdunensis* as an important opportunistic pathogen that is associated with severe cases of IE in humans (Carpenter *et al.*, 2012; Cevasco & Haime, 2012; Chung *et al.*, 2012; Sibal *et al.*, 2011; Stair *et al.*, 2012). Although infections are infrequent, it is remarkable that *S. lugdunensis* is associated with native valve endocarditis showing fulminant and a highly destructive clinical course. This distinguishes *S. lugdunensis* from

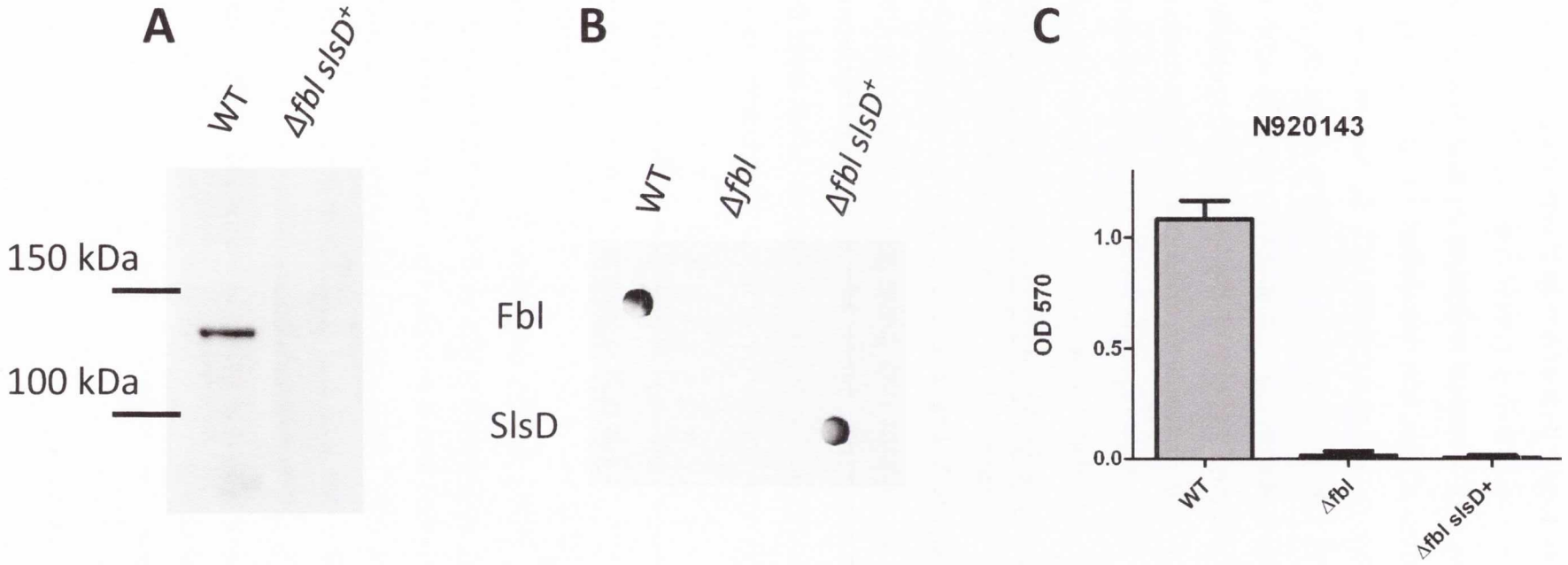

5.15 Expression of SlsD by strain N920143

(A) Western blot using concentrated cell culture supernatants. Proteins in the supernatants were separated by SDS-PAGE and blotted onto a PVDF membrane. SlsD was detected with mouse anti-SlsD serum followed by rabbit anti-mouse-IgG conjugated to HRP.

(B) Whole cell immunoblot for SlsD and Fbl expression. *S. lugdunensis* stationary phase cells were adjusted to OD_{578} = 1 and 5 µl of the suspension was dotted onto a nitrocellulose membrane. SlsD was detected with mouse anti-SlsD serum, Fbl was detected with rabbit anti-Fbl IgG. Primary antibodies were detected by rabbit anti-mouse-IgG conjugated to HRP or goat anti-rabbit-IgG conjugated to HRP, respectively.

(C) Adherence to immobilized Fg. *S. lugdunensis* cells (100 µl of OD_{578} = 1) were added to wells of microtiter plates coated with 10 µg/ml human Fg. Adhering cells were stained with crystal violet and the absorbance was measured in an ELISA plate reader at 570 nm. Values represent the mean and SEM of triplicate wells. The experiment was carried out three times with similar results.

the other CoNS which are normally primarily associated with prosthetic valve endocarditis (Frank *et al.*, 2008; Huebner & Goldmann, 1999).

For the first time, the virulence of a clinical isolate of *S. lugdunensis* was investigated in a rat endocarditis model and compared to two strains of *S. aureus*. Interestingly, *S. lugdunensis* strain N920143 did not display an elevated degree of virulence in this experimental model. In contrast, rats infected with N920143 survived longer and displayed lower levels of bactereamia than *S. aureus*-infected rats. In general, the level of bactereamia is regarded to be a good indication for the severity of endocarditis, since bacteria are constantly being released from the vegetation into the blood stream. However, reduced bactereamia and mortality in *S. lugdunensis*-infected rats could reflect differences in the clearance of bacteria from the blood stream rather than differences in the endocardial infections. Regarding immune evasion, a more effective clearance of *S. lugdunensis* seems a likely possibility. The analysis of two genome sequences has given some insight into the virulence potential of this species and genes encoding orthologues of *S. aureus* toxins and immune evasion factors were not detected. Altogether the virulence potential of *S. lugdunensis* compared to *S. aureus* seems to be limited.

Regarding size and density of the vegetations formed, *S. lugdunensis* showed similar characteristics to *S. aureus* COL. However, *S. aureus* Newman caused significantly bigger vegetations. It would be interesting to compare several other clinical isolates of *S. lugdunensis* with *S. aureus* to draw conclusions about virulence of *S. lugdunensis* in this model. In addition, it has to be considered that the rat endocarditis model might not be ideally suited for this organism. *S. lugdunensis* is the only CoNS with an iron responsive surface determinant locus (Isd), encoding cell wall-anchored haem-binding proteins, membrane transporters and a haem degrading monoxygenase. In *S. aureus*, this locus permits the utilization of haemoglobin as a source of nutrient iron. Recent studies by Haley *et. al.* (Haley *et al.*, 2011) and Zapotoczna *et al.* (Zapotoczna *et al.*, 2012a) showed that the Isd system in *S. lugdunensis* is active and functions in a similar fashion to that of *S. aureus*. However, the *S. lugdunensis* IsdB protein specifically binds human haemoglobin and has a low affinity for the rodent version (Zapotoczna *et al.*, 2012a). As a result,

S. lugdunensis cannot use mouse haemoglobin as a source of nutrient iron (Pishchany *et al.*, 2010; Zapotoczna *et al.*, 2012a). This might also be true for rat haemoglobin, since the α- and β-chains of mouse and rat haemoglobin show >84% sequence identity. In contrast the *S. aureus* Isd system is capable of using mouse haemoglobin, although not as efficiently as the human variant (Pishchany *et al.*, 2010). This adaption to the human host might help to explain the rather low virulence of *S. lugdunensis* N920143 in the rat infection model. It is important to underline that a single *S. lugdunensis* strain (N920143) was used in the endocarditis experiments. This strain was chosen since it represents a clinical isolate that expresses Fbl. However, the observed characteristics in the rat endocarditis model might represent strain specific characteristics rather than characteristics of the entire species. Additional *S. lugdunensis* isolates should be tested in the rat endocarditis model to investigate whether the species *S. lugdunensis* can be regarded as less virulent than *S. aureus*.

The importance of LPXTG-anchored proteins as virulence factors has been recognized (Que *et al.*, 2001; Que *et al.*, 2005). The expression of the *S. aureus* surface protein ClfA by *Lactococcus lactis* leads to increased virulence in an experimental rat endocarditis model (Moreillon *et al.*, 1995). Mutants of *S. aureus* deficient in sortase A displayed strongly reduced virulence in various infection models including experimental sepsis and infective endocarditis (Jonsson *et al.*, 2003; Weiss *et al.*, 2004). *srtA* mutants were recently discussed as vaccine candidates due to the attenuated but still immune-stimulating phenotype (Kim *et al.*, 2011). Here the *srtA* mutant of *S. lugdunensis* showed significant defects in virulence including reduced bacteraemia, reduced bacterial spreading to the kidneys and reduced size/density of endocardial vegetations. This highlights the importance of LPXTG-anchored proteins in pathogenesis.

The *S. lugdunensis* CWPs Fbl and vWbl bind to fibrinogen and von Willebrand Factor, respectively. Both ligands are important effector molecules in the blood clotting cascade making an involvement of Fbl and vWbl in the adherence to damaged heart tissue and the subsequent development of IE likely. Mutants defective in individual surface proteins Fbl and vWbl were not significantly less virulent than the wild-type, although trends towards reduced virulence were observed. This suggests that several surface proteins act in

concert to promote adhesion to the thrombus and possibly survival in the bloodstream. However, as soon as the thrombus on the heart valve is formed, surface proteins might only play a minor role and size and density develops independently.

Knowledge of the function of *S. lugdunensis* surface proteins is limited. Apart from fibrinogen for Fbl, von Willebrand Factor for vWbl and haem/haemoglobin for Isd proteins, no ligands have been identified for the remaining proteins. The experiments performed in this study failed to identify ECM molecules that serve as ligands for *S. lugdunensis* cell wall-anchored proteins. The potential ligands investigated in this study included ligands that are known to be important for *S. aureus* including fibronectin, cytokeratin 10 and loricrin. However, none of the *S. lugdunensis* strains in the TCD collection adhered to these molecules. The vWbl protein was reported to bind human vWF (Nilsson *et al.*, 2004b). The protein was not expressed detectably under *in vitro* conditions by most isolates tested, including N920143. Only two out of eleven strains expressed the protein on the cell surface *in vitro.* However, expression of the protein did not mediate adherence to immobilized human vWF. Earlier studies (Nilsson *et al.*, 2004b) reported that the C-terminal repeat region of vWbl binds to vWF, which is unusual. Normally the ligand binding domain is located within the N-terminal A domain of CWPs (Speziale *et al.*, 2009). C-terminal repeat regions are common in cell wall-anchored proteins. However, their function is usually to act as a stalk between the LPXTG cell wall anchor and the ligand binding domain. The stalk regions are needed so that proteins can bypass peptidoglycan and expose the ligand binding domain on the cell surface. The only exceptions known are the FnBPs of *S. aureus* where Fn binding is promoted by the repeat region (Schwarz-Linek *et al.*, 2003). Regarding vWbl it is conceivable that the repeat region is buried within the cell wall of *S. lugdunensis* and cannot promote adhesion to vWF. Perhaps vWbl binds to other ligands *in vivo*.

The adherence to fibrinogen promoted by Fbl might be influenced by the length of the stalk region. It is known that the presence of the *fbl* gene is a general characteristic of *S. lugdunensis* and PCR amplification of *fbl* has been proposed as an identification method for this species (Chatzigeorgiou *et al.*, 2010; Pereira *et al.*, 2010). Marlinghaus *et. al.* (Marlinghaus *et al.*, 2012) report

the presence of *fbl* in all of the 104 isolates in their study. Although Fbl is known to bind Fg, Marlinghaus *et. al.* reported that only 28% of their strains adhered to the ligand. Similar results were obtained when the *S. lugdunensis* strains of the TCD collection were tested for their ability to adhere to solid phase fibrinogen. However the experiments performed in this study showed that Fbl is detectable on the cell surface of most *S. lugdunensis* strains investigated although quantification of Fbl expression has not been performed, limiting the conclusions that can be drawn. However, strain-specific differences in the amino acid sequences of Fbl might account for the failure of some strains to bind to Fg. Comparing the *fbl* alleles of N920143 (strong adherence to Fg) and HKU09-01 (no adherence to Fg) revealed the only difference to be in the length of the stalk region. It was shown for ClfA of *S. aureus* that 60-110 residues in the stalk region are necessary for the functional display of the protein on the cell surface (Hartford *et al.*, 1997). The stalk of Fbl from N920143 possesses 224 residues while HKU09-01 possesses merely 74 residues. It is conceivable that differences in the length of the Fbl stalk regions are responsible for the different abilities of the strains to adhere to fibrinogen. However, additional experiments are necessary to validate this hypothesis.

Chapter 6
Duplication and amplification of the *isd* operon in HKU09-01

Introduction

Gene duplication and amplification (GDA) is a common genetic event that is known to occur in all three kingdoms of life (Romero & Palacios, 1997; Sandegren & Andersson, 2009) and is more and more recognised to be of fundamental evolutionary importance (Bergthorsson *et al.*, 2007; Näsvall *et al.*, 2012). GDA contributes to several human diseases, to phenotypic variation and to human susceptibility to infectious diseases (Beckmann *et al.*, 2007; Conrad & Antonarakis, 2007).

GDA events have best been studied in Gram-negative model organisms such as *Escherichia coli* (Andersson *et al.*, 1998) and *Salmonella species* (Anderson & Roth, 1981). Tandem repeat duplications are found in virtually all regions of the chromosome (Anderson & Roth, 1981) with the size of repeats ranging from a few kilobases up to several megabases (Sandegren & Andersson, 2009). The frequency of duplications seems to be high with an estimated 10% of cells in a bacterial culture carrying a duplication somewhere in the chromosome (Koch, 1987). The genetic mechanism for the creation of GDA is well described and involves non-equal homologous recombination mediated by RecA (Sandegren & Andersson, 2009). The repetitive sequences required for RecA-dependent recombination can be provided by short nucleotide repeats in different genes, ribosomal RNA operons (*rrn*) (Anderson & Roth, 1981), insertion sequences or transposable elements (Bertini *et al.*, 2007; Chandler *et al.*, 1979; Nicoloff *et al.*, 2007). During the replication of the bacterial chromosome, the two sister chromatids remain in close proximity for a short period of time. The RecA protein recognises homologous sequences (normally 100 or more nucleotides in length) upstream and downstream of the target sequence and promotes recombination. Thereby the target sequence is duplicated (Figure 6.1 A). The frequency of this recombination is dependent on the length of the homologous flanking sequences and has to be determined for every duplication separately. *In vitro*, the frequency of duplications in a bacterial culture can be measured using phage transduction assays. In *S. typhimurium* the frequency was found to vary between 10^{-2} and 10^{-5} per cell per generation (Pettersson *et al.*, 2009). Duplications arising without repeated sequences at the junction points are observed as well and arise in a RecA-independent

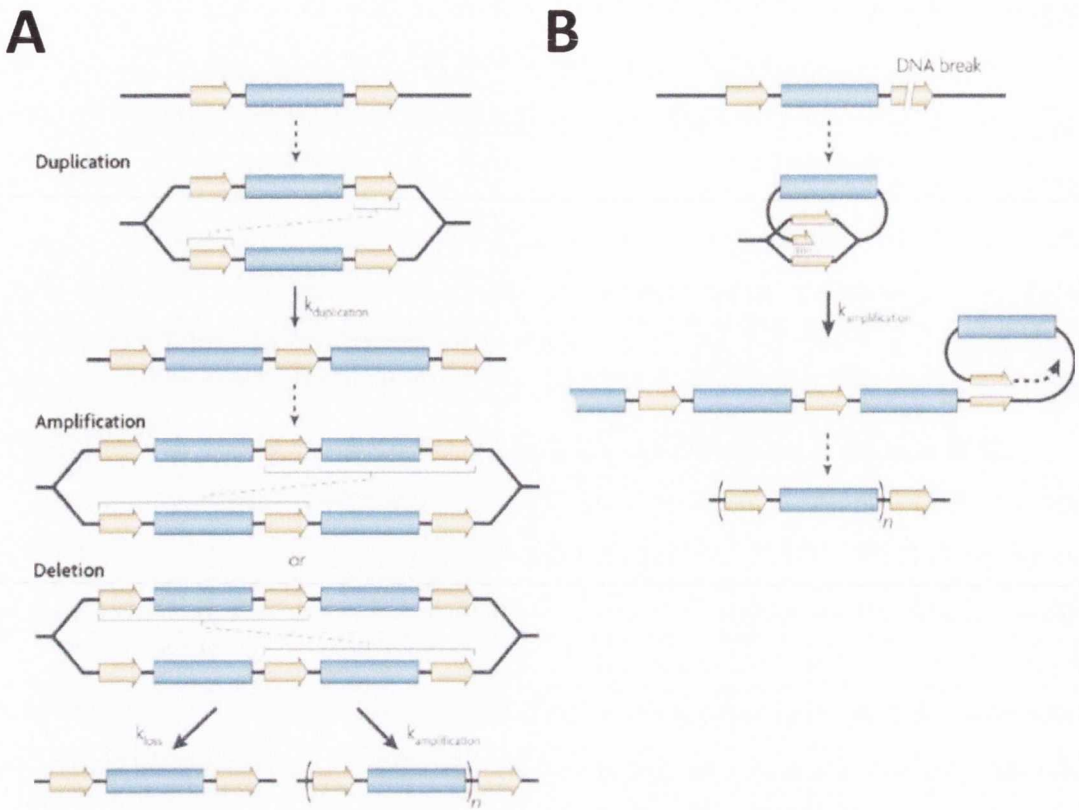

Figure 6.1 Mechanisms of gene duplication and amplification (GDA)
(A) Duplication occurs either through non-equal homologous recombination between directly orientated repeats or through RecA-independent mechanisms between short- or no-homology regions.
(B) GDA through rolling circle replication. A double-strand break allows single-strand invasion at a homologous or microhomologous site followed by replication.
Horizontal arrows denote regions of homology (long or short) involved in recombination (dashed lines) between sister chromatids that forms the initial duplication. Horizontal square brackets indicate the size of the region of homology. Vertical arrows denote the rate of formation of the initial duplication ($k_{duplication}$), the rate of further amplification ($k_{amplification}$) and loss of amplification or duplication (k_{loss}). The thickness of vertical arrows indicates relative rates of formation and loss. The region in vertical brackets denotes the amplified unit.
Adapted from (Sandegren & Andersson, 2009)

manner (Sandegren & Andersson, 2009). However, after the primary duplication event, long perfect tandem repeats are available and allow RecA-dependent amplification and the corresponding loss of the duplication (segregation) with a much higher frequency. Loss rates can be as high as 0.01-0.15 per cell per generation (Koch, 1987; Pettersson *et al.*, 2009).

Alternatively, higher level amplifications can arise without duplication intermediates by mechanisms based on rolling circle replication. This mechanism requires the RecA-dependent repair of double-strand breaks using the replication fork. Thereby it is possible to create long tandem arrays in a single generation (Figure 6.1 B) (Koch, 1987; Petit *et al.*, 1992).

A special function of GDAs is seen in the development of resistance to antibacterial agents (Sandegren & Andersson, 2009). Commonly encountered mechanisms of acquiring resistance against antibacterial drugs involve horizontal transfer of resistance determinants or spontaneous point mutations. However, GDAs confer resistance by increasing the gene dosage of antibiotic modifying enzymes (Clewell *et al.*, 1975; Yagi & Clewell, 1976), of the target gene (Min *et al.*, 2008; Yoon *et al.*, 2008), of unrelated genes (Nilsson *et al.*, 2006) and of drug efflux pumps (Nicoloff *et al.*, 2006; Nicoloff *et al.*, 2007). Resistance is often acquired in two steps. Firstly, the resistance mechanism is acquired by horizontal gene transfer and confers resistance with concomitant loss of bacterial fitness. Secondly, additional genetic changes compensate the loss of fitness. Those changes can include GDAs of the resistance determinant or of unrelated genes (Nilsson *et al.*, 2006).

In general GDAs have significant effects on protein expression due to increased gene dosage. A physiological burden is inherent in this. When the selective pressure that provides an advantage to cells with increased expression is absent, the GDA will rapidly be lost from the culture (Sandegren & Andersson, 2009). Because of their transient nature, some GDAs can be compared to regulatory responses rather than to permanent adaptive mutations (Sandegren & Andersson, 2009). One example is a study conducted in *S. aureus* (Morikawa *et al.*, 2012). Although *S. aureus* possesses Sigma Factor H (SigH)-controlled competence genes, bacteria do not take up extracellular DNA due to the lack of SigH expression under laboratory conditions. A tandem repeat duplication at the location of *sigH* can place one copy of the gene in a

new genomic context. A new promoter region becomes available to allow expression of SigH and subsequently the expression of competence genes. This duplication can be regarded as a strategy to allow a small subset of cells in a bacterial culture to take up extracellular DNA and extend genomic diversity.

Very little is known about the natural occurrence of GDAs in the chromosome of bacterial pathogens and their effects on the ability to cause disease. In *Vibrio cholera* the *ctxA* and *ctxB* genes encoding the two cholera toxin subunits are duplicated in many clinical isolates. This correlates with increased toxin production by these strains. Furthermore, the toxin locus was amplified during passage *in vivo*, going along with higher toxin expression (Goldberg & Mekalanos, 1986; Mekalanos, 1983). This raises the possibility that the duplication and amplification of virulence factors might play an important role for pathogens to adapt to *in vivo* growth. The *capB* locus of *Haemophilus influenzae* is another example. Most invasive isolates carry an amplified *capB* locus and the increased copy number correlates with an increase in invasiveness (Cerquetti *et al.*, 2006) and a decrease in complement mediated killing and opsonisation (Kroll *et al.*, 1991; Noel *et al.*, 1996). It was also noted that strains isolated from children who suffered vaccination failure possessed a higher copy number of the capsule locus (Cerquetti *et al.*, 2005) than strains isolated from the control group. Therefore duplication and amplification of the *capB* locus is regarded as a strategy to avoid host immune defences.

GDAs are also implicated in evolutionary processes. In 1988 Cairns *et al.* described an observation named "adaptive mutability" (Cairns *et al.*, 1988). The model described the high frequency of reversion of a *lac* frameshift mutation when the bacteria were grown with lactose as the sole carbon source. It was proposed that bacteria alter the level of target-specific mutability as part of their response to stress. It was suggested that bacteria direct mutability to selectively valuable sites (Boe, 1990; Foster & Cairns, 1992; Hall, 1990). Alternatively it was proposed that stress might induce a general hypermutable state (Torkelson *et al.*, 1997) but none of the proposed models explained all observations (Rosenberg *et al.*, 1998). Andersson *et al.* introduced a model to explain "adaptive mutability" involving GDA (Andersson *et al.*, 1998).

As discussed above, the duplication of chromosomal regions occurs randomly using repetitive sequences. However, only environmental pressure

will provide a growth advantage for the cells displaying a higher level of protein expression and the duplication becomes established within the population. As a result coding sequences of helpful proteins are present in increased numbers and provide long template sequences for mutations to occur. This allows mutations to be acquired at a higher frequency, improving the functions of proteins and making the increased gene dosage unnecessary. Subsequently, the amplified structure will collapse and only the improved gene copy will remain. Additionally, any harmful effects of point mutations (frameshifts and nonsense mutations as well as mutations decreasing protein function) are absorbed by GDAs since multiple copies are available and inactivated copies can be removed by recombination. Thus, GDAs serve as an efficient genetic tool to improve rapidly the function of selected genes. This could be shown using a *S. typhimurium* model (Andersson *et al.*, 1998; Kugelberg *et al.*, 2006). A *lac*$^-$ strain (harbouring a frameshift mutation within the *lac* locus) was grown with lactose as sole carbon source. It was shown that the *lac* frameshift allowed leaky expression of β-galactosidase enabling slow growth. Cells with amplifications of the leaky gene displayed faster growth. Thereby intermediate colonies arose with a Lac$^+$ phenotype carrying up to 100 copies of the leaky gene. However, these intermediates were unstable under non-selective conditions and reverted back to a Lac$^-$ phenotype due to a high frequency of segregation. Stable Lac$^+$ revertants (reversion of the frameshift) were recovered at a frequency 10 to 100 fold higher than expected for random point mutations in a single copy gene. This can be explained by the increased amount of template making mutations restoring the full activity of the gene more frequent. Subsequently, the amplified gene array was deleted by recombination, with a single reverted gene remaining. Taken together, the results suggest that target-specific mutagenesis is the result of an amplified target sequence and is not caused by an increase in the general rate of mutation.

Recent research concentrated on the development of novel gene functions from gene templates that were acquired by duplication events. GDAs were long suspected to provide templates for new genes (Soukup, 1974). However, a convincing genetic mechanism for this theory could not be suggested. The weakness of this hypothesis is that duplications are only stable within a culture when selective pressure allows a growth advantage to bacteria

with a higher gene dosage. Thus, the additional gene copies are not open for mutations to alter the gene function. Such mutations would interfere with the gene dosage effect maintaining the duplication and should thereby be eliminated from the culture. This problem has been referred to as "Ohno's dilemma" and as a possible solution the model of "Innovation, Amplification and Divergence" was proposed (Bergthorsson *et al.*, 2007). This model assumes that some enzymes possess weak side activities in addition to their main function. Under certain environmental conditions the side activity can become the main selective function and GDA increases the fitness. Accordingly, point mutations and recombination between genes that improve the side activity of the encoded protein can accumulate. This allows the stepwise creation of a new gene in one part of the gene array while the original function of the gene is maintained in additional copies. As a result, the original function is maintained on at least one copy of the gene while a new gene is created in which the original side function becomes dominant. Experimental proof of this hypothesis was gained recently by Nässvall *et. al.* (Näsvall *et al.*, 2012). The authors showed that the gene *hisA* encoding a histidine biosynthetic enzyme (possessing a weak tryptophan synthetic function) was amplified to allow slow growth under histidine/tryptophan limiting conditions. Subsequently, mutation and recombination created a new gene with the encoded enzyme possessing highly efficient tryptophan biosynthetic properties. However one copy of the original *hisA* gene remained intact. This study underlines the importance of GDAs in the evolution of new genes from already existing gene templates under continuous selection.

The genome sequence of *S. lugdunensis* HKU09-01 revealed the presence of a 32 kb tandem repeat duplication comprising the *isd* locus. The characteristics of this duplication and its effects on the physiology of *S. lugdunensis* are investigated within this chapter.

Results

6.1 Duplication of the *isd* operon in HKU09-01

The comparative analysis of the *S. lugdunensis* N920143 and HKU09-01 genome sequences revealed a 32 kb tandem repeat duplication in the latter strain. Analysis of the features affected by the duplication revealed that the complete *isd* operon is encoded within this region. Since the *isd* locus represents an outstanding characteristic of *S. lugdunensis*, the duplication was investigated in more detail.

Figure 6.2 B shows a schematic diagram of the duplication in HKU09-01. In N920143 (single copy of the region) three coding sequences (SLUG_00860, SLUG_00861, SLUG_00862) are present directly upstream of the *isdB* gene and encode a putative membrane-associated potassium transport system. 12.3 kb downstream of the *isd* operon the coding sequence SLUG_01140 encodes a putative multi drug efflux pump (upper part of Figure 6.2 B). The genes SLUG_00860 and SLUG_01140 possess a short stretch of identity (19 nucleotides in length with only one mismatch). Non-equal recombination must have occurred at this site in HKU09-01 thereby duplicating the 32 kb region between the genes (lower part in Figure 6.2 B). The potassium transport system in HKU09-01 is encoded by the genes SLGD_00058, SLGD_00059 and SLGD_00060. The putative drug efflux pump is encoded by SLGD_00116. The recombination event created a unique in-frame hybrid gene in HKU09-01 (SLGD_00087). This gene consists of the 5' end of SLGD_00058 and the 3' end of SLGD_00116. Both genes encode putative membrane associated proteins. However, SLGD_00058 encodes a protein that is predicted to be inserted into the membrane using hydrophobic helixes. In contrast SLGD_00116 encodes a protein that is predicted to be associated with the membrane using the attachment to lipoproteins. Consequently it is questionable whether the fusion gene encodes a functional protein.

Besides the ~16kb *isd* operon, the duplication comprises the genes encoding the SirABC transporter, a MarR family transcriptional regulator, and ten genes encoding proteins that are putatively involved in general metabolism and substrate import/export.

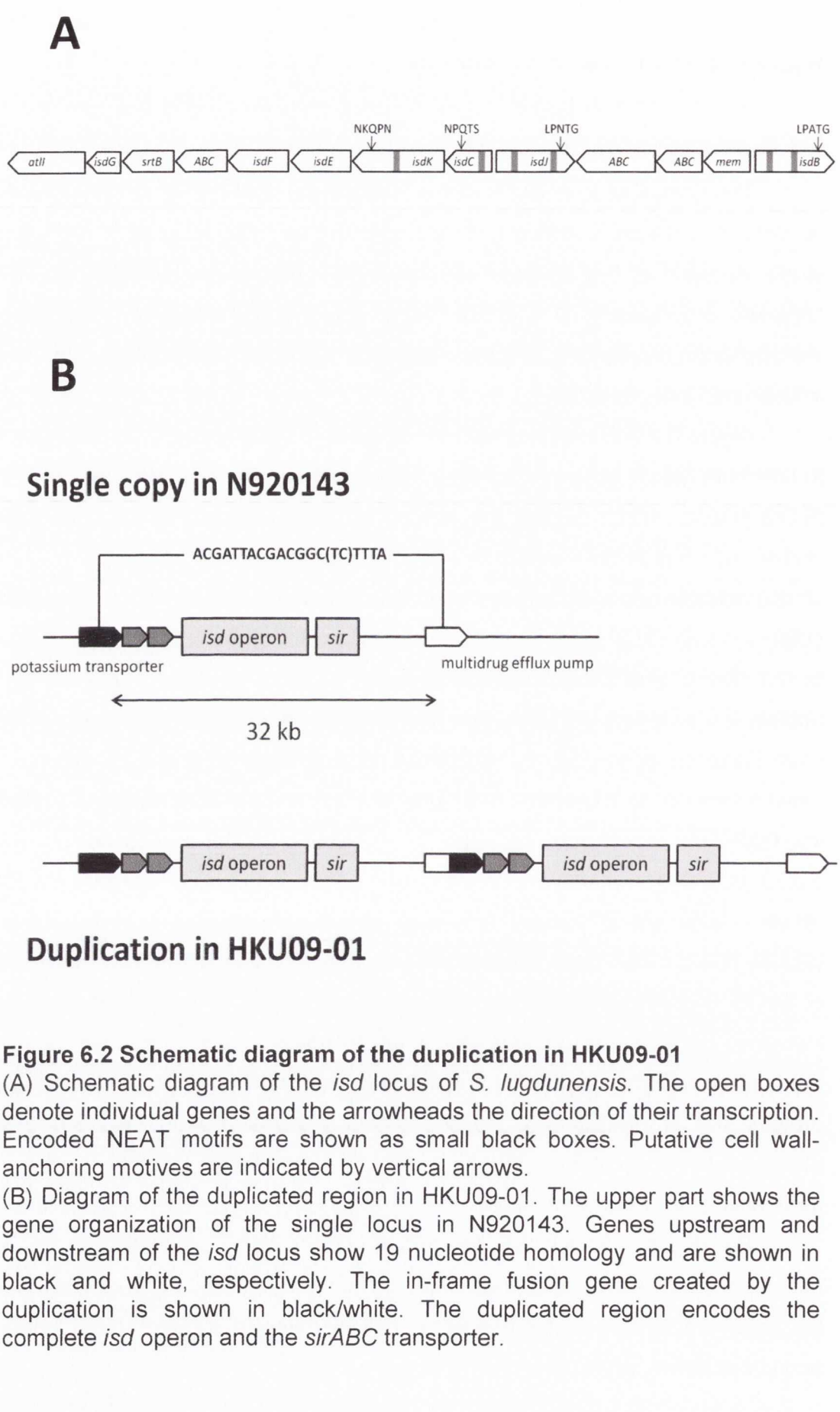

Figure 6.2 Schematic diagram of the duplication in HKU09-01
(A) Schematic diagram of the *isd* locus of *S. lugdunensis*. The open boxes denote individual genes and the arrowheads the direction of their transcription. Encoded NEAT motifs are shown as small black boxes. Putative cell wall-anchoring motives are indicated by vertical arrows.
(B) Diagram of the duplicated region in HKU09-01. The upper part shows the gene organization of the single locus in N920143. Genes upstream and downstream of the *isd* locus show 19 nucleotide homology and are shown in black and white, respectively. The in-frame fusion gene created by the duplication is shown in black/white. The duplicated region encodes the complete *isd* operon and the *sirABC* transporter.

6.2 Detection of the duplication

Southern blot experiments were undertaken to confirm the absence of the duplication in N920143 and its presence in the chromosome of HKU09-01. The acquisition of additional DNA is an inherent characteristic of duplications. The additional DNA carries additional restriction sites which will result in a change within the fragmentation profile of genomic DNA after cleavage. The genome sequences of HKU09-01 and N920143 allowed the identification of restriction endonucleases that will cleave the region into detectable fragments and will create a distinct banding pattern. The restriction enzyme ApaLI possesses four recognition sites in the single locus of N920143. A DNA probe labelled with digoxigenin (DIG) was amplified and detected a single 19.7 kb fragment created by ApaLI. This fragment contains the putative drug exporter involved into the creation of the duplication in HKU09-01 (Figure 6.3 A).

In contrast, ApaLI possesses seven restriction sites in the duplicated region of HKU09-01. The two copies of the region are identical. Therefore a second binding site for the DIG-labelled probe exists. As shown in Figure 6.3 A the second binding site allows the detection of a 15.3 kb fragment (surrounding the fusion gene) in addition to the 19.7 kb fragment detected in N920143.

The results of the Southern blot are shown in Figure 6.3 B. The detection of a ~15.3 kb and a ~19.7 kb fragment confirmed the presence of the duplication in HKU09-01, while a single ~19.7 kb fragment confirmed the absence of the duplication in N920143.

6.3 Stability of the duplication is RecA-dependent

6.3.1 Construction of a HKU09-01 Δ*recA* mutant

It is recognized that duplications give rise to a high frequency of RecA-mediated recombination events due to the long stretches of homology. This leads either to amplification of the locus, or to loss of the duplication (segregation) (see Figure 6.1). In order to investigate whether these processes happen in HKU09-01, a Δ*recA* deletion mutant of HKU09-01 was isolated by allelic replacement using the thermosensitive plasmid pIMAYZ. RecA is known to be an important mediator of the bacterial SOS response and *recA* mutants have a reduced ability to repair damaged DNA using recombination. UV light

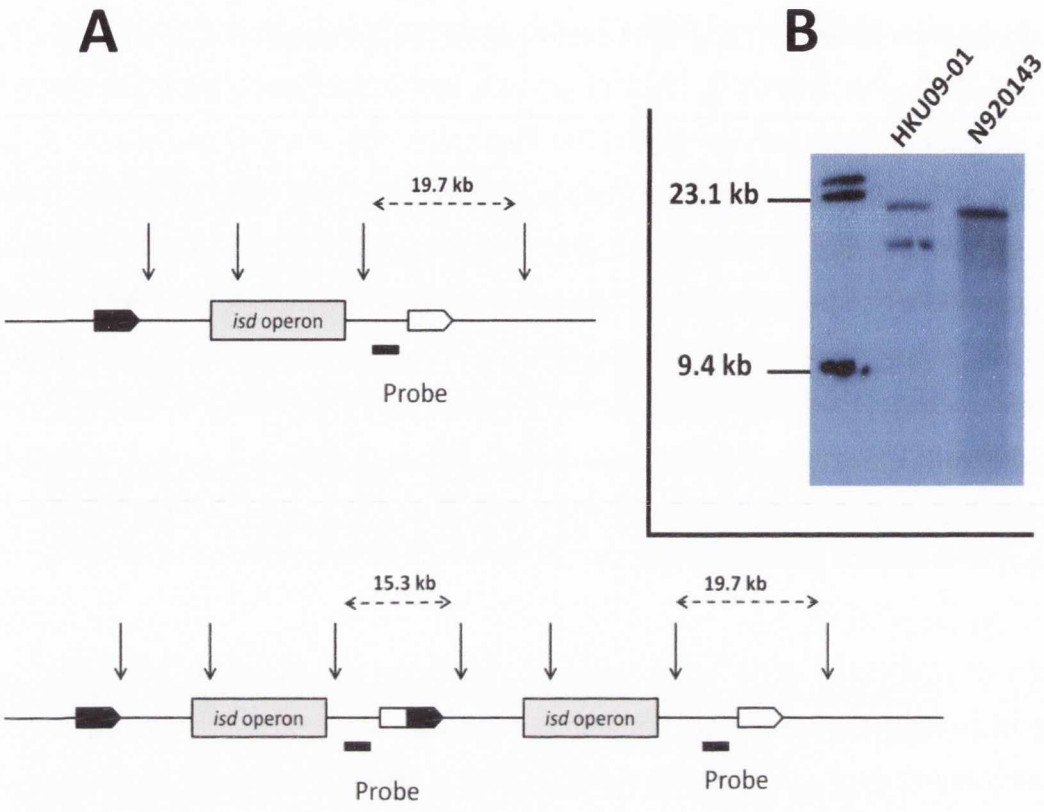

Figure 6.3 Southern blot to detect the duplication in HKU09-01
(A) Schematic diagram of the ApaLI restriction sites of the single region in N920143 and the duplication in HKU09-01. Restriction sites are indicated by vertical arrows. The binding site of the DIG-labelled probe is indicated by the black dash. Predicted sizes of the fragments recognized by the probe are indicated.
(B) Results of the Southern blot. 3 µg of chromosomal DNA of *S. lugdunensis* strains N920143 and HKU09-01 were digested with ApaLI and separated by electrophoresis. The DNA fragments were subsequently denatured, blotted onto a nylon membrane and hybridized with the DIG-labelled probe. Hybridization was detected using anti-DIG-Fab fragments conjugated to alkaline phosphatase.

catalyses the formation of pyrimidine dimers in the DNA backbone, blocking DNA replication. RecA-dependent recombination is an important repair mechanism of this damage. Therefore the ability of the HKU09-01 wild-type and the isogenic Δ*recA* mutant to tolerate UV exposure was assessed semi-quantitatively. The wild-type strain could tolerate UV light exposure for up to 20 seconds without an effect on growth, while the Δ*recA* mutant showed reduced viability already after 5 seconds of exposure (Figure 6.4 A). In addition, the Δ*recA* mutant displayed a longer lag phase (3 h 10 min) and a reduced growth rate (163 min per generation) compared to the wild-type strain (lag phase 2 h 30 min / 93 min per generation). Figure 6.4 B shows growth curves of the wild-type and the Δ*recA* mutant.

6.3.2 Stability of the duplication is RecA-dependent

A colony PCR screening method was developed for the rapid discrimination of HKU09-01 colonies harbouring or lacking the duplication. As shown in Figure 6.5 A, primers were designed facing the boundaries of the duplication. If a single copy of the locus is present in the chromosome, the primers face in opposite directions and thereby fail to produce a PCR product (upper part of Figure 6.5 A). If the locus is duplicated, a second binding site for each primer exists and the two primers face towards each other around the fusion point of the duplication, allowing the amplification of a 1.2 kb fragment. As shown in Figure 6.5 B chromosomal DNA of HKU09-01 WT (harbouring the duplication) allowed the amplification of the fragment while N920143 chromosomal DNA (no duplication) failed to amplify a PCR product.

In order to investigate the frequency of loss of the duplication, single colonies of the HKU09-01 wild-type and the isogenic Δ*recA* mutant were inoculated into broth to form independent cultures, grown overnight and dilutions were plated. Twenty two colonies were subsequently screened by PCR for the presence of the duplication. This sets the detection limit for the loss of the duplication to 4.5 %. Figure 6.5 B shows the result of one representative experiment. In the Δ*recA* strain all colonies maintained the duplication (<4.5 % loss) while in the wild-type a significant number of colonies had lost the duplication. In the experiment shown 9 / 22 colonies (40.9 %) had lost the duplication. The experiment was repeated seven times with independent

A

	WT	*recA*⁻
0 s	+++	+++
5 s	+++	++
10 s	+++	+
20 s	+++	-
30 s	++	-
60 s	-	-

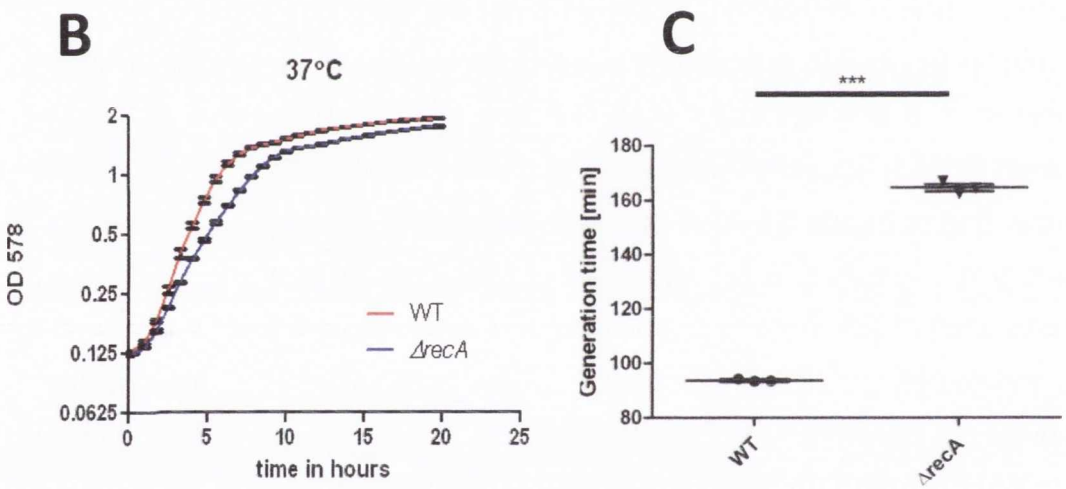

Figure 6.4 Phenotypes of the Δ*recA* mutant
(A) Semi-quantitative determination of UV sensitivity displayed by HKU09-01 and the isogenic Δ*recA* mutant. Exposure to short wave UV light is given in seconds. Growth was assessed after 24 hours of incubation. +++ – normal growth; ++ – weakly impaired growth; + – strongly impaired growth; - – no growth.
(B) Growth curves of HKU09-01 and the isogenic Δ*recA* mutant at 37°C. Shown is the mean and SEM of the OD_{578} at each time point of three independent growth curves.
(C) Generation times calculated for HKU09-01 wild-type and the isogenic Δ*recA* mutant. Shown are three generation times calculated from independent growth curves together with the mean and SEM.

Statistical evaluation was performed using an unpaired two tailed t-test. P-values <0.05 were regarded as significant and are indicated by *.
*** indicate P-values <0.0005.

overnight cultures (Figure 6.6) showing that the rate of loss in the wild-type ranged from <4.5 % to 45 %. The wide range in the frequency of loss of the duplication was not unexpected. The overnight culture represents ~11 generations of bacterial growth. Segregation leading to loss of the duplication can happen at each cell separation and is subsequently passed on to the daughter cells. A high frequency of loss of the duplication might therefore indicate that segregation had happened in the early stages of growth. Accordingly, cultures showing a low number of colonies without the duplication might represent cultures where segregation happened in the late stages of growth. In the Δ*recA* strain, not a single colony was detected that had lost the duplication, suggesting that segregation did not happen in this background. These experiments show that the duplication in HKU09-01 is intrinsically unstable and can be stabilized by the introduction of a *recA* mutation.

The *recA* mutation was introduced in each strain in the following experiments, to stabilize the *isd* copy number. The mutation is indicated by (R) in the strain designations.

6.4 Isolation of control strains

Two HKU09-01 strains were constructed with one and zero copies of the *isd* locus. One strain deficient in the duplication was chosen from the PCR-screen experiment described above. It possessed only one copy of the *isd* operon and was designated HKU-Δdup. This strain was used as the parental strain for the construction of a deletion mutant which lacked the entire *isd* operon (~16 kb). The thermosensitive plasmid pIMAY was used to delete all of the *isd* genes from *atlI* to *isdB* by allelic exchange using the technique described in Chapter 4 (see Figure 4.6). The resulting strain was designated HKU-Δisd. To construct strains that are genetically comparable to the strains described below, a tetracycline resistance determinant (*tet*) was integrated into the chromosome followed by a *recA* mutation. The resulting strains were designated HKU(R)-Δdup and HKU(R)-Δisd, respectively.

Schematic diagrams of the loci in HKU(R)-Δdup and HKU(R)-Δisd are included in the summary of the constructed strains shown later in this chapter (Figure 6.13).

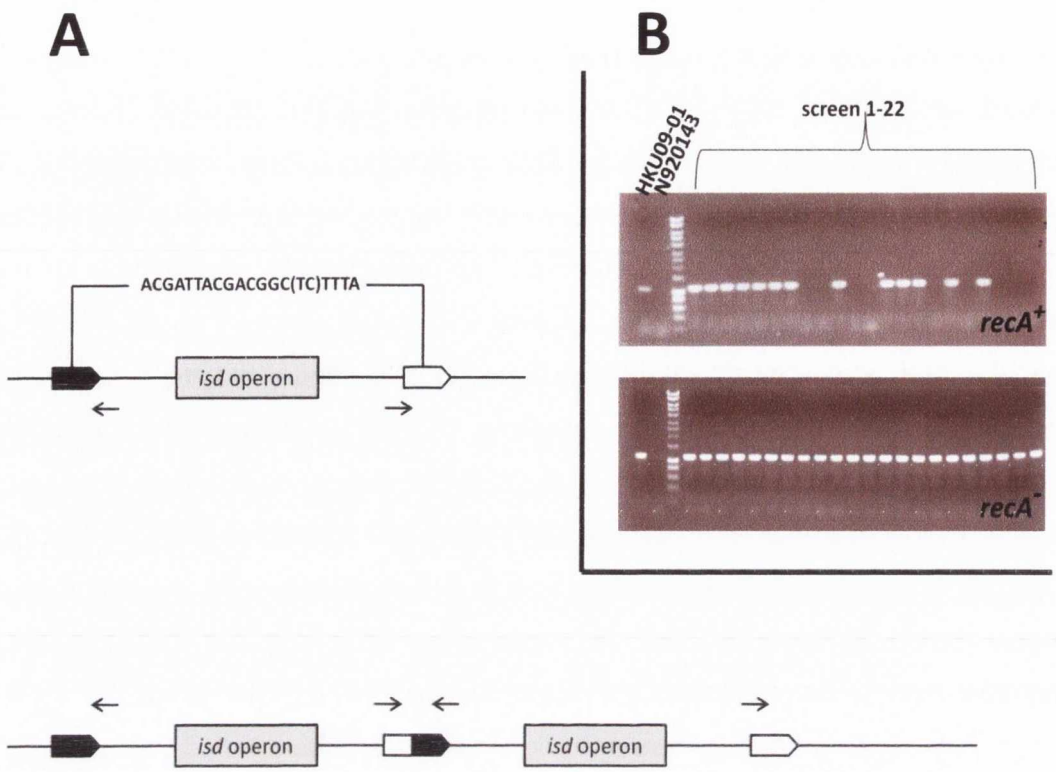

Figure 6.5 PCR screen to determine the stability of the duplication
(A) Schematic diagram of the single region and the duplication in HKU09-01. Primer binding sites and the direction of amplification are indicated by horizontal arrows. If the duplication is present, a 1.2 kb fragment will be amplified, containing the fusion point of the duplication.
(B) Result of one representative PCR screening experiment. HKU09-01 (wild-type and *recA* mutant) overnight cultures were plated out and 22 colonies were screened for the presence of the duplication.

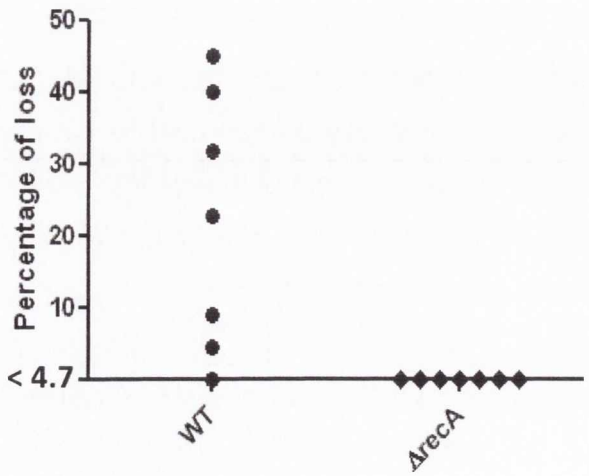

Figure 6.6 Stability of the duplication is *recA* dependent
HKU09-01 (wild-type and Δ*recA* mutant) cultures were plated out and 22 colonies were screened for the presence of the duplication.
The frequency of duplication loss of seven independent experiments is shown.

6.5. Amplification of the of the *isd* locus

The general model for gene duplication and amplification implies that as soon as a duplication is established, segregation and amplification occur hand in hand. During cell division, recombination can occur at a high frequency between the duplicated regions on the sister chromatids. Subsequent cell division results in two distinct daughter cells. One of them carries one copy of locus (segregation) while the other receives a further copy (amplification). The PCR screening experiments demonstrated that segregation occurred frequently during *in vitro* growth. This implicated that clones carrying multiple copies must also have been present. The PCR experiment is capable of distinguishing between one copy and two copies. However, it is not able to distinguish clones that carry either two or multiple copies. Therefore additional methods were needed to identify clones with multiple rather than two copies. A well-studied effect of GDAs is the increase in the level of antibiotic resistance when the gene dosage of the resistance determinant is increased. Therefore tetracycline resistance was employed to select for the higher copy number of amplimers.

6.5.1 Insertion of *a* tetracycline resistance determinant into the duplicated region

The tetracycline resistance determinant (*tet*) of the staphylococcal plasmid pT181 has been shown before to confer low tetracycline resistance in *S. aureus,* when a single copy was inserted into the chromosome (McDevitt *et al.*, 1993). The resistance level increased when the resistance cassette was amplified by GDA. Therefore, pIMAY was used to insert the *tet* gene of pT181 into the duplicated locus of HKU09-01 using a procedure similar to the construction of chromosomal reversions (described in Chapter 4). A *tet* cassette was constructed which contained 500 bp fragments upstream and downstream of the site chosen for the insertion. The pT181 *tet* determinant was inserted between the two fragments, (a schematic diagram is shown in Figure 6.7). Integration and subsequent excision of the thermosensitive plasmid allowed the isolation of the strain HKU::tet which carried the *tet* determinant within the duplicated region. The intergenic region between the CDSs SLGD_00110 and SLGD_00111 was chosen as the insertion point. The site is located at the 3' end of the duplication (Figure 6.7) and the flanking open reading frames are

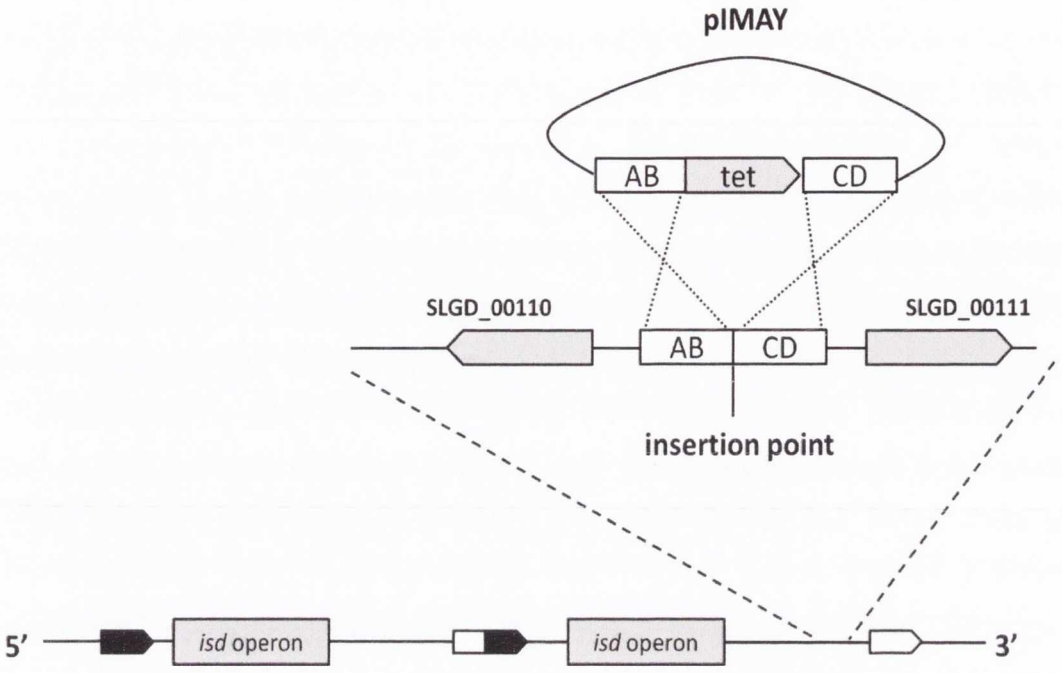

Figure 6.7 Schematic diagram of *tet* insertion site
The *tet* cassette was inserted at the 3' end of the duplicated region between the coding sequences SLGD_00110 and SLGD_00111. The *tet* integration cassette on the thermosensitive plasmid contained the *tet* gene flanked by regions upstream (AB) and downstream (CD) of the chosen insertion point. Insertion and excision of the thermosensitive plasmid allowed the exchange of plasmid and chromosomal segments and thereby the isolation of HKU::tet carrying the *tet* gene in the chromosome.

located on the reverse and on the forward strands of the chromosome, respectively. Therefore, integration of *tet* between the genes should avoid polar effects on the transcription of genes in the region. Furthermore, the site of integration is located on an ApaLI fragment recognized by the probe in the previously described Southern blot experiments (Figure 6.8). This allowed direct visualization of the success of the integration. The results of the Southern blot experiment and a schematic diagram are shown in Figure 6.8. Integration of the ~ 2.5 kb *tet* cassette into the locus resulted in the alteration of the size of the larger fragment which increased from 19.7 kb in the HKU09-01 wild-type to 22.3 kb in HKU::tet (Figure 6.8 B). The Southern blot also showed the presence of the smaller fragment (~15.3 kb) in both strains, confirming the presence of the duplication and indicating that *tet* was not integrated into the region upstream of the fusion gene. This possibility had to be considered since the sequences of the region upstream of the fusion gene and the region upstream of the last gene of the duplication are identical.

Growth of the strain in the presence of increasing concentrations of tetracycline revealed a minimal inhibitory concentration (MIC) of 8 μg/ml. Thus, one copy of *tet* allowed normal growth in the presence of 4 μg/ml tetracycline.

6.5.2 Isolation of clones with amplification of the *isd* locus

In a RecA$^+$ background any amplification of the *isd* locus was expected to be highly unstable. The introduction of a *recA* mutation using allelic exchange involves electroporation and several cycles of growth from single cell to colony for the integration and excision of the thermosensitive plasmid to be achieved. It was expected that maintenance of a higher copy number during this process would be difficult. Therefore the *recA* deletion plasmid (pIMAYZ:Δ*recA*) was introduced into HKU::tet and subsequently integrated into the chromosome before the process of selection of clones with increased *isd* copy number was started. The resulting strain HKU::tet::pIMAYZ:Δ*recA* remained RecA$^+$, since a functional copy of the wild-type *recA* gene was present in the chromosome. However, after the selection of amplifications, excision of pIMAYZ:Δ*recA* could be induced by a single temperature shift to 28°C and Δ*recA* mutants could be isolated. This allowed rapid stabilization of amplifications.

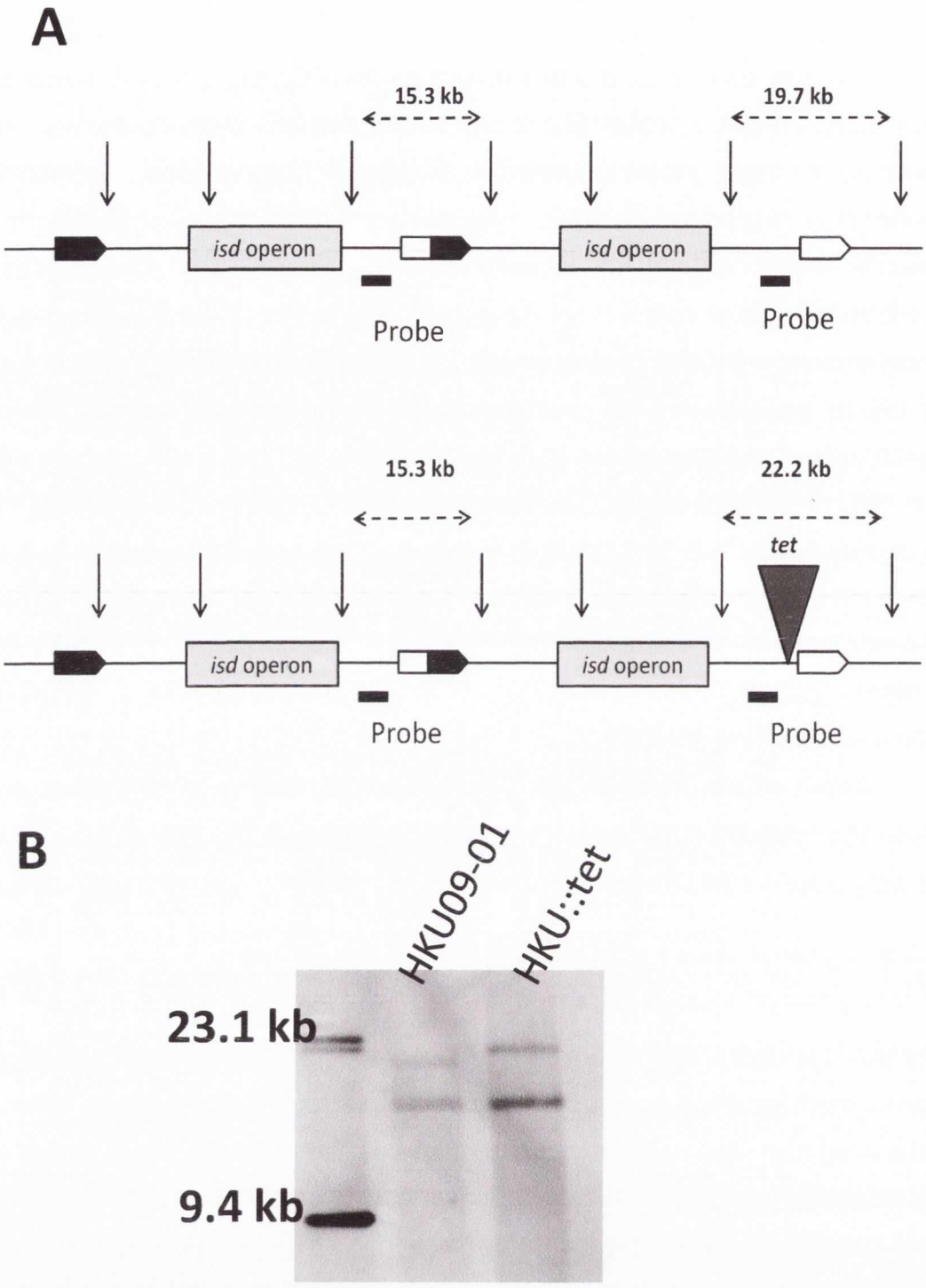

Figure 6.8 Southern blot to confirm the insertion of the *tet* in the duplicated region

(A) Schematic diagram of the ApaLI restriction profile of the duplication in HKU09-01 (top) and HKU::tet (bottom). Restriction sites are indicated by vertical arrows. The binding site of the DIG-labelled probe is indicated by the black dash. Predicted fragment sizes labelled by the probe are indicated.

(B) Results of the Southern blot. 3 µg of chromosomal DNA of strains HKU09-01 and HKU::tet were digested with ApaLI and separated by electrophoresis. The DNA fragments were subsequently denatured, blotted onto a nylon membrane and hybridized with the DIG-labelled probe. Hybridization was detected using anti-DIG-Fab fragments conjugated to alkaline phosphatase.

As described above the strain HKU::tet::pIMAYZ:Δ*recA* which possessed a single copy of *tet* in the duplicated region was not able to form colonies on TSA containing 8 µg/ml tetracycline (upper plate in Figure 6.9). Amplification and segregation occurs during cell division. To allow amplification to occur an overnight culture of HKU::tet::pIMAYZ:Δ*recA* was grown and subsequently plated on TSA containing 8 µg/ml tetracycline. Growth of single colonies could be detected after 24 hours of incubation (lower plate in Figure 6.9) and these colonies were assumed to carry multiple copies of *tet*. The colonies showed a high degree of variability in size ranging from ~0.1 mm to ~1.5 mm (Figure 6.9 lower plate) suggesting that they harboured different copy numbers of *tet* which lead to different resistance levels. Several colonies of different sizes were picked, grown at 28°C to promote excision of pIMAYZ:Δ*recA* and a Δ*recA* mutant of each strain was isolated. The increased UV sensitivity associated with the *recA* mutation was tested and confirmed for each strain. The strains were designated HKU(R)-K4, HKU(R)-K4-2, HKU(R)-X1, HKU(R)-Y1 and HKU(R)-Z1 with minimal inhibitory concentrations of tetracycline of 40 µg/ml, 40 µg/ml, 28 µg/ml, 24 µg/ml and 16 µg/ml, respectively. Besides the increase in UV sensitivity, the *recA* mutation is associated with a slower growth. Thus incubation for two days was needed to achieve reliable results in the MIC analysis. Therefore, measurement of the MIC of strain HKU(R)-WT which carries one copy of *tet* was repeated under the same conditions and an increased MIC of 12 µg/ml tetracycline was measured compared to the MIC of 8 µg/ml tetracycline described above (Section 6.5.1).

6.5.3 Southern blot experiments to determine recombination events leading to the increased copy number of *tet*

The selection of clones with an increase in the MIC to tetracycline only reflects an increase in the copy number of *tet*. Since *tet* and *isd* are located on the same duplicated region, the amplification of *tet* also includes amplification of *isd* (Figure 6.10).

Initially recombination can occur anywhere along the duplicated region. However, recombination occurring upstream of *tet* will result in segregation and amplification of the *isd* locus but will not change the *tet* copy number in the two daughter cells (Figure 6.10 A). Only a specific recombination event (here

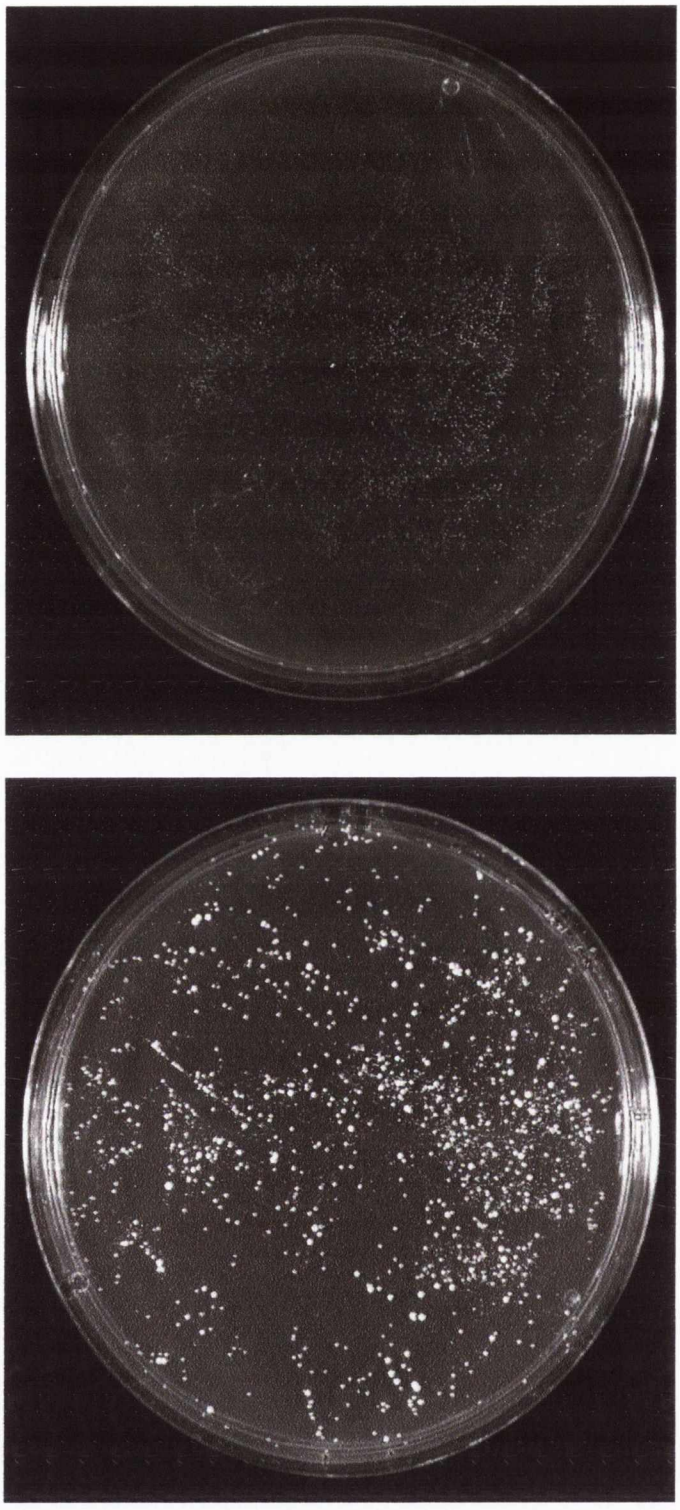

Figure 6.9 Selection of colonies with increased tetracycline resistance

A single HKU::tet::pIMAYZ:Δ*recA* colony was either resuspended in PBS and dilutions were plated directly on TSA containing 8 µg/ml tetracycline (upper plate) or a single colony was used to inoculate a TSB overnight culture of which dilutions were subsequently plated on TSA containing 8 µg/ml tetracycline (lower plate). Growth was assessed after 24 h of incubation at 37°C.

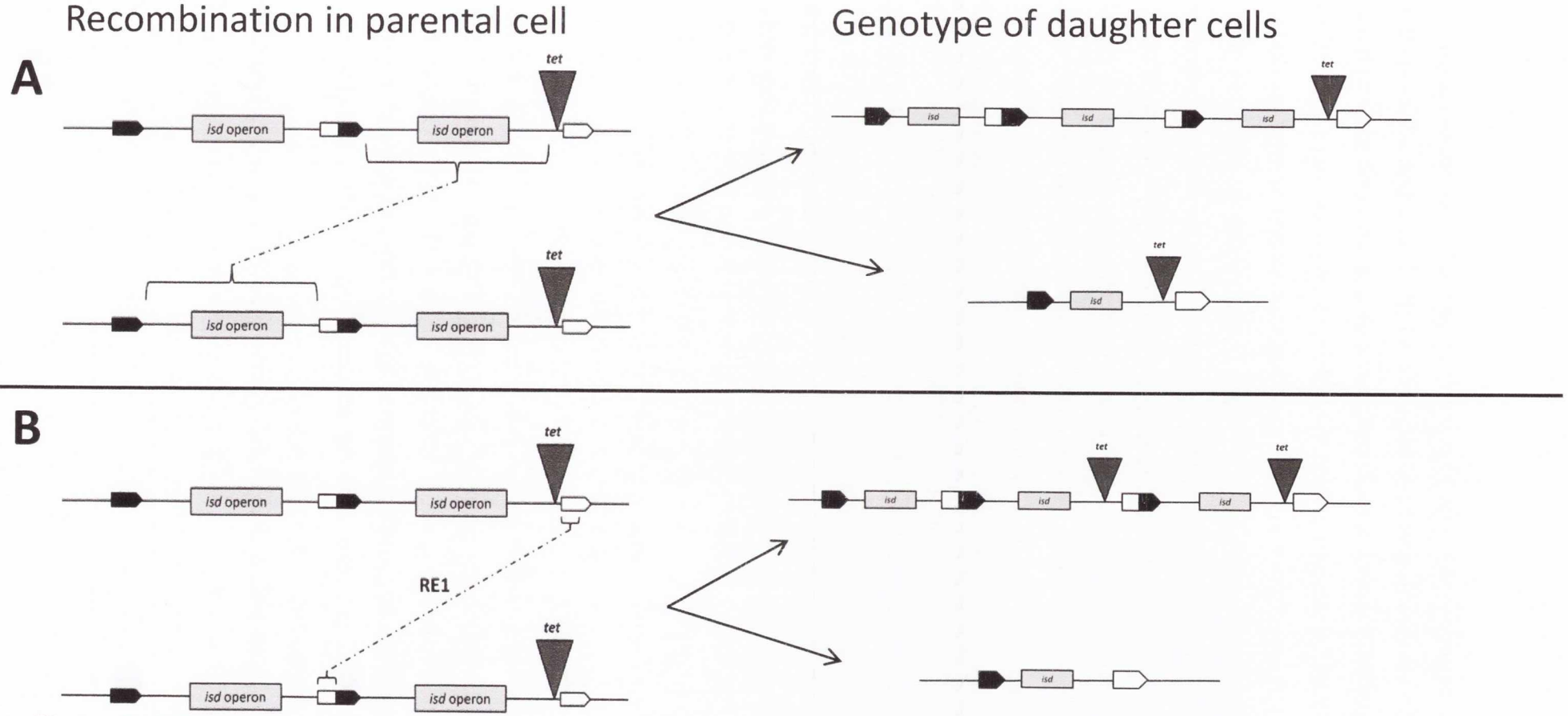

Figure 6.10 Schematic diagram of recombination events and genotypes of daughter cells

(A) Recombination occurring upstream of the *tet* determinant results in amplification of *isd* operon but does not allow the amplification of *tet*.

(B) Recombination occurring in the ~6 kb region downstream of the *tet* determinant (RE1) allows amplification of the *isd* operon together with the *tet* determinant. This creates a novel *tet* insertion point upstream of a second fusion gene in the daughter cell carrying the amplified locus.

named recombination event 1 – RE1) occurring downstream of *tet* results in the duplication of *tet* in one daughter cell (Figure 6.10 B). The region allowing RE1 is ~6.5 kb in size. RE1 results in the creation of one daughter cell carrying three *isd* loci and two *tet* genes and a second carrying a single *isd* locus and no *tet* (Figure 6.10 B). As mentioned above, the site of introduction of *tet* is located in the ApaLI fragment recognized by the probe. Therefore the amplification of *tet* resulted in the creation of third fragment of ~17.8 kb. This fragment carries a *tet* gene upstream of the second fusion gene in the middle of the amplified array (Figure 6.11 A). RE1 is the basis for further amplification of *tet* and the novel fragment was present in all subclones with increased tetracycline resistance (Figure 6.11 B). In subsequent generations, recombination (recombination event 2 - RE2) can occur at different sites and promote further amplification of *tet* (Figure 6.11 A). For example, recombination occurring between the middle region and the first region of the two sister chromatids, respectively (RE2-1), results in the duplication of the smallest (15.3 kb) fragment and maintains one intermediate fragment (17.8 kb) and one large fragment (22.2 kb). RE2-1 will therefore not change the number of *tet* determinants within the daughter cells. Recombination occurring between the third region and the first region of the two sister chromatids (RW2-1') will also result in the duplication of the smallest fragment. However two or three intermediate sized fragments (17.3 kb) will be created depending on whether recombination occurred upstream or downstream of the second *tet* gene. In contrast, recombination between the third and the second region of the two sister chromatids (RE2-2) will not duplicate the smallest fragment but will amplify the intermediate fragment to two or three copies depending on the exact site of recombination. Segregation occurring between the first and the second region of the two sister chromatids (RE2-3) will result in the deletion of the smallest fragment while the other two fragments are maintained at a single copy.

All RE2 events (RE2-1, RE2-1' RE2-2 and RE2-3 in Figure 6. 11 A) have the common factor, that they create daughter cells that carry only one copy of the largest fragment (22.2 kb). However, the two smaller fragments (15.3 kb and 17.8 kb) are present in variable numbers depending on the site of recombination. This is also true for all recombination events that occur during subsequent cell divisions. The largest fragment is always present in a single

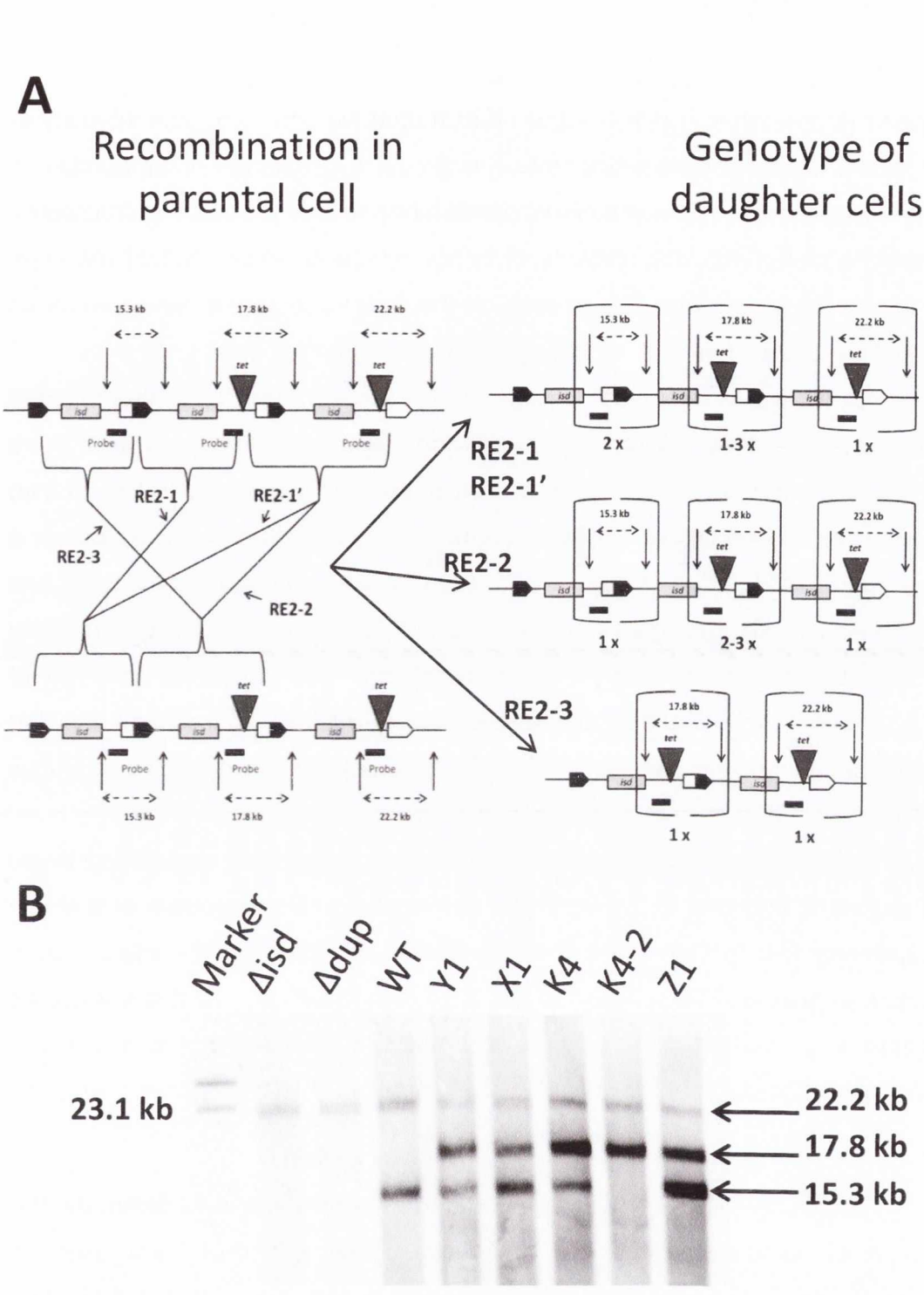

Figure 6.11 Southern blot to determine the site of recombination leading to *tet* amplification

(A) Schematic diagram of RE2 events leading to the different numbers of fragments labelled in the Southern blot experiment (see text for explanation).

(B) Results of the Southern blot. 3 µg of chromosomal DNA of HKU(R) strains with different tetracycline resitance levels were digested with ApaLI and separated by electrophoresis. The DNA fragments were subsequently denatured, blotted onto a nylon membrane and hybridized with the DIG-labelled probe. Hybridization was detected using anti-DIG-Fab fragments conjugated to alkaline phosphatase. Comparison of the relative intensities of the bands allows an estimation of the copy number of fragments within the band.

copy, while the copy number of the other fragments can vary. The intensity of the bands detected in Southern blot experiments is dependent of the number of fragments present (one molecule of probe binds to one molecule of fragment). Therefore, comparing the intensity of bands allows an estimation of the copy number of the fragments. The intensity of the 22.3 kb fragment can serve as an internal standard since it occurs at one copy per chromosome.

Southern blot experiments were carried out with the five different clones displaying increased tetracycline resistance (Figure 6. 11 B). The 17.8 kb fragment in clone HKU(R)-K4 showed a high intensity compared to the 15.3 kb and 22.2 kb fragments, so amplification most likely occurred at site RE2-2, or a combination of RE2-1 and RE-2-2 over several generations (Figure 6.11 A and B). The 15.3 kb fragment in clone HKU(R)-Z1 showed a high intensity compared to the other fragments, indicating that recombination occurred at RE2-1. Interestingly, clone HKU(R)-K4-2 had lost the 15.3 kb fragment showing that recombination had occurred at RE2-3 to delete one copy of the *isd* locus but maintaining the increased *tet* copy number.

The two control strains HKU(R)-Δdup (one copy of *isd*) and HKU(R)-Δisd (no *isd*) were included in the Southern blot analysis. The presence of a single 22.2 kb fragment confirmed the absence of the duplication and the integration of *tet* in both strains. The deletion of the *isd* locus in HKU(R)-Δisd could not be confirmed by Southern blot since the probe was not directed against fragments carrying *isd* genes.

6.5.4 Determination of the *isd* copy number by qPCR

Quantitative PCR (qPCR) is the state of the art method to determine the amount of template within PCR reactions. This procedure was used to determine the *isd* copy number of the different strains. The origin of replication (*ori*) served as a standard for the experiment since there is only one copy of *ori* per chromosome. Three independent qPCR experiments were carried out using chromosomal DNA of each of the strains and the relative amount of template for *ori* and *isdJ* was determined. Figure 6.12 shows the relative template concentrations of one representative experiment. A shift in the ratio of *ori* : *isdJ* indicates a change in the copy number of *isdJ*. Genomic DNA of the strain HKU(R)-Δdup showed an *ori* : *isdJ* ratio of 1 : 1. In contrast, HKU(R)-WT DNA

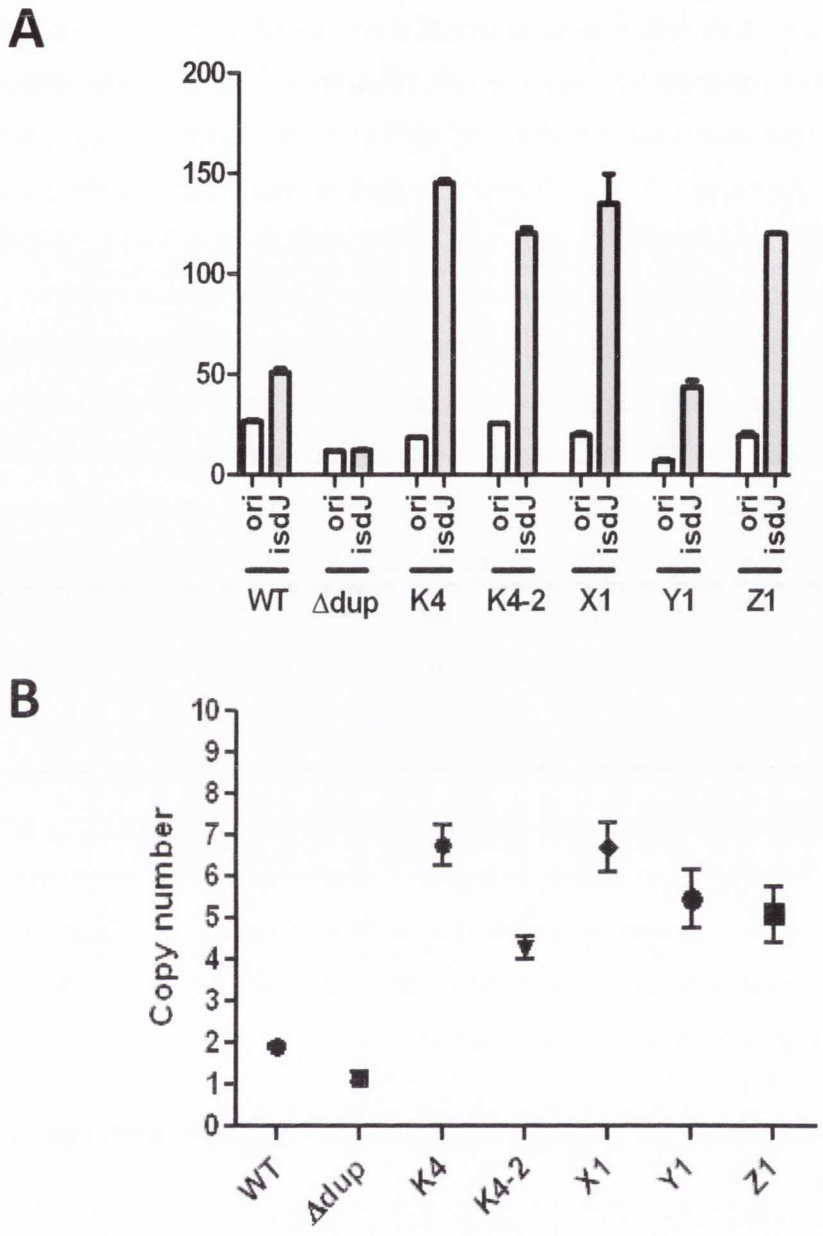

Figure 6.12 qPCR experiment to determine the *isd* copy number
(A) Absolute values from one qPCR experiment. Numbers derive from the comparison with the standard curve using known concentrations of N920143 DNA (one copy of *isd*). Different relative amounts of template *ori* and *isdJ* within the sample indicate differences in the *isd* copy number.
(B) Combination of three qPCR experiments. The value for *ori* was set to 1 and the template amount of *isdJ* was expressed in relation to this value, thereby giving the copy number of *isdJ* in the chromosome of each strain. The mean and SEM of three experiments is shown.

showed a ratio of 1 : 2 indicating two copies of *isdJ*. The subclones with increased tetracycline resistance showed a further increase in *isdJ* compared to *ori*, indicating increased *isdJ* copy numbers. The three independent experiments showed that HKU(R)-K4, HKU(R)-K4-2, HKU(R)-X1, HKU(R)-Y1 and HKU(R)-Z1 carried 7, 4, 7, 5 and 5 copies of *isdJ*, respectively (Figure 6.12 B). The control strains HK(R)-Δdup and HK(R)-WT carried 2 and 1 copies of *isd* respectively (Figure 6.12 B).

The qPCR copy number data correlates well with the MIC analysis and the Southern blotting (Figure 6.11). Clones HKU(R)-K4 and HKU(R)-K4-2 had the highest tetracycline MIC suggesting the highest *tet* copy number. The Southern blot showed that K4 had maintained the 15.3 kb fragment, indicating that at least one *isd* copy was maintained although this did not carry a *tet* determinant. In contrast K4-2 had lost this fragment. This explains the identical MICs and the difference in the *isd* copy number calculated from the qPCR results.

The *isd* copy number was integrated into the strain designations and the strains HKU(R)-Δisd$^{(0)}$, HKU(R)-Δdup$^{(1)}$, HKU(R)-WT$^{(2)}$ and HKU(R)-X1$^{(7)}$ were chosen for phenotypic characterization. Their genotypic and phenotypic characteristics are summarized in Table 6.1. Schematic diagrams of the organization of the single, duplicated and amplified regions present in the different strains are shown in Figure 6.13.

6.6 Chromosomal *isd* copy number correlates with Isd protein expression

6.6.1 Whole cell immunoblot

In order to quantify the expression of Isd proteins, strains were grown in the iron-restricted medium RPMI to induce the locus. Surface protein expression was assessed using whole cell immunoblotting. The concentration of cells was adjusted to OD_{578} = 5 and doubling dilutions were dotted onto a nitrocellulose membrane and stained for the presence of IsdB and IsdC. Both of these proteins have been reported previously to be exposed on the cell surface (Zapotoczna *et al.*, 2012a). The fibrinogen binding protein Fbl served as a loading control, since a single copy of the gene is present in each strain. As shown in Figure 6.14, all strains showed similar intensities when stained for Fbl.

Table 6.1 Characteristics of the strains with different *isd* copy numbers

	colony size † (mm)	Tetracycline MIC (μg/ml)	*isd* copy number (qPCR)	Doubling time in TSB (min)	Doubling time in RPMI (min)
HKU(R)-Δisd	n.a.	n.a.	n.a.	143.6	232.2
HKU(R)-Δdup	n.a.	n.a.	1	142.0	260.8
HKU(R)-WT	n.a.	12	2	145.6	262.2
HKU(R)-K4	1.5	40	7	n.a.	n.a.
HKU(R)-K4-2	1.5	40	4	n.a.	n.a.
HKU(R)-X1	1.5	28	7	152.6	364.2
HKU(R)-Y1	0.5	24	5	n.a.	n.a.
HKU(R)-Z1	0.5	16	5	n.a.	n.a.

† – on TSB_{tet8} – prior to introduction of the *recA* mutation (Section 6.5.2)
n.a. not applicable

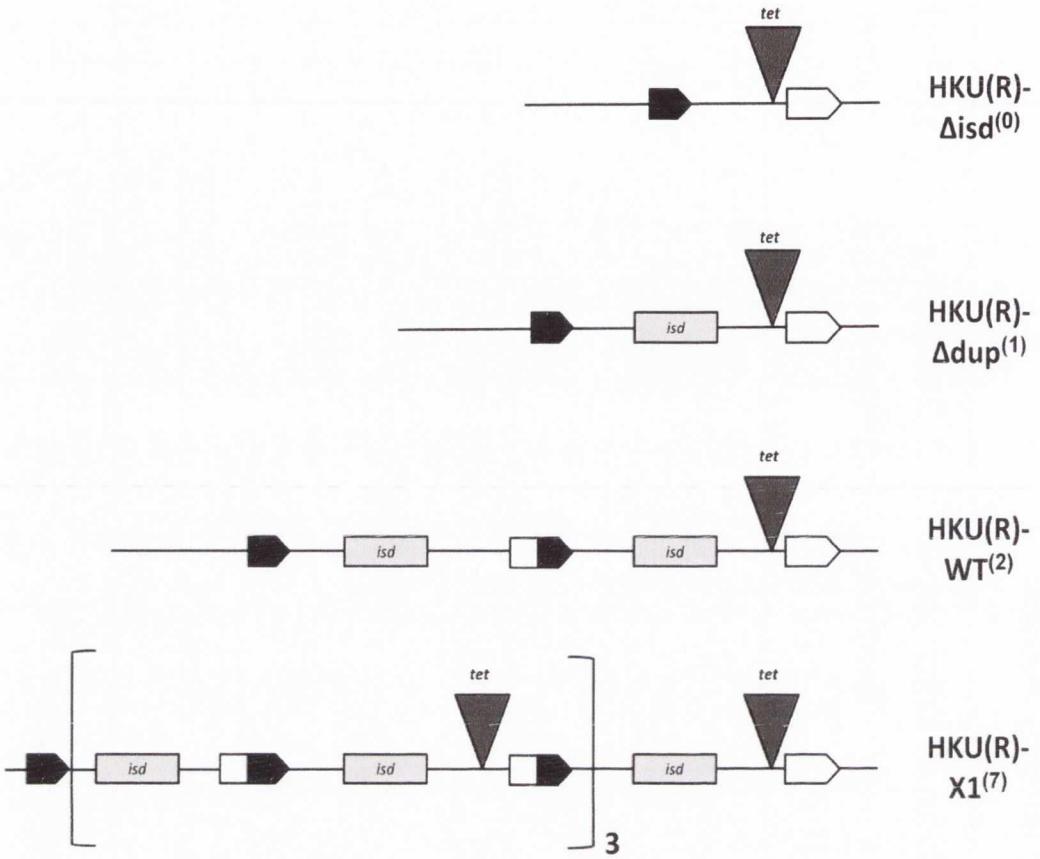

Figure 6.13 Organization of the *isd* loci of strains with different *isd* copy numbers

Schematic diagrams of the chromosomal *isd*-encoding regions in the different strains are shown. Brackets indicate the amplified region in HKU(R)-X1$^{(7)}$.

The strains HKU(R)-Δisd$^{(0)}$; HKU(R)-Δdup$^{(1)}$; HKU(R)-WT$^{(2)}$; HKU(R)-X1$^{(7)}$ carry 0, 1, 2 and 7 copies of *isd,* respectively.

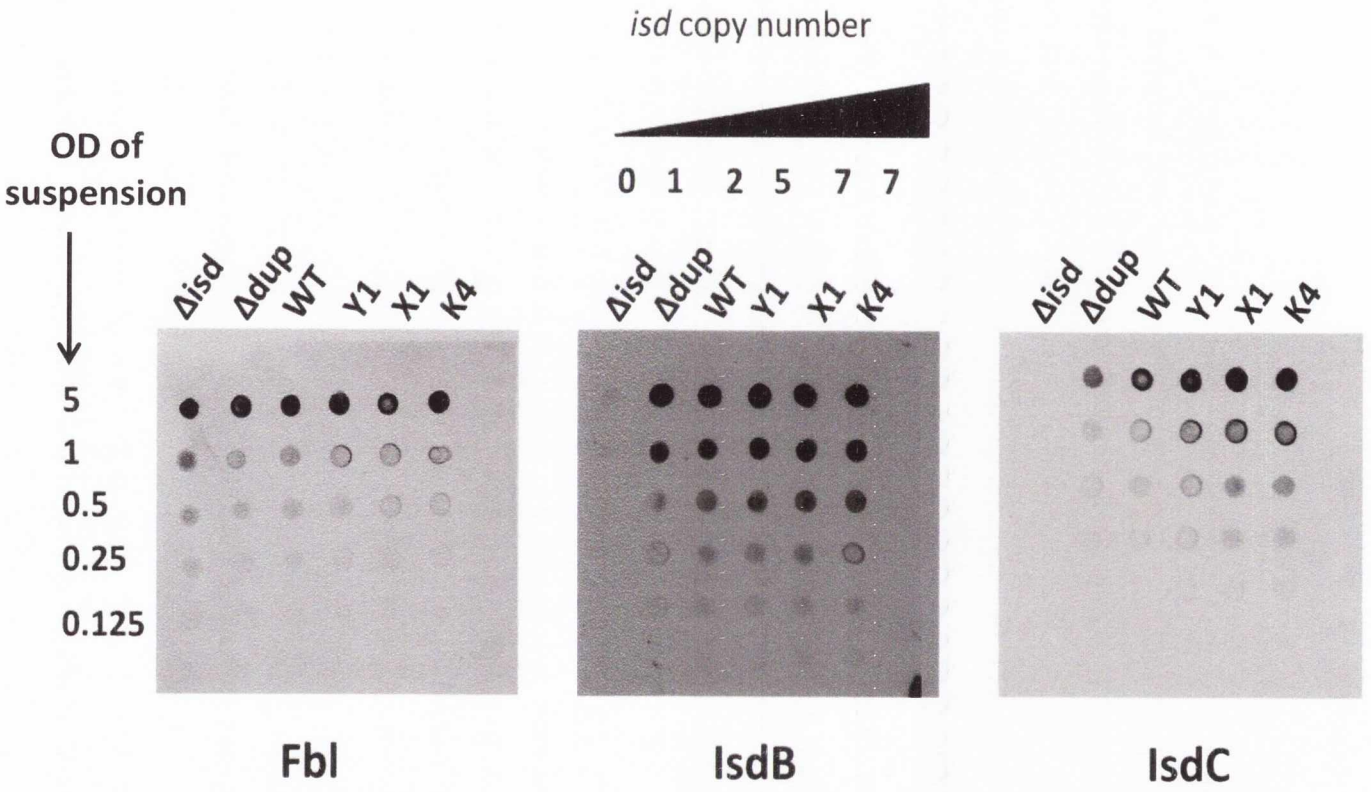

Figure 6.14 Whole cell immunoblotting to estimate the amount of Isd protein expressed on the cell surface

Overnight cultures were grown in RPMI, adjusted to OD_{578} = 5 and doubling dilutions were spotted on the membrane. Detection of FbI served as a loading control. FbI and Isd proteins were detected with specific rabbit serum followed by goat anti-rabbit IgG conjugated to HRP.

However, the amount of IsdB and IsdC differed between the strains. Strain HKU(R)-Δisd$^{(0)}$ did not express either of the two proteins which is consistent with the loss of the entire *isd* locus. With the increasing copy number of *isd* an increase in the level of IsdB and IsdC expression was observed which is consistent with a gene-dosage effect.

6.6.2 Cell fractionation analysis

Although the IsdK and IsdJ proteins are known not be exposed on the cell surface, they can be detected in the membrane and cell wall fractions of *S. lugdunensis* (Zapotoczna *et al.*, 2012a). Therefore cell fractionation was performed followed by Western immunoblotting. The results confirmed that the increase in *isd* copy number led to an increase in the amount of protein expressed (Figure 6.15).

6.6.3 Effects of the *isd* copy number on growth with human haemoglobin

The *isd* operon was previously shown to support the growth of *S. lugdunensis* N920143 with haemoglobin as the sole source of nutrient iron (Zapotoczna *et al.*, 2012a). This was shown by measuring the rate of growth of the wild-type and the isogenic Δ*isd* mutant in iron-deficient medium supplemented with 10 μg/ml human haemoglobin. Therefore the possibility that an increase in Isd protein expression in HKU09-01 might provide a growth advantage under these conditions was investigated. The growth rate of *isd* copy number variants was determined in iron-deficient medium in the presence or absence of human haemoglobin (Figure 6.16). All strains failed to grow in the absence of haemoglobin which confirmed the effectiveness of removing iron from the growth medium. However, the comparison of the growth rates in the presence of haemoglobin proved to be difficult and no significant differences could be determined. Since all strains carried *recA* mutations growth in the iron-limited medium was very slow and the high level of variation between the experiments made an accurate determination of doubling times impossible. The strain HKU(R)-Δisd$^{(0)}$ (no Isd proteins) showed a trend towards a decreased growth rate compared to the strains expressing Isd proteins (HKU(R)-Δdup$^{(1)}$, HKU(R)-WT$^{(2)}$, HKU(R)-X1$^{(7)}$). However, the observed differences were not significant at any time point (Figure 6.16 C shows data from 48 h time point). There was no difference in the outcome when lower concentrations of

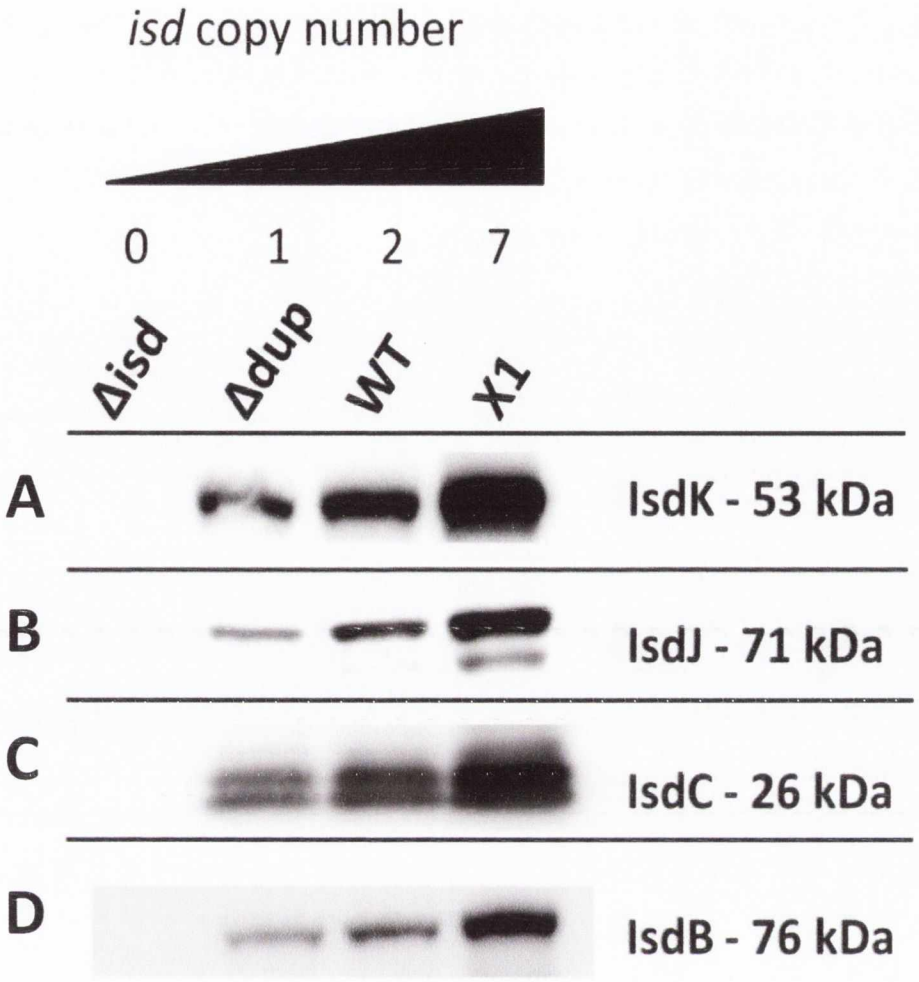

Figure 6.15 Western immunoblotting to investigate Isd protein expression

Strains were grown in RPMI, adjusted to OD_{578}= 5 and the cell wall was digested with lysostaphin and mutanolysin in the presence of 500 mM sucrose to stabilize the protoplasts. Cell wall and membrane fractions were separated by SDS-PAGE and blotted onto a PVDF membrane. Isd proteins were detected using specific rabbit serum followed by goat anti-rabbit IgG conjugated to HRP.

(A) IsdK in the membrane fraction.
(B) IsdJ in the cell wall fraction.
(C) IsdC in the cell wall fraction.
(D) IsdB in the cell wall fraction.

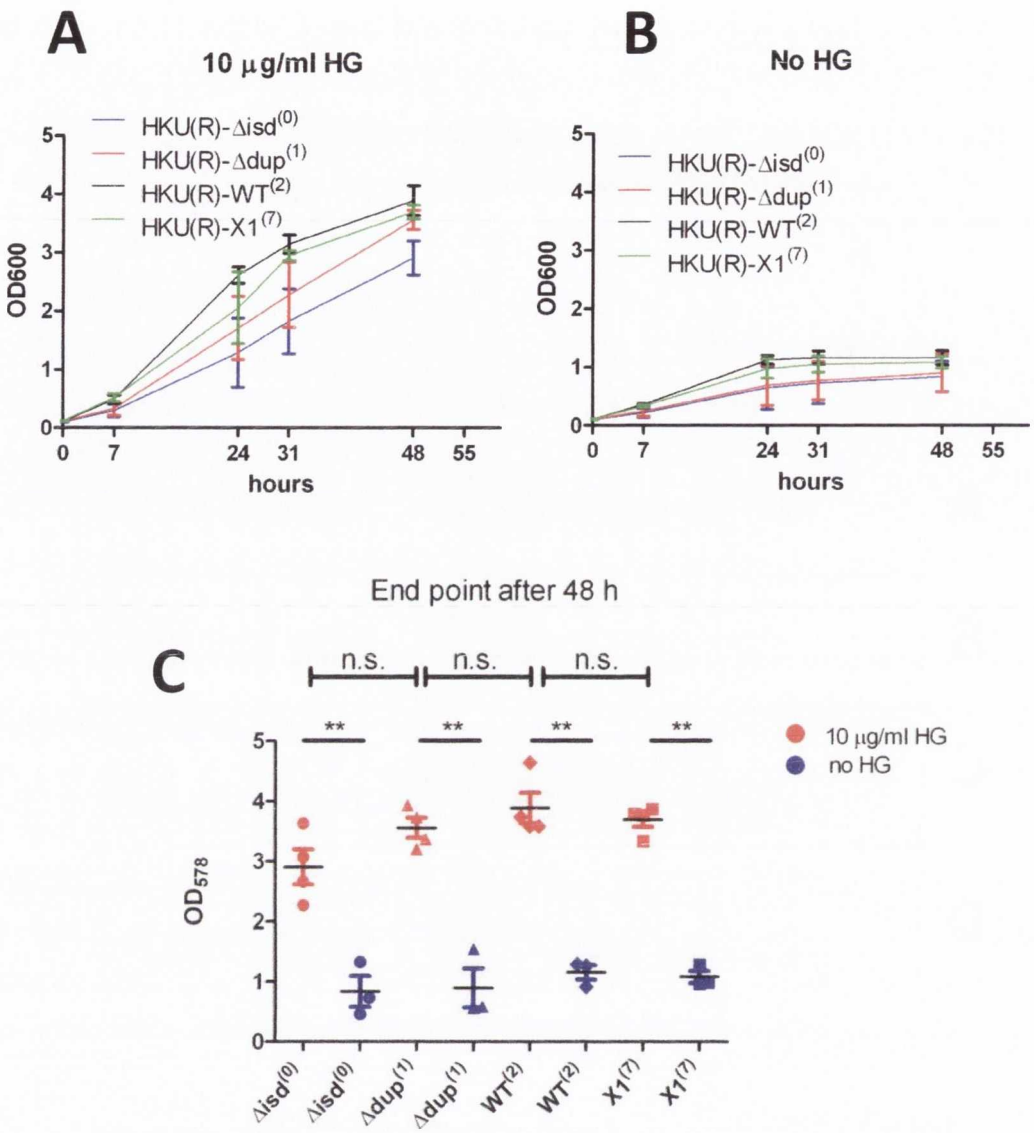

Figure 6.16 Growth on human haemoglobin

Overnight cultures were grown in RPMI and used to inoculate completely iron-deficient medium DD-RPMI supplemented with human haemoglobin (HG) (10 µg/ml) or unsupplemented.

(A) Growth curves in DD-RPMI supplemented with haemoglobin for 48 h. The mean and SEM of four independent experiments is shown.

(B) Growth curves in DD-RPMI without supplementation for 48 h. The mean and SEM of four independent experiments is shown.

(C) End point of the experiments after 48 h of growth. The values of individual experiments are shown as well as the mean and SEM. None of the differences between the HG supplemented cultures reached statistical significance.

Statistical evaluation was performed using an unpaired two tailed t-test. P-values <0.05 were regarded as significant and are indicated by *.
** indicate P-values <0.005.

haemoglobin were used (5 μg/ml; 2.5 μg/ml) in single experiments (data not shown). Taken together these experiments suggested that there might have been differences in the growth rates of the *isd* copy number variants under the conditions used but the experimental setup was not appropriate. Therefore a more sensitive approach was needed for the comparison of the strains.

6.7 The phage integrase vector pIPI03

Competitive growth of two different strains under identical conditions within the same culture is powerful method for comparing fitness. By growing a mixed culture to stationary phase, diluting it into fresh medium and repeating the process multiple times, small differences in fitness can be revealed over a large number of generations. In order to detect differences in growth between two strains they must be labelled in such a way that they can be differentiated in mixed cultures. This can be achieved by the integration of antibiotic resistance determinants into the chromosome. Labelling with antibiotic resistance cassettes represented a challenge since most methods for integration involve homologous recombination which was not available here since the *isd* copy number variants were deficient in RecA. Bacteriophage integrases recognize attachment sites (*attB*) in the bacterial chromosome and mediate site-specific, RecA-independent recombination with the *attP* site on the phage chromosome. The target site in the bacterial chromosome is disrupted when a single copy of the phage chromosome is inserted (Hirano et al., 2011). It has been previously demonstrated that phage integrases can be used to promote site-specific integration of plasmids harbouring the corresponding *attP* site into the bacterial chromosome at the *attB* site. Such integrative plasmids have been used successfully in various Gram-negative and Gram-positive bacteria including *Lactococcus lactis* (Petersen et al., 2013) and *S. aureus* (Lei et al., 2012). Since recombination using phage integrases is RecA-independent, this approach offered the prospect of labelling the *recA* mutants of *S. lugdunensis*.

6.7.1 Construction of the phage integrase vector pIPI03

As mentioned in Chapter 3, *S. lugdunensis* N920143 carries the lysogenic phage ϕSL01. The phage genome is integrated within the gene SLUG_08250 which encodes a putative phosphosugar transport protein. This

gene is conserved in the strain HKU09-01 and does not harbour a phage genome.

The *attP* site and the adjacent recombinase gene *ccrB* of ϕSL1 were amplified from a circularized template after the phage was induced to enter lytic cycle replication by mitomycin C. The PCR amplimer was cloned into the thermosensitive vector pIMAY. The phage integrase gene was inserted directly downstream of the *cat* gene thereby creating a transcriptional fusion and constitutive expression from the Phelp promoter (Figure 6.17 A).

IPTG-inducible kanamycin and erythromycin resistance cassettes for use in Gram-positive bacteria have been described previously (Monk *et al.*, 2008). They harbour a Phelp promoter (containing a LacO repressor binding site) followed by the resistance determinant. In addition the LacI (repressor) coding sequence is present and its expression is driven by a second Phelp promoter. Thus the antibiotic resistance genes are repressed unless induced by IPTG. To create two versions of pIPI03 with different selectable markers, the two resistance cassettes were cloned into the multiple cloning site of pIPI03 (Figure 6. 17 B). The plasmids were designated pIPI03:*ery* and pIPI03:*kan.*

6.7.2 Integration of pIPI03

S. lugdunensis HKU09-01 was transformed with pIPI03 at 28°C, the permissive temperature for plasmid replication. Subsequent plating at 37°C allowed the selection of clones with an integrated plasmid. Determination of the number of CFUs growing at 28°C and at 37°C revealed that 0.09% to 0.13% of cells present within a colony carried the plasmid integrated in the chromosome.

PCR experiments using primer combinations recognizing sequences in the chromosome and the pIPI03 backbone showed that the plasmid had integrated at the same site as phage ϕSL01 in N920143. PCR1 using the chromosomal primers scr.F and scr.R yielded a 600 bp fragment with DNA isolated from HKU09-01 (pIPI03) grown at 28°C showing that the phage attachment site was not occupied in this strain (Figure 6.18 B). PCR1 did not produce a product with DNA from HKU09-01::pIPI03 grown at 37°C indicating that the site was occupied by the integrated plasmid. PCR2 using primers ccrB. F and attP. R confirmed the presence of replicating plasmid in HKU09-01 (pIPI03). PCR2 failed to detect autonomous plasmid DNA in HKU09-01::pIPI03

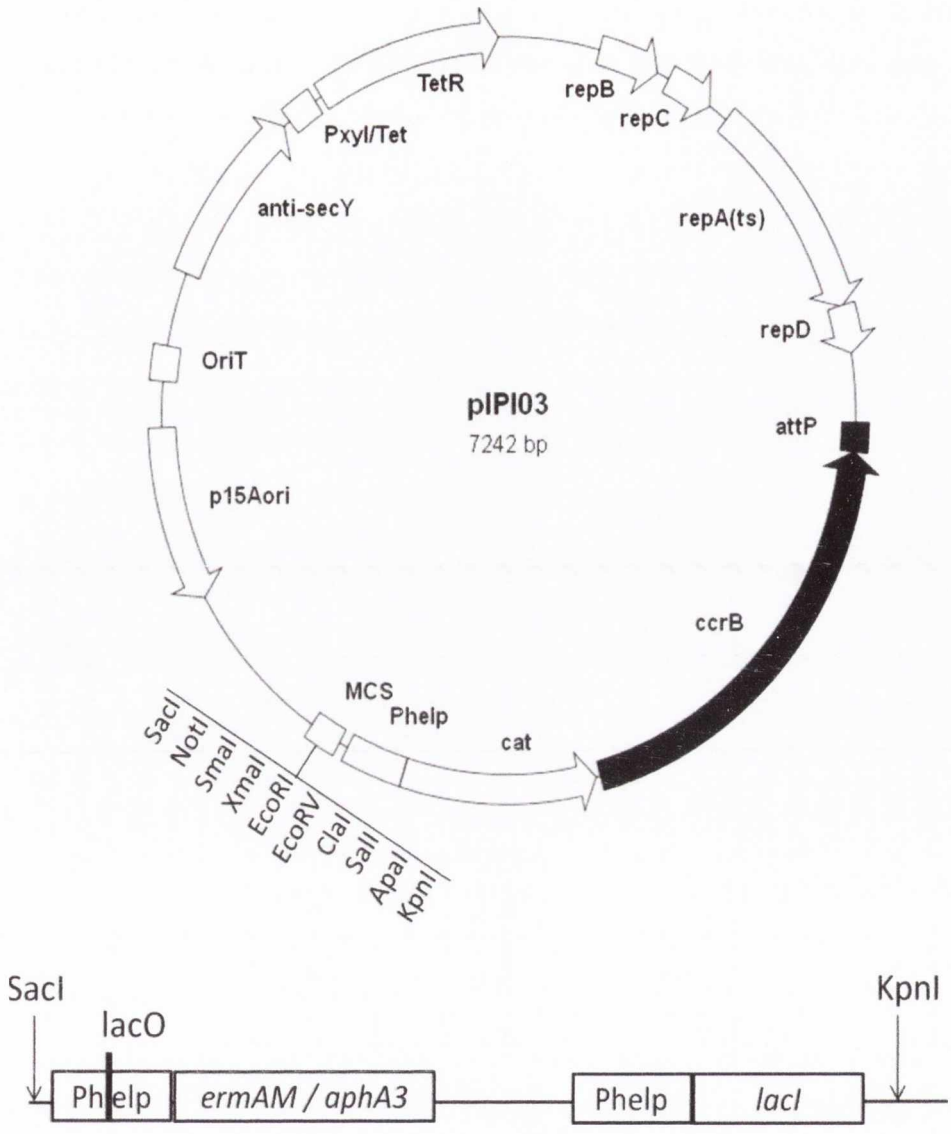

Figure 6.17 The phage integrase vector pIPI03

(A) Schematic diagram of pIPI03. The coding sequences on the thermosensitive plasmid pIMAY are shown in white. Coding sequences of the ϕSL01 integrase (*ccrB*) and the corresponding attachment site (*attP*) are shown in black. The restriction sites shown are unique. For sequencing purposes, T3 and T7 primer binding sites are present before the KpnI and after the SacI restriction sites, respectively.

(B) Schematic diagram of the IPTG-inducible antibiotic resistance cassettes.

The cassettes were cloned into the MCS of pIPI03 using SacI, KpnI. *ermAM* – erythromycin resistance; *aphA3* – kanamycin resistance.

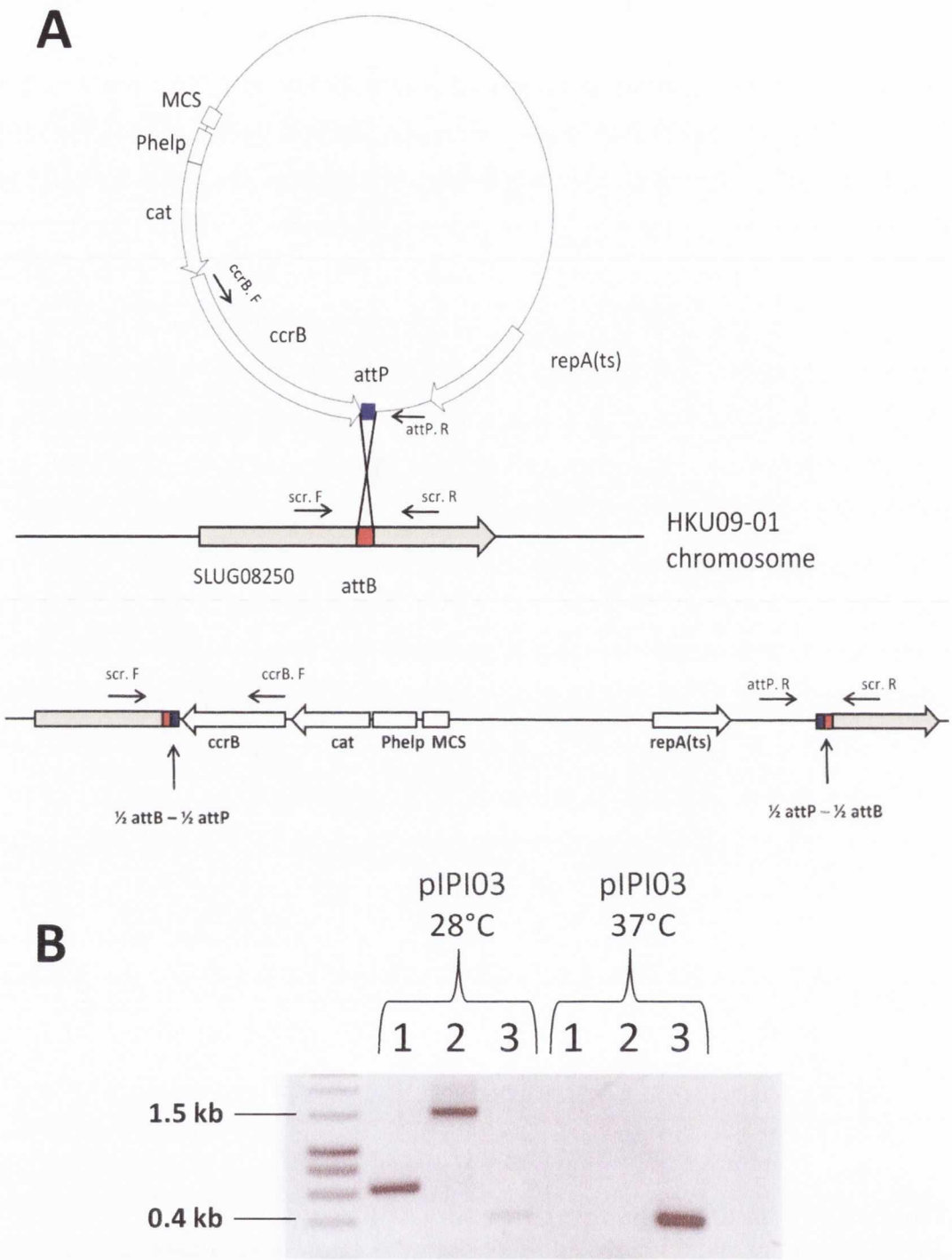

Figure 6.18 Integration of pIPI03

(A) Schematic diagram of the integration of pIPI03. The plasmid-encoded genes are shown in white. The *attP* site on the plasmid is shown in blue. The gene SLUG_08250 harboring the *attB* site (red) in the HKU09-01 chromosome is shown in tan. Arrows indicate the location of primers for the detection of integration by PCR. Integration of pIPI03 disrupts the attachment sites resulting in *½ attB* and *½ attP* on either side of the integrated plasmid.

(B) PCR to detect the integration of pIPI03. Primer combination 1 (scr. F / scr. R) was used to determine if the chromosomal *attB* site was occupied or not. Primer combination 2 (ccrB. F / attP. R) was used to detect autonomous plasmid. Primer combination 3 (attP. R / scr. R) determined if pIPI03 was integrated into the *attB* site on the chromosome.

(Figure 6.18 B). The primers used in PCR3 (scr. R and attP. R) bound to the chromosome and the plasmid, respectively, and yielded a 400 bp fragment with DNA from HKU09-01::pIPI03. This confirmed the site-specific integration of the plasmid. Interestingly, this PCR experiment produced a faint product with HKU09-01 (piPI03) (Figure 6.18 B), showing that with growth at 28 °C a small subpopulation of cells carried the plasmid integrated into the chromosome.

The integration of pIPI03 into the chromosome was found to be very stable at both 37°C and 28°C. Loss of Cm resistance (<2%) could not be detected when strains with integrated plasmid were grown for four consecutive cultures (ca. 40 generations) in TSB without antibiotic. To confirm that the integrated plasmid was maintained, 10 representative colonies grown after the incubation of broth cultures at 28°C or 37°C were screened by PCR using the primers described above. All clones tested carried an integrated copy of the plasmid and no autonomous plasmid was detected (data not shown). These results suggest that the phage integrase of ϕSL01 is only responsible for the insertion of the plasmid/phage into the chromosome and not for excision.

Recently, MLST typing revealed five clonal complexes (CCs) for *S. lugdunensis* (Chassaîn *et al.*, 2012). PCR1 experiments using primers scr.F and scr.R showed that none of the strains in the TCD collection carried a lysogenic phage at the chromosomal *attB* site of ϕSL01 (data not shown). Therefore the ability of pIPI03 to integrate into the *attB* site of strains from different CCs was investigated. HKU09-01 is a member of CC1. Five isolates SL71 (CC2), SL27 (CC3), SL37 (CC3), SL62 (CC4) and SL81 (CC5) were chosen for the experiments. All strains could be transformed with pIPI03 and the plasmid integrated specifically into the *attB* site as confirmed by PCR using the primer combination scr.R and attP.R (data not shown).

The integration of pIPI03 was independent of RecA and pIPI03 integration could be achieved with the same experimental procedure and at the same frequency in the wild-type and the *recA* mutant strain. This supports the idea that CcrB does not need RecA-mediated processes to mediate integration into the chromosome and allowed *recA* deficient strains to be labelled with pIPI03.

6.7.3 Effects of pIPI03 integration on bacterial fitness

In pIPI03 the *ccrB* gene is expressed constitutively from the Phelp promoter. Growth curve analysis was performed to determine if this influences bacterial fitness. When incubated at 37°C the HKU09-01 wild-type and HKU09-01::pIPI03 strains had identical lag times (ca. 2,5 h) and similar rates of exponential growth (generation times of 93 min and 98 min, respectively) (Figure 6.19 A). This shows that *ccrB* expression did not have any deleterious effects. However, when the strains were grown at a temperature that allowed the plasmid to initiate replication (28°C), the presence of pIPI03 had a significant effect on the growth rate (Figure 6. 19 B). At 28°C, both strains had a lag time of ca. 4 h 20 min. However, the wild-type strain had a generation time of 181 min while the strain with integrated plasmid needed 246 min per cell division. This is most likely due to the thermosensitive replication machinery of pIPI03 inducing replication at the permissive temperature which subsequently interfered with the chromosomal replication.

6.7.4 Competitive growth experiments using pIPI03 labelled strains

In order to demonstrate that pIPI03:*ery* and pIPI03:*kan* can be used in competitive growth experiments, both plasmids were integrated into the chromosome of the HKU09-01 wild-type strain, creating HKU(WT):ery and HKU(WT):kan. TSB was inoculated with the two strains in a ratio of 1:1. The culture was grown overnight, and used to inoculate fresh broth. The experiment continued for four consecutive subcultures. The ratio of erythromycin : kanamycin resistant cells was determined both for the starter culture and for each of the four subcultures by performing viable counts on agar plates containing antibiotics. Figure 6.20 (red line) shows that the ratio of erythromycin : kanamycin resistant bacteria remained constant over the course of the experiment. This indicates that the nature of the resistance cassette did not influence the strains in the competition experiment.

The Δ*recA* mutant of HKU09-01 showed a growth defect when the growth rate was compared to the wild-type in the growth curve analysis (compare paragraph 6.3.1, Figure 6.4). Both plasmids were integrated into the RecA$^-$ strain creating HKU(R):ery and HKU(R):kan and competitive growth experiments were performed. No differences were observed in the outcome

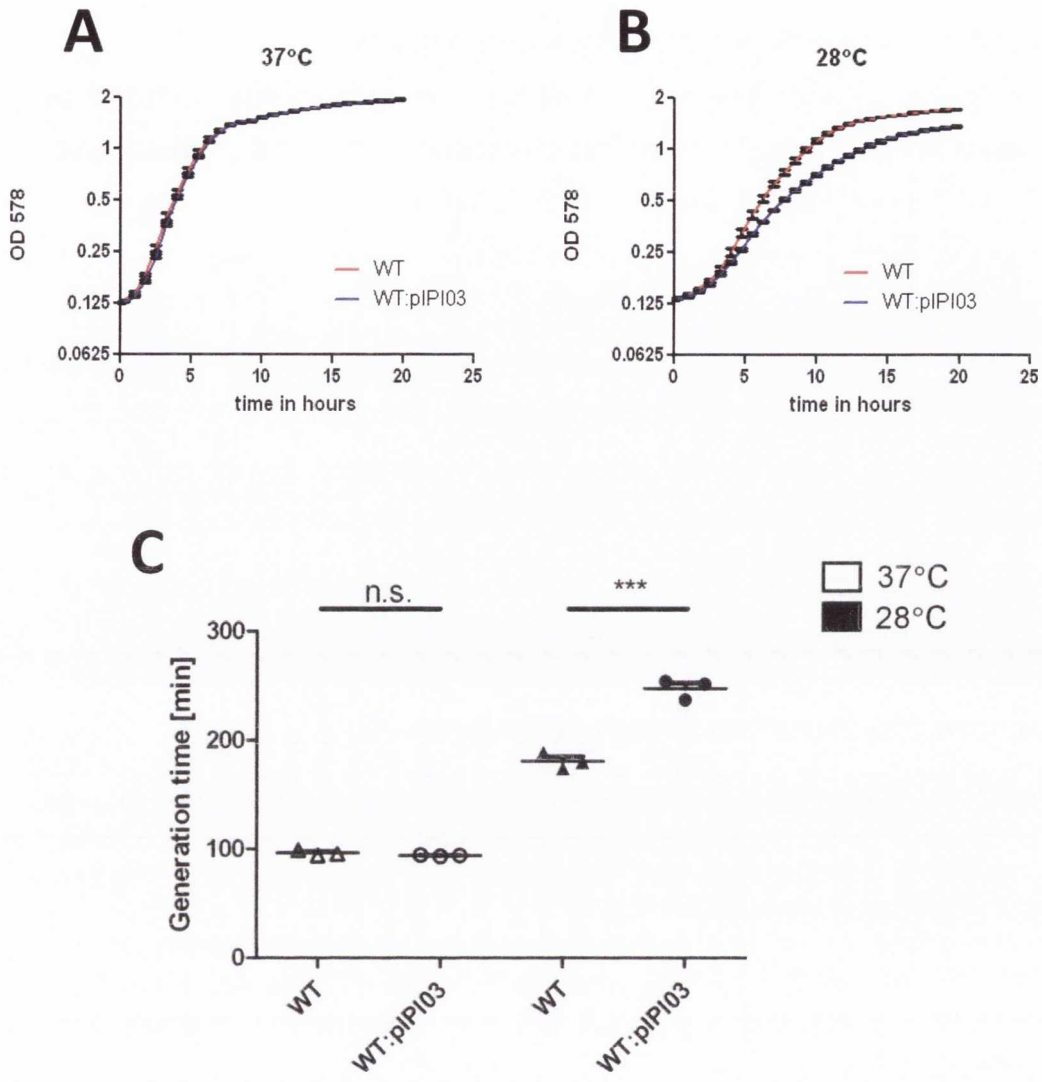

Figure 6.19 Influence of pIPI03 integration on bacterial growth
(A) Growth curves of HKU09-01 and HKU09-01::pIPI03 (integrated plasmid) at 37°C. The mean and SEM of three independent growth curves at each time point are shown.
(B) Growth curves of HKU09-01 and HKU09-01::pIPI03 (integrated plasmid) at 28°C. The mean and SEM of three independent growth curves at each time point are shown.
(C) Generation times calculated for HKU09-01 wild-type and HKU09-01::pIPI03 at different temperatures. Shown are three generation times calculated from independent growth curves together with the mean and SEM.

Statistical evaluation was performed using an unpaired two tailed t-test. P-values <0.05 were regarded as significant and are indicated by *.
*** indicate P-values <0.0005.

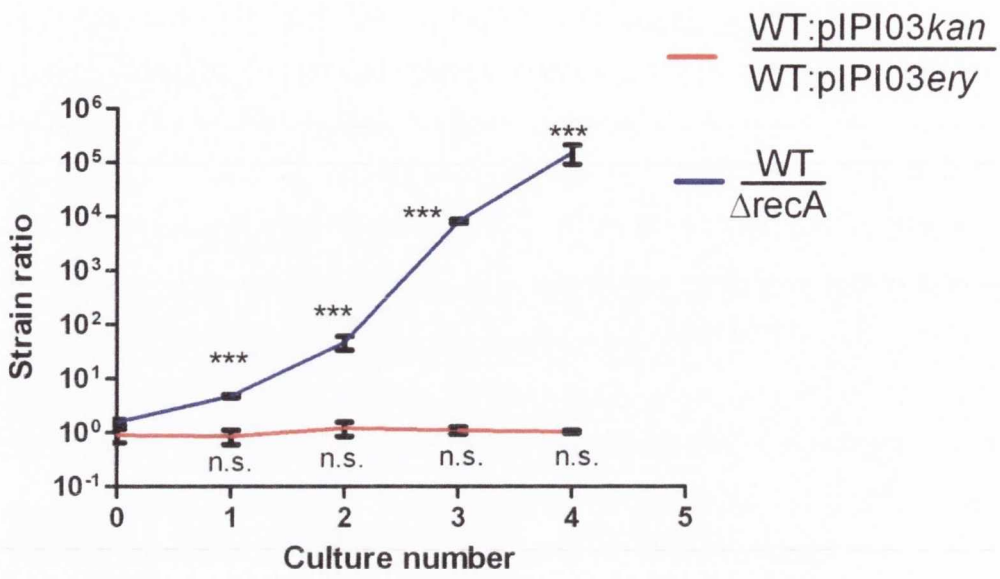

Figure 6.20 Competitive growth experiments

TSB was inoculated with two strains (labelled with pIPI03*kan* and pIPI03*ery* respectively) and passaged over four consecutive cultures. CFUs were determined for every culture and the ratio of erythromycin : kanamycin resistant cells was calculated. The mean and SEM of three independent experiments is shown.

The red line represents competitive growth of HKU09-01(WT):ery and HK(WT):kan. The number of erythromycin resistant CFUs was set to 1 and the number of kanamycin resistant CFUs was expressed in relation to this value.

The blue line represents competitive growth of HKU(WT) and the isogenic Δ*recA* mutant HKU(R). The number of HKU(R) CFUs was set to 1 and the number of HKU(WT) CFUs was expressed in relation to this value.

* Indicates a significant change in the strain ratio compared to the previous culture.

Statistical evaluation was performed using an unpaired two tailed t-test. P-values <0.05 were regarded as significant and are indicated by *.

*** indicate P-values <0.0005.

when the competition between HKU(R):ery and HKU(WT):kan was compared to the competition of HKU(R):kan and HKU(WT):ery. Therefore the experimental data was combined into one curve to compare HKU(R) with HKU(WT) (blue line in Figure 6.20). The data showed the strong growth advantage of the wild-type strain over the RecA mutant. The experiment began with equal numbers of the two strains. However, the RecA mutant was rapidly outcompeted and was present at a 10^5-fold lower number at the end of the experiment.

The experiments showed a strong statistical significance with only three replicates, due to the strong growth advantage of the wild-type strain and the small variation between the individual experiments.

6.8 Competitive growth of strains with different *isd* copy numbers

The *isd* genes of *S. aureus* and of *S. lugdunensis* have been reported to support the growth of these bacteria under iron-limited conditions in the presence of haemoglobin (Hammer & Skaar, 2011; Zapotoczna *et al.*, 2012a). Thus it was investigated whether the increase in the *isd* copy number provides a further growth advantage under these conditions. The strains HKU(R)-Δisd$^{(0)}$, HKU(R)-Δdup$^{(1)}$, HKU(R)-WT$^{(2)}$ and HKU(R)-X1$^{(7)}$ have 0, 1, 2 and 7 copies of the *isd* operon, respectively. Each strain was labelled with both pIPI03:*ery* and pIPI03:*kan* conferring an erythromycin resistant phenotype and a kanamycin resistant phenotype. This allowed a direct comparison of all copy number variants in any pairwise combination. The competitive growth experiments were carried out in iron-deficient medium (DD-RPMI). This medium has been described previously (Pishchany *et al.*, 2010; Zapotoczna *et al.*, 2012a) and consisted of RPMI treated with the iron-chelator Chelex 100 (Sigma) and contained 25 μM of the iron-chelator EDDHA (see Chapter 2). Without the addition of any source of iron *S. lugdunensis* grew poorly in this medium (see paragraph 6.6.3 Figure 6.16B). To allow bacterial growth, the medium was supplemented with either 4 μg/ml haemoglobin or 0.5 mM $FeCl_3$.

These conditions were chosen since preliminary experiments showed that 4 μg/ml haemoglobin was sufficient to allow growth to ca. OD_{578} = 4 after 24 hours of incubation. Lower concentrations failed to allow reliable growth (data not shown). Zapotoczna *et. al.* (Zapotoczna *et al.*, 2012a) showed that

S. lugdunensis expresses Isd proteins in RPMI and expression is suppressed when 1 mM $FeCl_3$ was added to the medium. However, $FeCl_3$ concentrations lower than 1 mM still induced Isd protein expression (Zapotoczna *et al.*, 2012a). Thus, the addition of 0.5 mM $FeCl_3$ to DD-RPMI in these experiments generated conditions where sufficient free iron is available to support bacterial growth without complete suppression of Isd protein expression.

In order to determine if these experimental conditions indeed allowed Isd expression, two independent competitive growth experiments in culture C2 (described below) were investigated by whole cell immunoblotting for the expression of Isd proteins (Figure 6.21). The results revealed that IsdB was expressed on the cell surface of the cells with both haemoglobin and $FeCl_3$ added, confirming iron-limitation.

6.8.1 Competitive growth of HKU(R)-Δisd$^{(0)}$ and HKU(R)-Δdup$^{(1)}$

In order to confirm the importance of Isd proteins in competitive growth assays with haemoglobin as the sole source of nutrient iron, strains HKU(R)-Δisd$^{(0)}$ (0 copies of *isd*) and HKU(R)-Δdup$^{(1)}$ (1 copy of *isd*) were compared. The results of the experiments are shown in Figure 6.22 A. The results showed that the presence of the *isd* operon conferred a growth advantage to bacteria grown in DD-RPMI supplemented with haemoglobin. Both strains began the experiment with the same number of cells. The ratio remained constant for the first 24 h of growth. Of note, the starter cultures used for the inoculation of the C0 culture were grown in iron-rich TSB to allow comparable physiological states of the strains at the beginning of the experiment. Most likely, the first joint culture in DD-RPMI was not iron-limited, since the bacteria might have used internally stored iron. This could explain the constant ratio after the first period of growth. However, over the course of the experiment (C2-C4) the strain expressing *isd* possessed a growth advantage and was present at a 6-70 fold higher number at the end of the experiment. However, high variation between the experiments did not allow the conclusion that the change in strain-ratio is of statistical significance. Three replicates were performed in these experiments but the complex experimental design of competitive growth experiments requires a minimum of 5 to 8 replicates to draw reliable conclusions about statistical significance if the growth differences between the strains are small

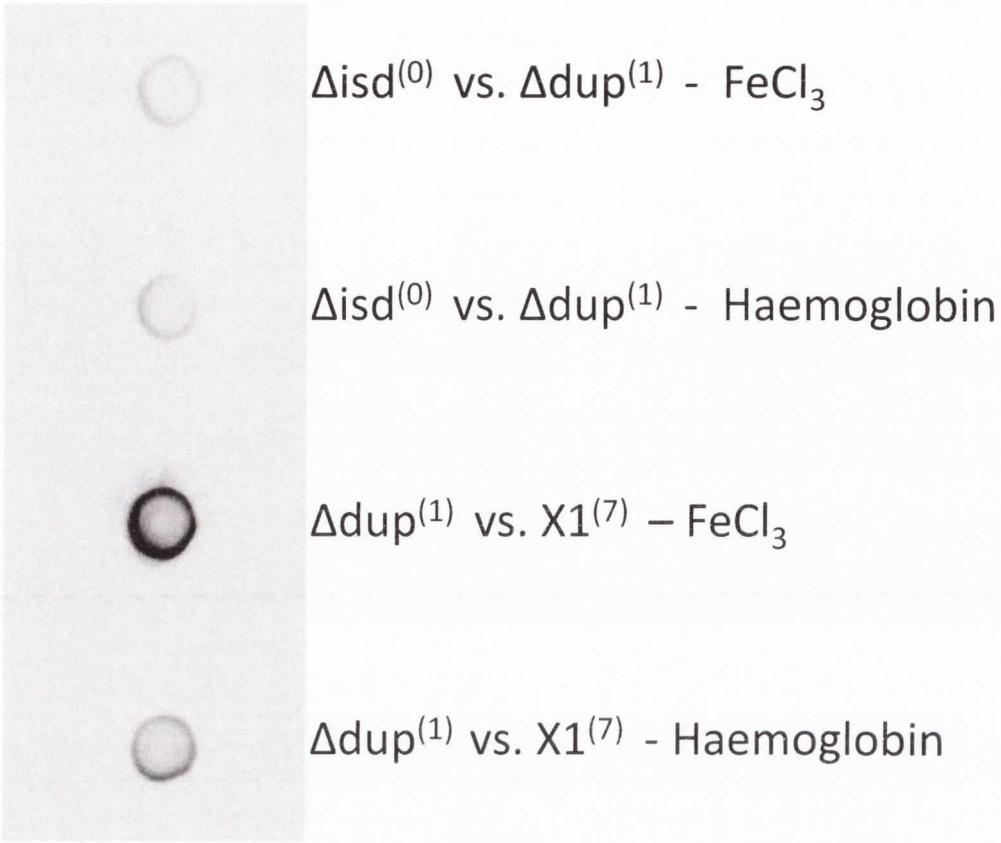

Figure 6.21 Isd protein expression during competitive growth
Samples were taken during one competitive growth experiment (C2), adjusted to OD_{578} = 1 and spotted on a nitrocellulose membrane. IsdB was detected with specific rabbit serum followed by goat anti-rabbit IgG conjugated to HRP.

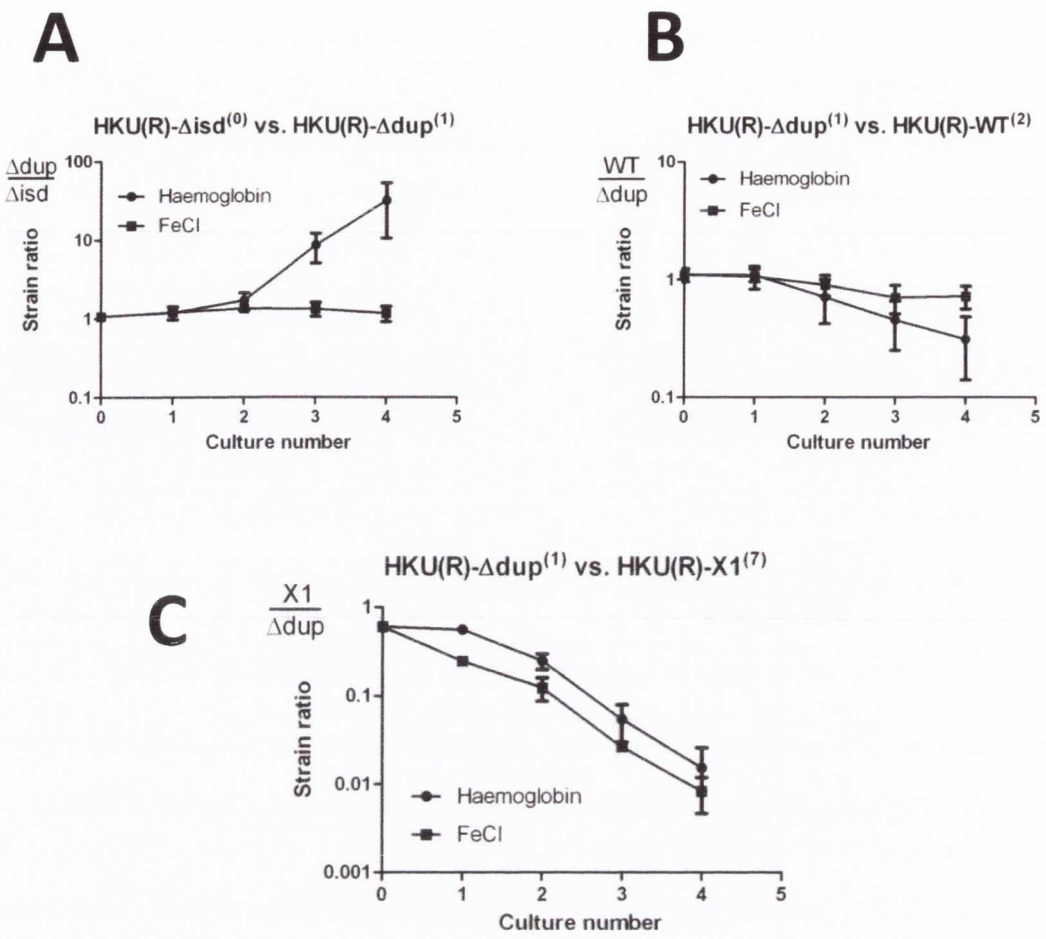

Figure 6.22 Competitive growth of strains with different *isd* copy number

DD-RPMI cultures were supplemented with 4 µg/ml haemoglobin or 0.5 mM $FeCl_3$ and inoculated with two strains (labelled with pIPI03*kan* and pIPI03*ery* respectively) and passaged over four consecutive cultures. CFUs were determined for every culture and the ratio of erythromycin : kanamycin resistant cells was calculated. The mean and SEM of three independent experiments are shown.

(A) Competitive growth of HKU(R)-Δisd(0) and HKU(R)-Δdup(1). CFUs of HKU(R)-Δisd(0) in each culture was set to 1 and CFUs of HKU(R)-Δdup(1) was expressed in relation to this value.

(B) Competitive growth of HKU(R)-Δdup(1) and HKU(R)-WT(2). CFUs of HKU(R)-Δdup(1) in each culture was set to 1 and CFUs of HKU(R)-WT(2) was expressed in relation to this value.

(C) Competitive growth of HKU(R)-Δdup(1) and HKU(R)-X1(7). CFUs of HKU(R)-Δdup(1) in each culture was set to 1 and CFUs of HKU(R)-X1(7) was expressed in relation to this value.

Statistical evaluation was performed using an unpaired two tailed t-test, comparing the strain ratio in each culture to the strain ratio in the previous culture and to the starter culture C0. Non of the differences was found to be of significance ($P<0.05$)

and the variation between individual experiments are high (Personal communication, K. Roberts).

The ratio of the two strains remained constant when $FeCl_3$ was added to the medium instead of haemoglobin. Under these conditions the expression of *isd* proteins did not confer a growth advantage since the proteins do not provide an uptake system for free iron.

6.8.2 Competitive growth of HKU(R)-dup$^{(1)}$ vs. HKU(R)-WT$^{(2)}$ and HKU(R)-X1$^{(7)}$

In order to investigate whether increased expression of Isd proteins allows a more efficient growth with haemoglobin as the sole source of nutrient iron, two further competitive growth experiments were carried out. The first compared HKU(R)-Δdup$^{(1)}$ and HKU(R)-WT$^{(2)}$ (one vs. two copies) and the second compared HKU(R)-Δdup$^{(1)}$ and HKU(R)-X1$^{(7)}$ (one vs. seven copies) (Figure 6.22 B and C). Interestingly, the results showed that the presence of multiple copies did not provide a growth advantage under either haemoglobin or $FeCl_3$ conditions. In the competition between HKU(R)-Δdup$^{(1)}$ and HKU(R)-WT$^{(2)}$ (Figure 6.22 B), the ratio remained constant with $FeCl_3$ with only a small drop in the HKU(R)-Δdup$^{(1)}$: HKU(R)-WT$^{(2)}$ ratio. This indicated a minor growth advantage for the low copy number isolate. A growth advantage of one copy compared to two copies was observed with haemoglobin. The two copy strain HKU(R)-WT$^{(2)}$ was present in a 5-8 fold lower number than the single copy strain HKU(R)-Δdup$^{(1)}$ at the end of the experiment.

The effect became more pronounced in the competition between HKU(R)-Δdup$^{(1)}$ (one *isd* copy) and HKU(R)-X1$^{(7)}$ (seven *isd* copies) (Figure 6.22 C). With both $FeCl_3$ and haemoglobin, the growth advantage of the HKU(R)-Δdup$^{(1)}$ strain was strong and the HKU(R)-X1$^{(7)}$ was present at a 50-100 fold lower number than the HKU(R)-Δdup$^{(1)}$ strain at the end of the experiment.

As described above, the three replicates performed in these experiments showed trends towards a reduced fitness of HKU(R)-ΔWT$^{(2)}$ and HKU(R)-X1$^{(7)}$ However, additional replicates are needed to draw conclusions about the statistical significance of these experiments.

6.9 Physiological burden associated with the amplification of *isd*

6.9.1 Growth analysis under iron-rich and iron-deficient conditions

The competitive growth experiments indicated a strong growth disadvantage for the HKU(R)-X1$^{(7)}$ strain. It was investigated whether the observed differences were due to the gene-dosage-dependent over-expression of the Isd proteins.

TSB is iron-rich and the *S. lugdunensis* Isd proteins were shown not to be expressed in this medium (Zapotoczna *et al.*, 2012a). RPMI medium is iron-limited and it was shown previously that iron-limitation is strong enough to induce *isd* expression in *S. lugdunensis* (Zapotoczna *et al.*, 2012a). Nonetheless, the medium contains enough free iron to allow bacterial growth. The four strains with different *isd* copy numbers showed similar growth characteristics in TSB (Figure 6.23 A). The generation times in this medium for HKU(R)-Δisd$^{(0)}$, HKU(R)-Δdup$^{(1)}$, HKU(R)-WT$^{(2)}$, HKU(R)-X1$^{(7)}$ were 143.6 min, 142.0 min, 145.6 min and 152.6 min, respectively. Although the differences appear small, they were found to be of statistical significance. This indicated that a distinct physiological burden exists which is independent of *isd* expression. The growth in iron-limited RPMI also showed differences between the strains. Although the growth curves of the strains appeared similar (Figure 6.23 B), the generation times for HKU(R)-Δisd$^{(0)}$, HKU(R)-Δdup$^{(1)}$, HKU(R)-WT$^{(2)}$, HKU(R)-X1$^{(7)}$ were 232.2 min, 260.8 min, 262.2 min and 364.2 min, respectively (Figure 6.23 C). Due to a higher variation between the experiments, only the differences between the generation times of HKU(R)-Δisd$^{(0)}$ and HKU(R)-X1$^{(7)}$ were statistically significant in these experiments.

6.9.1 A role for AtlI

A unique characteristic of the *S. lugdunensis isd* locus is the presence of the gene *atlI* (Figure 6.2 A). The encoded protein possesses a glucosaminidase domain and is likely to represent an autolysin involved in the hydrolysis of peptidoglycan (PG). Overexpression of this gene due to an increased copy number might decrease bacterial viability. In order to investigate this possibility, zymogram analysis was performed. The HKU(R) strains were grown under iron-limiting conditions and cell fractionation was performed. The fractions were

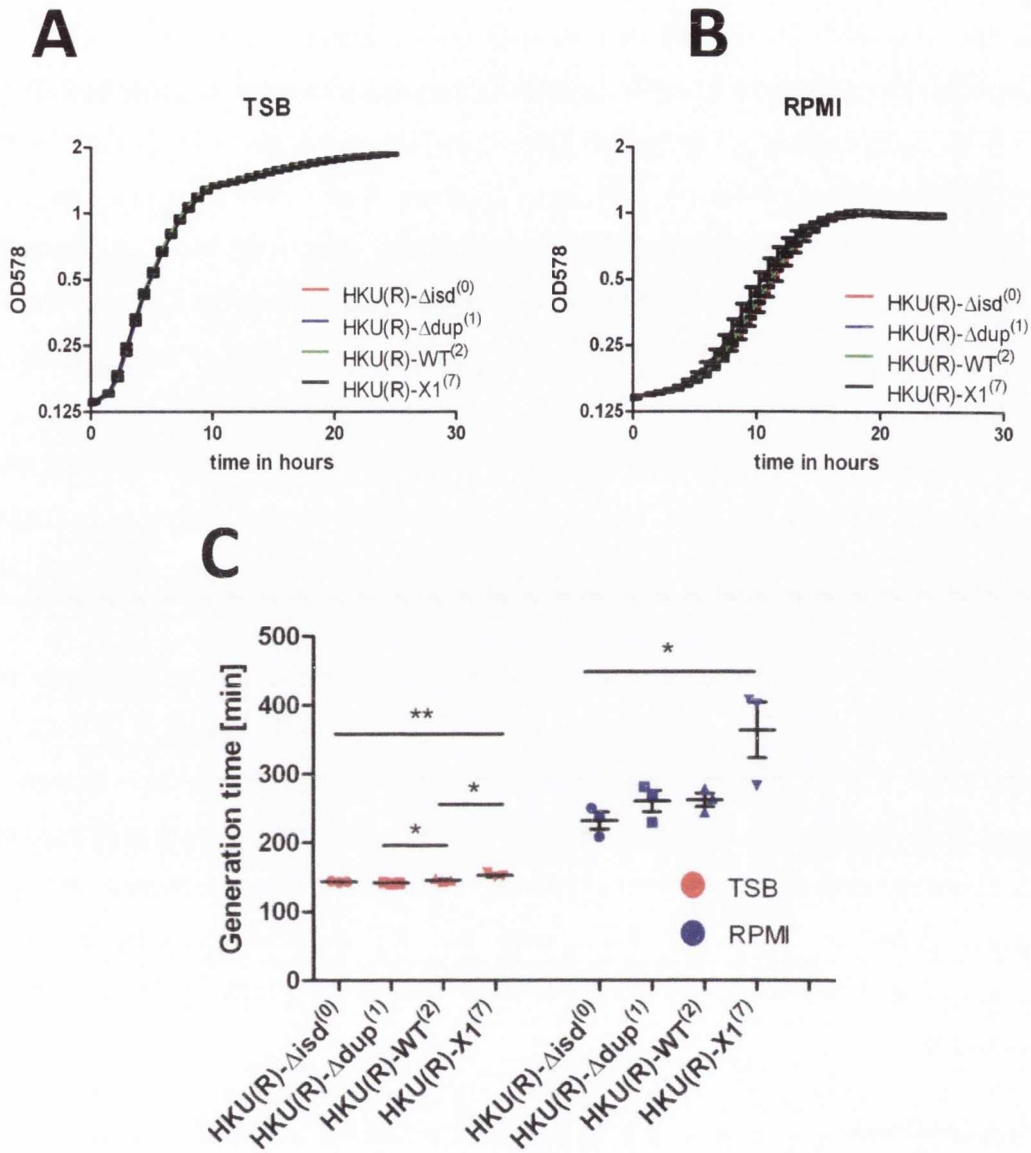

Figure 6.23 Growth in TSB and RPMI

(A) Growth curves of strains with different *isd* copy number in TSB at 37°C. The mean and SEM of three independent growth curves are shown.

(B) Growth curves of strains with different *isd* copy number in RPMI at 37°C. The mean and SEM of three independent growth curves are shown.

(C) Generation times of strains in TSB and RPMI calculated using the growth curves in A and B. The generation time was calculated for each growth curve. The mean and SEM of the three experiments are shown.

Statistical evaluation was performed using an unpaired two tailed t-test. P-values <0.05 were regarded as significant and are indicated by *. ** indicate P-values <0.005.

subsequently separated by SDS-PAGE containing lyophilized *Micrococcus lysodeikticus* cells and autolysin activity was assessed (Figure 6.24 A). No difference in the pattern of hydrolysis between the strains was observed. Since HKU(R)-Δisd$^{(0)}$ lacks *altI* a missing band in this strain would have correlated with AtlI activity. The result can have various explanations (i) AtlI does not possess autolysin activity; (ii) AtlI autolysin activity is specific for *S. lugdunensis* PG and does not recognize *Micrococcus lysodeikticus* PG; (iii) AtlI is unable to refold under the conditions used; (iv) expression of AtlI is too low to be detected.

In order to narrow down the possibilities, autolysis experiments were performed (Figure 6.24 B/C). All the strains showed the same level of autolysis, independently of the growth conditions (iron-limited / iron-rich). This indicates that AtlI did not contribute significantly to bacterial autolysis.

In order to investigate the effects of *atlI* over-expression, the gene was cloned into the inducible expression vector pRMC2 and the plasmid pRMC2:*atlI* was used to transform wild-type HKU09-01. The strain was grown to exponential phase and *atlI* expression was induced with anhydrotetracycline. Induction did not influence the bacterial growth and did not increase autolysis (Figure 6.24 D). However, AtlI could not be detected directly in these experiments, therefore it has to be considered, that the protein was not actually expressed.

Discussion

Gene duplication and amplification (GDA) are common genetic events that have been shown to be of importance for the rapid adaption to new environmental conditions and for the development of new genes (Andersson *et al.*, 1998; Näsvall *et al.*, 2012). It is well understood that RecA-mediated processes are responsible of the amplification and segregation of duplicated chromosomal regions (Sandegren & Andersson, 2009). The work presented here demonstrates that these mechanisms also apply to the amplification and segregation of the duplicated region in HKU09-01. It was demonstrated that the duplication was intrinsically unstable during growth under non-selective conditions and could be stabilized by the introduction of a *recA* mutation.

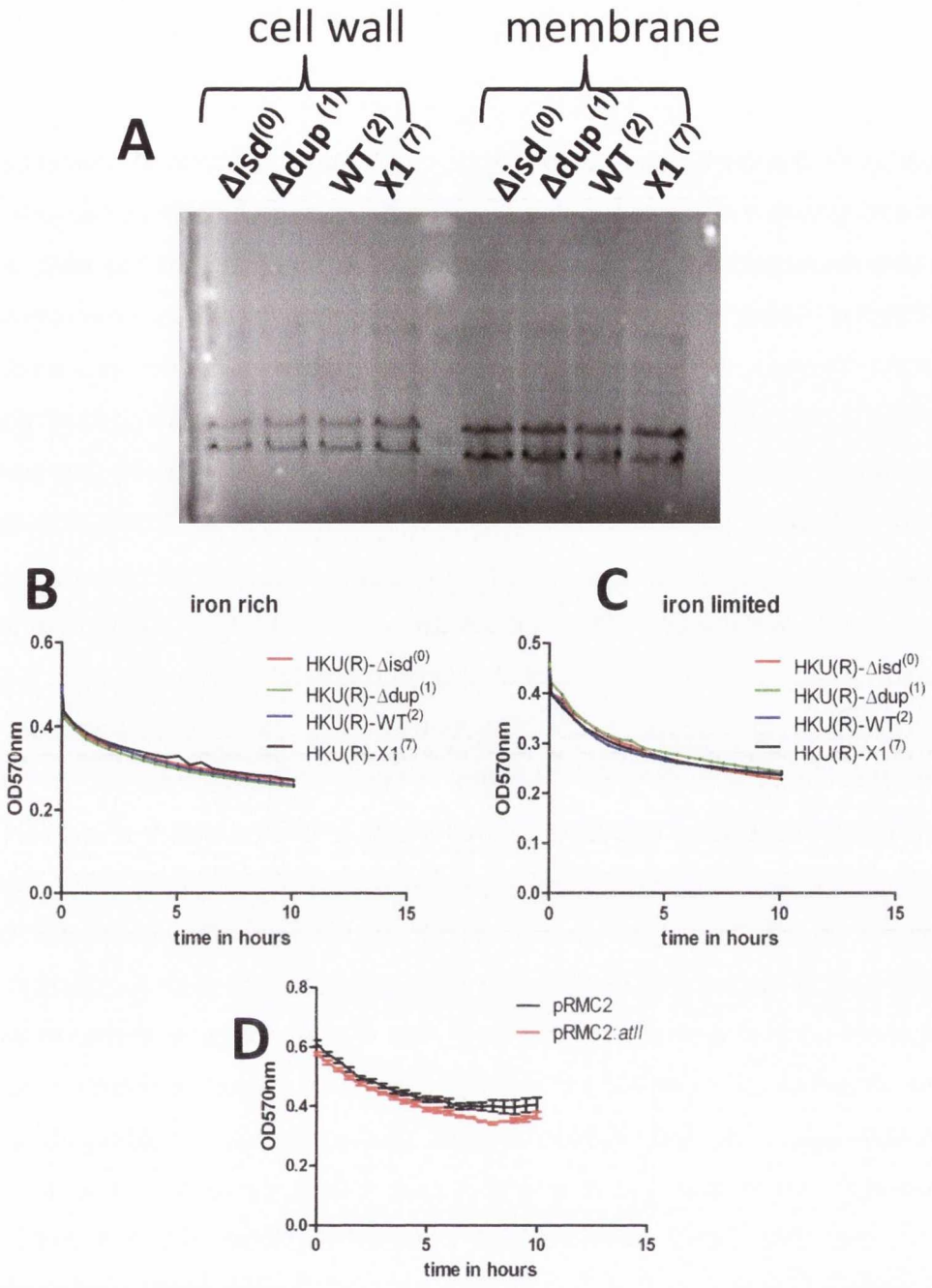

Figure 6.24 Atll activity

(A) Zymogram using cell fractions of the HKU(R) strains with different *isd* copy number. The SDS PAGE contained 1% lyophilized *Micrococcus lysodeikticus* cells. Bands show zones of PG degradation after overnight incubation in renaturation buffer at 37°C.

(B/C) Autolysis of HKU(R) strains grown under iron-rich or iron-limited conditions (TSB or RPMI). Exponential phase cells were adjusted to OD_{578} = 0.5 and the decrease in optical density was measured over time during incubation at 37°C. The mean and SEM of triplicate wells of one experiment are shown. The experiment was repeated three times with similar results.

(D) Autolysis of HKU09-01 transformed with pRMC2 or pRMC2:*atlI*. Exponential phase cells were induced for 2 h with anhydrotetracycline, adjusted to OD_{578} = 0.7 and the decrease in optical density was measured as in (B/C). The mean and SEM of triplicate wells are shown. The experiment was repeated three times with similar results.

Statistical evaluation using an unpaired two tailed t-test did not identify any significant ($P<0.05$) differences in cell-lyses between the strains.

Furthermore, the duplication was shown to be the subject of amplification events and strains harbouring multiple copies of the region could be isolated.

The current model of the function of GDAs implies that the associated gene-dosage effect improves bacterial fitness under certain environmental conditions. Thereby the selective pressure stabilizes the GDA within a bacterial population. The amplification of the DNA region encoding important genes allows mutations to occur with a higher frequency thereby speeding up the evolution of important chromosomal regions (Kugelberg *et al.*, 2006). However, GDAs are always associated with a physiological burden due to the increased level of protein expression. Thus GDAs are under constant pressure and as soon as the selective pressure which favoured bacterial cells harbouring a GDA is lifted, GDAs are subject to high-frequency RecA-mediated segregation and are thereby eliminated from the bacterial culture. This characteristic of GDAs makes any investigation of GDAs providing an unknown selective advantage challenging. Research conducted to date focused on GDAs with known phenotypic effects to enable specific experimental setups to select for GDA events in model organisms (Andersson *et al.*, 1998; Näsvall *et al.*, 2012). The experiments conducted here addressed a naturally occurring duplication within the chromosome of a clinical isolate. The selective pressure maintaining the duplication was unknown which made the experimental analysis more complicated. The introduction of a tetracycline resistance determinant (*tet*) was used to circumvent this problem. The point of *tet* introduction allowed the amplification of *tet* only in combination with the amplification of the entire region, comprising *isd*, *sir* and 11 genes of unknown function. Thereby the gene-dosage effect associated with the amplification of *tet* allowed the isolation of clones with variable numbers of *isd* loci. However, this selection is artificial and the natural function of the duplication remains to be elucidated.

The genes encoded within the duplicated region of HKU09-01 give a good indication about the phenotypes that might be associated with the duplication. The *isd* locus of *S. lugdunensis* is of particular interest since it links this species more closely to *S. aureus* and to the evolution towards a more invasive behaviour than other CoNS. The locus is well described in *S. aureus* and a plethora of different functions associate this locus with invasive disease. Most importantly, the locus of *S. aureus* provides a haem transport system

allowing the efficient acquisition of nutrient iron during infection (Mazmanian *et al.*, 2002; Mazmanian *et al.*, 2003; Pishchany *et al.*, 2010). Recent research showed that the *S. lugdunensis* Isd proteins fulfil the same function (Haley *et al.*, 2011; Zapotoczna *et al.*, 2012a) although no *in vivo* experiments have been performed to date. In this regard the duplication in HKU09-01 is of special interest. The duplication comprises the complete *isd* operon together with the siderophore uptake system *sirABC*. Both loci are involved in iron acquisition in *S. aureus* and among all staphylococci sequenced only *S. lugdunensis* and *S. aureus* encode these loci. The GDA in HKU09-01 was shown to promote an increase in the level of expression of Isd proteins and might therefore indicate special importance of iron acquisition for *S. lugdunensis.* The strain HKU09-01 is a clinical isolate, although the type of infection caused by this strain was not described precisely in the original publication (Tse *et al.*, 2010). It was described as "isolated from pus" indicating abscess formation or a similar superficial skin infection. It was shown previously that erythrocytes are present within abscesses making haemoglobin an available source of iron at this site (Cheng *et al.*, 2009). Accordingly, it can be speculated that iron-limitation in the presence of haemoglobin might have selected for the duplication of the *isd* region in HKU09-01. Competitive growth experiments comparing a strain without *isd* to a strain harbouring a single copy showed that the presence of *isd* confers a growth advantage under iron-limited conditions in the presence of haemoglobin. Nonetheless the strain without *isd* was not lost entirely from the mixed culture and the strain was single-handedly able to grow in DD-RPMI supplemented with haemoglobin. This suggests that apart from *isd* *S. lugdunensis* possesses at least one additional heam-uptake system.

However, the *in vitro* experiments conducted here did not support the idea that a gene-dosage dependent increase in Isd protein expression results in an improved ability to acquire nutrient iron from haemoglobin. In contrast, strains with multiple copies of *isd* proved to have a growth disadvantage in competitive growth experiments and were outcompeted by the single copy variant. These experiments suggest that one copy of *isd* is sufficient to allow the satisfactory uptake of haemoglobin to support optimal bacterial growth. The reasons for this remain speculative but multiple explanations have to be considered. Firstly, for individual bacteria within a culture, GDAs have to be

understood as a mixed blessing. Only if the conditions are right and the positive effects of the improved gene-dosage outweigh the inherent negative side-effects (maintainance of DNA, stochiometric imbalance, physiological cost of protein over-expression etc.) the duplication will improve the bacterial fitness and allow stabilization throughout the culture. The duplication of the region in HKU09-01 possesses a realistic threat of strong negative side-effects. The duplicated region comprises 29 genes of which 18 encode putatively-membrane associated proteins. Over expression of all proteins simultaneously might cause significant metabolic problems. Not only do the physiological costs of the over-expression have to be considered, but also the over-representation of proteins within the membrane. Growth curve analysis showed that the increase in copy number correlated with an increase in the generation time, highlighting the physiological disadvantage of GDAs under non-selective conditions. Thus the environmental conditions are crucial to maintain the duplication within the culture.

The GDA in HKU09-01 encodes the *isd* locus and the *sirABC* locus. Both of these systems are known to be repressed in the presence of iron (Dale *et al.*, 2004b; Hammer & Skaar, 2011; Mazmanian *et al.*, 2002). In *S. aureus* Fur regulated genes are highly expressed under iron-limiting conditions and IsdA is the most abundant surface-associated protein in this setting (Clarke *et al.*, 2007). Assuming that the same is true for *S. lugdunensis,* it is conceivable that amplification of these genes might have severe impacts on the cell physiology. The *S. lugdunensis isd* gene *atlI* encodes a putative autolysin. Thus it seemed likely that over-expression of this gene might lead to an increase in autolytic activity, representing a further negative effect of the duplication. It could not be proven experimentally that an increase of the *isd* copy number leads to AtlI over-expression. However this was shown for IsdB, IsdC, IsdJ and IsdK and since all genes are Fur regulated it can be assumed that AtlI was also over-expressed. Strains with increased *isd* copy number did not display a significant increase in their autolytic activity. The same was true when the protein was cloned and induced using pRMC2 which should result in strong over-expression. These results suggest that over-expression of AtlI is not exclusively responsible for the growth disadvantage of HKU(R)-X1$^{(7)}$ observed in competitive growth experiments. Although more experiments are needed to

understand the role of *atlI*, over-expression of the protein seems not to be toxic for to bacterial cells and *atlI* over-expression in HKU(R)-X1[(7)] is unlikely to cause the decreased growth rate observed under iron-limiting conditions.

The duplicated region in HKU09-01 comprises iron uptake systems, which opens a further avenue of putative negative effects. Although iron is essential for bacterial survival and growth, the reactivity of the metal has severe toxic side-effects. It is conceivable that *isd* and *sir*-dependent iron uptake is too effective in strains with higher copy numbers thereby increasing the iron-mediated toxicity. Not only an excess of free iron, but also an excess of haem is known to be toxic for bacterial cells (Anzaldi & Skaar, 2010). *S. aureus* encodes a haem sensing two component system and a haem efflux ABC transporter to avoid an excess of haem within the cytoplasm (Stauff *et al.*, 2007; Torres *et al.*, 2007). This system was found not be conserved in *S. lugdunensis* and rises the general question how *S. lugdunensis* might avoid haem mediated toxicity. This question has not been addressed in the experiments conducted within this thesis, but it is conceivable that an amplification of the *isd* locus might overpower the haem detoxification systems of *S. lugdunensis*. This would suggest that only moderate amplification of the locus results in improved fitness, while high level amplification results in negative side-effects. However, before this can be investigated, further experiments are needed to confirm that the gene-dosage effect does indeed mediate an improved import of haem / iron.

Furthermore it has to be underlined that, in order to stabilize the *isd* copy number, a *recA* mutation was introduced in all strains used for competitive experiments. It was shown that the *recA* mutation itself confers a strong growth disadvantage. The effect of this mutation might make it more difficult to detect small differences in the relative fitness conferred by the increased *isd* copy number. This might be especially important for experiments investigating iron uptake. It is widely recognized that high concentrations of free intracellular iron and especially haem-iron possess toxic effects. Both, radicals released by free iron in Fenton reactions and the monooxygenase-like activity of haem have toxic effects. Although the mechanism of toxicity is not understood in much detail, it is suggested that protein and DNA damage is a result of these processes (Anzaldi & Skaar, 2010). An important mechanism of DNA repair is RecA-dependent recombination which is not possible in the strains used in the

experiments conducted here. It is therefore conceivable, that the haem uptake in strains with increased Isd protein expression is so effective that it leads to DNA damage that cannot be tolerated in the artificial *recA*$^-$ background. Therefore it should be considered to redesign the experimental setup used in these experiments. Exemplarily the *isd* copy number might be stabilized by the expression of an inducible *recA*-antisense RNA located on a plasmid. After the start of haem uptake experiments *recA* expression can be allowed in the absence of the inducer. Alternatively the concentration of haem used in the experiments might be lowered to reduce the intracellular accumulation.

Animal experiments using *recA*$^+$ cells carrying two copies of *isd* might give additional insights into the importance of this duplication. In case the duplication of *isd* does indeed confer a growth advantage during infection, the duplication should be stable within the mouse and should be subject to amplification. Both stability and amplification of the duplication can be addressed using the techniques described within this thesis. *In vivo* experiments might therefore help to understand the biological significance of this process.

Additionally it has to be considered that haem / iron uptake does not provide a selective advantage, selecting for an increased gene-dosage. The *isd* genes of *S. aureus* are associated with a plethora of different unrelated phenotypes. IsdA promotes resistance to innate immune defences such as antibacterial peptides, antimicrobial fatty acids or apolactoferrin protease activity (Clarke *et al.*, 2007; Clarke & Foster, 2008). IsdJ of *S. lugdunensis* shows significant homology to IsdA and is located at the same site in the locus. Furthermore IsdJ was shown to confer resistance against linoleic acid when expressed in the surrogate host *L. lactis* (Zapotoczna *et al.*, 2012a). Therefore the gene-dosage effect might improve resistance levels and experiments regarding this are currently being conducted. IsdB of *S. aureus* allows the interaction with and activation of platelets (Miajlovic *et al.*, 2010). Additionally it promotes integrin-mediated invasion of non-phagocytic cells (Zapotoczna *et al.*, 2012b). If IsdB of *S. lugdunensis* possesses the same functions, the gene dosage effect might improve these processes.

Finally it has to be considered that the proteins encoded by the *isd* operon do not possess the functions that stabilized the duplication. The

duplicated region HKU09-01 comprises 13 genes that are not related to *isd* or *sir*. Since no experimental evidence is available for similar proteins, it is impossible to predict the effects that duplication of these genes might have on bacterial physiology. Yet any of these proteins might possess functions that are improved by a higher gene-dosage. Additionally the duplication created a unique hybrid gene. Maybe the function provided by the encoded protein confers a favourable phenotype that is selected.

Also *S. aureus* has the potential to express up to 21 different cell wall-anchored proteins. Many of these proteins allow it to evade innate immune factors such as neutrophils and complement. *S. lugdunensis* encodes only nine putative cell wall-anchored proteins. It is conceivable that the cell-surface of *S. lugdunensis* might be less decorated with protein. The amplification of *isd* and the associated over-expression of cell surface-associated proteins might help in this regard.

The experiments reported here failed to model *in vitro* the environmental conditions that selected for an increased copy number by the GDA in HKU09-01 *in vivo*. However, a multitude of additional putative functions of the *S. lugdunensis* Isd proteins can be addressed in future experiments in order to elucidate the function of the GDA. Of special interest will be *in vivo* models, since multiple pressures are present simultaneously during infection. Besides iron-limitation, host immune defence mechanisms must be avoided within the host. It is conceivable that only the combination of multiple selective pressures present *in vivo* will allow the detection of a growth advantage provided by the GDA in HKU09-01. Since *S. lugdunensis* Isd proteins were shown to recognize only human haemoglobin (Pishchany *et al.*, 2010; Zapotoczna *et al.*, 2012a), transgenic mice expressing human haemoglobin (Pishchany *et al.*, 2010) will be used for these experiments.

Site-specific integrative plasmids are important tools for modern molecular microbiology since they allow the efficient insertion of DNA in a specific genomic region. In principle phage-integrase vectors can be constructed for any species as needed. Only the *ccrB* gene together with the corresponding *attP* site of a phage are required. As long as the strain to be tested is not lysogenic and the CcrB protein does not promote excision of the

phage, phage-integrase vectors will integrate stably into the bacterial chromosome.

The constructed site-specific integration vector for *S. lugdunensis* uses the coding sequence of the CcrB integrase and the corresponding *attP* site of phage ϕSL01. The plasmid was found to integrate specifically, irreversibly and RecA-independently into the *attB* site of HKU09-01. The constitutive expression of *ccrB* in this vector did not have a negative effect on bacterial fitness. However, the integrated plasmid led to a reduction in growth rate at 28°C. This is most likely due to the thermosensitive nature of the plasmid replication system, which allows replication to be attempted at 28°C. This most likely interferes with the chromosomal replication. This should be borne in mind when pIPI03 is employed to complement mutants, for example. Despite this no plasmid loss was detected after 40 generations of growth at 28°C. None of the 10 *S. lugdunensis* strains from CC1-CC5 harboured a lysogenic phage in the *attB* site recognized by CcrB of ϕSL1. Consequently pIPI03 could be integrated into the chromosome of every strain investigated. This demonstrates the broad range of *S. lugdunensis* strains that can conveniently be labelled using pIPI03.

There are many possible applications of site-specific integrative plasmids such as pIPI03. The extensive multiple cloning site of pIPI03 facilitates insertion of DNA fragments into the plasmid. Two IPTG-inducible antibiotic resistance cassettes were cloned into pIPI03 and the use of the two variants in competitive growth experiments was demonstrated. Competitive growth is a powerful technique to investigate the effects of the controlled expression of a single gene on the cell physiology under identical growth conditions and can be used both *in vitro* and *in vivo* (Monk *et al.*, 2008). pIPI03:*ery* and pIPI03:*kan* allowed easy labelling of *S. lugdunensis* strains with clearly distinguishable phenotypes and hence the accurate determination of the ratio of the two strains in competitive growth experiments. It is possible to detect subtle differences by prolonged competitive growth when differences in growth rate/yield in conventional growth curve experiment would not be seen. Furthermore, the growth of different strains in the same culture allows the comparison of the effects of environmental stress factors, such as antibacterial compounds or nutrient limitation.

Another application of integration vectors is complementation of mutants. This would be particularly attractive for experiments involving growth in experimental animals where selection for an autonomously replicating plasmid is difficult and where plasmid loss is magnified by stressful conditions of growth *in vivo*. Furthermore complementation may be distorted by the gene-dosage effect of expressing the wild-type gene from a multicopy plasmid. The integrated vector is very stable and provides expression from a single copy of the wild-type gene.

The *S. lugdunensis* integrative plasmid pIPI03 is ideally suited for these applications and will facilitate future experiments to allow a deeper understanding of the virulence potential of this neglected coagulase negative pathogen.

Chapter 7
Discussion

S. lugdunensis is an unusual pathogen. It is a coagulase negative staphylococcus (CoNS) and therefore in general regarded as less virulent than the coagulase positive *S. aureus*. Nevertheless *S. lugdunensis* is associated with a wide array of different invasive infections and diseases that are more akin to

S. aureus infections than to CoNS infections (Frank *et al.*, 2008). Although *S. lugdunensis* is more and more recognized to be an important staphylococcal pathogen, hypothesis-driven research has been widely neglected and very little is known about the virulence and immune evasion factors that might account for any increased invasiveness.

The analysis of the first genome sequences of *S. lugdunensis* N920143 (this thesis) and HKU09-01 (Tse *et al.*, 2010) identified several interesting genes and loci that seem to place *S. lugdunensis* between *S. aureus* and the CoNS. Several features are consistent with *S. lugdunensis* being a skin commensal. Both HKU09-01 and N920143 encode a putative lantibiotic resistance determinant and three nonribosomal peptide synthesis systems (NRPS). Although the functionality of the lantibiotic resistance needs to be proven experimentally and the identity and functionality of the nonribosomal peptides need to be determined, it seems conceivable that these factors promote the survival of *S. lugdunensis* within the microbiome of the human skin by providing resistance to secreted inhibitors, by facilitating the uptake of rare ions or by inhibiting other commensals.

However other factors seem to underline the virulence potential of the species. *S. lugdunensis* has the potential to express a putative streptolysin S–like toxin which among staphylococci is only described for the bovine *S. aureus* isolate RF122 (Lee *et al.*, 2008). Furthermore *S. lugdunensis* encodes the haemolytic SLUSH peptides, a putative haemolysin III and a putative β-toxin. It possesses the genetic loci for the expression of a polysaccharide and polyglutamic acid capsule. However, experimental evidence is needed to confirm that these factors are indeed expressed and represent virulence factors. Interestingly, *S. lugdunensis* was found not to encode cytotoxic or immunostimulatory toxins that are produced by *S. aureus*. Neither superantigens nor pore-forming toxins are encoded. Furthermore immune

evasion molecules such as SCIN, CHIPS, staphylokinase, protein A or Eap are not encoded. However, *S. lugdunensis* is known to cause invasive disease in immunocompetent individuals. Consequently strategies to avoid host immune responses must be present. The factors employed by *S. lugdunensis* might be different from the factors used by *S. aureus*. A noticeable characteristic of the two investigated genome sequences is the small number of mobile genetic elements (MGE) present. Neither strain carries any free or integrated plasmids, or SCC-elements. Both strains carry a single prophage (distinct in each strain) and HKU09-01 carries two identical transposons encoding β-lactamase. Apart from the transposon-encoded resistances no obvious virulence or immune evasion factors are associated with the MGEs in N920143 and HKU09-01. It is recognised that MGEs are important vehicles for *S. aureus* to acquire/impart antibiotic resistance determinants and virulence factors from/to closely related strains (Lindsay & Holden, 2004). It is reported that clinical *S. lugdunensis* isolates are remarkably sensitive to the antibiotics used in clinical practice and strains carrying multiple resistances do not seem to accumulate (Frank *et al.*, 2008). It might be speculated that a lack of MGEs might limit the ability of the species *S. lugdunensis* to acquire novel genes by lateral gene transfer. Interestingly, *S. lugdunensis* carries a CRISPR (clustered regularly interspaced short palindromic repeats) locus. This kind of locus was identified in *S. epidermidis* RP62a but not *S. aureus* strains and is recognised to represent a sequence-specific and heritable defence mechanism of bacteria against phage infection and the transfer of plasmids by conjugation (Marraffini & Sontheimer, 2008; Richter *et al.*, 2012). Thereby the system also limits the transfer of mobile genetic elements. It is tempting to speculate that this system might be responsible for the apparent low number of MGEs present in the *S. lugdunensis* genome sequences and might be linked to the apparent slow spread of resistance determinants within the species. However, many factors are known to influence the lateral transfer of MGEs e.g. restriction modification systems or the masking of phage receptors on the surface of the bacterial cell (Labrie *et al.*, 2010). Therefore experimental evidence is needed to determine the effect of CRISPR expression on the ability of *S. lugdunensis* to acquire MGEs. Furthermore a wider range of *S. lugdunensis* genomes need to be sequenced

and analysed to determine whether a general lack of MGEs is indeed associated with the species.

In order to investigate putative virulence factors of *S. lugdunensis*, a genetic system was developed to allow the efficient genetic manipulation of the species. N920143 and HKU09-01 possess a single Type I restriction modification (RM) system (SluI) which is solely responsible the prevention of transformation with *E. coli*-derived DNA. Unlike *S. aureus* and *S. epidermidis*, neither of the sequenced *S. lugdunensis* strains encodes a Type IV restriction system (SauUSI) that recognises cytosine methylation conferred by Dcm of *E. coli* K12. Therefore plasmid DNA isolated from the *dcm*⁻ *E. coli* cloning strain DC10B (Monk *et al.*, 2012) did not facilitate the transformation of N920143 and HKU09-01. The same was true for all strains included in this thesis, suggesting that a SauUSI homologue is not present in *S. lugdunensis* strains. It is an interesting observation that *S. lugdunensis* CC1 strains seem to possess a single allele of the Type I RM system while most *S. aureus* strains possess two alleles of a Type I system and additionally a Type IV restriction system (Monk *et al.*, 2012; Roberts *et al.*, 2013). In general, Type I restriction systems recognise strain-specific methylation patterns and are therefore able to recognize and cleave DNA even from closely related strains of the same species if their HsdS proteins show differences in the target recognition domains (TRD). The presence of two distinct alleles in most *S. aureus* strains leads to a tight restriction barrier that allows DNA transfer only between closely related lineages that have identical TRDs in both HsdS variants (Roberts *et al.*, 2013). *S. aureus* tightens this barrier further by the expression of the Type IV system (SauUSI) that is specific for cytosine methylation patterns created by Dcm which is only described in the family Enterobacteriaceae (Gomez-Eichelmann *et al.*, 1991), although it cannot be excluded that other species possess systems that confer the same methylation. The SauUSI system does not impact the transfer of DNA between *S. aureus* strains (Roberts *et al.*, 2013), but represents an additional barrier against the transfer of DNA derived from Enterobacteriaceae. The evolutionary importance of this system for *S. aureus* is not yet understood. However, *S. lugdunensis* does not seem to rely on an additional RM system to prevent the uptake of DNA derived from Enterobactericeae. These findings simplify the transformation of *S. lugdunensis* and together with the *E. coli*

cloning strain SL01B that expresses the SluI HsdM/S subunits of *S. lugdunensis* CC1, a convenient genetic system is now available. Plasmid DNA derived from the PAM (plasmid artificial modification) strain SL01B allowed the improved transformation of all strains from CC1 and CC2 suggesting that the Type I system (including the TRD-sequences of HsdS) is conserved within these strains. *S. lugdunensis* strains from CC3, CC4 and CC5 could not be transformed with an increased efficiency when SL01B-derived plasmid DNA was used suggesting that the RM system in these CCs is not bypassed by the methylation pattern conferred by SL01B. Differences in the TRDs of SluI or the presence of additional *hsdM/S* alleles seem most likely to account for this phenomenon. However addition experiments are needed to verify this hypothesis.

The analysis of the *S. lugdunensis* genome sequences revealed the presence of 13 genes with the potential to encode cell wall-anchored proteins (CWPs). The established genetic system was used to create N920143 mutants deficient in sortase A or the individual CWPs vWbl (binds to von Willebrand factor) or Fbl (binds to fibrinogen). A catheter-induced rat endocarditis model was used to investigate the ability of N920143 wild-type and the isogenic mutants to cause infective endocarditis. Although *S. lugdunensis* N920143 was less virulent than *S. aureus* Newman in this model, it formed endocardial vegetations that were comparable to those formed by *S. aureus* strain COL (MRSA). CWPs were shown to be important for the development of the disease since the Δ*srt* mutant was significantly impaired. However mutants deficient in Fbl or vWbl alone were not significantly different from the wild-type. It is conceivable that the combined functions of several CWPs are important for the development of the disease. *S. lugdunensis* possesses a multitude of different CWPs and the experiments performed showed that the proteins are expressed in a strain- and growth phase-dependent manner. Previous studies confirmed that *S. lugdunensis* strains possess the capacity to bind to various extracellular matrix (ECM) molecules (Paulsson *et al.*, 1993). However, the experiments conducted in this study failed to identify ECM molecules that serve as ligands for *S. lugdunensis*, apart from Fbl-dependent adherence to fibrinogen. None of the strains tested adhered to fibronectin, cytokeratin 10, or loricrin, ligands that are known to be important for *S. aureus* colonisation and disease (Mulcahy *et*

al., 2012; Speziale *et al.*, 2009). Furthermore, vWbl-expressing strains did not adhere to von Willebrand factor (vWF), raising the question as to whether vWbl does indeed represent a vWF binding protein when expressed on the cell surface of *S. lugdunensis* or if it binds to other ligands. Interestingly vWbl and SlsE of *S. lugdunensis* possess one and two Arg-Gly-Asp (RGD) motifs, respectively. In contrast, not a single *S. aureus* CWP possessing an RGD motif has been described. RGD motifs are recognized specifically by many eukaryotic integrins and are present in a multitude of ligands such as fibronectin, vitronectin, fibrinogen, von Willebrand factor and collagens (Ruoslahti & Pierschbacher, 1986; Ruoslahti, 1996). It is conceivable that vWbl and SlsE allow a direct interaction between the bacterial cell and integrins on eukaryotic cells. Similar interactions have been shown to be important for *S. aureus.* IsdB of *S. aureus* does not contain an RGD motive, nonetheless the direct interaction between IsdB and RGD binding integrins allows the invasion of eukaryotic cells (Zapotoczna *et al.*, 2012b). A direct Interaction of IsdB with the platelet integrin αIIbβ3 allows the adhesion to and activation of platelets (Miajlovic *et al.*, 2010). Furthermore an indirect interaction is established by ClfA and FnBPA binding to fibrinogen which is also bound by the platelet integrin αIIbβ3. The fibrinogen bridge together with a second bridge of specific IgG bound to ClfA/FnBPA and to the platelet Fc-receptor allows the activation of platelets (Fitzgerald *et al.*, 2006a; Fitzgerald *et al.*, 2006b). If vWbl and SlsE promote a direct interaction with eukaryotic integrins, these CWPs might possess important functions during infection.

However, the experiments performed in this thesis are not comprehensive and more studies have to be undertaken to understand the role of CWPs of *S. lugdunensis*. The set of putative ligands tested is rather short and additional ECM molecules such as collagens or elastin should be considered in further experiments. Also integrin-mediated binding to eukaryotic cells should be investigated. CWPs are also known to possess anti-phagocytic properties (Higgins *et al.*, 2006) and they allow the interaction with complement regulatory proteins (Kang *et al.*, 2013; Sharp *et al.*, 2012). CWPs of *S. lugdunensis* might possess similar properties and experiments regarding this have not yet been undertaken.

S. lugdunensis expresses the CWP SlsF which encodes a protein possessing a putative albumin binding domain. It was shown that the protein is expressed and surface-associated in strain N940164. However, recombinant $SlsF_{42-778}$ did not bind to immobilized albumin and N940164 did not adhere detectably to the ligand, suggesting that the protein does not represent an albumin binding protein. Recently the SlsF homologue SssF of *S. saprophyticus* was shown to confer resistance against the antibacterial fatty acid linoleic acid (King *et al.*, 2012). A similar effect might be associated with the expression of SlsF in *S. lugdunensis*.

The significantly reduced virulence of the Δ*srtA* mutant in the rat endocarditis model shows that appropriately displayed CWPs are crucial for the development of the disease. Most likely several CWPs of *S. lugdunensis* fulfil important functions and the deletion of SrtA results in the abrogation of all these functions simultaneously, resulting in the decrease in virulence. However, single CWPs and their functions in adhesion and immune evasion of *S. lugdunensis* have yet to be described.

S. lugdunensis is the only CoNS sequenced up to date that encodes an iron responsive surface determinant locus (*isd*). A similar system is well described for *S. aureus* and allows the extraction of haem from haemoglobin and haemoglobin-haptoglobin complexes. Isd proteins allow the transfer of haem across the cell envelope and its degradation within the cytoplasm to release nutrient iron. Recent studies showed the Isd proteins of *S. lugdunensis* function in a similar fashion (Haley *et al.*, 2011; Zapotoczna *et al.*, 2012a).

The *isd* loci of *S. aureus* and *S. lugdunensis* are located in a different chromosomal context and show interesting similarities and differences, all indicating that the loci have been acquired independently from different sources. The *S. aureus isd* locus has been shown to be important for full virulence (Clarke *et al.*, 2007; Clarke & Foster, 2008; Pishchany *et al.*, 2010), thus the presence of an independently acquired *isd* locus in *S. lugdunensis* points to a convergent evolution towards an invasive behaviour that has not been described for any other CoNS and might in part explain the apparent *S. aureus*-like infections caused by *S. lugdunensis*. The haemoglobin receptor IsdB is conserved in both *S. aureus* and *S. lugdunensis*. It has been shown for *S. aureus* that IsdB is the lynchpin for haem acquisition *in vivo* and deletion of IsdB

significantly decreases virulence (Pishchany *et al.*, 2010). Interestingly, IsdB expression is most prominent in the heart of infected mice and using an Δ*isdB* mutant, 100-fold fewer bacteria were recovered from the heart of infected animals (Pishchany *et al.*, 2010). It is therefore tempting to speculate that the *isd* system of *S. lugdunensis* and the expression of IsdB are in part the reason for the observed association of *S. lugdunensis* with infectious endocardits in humans. Experimental investigation of this hypothesis has not yet had good prospects since the Isd proteins of *S. lugdunensis* were shown to be highly specific for human haemoglobin (Pishchany *et al.*, 2010; Zapotoczna *et al.*, 2012a). Accordingly mouse or rat models are not appropriate to investigate the effects of *S. lugdunensis* IsdB. However, a transgenic mouse strain is available expressing human haemoglobin which was successfully used to demonstrate the importance of *S. aureus* Isd (Pishchany *et al.*, 2010). This mouse strain is currently being used to investigate the importance of *S. lugdunensis* Isd during infection.

S. lugdunensis encodes the staphylococcal iron regulated transporter (*sirABC*) in close proximity to the *isd* locus, The transporter is well characterized in *S. aureus* and allows the uptake of the iron scavenging siderophore staphyloferrin B (Dale *et al.*, 2004b). Interestingly, *S. lugdunensis* does not encode proteins for the biosynthesis of staphyloferrin B. However, the SirABC transporter should allow the theft of this molecule during mixed infection. Of note the Sir transporter is not encoded by any other sequenced CoNS species thereby linking *S. aureus* and *S. lugdunensis* closer together. Additionally the presence of these iron acquisition systems suggest that the species has adapted to an environment where free iron is strongly limited which might be interpreted as an adaptation towards invasive behaviour.

The importance of Isd and SirABC might be further underlined by the presence of a tandem repeat duplication in HKU09-01 that leads to an increased gene dosage of the coding sequences for both iron acquisition systems. The experiments conducted in this study showed that this duplication is intrinsically unstable and subject to high frequent RecA-dependent amplification and segregation events. In general these genetic mechanisms allow rapid increase in the expression level of important proteins which results in an increased fitness under certain environmental conditions (Sandegren &

Andersson, 2009). The experiments conducted in this study failed to associate the increase in the expression of Isd proteins with improved growth under iron limited conditions in the presence of haemoglobin as the sole source of nutrient iron. Yet, the duplication of two iron uptake systems (Isd and Sir) strongly suggests that iron is of special importance for *S. lugdunensis*. The Sst siderophore uptake system is a further iron acquisition system. It is conserved amongst all sequenced staphylococcal species and has been shown to allow the uptake of catechol siderophores and to promote virulence in *S. aureus* (Beasley *et al.*, 2011). Interestingly this system is duplicated in both sequenced *S. lugdunensis* strains and a similar duplication is not present in any other staphylococcal species.

The presence and duplication of the iron uptake systems in HKU09-01 suggest that this strain has been exposed to environmental conditions where iron is rare and an increased gene dosage of the iron uptake systems was of advantage. It is tempting to suggest that these conditions were present during invasive disease, caused by "nutritional immunity" (Hood & Skaar, 2012). Nonetheless, experimental evidence showing that the duplication and amplification of haem/siderophore transport systems allows a more efficient uptake of nutrient iron *in vitro* is not available. Furthermore no *in vivo* experiments were performed showing that strains harbouring the duplication have a growth advantage *in vivo*. Therefore it cannot be decided whether the duplication in HKU09-01 occurred *in vivo* and is of evolutionary significance or whether it is an artefact created randomly after the isolation of the clone.

However, following the hypothesis that the duplication of *isd* and *sir* represented an *in vivo* growth advantage for *S. lugdunensis* HKU09-01 during invasive disease opens a further area for future investigations. Gene duplication and amplification (GDA) is understood to represent means for the rapid adaption to new environmental conditions, where an increased gene dosage leads to an improved fitness. Only genes and loci will be affected that possess an impaired function or a weak side activity. Overexpression allows bacteria to overcome the problem with the function of the protein and the increase in the DNA template amount allows an increased mutation frequency and thereby an improvement of the protein (Anderson & Roth, 1981; Kugelberg *et al.*, 2006). Alternatively new genes can develop where the side function becomes

dominant (Näsvall *et al.*, 2012). Evidence for such processes is found is *S. aureus*. The staphylococcal superantigen-like toxins (*ssl*) secreted by *S. aureus* are always located in an operon of very similar genes showing only minor differences. The small differences are however big enough to produce toxins recognizing different Vβ chains of T cell receptors. Phylogenetic analysis of *ssl* genes from various *S. aureus* clinical isolates suggested that new genes arise from this operon, allowing the diversification of specificity (Jarraud *et al.*, 2001).

Looking at the duplication of *isd* and *sir* in an evolutionary context might therefore lead to several interesting questions. Is the *isd* operon in *S. lugdunensis* not functioning very well in HKU09-01? The presence of *isd* seems unusual for CoNS, maybe the species acquired the locus only recently and is in a process of development from being a skin commensal to being a pathogen. Are there side activities present in the loci that need to be improved? Membrane transport systems seem to be promising candidates. It is easily imaginable that the substrate specificity is not elusive and the transport of various molecules might be allowed with different efficiencies. GDA might therefore improve the import/export of molecules other then haem and sidorphores. However, such questions are very difficult to address with the experimental systems available up to date, especially if the main function and putative side function of the proteins of interest are only poorly described. Therefore these questions have to remain speculation for the time being.

Investigations regarding the creation of the duplication of *isd* and *sir* in other clinical isolates of *S. lugdunensis* will also be of interest for further investigation. The homologous regions that allowed the duplication in HKU09-01 are only 19 nucleotides in length. This length of sequence homology seems to be barely long enough for normal RecA-mediated recombination which needs at least 20 nucleotides of homology in *E. coli* (Watt *et al.*, 1985). However, a RecA-independent mechanism might have been involved in the creation of the duplication. In HKU09-01 homologous recombination has also occurred between homologous sequences (29 nucleotides in length) in *slush-B* and *slush-C* thereby deleting the gene for one of the peptides and creating the chimeric gene *slush-B2*. Again, the length of the homology seems to be rather short. It might be possible that these recombination events between short

sequences were driven by RecA-independent mechanisms that are not yet identified.

The investigation of *S. lugdunensis* genome sequences gave insight into the genetic capacity of this unusually virulent but neglected CoNS. Several discovered features might represent targets for a specific treatment of *S. lugdunensis* infections. The putative secreted streptolysin S-like toxin might represent a virulence factor of *S. lugdunensis.* Similar toxins are secreted by numerous Gram-positive pathogens including *Streptococcus spp.*, *Lsteria spp.* and *Clostridium spp.* and rational vaccine design has been suggested to prevent infections caused by these organisms (Molloy *et al.*, 2011). Such a vaccine might also be potent to prevent *S. lugdunensis* infection.

Furthermore *S. lugdunensis* possesses features shared exclusively with the coagulase positive *S. aureus*. These features might represent interesting targets for therapies aiming solely on the aggressive pathogens *S. aureus* and *S. lugdunensis* while other staphylococcal species would not be affected by the treatment. Among these features is the ESAT6-like toxin synthesis and secretion system Esx. Blocking of the effector function of these toxins or specific vaccination might be interesting for further investigation. However, of special interest is the presence, conserved regulation and conserved function of Isd proteins in *S. aureus* and *S. lugdunensis*. Several other Gram-positive bacterial species causing invasive disease such as *Listeria ssp.*, *Clostridium ssp.* or *Bacillus ssp.*, express Isd proteins to overcome iron limitation within the host (Anzaldi & Skaar, 2010). This system might therefore be used to create pathogen-specific treatment options. Substances binding with high affinity to the NEAT domains of Isd proteins might be developed to block the acquisition of haem by this pathway. Alternatively toxic components linked to haem could be used to specifically kill bacteria with the ability to bind and take up haem.

Although the development of a specific vaccine against *S. aureus* has not been successful up to date, several promising targets have been identified. Among those are the cell wall anchored proteins clumping factor A (ClfA) and IsdB (Daum & Spellberg, 2012; Joshi *et al.*, 2012). IsdB was found to be conserved in *S. lugdunensis* and Fbl shows high sequence and functional homology to ClfA of *S. aureus* (Geoghegan et al., 2010). It can therefore be anticipated that a vaccine design against *S. aureus* IsdB and ClfA might also

have protective effects against *S. lugdunensis* infections. The described cell wall-anchored proteins of *S. lugdunensis* can represent further promising targets for the development of a specific vaccine. It would be interesting to use convalescent serum of patients that suffered from *S. lugdunensis* infection to investigate whether the SIsA-G proteins are expressed during infection and whether an effective immune response is mounted against these epitopes. This would help to identify promising targets for a *S. lugdunensis* specific vaccine.

The established protocols for transformation and genetic manipulation cleared the way for hypothesis driven research to identify factors that contribute to the apparent *S. aureus*-like behaviour of *S. lugdunensis*. This project opened a multitude of avenues for further research regarding *S. lugdunensis* and especially Isd-dependent haem acquisition, its importance for virulence and the role of GDAs in this process will be interesting for further investigation.

References

Alber, G., Hammer, D. K. & Fleischer, B. (1990). Relationship between enterotoxic- and T lymphocyte-stimulating activity of staphylococcal enterotoxin B. *J Immunol* **144**, 4501-4506.

Alberts, B. & Lewis, J. (2002). *Molecular Biology of the Cell*, 4 edn. New York: Garland Science.

Alonzo, F., 3rd, Kozhaya, L., Rawlings, S. A., Reyes-Robles, T., DuMont, A. L., Myszka, D. G., Landau, N. R., Unutmaz, D. & Torres, V. J. (2013). CCR5 is a receptor for *Staphylococcus aureus* leukotoxin ED. *Nature* **493**, 51-55.

Anderson, P. & Roth, J. (1981). Spontaneous tandem genetic duplications in *Salmonella typhimurium* arise by unequal recombination between rRNA (*rrn*) cistrons. *Proc Natl Acad Sci U S A* **78**, 3113-3117.

Andersson, D. I., Slechta, E. S. & Roth, J. R. (1998). Evidence that gene amplification underlies adaptive mutability of the bacterial *lac* operon. *Science* **282**, 1133-1135.

Andrews, S. C., Robinson, A. K. & Rodriguez-Quinones, F. (2003). Bacterial iron homeostasis. *FEMS Microbiol Rev* **27**, 215-237

Anguera, I., Del Rio, A., Miro, J. M., Matinez-Lacasa, X., Marco, F., Guma, J. R., Quaglio, G., Claramonte, X., Moreno, A., Mestres, C. A., Mauri, E., Azqueta, M., Benito, N., Garcia-de la Maria, C., Almela, M., Jimenez-Exposito, M. J., Sued, O., De Lazzari, E. & Gatell, J. M. (2005). *Staphylococcus lugdunensis* infective endocarditis: description of 10 cases and analysis of native valve, prosthetic valve, and pacemaker lead endocarditis clinical profiles. *Heart* **91**, e10.

Anzaldi, L. L. & Skaar, E. P. (2010). Overcoming the heme paradox: heme toxicity and tolerance in bacterial pathogens. *Infect Immun* **78**, 4977-4989.

Arias, M., Tena, D., Apellaniz, M., Asensio, M. P., Caballero, P., Hernandez, C., Tejedor, F. & Bisquert, J. (2010). Skin and soft tissue infections caused by *Staphylococcus lugdunensis*: report of 20 cases. *Scand J Infect Dis* **42**, 879-884.

Athanasopoulos, A. N., Economopoulou, M., Orlova, V. V., Sobke, A., Schneider, D., Weber, H., Augustin, H. G., Eming, S. A., Schubert, U., Linn, T., Nawroth, P. P., Hussain, M., Hammes, H. P., Herrmann, M., Preissner, K. T. & Chavakis, T. (2006). The extracellular adherence protein (Eap) of *Staphylococcus aureus* inhibits wound healing by interfering with host defense and repair mechanisms. *Blood* **107**, 2720-2727.

Augustin, J. & Götz, F. (1990). Transformation of *Staphylococcus epidermidis* and other staphylococcal species with plasmid DNA by electroporation. *FEMS Microbiol Lett* **54**, 203-207.

Aury, J. M., Cruaud, C., Barbe, V., Rogier, O., Mangenot, S., Samson, G., Poulain, J., Anthouard, V., Scarpelli, C., Artiguenave, F. & Wincker, P. (2008). High quality draft sequences for prokaryotic genomes using a mix of new sequencing technologies. *BMC Genomics* **9**, 603.

Bae, T. & Schneewind, O. (2006). Allelic replacement in *Staphylococcus aureus* with inducible counter-selection. *Plasmid* **55**, 58-63.

Barbu, E. M., Ganesh, V. K., Gurusiddappa, S., Mackenzie, R. C., Foster, T. J., Sudhof, T. C. & Hook, M. (2010). beta-Neurexin is a ligand for the *Staphylococcus aureus* MSCRAMM SdrC. *PLoS Pathog* **6**, e1000726.

Bayer, A. S., Schneider, T. & Sahl, H. G. (2013). Mechanisms of daptomycin resistance in *Staphylococcus aureus*: role of the cell membrane and cell wall. *Ann N Y Acad Sci* **1277**, 139-158.

Beasley, F. C., Vines, E. D., Grigg, J. C., Zheng, Q., Liu, S., Lajoie, G. A., Murphy, M. E. & Heinrichs, D. E. (2009). Characterization of staphyloferrin A biosynthetic and transport mutants in *Staphylococcus aureus*. *Mol Microbiol* **72**, 947-963.

Beasley, F. C., Marolda, C. L., Cheung, J., Buac, S. & Heinrichs, D. E. (2011). *Staphylococcus aureus* transporters Hts, Sir, and Sst capture iron liberated from human transferrin by Staphyloferrin A, Staphyloferrin B, and catecholamine stress hormones, respectively, and contribute to virulence. *Infect Immun* **79**, 2345-2355.

Becker, K., Pagnier, I., Schuhen, B., Wenzelburger, F., Friedrich, A. W., Kipp, F., Peters, G. & von Eiff, C. (2006). Does nasal cocolonization by methicillin-resistant coagulase-negative staphylococci and methicillin-susceptible *Staphylococcus aureus* strains occur frequently enough to represent a risk of false-positive methicillin-resistant *S. aureus* determinations by molecular methods? *J Clin Microbiol* **44**, 229-231.

Beckmann, J. S., Estivill, X. & Antonarakis, S. E. (2007). Copy number variants and genetic traits: closer to the resolution of phenotypic to genotypic variability. *Nat Rev Genet* **8**, 639-646.

Beenken, K. E., Spencer, H., Griffin, L. M. & Smeltzer, M. S. (2012). Impact of extracellular nuclease production on the biofilm phenotype of *Staphylococcus aureus* under *in vitro* and *in vivo* conditions. *Infect Immun* **80**, 1634-1638.

Ben Zakour, N. L., Beatson, S. A., van den Broek, A. H., Thoday, K. L. & Fitzgerald, J. R. (2012). Comparative genomics of the *Staphylococcus intermedius* group of animal pathogens. *Front Cell Infect Microbiol* **2**, 44.

Benson, D. A., Cavanaugh, M., Clark, K., Karsch-Mizrachi, I., Lipman, D. J., Ostell, J. & Sayers, E. W. (2013). GenBank. *Nucleic Acids Res* **41**, D36-42.

Bentley, D. R. (2006). Whole-genome re-sequencing. *Curr Opin Genet Dev* **16**, 545-552.

Berends, E. T., Horswill, A. R., Haste, N. M., Monestier, M., Nizet, V. & von Kockritz-Blickwede, M. (2010). Nuclease expression by *Staphylococcus aureus* facilitates escape from neutrophil extracellular traps. *J Innate Immun* **2**, 576-586.

Bergthorsson, U., Andersson, D. I. & Roth, J. R. (2007). Ohno's dilemma: evolution of new genes under continuous selection. *Proc Natl Acad Sci U S A* **104**, 17004-17009.

Bertini, A., Poirel, L., Bernabeu, S., Fortini, D., Villa, L., Nordmann, P. & Carattoli, A. (2007). Multicopy *blaOXA-58* gene as a source of high-level resistance to carbapenems in *Acinetobacter baumannii*. *Antimicrob Agents Chemother* **51**, 2324-2328.

Bieber, L. & Kahlmeter, G. (2010). *Staphylococcus lugdunensis* in several niches of the normal skin flora. *Clin Microbiol Infect* **16**, 385-388.

Biswas, R., Martinez, R. E., Gohring, N., Schlag, M., Josten, M., Xia, G., Hegler, F., Gekeler, C., Gleske, A. K., Götz, F., Sahl, H. G., Kappler, A. & Peschel, A. (2012). Proton-binding capacity of *Staphylococcus aureus* wall teichoic acid and its role in controlling autolysin activity. *PLoS One* **7**, e41415.

Bocher, S., Tonning, B., Skov, R. L. & Prag, J. (2009). *Staphylococcus lugdunensis*, a common cause of skin and soft tissue infections in the community. *J Clin Microbiol* **47**, 946-950.

Boe, L. (1990). Mechanism for induction of adaptive mutations in *Escherichia coli*. *Mol Microbiol* **4**, 597-601.

Boles, B. R. & Horswill, A. R. (2008). Agr-mediated dispersal of *Staphylococcus aureus* biofilms. *PLoS Pathog* **4**, e1000052.

Boman, H. G. (2003). Antibacterial peptides: basic facts and emerging concepts. *J Intern Med* **254**, 197-215.

Bork, P., Downing, A. K., Kieffer, B. & Campbell, I. D. (1996). Structure and distribution of modules in extracellular proteins. *Q Rev Biophys* **29**, 119-167.

Bou-Abdallah, F. (2010). The iron redox and hydrolysis chemistry of the ferritins. *Biochim Biophys Acta* **1800**, 719-731.

Bourgeois, I., Pestel-Caron, M., Lemeland, J. F., Pons, J. L. & Caron, F. (2007). Tolerance to the glycopeptides vancomycin and teicoplanin in coagulase-negative staphylococci. *Antimicrob Agents Chemother* **51**, 740-743.

Bowden, M. G., Heuck, A. P., Ponnuraj, K., Kolosova, E., Choe, D., Gurusiddappa, S., Narayana, S. V., Johnson, A. E. & Hook, M. (2008). Evidence for the "dock, lock, and latch" ligand binding mechanism of the staphylococcal microbial surface component recognizing adhesive matrix molecules (MSCRAMM) SdrG. *J Biol Chem* **283**, 638-647.

Brown, S., Xia, G., Luhachack, L. G., Campbell, J., Meredith, T. C., Chen, C., Winstel, V., Gekeler, C., Irazoqui, J. E., Peschel, A. & Walker, S. (2012). Methicillin resistance in *Staphylococcus aureus* requires glycosylated wall teichoic acids. *Proc Natl Acad Sci U S A* **109**, 18909-18914.

Burke, F. M., Di Poto, A., Speziale, P. & Foster, T. J. (2011). The A domain of fibronectin-binding protein B of *Staphylococcus aureus* contains a novel fibronectin binding site. *FEBS J* **278**, 2359-2371.

Burts, M. L., Williams, W. A., DeBord, K. & Missiakas, D. M. (2005). EsxA and EsxB are secreted by an ESAT-6-like system that is required for the pathogenesis of *Staphylococcus aureus* infections. *Proc Natl Acad Sci U S A* **102**, 1169-1174.

Cairns, J., Overbaugh, J. & Miller, S. (1988). The origin of mutants. *Nature* **335**, 142-145.

Carpenter, R. J., Price, G. D., Boswell, G. E., Nayak, K. R. & Ramirez, A. R. (2012). Gerbode defect with *Staphylococcus lugdunensis* native tricuspid valve infective endocarditis. *J Card Surg* **27**, 316-320.

Carver, T., Thomson, N., Bleasby, A., Berriman, M. & Parkhill, J. (2009). DNAPlotter: circular and linear interactive genome visualization. *Bioinformatics* **25**, 119-120.

Carver, T. J., Rutherford, K. M., Berriman, M., Rajandream, M. A., Barrell, B. G. & Parkhill, J. (2005). ACT: the Artemis Comparison Tool. *Bioinformatics* **21**, 3422-3423.

Casanova-Roman, M., Sanchez-Porto, A. & Casanova-Bellido, M. (2004). Urinary tract infection due to *Staphylococcus lugdunensis* in a healthy child. *Scand J Infect Dis* **36**, 149-150.

Cassat, J. E. & Skaar, E. P. (2013). Iron in infection and immunity. *Cell Host Microbe* **13**, 509-519.

CDC (2002). *Staphylococcus aureus* resistant to vancomycin--United States, 2002. *MMWR Morb Mortal Wkly Rep* **51**, 565-567.

Cedergren, L., Andersson, R., Jansson, B., Uhlen, M. & Nilsson, B. (1993). Mutational analysis of the interaction between staphylococcal protein A and human IgG1. *Protein Eng* **6**, 441-448.

Cerquetti, M., Cardines, R., Ciofi Degli Atti, M. L., Giufre, M., Bella, A., Sofia, T., Mastrantonio, P. & Slack, M. (2005). Presence of multiple copies of the capsulation b locus in invasive *Haemophilus influenzae* type b (Hib) strains isolated from children with Hib conjugate vaccine failure. *J Infect Dis* **192**, 819-823.

Cerquetti, M., Cardines, R., Giufre, M., Castella, A., Rebora, M., Mastrantonio, P. & Ciofi Degli Atti, M. L. (2006). Detection of six copies of the capsulation b locus in a *Haemophilus influenzae* type b strain isolated from a splenectomized patient with fulminant septic shock. *J Clin Microbiol* **44**, 640-642.

Cevasco, M. & Haime, M. (2012). Aortic valve endocarditis from *Staphylococcus lugdunensis*. *J Card Surg* **27**, 299-300.

Chain, P. S., Grafham, D. V., Fulton, R. S., Fitzgerald, M. G., Hostetler, J., Muzny, D., Ali, J., Birren, B., Bruce, D. C., Buhay, C., Cole, J. R., Ding, Y., Dugan, S., Field, D., Garrity, G. M., Gibbs, R., Graves, T., Han, C. S., Harrison, S. H., Highlander, S., Hugenholtz, P., Khouri, H. M., Kodira, C. D., Kolker, E., Kyrpides, N. C., Lang, D., Lapidus, A., Malfatti, S. A., Markowitz, V., Metha, T., Nelson, K. E., Parkhill, J., Pitluck, S., Qin, X., Read, T. D., Schmutz, J., Sozhamannan, S., Sterk, P., Strausberg, R. L., Sutton, G., Thomson, N. R., Tiedje, J. M., Weinstock, G., Wollam, A. & Detter, J. C. (2009). Genomics. Genome project standards in a new era of sequencing. *Science* **326**, 236-237.

Chandler, M., de la Tour, E. B., Willems, D. & Caro, L. (1979). Some properties of the chloramphenicol resistance transposon Tn9. *Mol Gen Genet* **176**, 221-231.

Chassaîn, B., Lemée, L., Didi, J., Thiberge, J. M., Brisse, S., Pons, J. L. & Pestel-Caron, M. (2012). Multilocus sequence typing analysis of *Staphylococcus lugdunensis* implies a clonal population structure. *J Clin Microbiol* **50**, 3003-3009.

Chatzigeorgiou, K. S., Siafakas, N., Petinaki, E. & Zerva, L. (2010). *fbl* gene as a species-specific target for *Staphylococcus lugdunensis* identification. *J Clin Lab Anal* **24**, 119-122.

Chavakis, T., Hussain, M., Kanse, S. M., Peters, G., Bretzel, R. G., Flock, J. I., Herrmann, M. & Preissner, K. T. (2002). *Staphylococcus aureus* extracellular adherence protein serves as anti-inflammatory factor by inhibiting the recruitment of host leukocytes. *Nat Med* **8**, 687-693.

Chen, Y., McClane, B. A., Fisher, D. J., Rood, J. I. & Gupta, P. (2005). Construction of an alpha toxin gene knockout mutant of *Clostridium perfringens* type A by use of a mobile group II intron. *Appl Environ Microbiol* **71**, 7542-7547.

Cheng, A. G., Kim, H. K., Burts, M. L., Krausz, T., Schneewind, O. & Missiakas, D. M. (2009). Genetic requirements for *Staphylococcus aureus* abscess formation and persistence in host tissues. *FASEB J* **23**, 3393-3404.

Cheng, A. G., McAdow, M., Kim, H. K., Bae, T., Missiakas, D. M. & Schneewind, O. (2010). Contribution of coagulases towards *Staphylococcus aureus* disease and protective immunity. *PLoS Pathog* **6**, e1001036.

Cheung, G. Y., Duong, A. C. & Otto, M. (2012). Direct and synergistic hemolysis caused by Staphylococcus phenol-soluble modulins: implications for diagnosis and pathogenesis. *Microbes Infect* **14**, 380-386.

Cheung, J., Beasley, F. C., Liu, S., Lajoie, G. A. & Heinrichs, D. E. (2009). Molecular characterization of staphyloferrin B biosynthesis in *Staphylococcus aureus*. *Mol Microbiol* **74**, 594-608.

Chiquet, C., Pechinot, A., Creuzot-Garcher, C., Benito, Y., Croize, J., Boisset, S., Romanet, J. P., Lina, G. & Vandenesch, F. (2007). Acute postoperative endophthalmitis caused by *Staphylococcus lugdunensis*. *J Clin Microbiol* **45**, 1673-1678.

Choi, Y., Lafferty, J. A., Clements, J. R., Todd, J. K., Gelfand, E. W., Kappler, J., Marrack, P. & Kotzin, B. L. (1990). Selective expansion of T cells expressing V beta 2 in toxic shock syndrome. *J Exp Med* **172**, 981-984.

Christner, M., Franke, G. C., Schommer, N. N., Wendt, U., Wegert, K., Pehle, P., Kroll, G., Schulze, C., Buck, F., Mack, D., Aepfelbacher, M. & Rohde, H. (2010). The giant extracellular matrix-binding protein of *Staphylococcus epidermidis* mediates biofilm accumulation and attachment to fibronectin. *Mol Microbiol* **75**, 187-207.

Chung, K. P., Chang, H. T., Liao, C. H., Chu, F. Y. & Hsueh, P. R. (2012). *Staphylococcus lugdunensis* endocarditis with isolated tricuspid valve involvement. *J Microbiol Immunol Infect* **45**, 248-250.

Clarke, S. R., Wiltshire, M. D. & Foster, S. J. (2004). IsdA of *Staphylococcus aureus* is a broad spectrum, iron-regulated adhesin. *Mol Microbiol* **51**, 1509-1519.

Clarke, S. R., Mohamed, R., Bian, L., Routh, A. F., Kokai-Kun, J. F., Mond, J. J., Tarkowski, A. & Foster, S. J. (2007). The *Staphylococcus aureus* surface protein IsdA mediates resistance to innate defenses of human skin. *Cell Host Microbe* **1**, 199-212.

Clarke, S. R. & Foster, S. J. (2008). IsdA protects *Staphylococcus aureus* against the bactericidal protease activity of apolactoferrin. *Infect Immun* **76**, 1518-1526.

Clarke, S. R., Andre, G., Walsh, E. J., Dufrene, Y. F., Foster, T. J. & Foster, S. J. (2009). Iron-regulated surface determinant protein A mediates adhesion of *Staphylococcus aureus* to human corneocyte envelope proteins. *Infect Immun* **77**, 2408-2416.

Clauditz, A., Resch, A., Wieland, K. P., Peschel, A. & Götz, F. (2006). Staphyloxanthin plays a role in the fitness of *Staphylococcus aureus* and its ability to cope with oxidative stress. *Infect Immun* **74**, 4950-4953.

Clewell, D. B., Yagi, Y. & Bauer, B. (1975). Plasmid-determined tetracycline resistance in *Streptococcus faecalis*: evidence for gene amplification during growth in presence of tetracycline. *Proc Natl Acad Sci U S A* **72**, 1720-1724.

Conrad, B. & Antonarakis, S. E. (2007). Gene duplication: a drive for phenotypic diversity and cause of human disease. *Annu Rev Genomics Hum Genet* **8**, 17-35.

Conrady, D. G., Wilson, J. J. & Herr, A. B. (2013). Structural basis for Zn2+-dependent intercellular adhesion in staphylococcal biofilms. *Proc Natl Acad Sci U S A* **110**, E202-211.

Corrigan, R. M. & Foster, T. J. (2009). An improved tetracycline-inducible expression vector for *Staphylococcus aureus*. *Plasmid* **61**, 126-129.

Corvaglia, A. R., Francois, P., Hernandez, D., Perron, K., Linder, P. & Schrenzel, J. (2010). A type III-like restriction endonuclease functions as a major barrier to horizontal gene transfer in clinical *Staphylococcus aureus* strains. *Proc Natl Acad Sci U S A* **107**, 11954-11958.

Cotton, J. L., Tao, J. & Balibar, C. J. (2009). Identification and characterization of the *Staphylococcus aureus* gene cluster coding for staphyloferrin A. *Biochemistry* **48**, 1025-1035.

Courcol, R. J., Trivier, D., Bissinger, M. C., Martin, G. R. & Brown, M. R. (1997). Siderophore production by *Staphylococcus aureus* and identification of iron-regulated proteins. *Infect Immun* **65**, 1944-1948.

Cramton, S. E., Gerke, C., Schnell, N. F., Nichols, W. W. & Götz, F. (1999). The intercellular adhesion (*ica*) locus is present in *Staphylococcus aureus* and is required for biofilm formation. *Infect Immun* **67**, 5427-5433.

Crosa, J. H. & Walsh, C. T. (2002). Genetics and assembly line enzymology of siderophore biosynthesis in bacteria. *Microbiol Mol Biol Rev* **66**, 223-249.

Dale, S. E., Doherty-Kirby, A., Lajoie, G. & Heinrichs, D. E. (2004a). Role of siderophore biosynthesis in virulence of *Staphylococcus aureus*: identification and characterization of genes involved in production of a siderophore. *Infect Immun* **72**, 29-37.

Dale, S. E., Sebulsky, M. T. & Heinrichs, D. E. (2004b). Involvement of SirABC in iron-siderophore import in *Staphylococcus aureus*. *J Bacteriol* **186**, 8356-8362.

de Haas, C. J., Veldkamp, K. E., Peschel, A., Weerkamp, F., Van Wamel, W. J., Heezius, E. C., Poppelier, M. J., Van Kessel, K. P. & van Strijp, J. A. (2004). Chemotaxis inhibitory protein of *Staphylococcus aureus*, a bacterial antiinflammatory agent. *J Exp Med* **199**, 687-695.

De Paulis, A. N., Predari, S. C., Chazarreta, C. D. & Santoianni, J. E. (2003). Five-test simple scheme for species-level identification of clinically significant coagulase-negative staphylococci. *J Clin Microbiol* **41**, 1219-1224.

Deisenhofer, J. (1981). Crystallographic refinement and atomic models of a human Fc fragment and its complex with fragment B of protein A from *Staphylococcus aureus* at 2.9- and 2.8-A resolution. *Biochemistry* **20**, 2361-2370.

Deivanayagam, C. C., Wann, E. R., Chen, W., Carson, M., Rajashankar, K. R., Hook, M. & Narayana, S. V. (2002). A novel variant of the immunoglobulin fold in surface adhesins of *Staphylococcus aureus*: crystal structure of the fibrinogen-binding MSCRAMM, clumping factor A. *EMBO J* **21**, 6660-6672.

Delcher, A. L., Harmon, D., Kasif, S., White, O. & Salzberg, S. L. (1999). Improved microbial gene identification with GLIMMER. *Nucleic Acids Res* **27**, 4636-4641.

Diekema, D. J., Pfaller, M. A., Schmitz, F. J., Smayevsky, J., Bell, J., Jones, R. N. & Beach, M. (2001). Survey of infections due to Staphylococcus species: frequency of occurrence and antimicrobial susceptibility of isolates collected in the United States, Canada, Latin America, Europe, and the Western Pacific region for the SENTRY Antimicrobial Surveillance Program, 1997-1999. *Clin Infect Dis* **32 Suppl 2**, S114-132.

Doery, H. M., Magnusson, B. J., Cheyne, I. M. & Sulasekharam, J. (1963). A phospholipase in staphylococcal toxin which hydrolyses sphingomyelin. *Nature* **198**, 1091-1092.

Donlan, R. M. (2001). Biofilms and device-associated infections. *Emerg Infect Dis* **7**, 277-281.

Donvito, B., Etienne, J., Denoroy, L., Greenland, T., Benito, Y. & Vandenesch, F. (1997). Synergistic hemolytic activity of *Staphylococcus lugdunensis* is mediated by three peptides encoded by a non-agr genetic locus. *Infect Immun* **65**, 95-100.

Drabkin, D. L. (1951). Metabolism of the hemin chromoproteins. *Physiol Rev* **31**, 345-431.

Dryla, A., Hoffmann, B., Gelbmann, D., Giefing, C., Hanner, M., Meinke, A., Anderson, A. S., Koppensteiner, W., Konrat, R., von Gabain, A. & Nagy, E. (2007). High-affinity binding of the staphylococcal HarA protein to haptoglobin and hemoglobin involves a domain with an antiparallel eight-stranded beta-barrel fold. *J Bacteriol* **189**, 254-264.

Du, Y., He, Y. X., Zhang, Z. Y., Yang, Y. H., Shi, W. W., Frolet, C., Guilmi, A. M., Vernet, T., Zhou, C. Z. & Chen, Y. (2011). Crystal structure of the mucin-binding domain of Spr1345 from *Streptococcus pneumoniae*. *J Struct Biol* **174**, 252-257.

Ferguson, K. P., Lambe, D. W., Jr., Keplinger, J. L. & Kalbfleisch, J. H. (1991). Comparison of the pathogenicity of three species of coagulase-negative Staphylococcus in a mouse model with and without a foreign body. *Can J Microbiol* **37**, 722-724.

Finn, R. D., Mistry, J., Tate, J., Coggill, P., Heger, A., Pollington, J. E., Gavin, O. L., Gunasekaran, P., Ceric, G., Forslund, K., Holm, L., Sonnhammer, E. L., Eddy, S. R. & Bateman, A. (2010). The Pfam protein families database. *Nucleic Acids Res* **38**, D211-222.

Fitzgerald, J. R., Foster, T. J. & Cox, D. (2006a). The interaction of bacterial pathogens with platelets. *Nat Rev Microbiol* **4**, 445-457.

Fitzgerald, J. R., Loughman, A., Keane, F., Brennan, M., Knobel, M., Higgins, J., Visai, L., Speziale, P., Cox, D. & Foster, T. J. (2006). Fibronectin-binding proteins of *Staphylococcus aureus* mediate activation of human platelets via fibrinogen and fibronectin bridges to integrin GPIIb/IIIa and IgG binding to the FcgammaRIIa receptor. *Mol Microbiol* **59**, 212-230.

Fleurette, J., Bes, M., Brun, Y., Freney, J., Forey, F., Coulet, M., Reverdy, M. E. & Etienne, J. (1989). Clinical isolates of *Staphylococcus lugdunensis* and *S. schleiferi*: bacteriological characteristics and susceptibility to antimicrobial agents. *Res Microbiol* **140**, 107-118.

Foster, P. L. & Cairns, J. (1992). Mechanisms of directed mutation. *Genetics* **131**, 783-789.

Foster, T. J. (1998). *Molecular Genetic Analysis of Staphylococcal Virulence*: Academic Press.

Foster, T. J. (2005). Immune evasion by staphylococci. *Nat Rev Microbiol* **3**, 948-958.

Foster, T. J., Geoghegan, J. A., Ganesh, V. K. & Hook, M. (2013). Adhesion, Invasion, Evasion: The Many Functions of *Staphylococcus aureus*' Surface Proteins. *Nat Rev Microbiol* **under revison**.

Frank, K. L. & Patel, R. (2007). Poly-N-acetylglucosamine is not a major component of the extracellular matrix in biofilms formed by *icaADBC*-positive *Staphylococcus lugdunensis* isolates. *Infect Immun* **75**, 4728-4742.

Frank, K. L., Reichert, E. J., Piper, K. E. & Patel, R. (2007). *In vitro* effects of antimicrobial agents on planktonic and biofilm forms of *Staphylococcus lugdunensis* clinical isolates. *Antimicrob Agents Chemother* **51**, 888-895.

Frank, K. L., Del Pozo, J. L. & Patel, R. (2008). From clinical microbiology to infection pathogenesis: how daring to be different works for *Staphylococcus lugdunensis*. *Clin Microbiol Rev* **21**, 111-133.

Freney, J., Brun, Y., Bes, M., Meugnier, H., Grimont, F., Grimont, P. A. D., Nervi, C. & Fleurette, J. (1988). *Staphylococcus lugdunensis* sp. nov. and *Staphylococcus schleiferi* sp. nov., Two Species from Human Clinical Specimens. *Int J Syst Bacteriol* **38**, 168-172.

Friedman, D. B., Stauff, D. L., Pishchany, G., Whitwell, C. W., Torres, V. J. & Skaar, E. P. (2006). *Staphylococcus aureus* redirects central metabolism to increase iron availability. *PLoS Pathog* **2**, e87.

Frishman, D., Mironov, A., Mewes, H. W. & Gelfand, M. (1998). Combining diverse evidence for gene recognition in completely sequenced bacterial genomes. *Nucleic Acids Res* **26**, 2941-2947.

Geoghegan, J. A., Corrigan, R. M., Gruszka, D. T., Speziale, P., O'Gara, J. P., Potts, J. R. & Foster, T. J. (2010a). Role of surface protein SasG in biofilm formation by *Staphylococcus aureus*. *J Bacteriol* **192**, 5663-5673.

Geoghegan, J. A., Ganesh, V. K., Smeds, E., Liang, X., Hook, M. & Foster, T. J. (2010b). Molecular characterization of the interaction of staphylococcal microbial surface components recognizing adhesive matrix molecules (MSCRAMM) ClfA and Fbl with fibrinogen. *J Biol Chem* **285**, 6208-6216.

Geoghegan, J. A., Monk, I. R., O'Gara, J. P. & Foster, T. J. (2013). Subdomains N2N3 of fibronectin binding protein A mediate *Staphylococcus aureus* biofilm formation and adherence to fibrinogen using distinct mechanisms. *J Bacteriol* **195**, 2675-2683.

Ghebremedhin, B., Layer, F., Konig, W. & Konig, B. (2008). Genetic classification and distinguishing of *Staphylococcus species* based on different partial gap, 16S rRNA, hsp60, rpoB, sodA, and tuf gene sequences. *J Clin Microbiol* **46**, 1019-1025.

Gill, S. R., Fouts, D. E., Archer, G. L., Mongodin, E. F., Deboy, R. T., Ravel, J., Paulsen, I. T., Kolonay, J. F., Brinkac, L., Beanan, M., Dodson, R. J., Daugherty, S. C., Madupu, R., Angiuoli, S. V., Durkin, A. S., Haft, D. H., Vamathevan, J., Khouri, H., Utterback, T., Lee, C., Dimitrov, G., Jiang, L., Qin, H., Weidman, J., Tran, K., Kang, K., Hance, I. R., Nelson, K. E. & Fraser, C. M. (2005). Insights on evolution of virulence and resistance from the complete genome analysis of an early methicillin-resistant *Staphylococcus aureus* strain and a biofilm-producing methicillin-resistant *Staphylococcus epidermidis* strain. *J Bacteriol* **187**, 2426-2438.

Gladstone, G. P. & Walton, E. (1971). The effect of iron and haematin on the killing of staphylococci by rabbit polymorphs. *Br J Exp Pathol* **52**, 452-464.

Goldberg, I. & Mekalanos, J. J. (1986). Effect of a *recA* mutation on cholera toxin gene amplification and deletion events. *J Bacteriol* **165**, 723-731.

Gomez-Eichelmann, M. C., Levy-Mustri, A. & Ramirez-Santos, J. (1991). Presence of 5-methylcytosine in CC(A/T)GG sequences (Dcm methylation) in DNAs from different bacteria. *J Bacteriol* **173**, 7692-7694.

Gomez, M. I., Lee, A., Reddy, B., Muir, A., Soong, G., Pitt, A., Cheung, A. & Prince, A. (2004). *Staphylococcus aureus* protein A induces airway epithelial inflammatory responses by activating TNFR1. *Nat Med* **10**, 842-848.

Gomez, M. I., O'Seaghdha, M., Magargee, M., Foster, T. J. & Prince, A. S. (2006). *Staphylococcus aureus* protein A activates TNFR1 signaling through conserved IgG binding domains. *J Biol Chem* **281**, 20190-20196.

Götz, F. (2002). Staphylococcus and biofilms. *Mol Microbiol* **43**, 1367-1378.

Graille, M., Stura, E. A., Corper, A. L., Sutton, B. J., Taussig, M. J., Charbonnier, J. B. & Silverman, G. J. (2000). Crystal structure of a *Staphylococcus aureus* protein A domain complexed with the Fab fragment of a human IgM antibody: structural basis for recognition of B-cell receptors and superantigen activity. *Proc Natl Acad Sci U S A* **97**, 5399-5404.

Grigg, J. C., Vermeiren, C. L., Heinrichs, D. E. & Murphy, M. E. (2007). Haem recognition by a *Staphylococcus aureus* NEAT domain. *Mol Microbiol* **63**, 139-149.

Grigg, J. C., Ukpabi, G., Gaudin, C. F. & Murphy, M. E. (2010). Structural biology of heme binding in the *Staphylococcus aureus* Isd system. *J Inorg Biochem* **104**, 341-348.

Gross, M., Cramton, S. E., Götz, F. & Peschel, A. (2001). Key role of teichoic acid net charge in *Staphylococcus aureus* colonization of artificial surfaces. *Infect Immun* **69**, 3423-3426.

Grupper, M., Potasman, I., Rosner, I., Slobodin, G. & Rozenbaum, M. (2010). Septic arthritis due to *Staphylococcus lugdunensis* in a native joint. *Rheumatol Int* **30**, 1231-1233.

Haile, D. T., Hughes, J., Vetter, E., Kohner, P., Snyder, R., Patel, R. & Cockerill, F. R., 3rd (2002). Frequency of isolation of *Staphylococcus lugdunensis* in consecutive urine cultures and relationship to urinary tract infection. *J Clin Microbiol* **40**, 654-656.

Hair, P. S., Ward, M. D., Semmes, O. J., Foster, T. J. & Cunnion, K. M. (2008). *Staphylococcus aureus* clumping factor A binds to complement regulator factor I and increases factor I cleavage of C3b. *J Infect Dis* **198**, 125-133.

Haley, K. P., Janson, E. M., Heilbronner, S., Foster, T. J. & Skaar, E. P. (2011). *Staphylococcus lugdunensis* IsdG Liberates Iron from Host Heme. *J Bacteriol* **193**, 4749-4757.

Hall, B. G. (1990). Spontaneous point mutations that occur more often when advantageous than when neutral. *Genetics* **126**, 5-16.

Hammer, N. D. & Skaar, E. P. (2011). Molecular mechanisms of *Staphylococcus aureus* iron acquisition. *Annu Rev Microbiol* **65**, 129-147.

Harris, S. R., Feil, E. J., Holden, M. T., Quail, M. A., Nickerson, E. K., Chantratita, N., Gardete, S., Tavares, A., Day, N., Lindsay, J. A., Edgeworth, J. D., de Lencastre, H., Parkhill, J., Peacock, S. J. & Bentley, S. D. (2010). Evolution of MRSA during hospital transmission and intercontinental spread. *Science* **327**, 469-474.

Harris, S. R., Cartwright, E. J., Torok, M. E., Holden, M. T., Brown, N. M., Ogilvy-Stuart, A. L., Ellington, M. J., Quail, M. A., Bentley, S. D., Parkhill, J. & Peacock, S. J. (2013). Whole-genome sequencing for analysis of an outbreak of meticillin-resistant *Staphylococcus aureus*: a descriptive study. *Lancet Infect Dis* **13**, 130-136.

Hartford, O., Francois, P., Vaudaux, P. & Foster, T. J. (1997). The dipeptide repeat region of the fibrinogen-binding protein (clumping factor) is required for functional expression of the fibrinogen-binding domain on the *Staphylococcus aureus* cell surface. *Mol Microbiol* **25**, 1065-1076.

Hartman, B. & Tomasz, A. (1981). Altered penicillin-binding proteins in methicillin-resistant strains of *Staphylococcus aureus*. *Antimicrob Agents Chemother* **19**, 726-735.

Heilbronner, S., Holden, M. T., van Tonder, A., Geoghegan, J. A., Foster, T. J., Parkhill, J. & Bentley, S. D. (2011). Genome sequence of *Staphylococcus lugdunensis* N920143 allows identification of putative colonization and virulence factors. *FEMS Microbiol Lett* **322**, 60-67.

Heilmann, C., Schweitzer, O., Gerke, C., Vanittanakom, N., Mack, D. & Götz, F. (1996). Molecular basis of intercellular adhesion in the biofilm-forming *Staphylococcus epidermidis*. *Mol Microbiol* **20**, 1083-1091.

Heilmann, C., Hussain, M., Peters, G. & Götz, F. (1997). Evidence for autolysin-mediated primary attachment of *Staphylococcus epidermidis* to a polystyrene surface. *Mol Microbiol* **24**, 1013-1024.

Hentze, M. W., Muckenthaler, M. U. & Andrews, N. C. (2004). Balancing acts: molecular control of mammalian iron metabolism. *Cell* **117**, 285-297.

Herrick, S., Blanc-Brude, O., Gray, A. & Laurent, G. (1999). Fibrinogen. *Int J Biochem Cell Biol* **31**, 741-746.

Higgins, J., Loughman, A., van Kessel, K. P., van Strijp, J. A. & Foster, T. J. (2006). Clumping factor A of *Staphylococcus aureus* inhibits phagocytosis by human polymorphonuclear leucocytes. *FEMS Microbiol Lett* **258**, 290-296.

Hiramatsu, K., Cui, L., Kuroda, M. & Ito, T. (2001). The emergence and evolution of methicillin-resistant *Staphylococcus aureus*. *Trends Microbiol* **9**, 486-493.

Hirano, N., Muroi, T., Takahashi, H. & Haruki, M. (2011). Site-specific recombinases as tools for heterologous gene integration. *Appl Microbiol Biotechnol* **92**, 227-239.

Hofstad, T. (1999). *The Ever Present Pathogens*. Göteborg: Rosell & Co.

Hoiby, N., Bjarnsholt, T., Givskov, M., Molin, S. & Ciofu, O. (2010). Antibiotic resistance of bacterial biofilms. *Int J Antimicrob Agents* **35**, 322-332.

Holden, M. T., Feil, E. J., Lindsay, J. A., Peacock, S. J., Day, N. P., Enright, M. C., Foster, T. J., Moore, C. E., Hurst, L., Atkin, R., Barron, A., Bason, N., Bentley, S. D., Chillingworth, C., Chillingworth, T., Churcher, C., Clark, L., Corton, C., Cronin, A., Doggett, J., Dowd, L., Feltwell, T., Hance, Z., Harris, B., Hauser, H., Holroyd, S., Jagels, K., James, K. D., Lennard, N., Line, A., Mayes, R., Moule, S., Mungall, K., Ormond, D., Quail, M. A., Rabbinowitsch, E., Rutherford, K., Sanders, M., Sharp, S., Simmonds, M., Stevens, K., Whitehead, S., Barrell, B. G., Spratt, B. G. & Parkhill, J. (2004). Complete genomes of two clinical *Staphylococcus aureus* strains: evidence for the rapid evolution of virulence and drug resistance. *Proc Natl Acad Sci U S A* **101**, 9786-9791.

Holden, M. T., Hauser, H., Sanders, M., Ngo, T. H., Cherevach, I., Cronin, A., Goodhead, I., Mungall, K., Quail, M. A., Price, C., Rabbinowitsch, E., Sharp, S., Croucher, N. J., Chieu, T. B., Mai, N. T., Diep, T. S., Chinh, N. T., Kehoe, M., Leigh, J. A., Ward, P. N., Dowson, C. G., Whatmore, A. M., Chanter, N., Iversen, P., Gottschalk, M., Slater, J. D., Smith, H. E., Spratt, B. G., Xu, J., Ye, C., Bentley, S., Barrell, B. G., Schultsz, C., Maskell, D. J. & Parkhill, J. (2009). Rapid evolution of virulence and drug resistance in the emerging zoonotic pathogen *Streptococcus suis*. *PLoS One* **4**, e6072.

Holden, M. T., Hsu, L. Y., Kurt, K., Weinert, L. A., Mather, A. E., Harris, S. R., Strommenger, B., Layer, F., Witte, W., de Lencastre, H., Skov, R., Westh, H., Zemlickova, H., Coombs, G., Kearns, A. M., Hill, R. L., Edgeworth, J., Gould, I., Gant, V., Cooke, J., Edwards, G. F., McAdam, P. R., Templeton, K. E., McCann, A., Zhou, Z., Castillo-Ramirez, S., Feil, E. J., Hudson, L. O., Enright, M. C., Balloux, F., Aanensen, D. M., Spratt, B. G., Fitzgerald, J. R., Parkhill, J., Achtman, M., Bentley, S. D. & Nubel, U. (2013).A genomic portrait of the emergence, evolution, and global spread of a methicillin-resistant *Staphylococcus aureus* pandemic. *Genome Res* **23**, 653-664.

Hood, M. I. & Skaar, E. P. (2012). Nutritional immunity: transition metals at the pathogen-host interface. *Nat Rev Microbiol* **10**, 525-537.

Horsburgh, M. J., Ingham, E. & Foster, S. J. (2001). In *Staphylococcus aureus*, fur is an interactive regulator with PerR, contributes to virulence, and Is necessary for oxidative stress resistance through positive regulation of catalase and iron homeostasis. *J Bacteriol* **183**, 468-475.

Huebner, J. & Goldmann, D. A. (1999). Coagulase-negative staphylococci: role as pathogens. *Annu Rev Med* **50**, 223-236.

Hung, T., Zaghi, S., Yousefzadeh, J. & Leibowitz, M. (2012). Necrotizing Fasciitis Associated with *Staphylococcus lugdunensis*. *Case Rep Infect Dis* **2012**, 453685.

Hussain, M., Herrmann, M., von Eiff, C., Perdreau-Remington, F. & Peters, G. (1997). A 140-kilodalton extracellular protein is essential for the accumulation of *Staphylococcus epidermidis* strains on surfaces. *Infect Immun* **65**, 519-524.

Hussain, M., Becker, K., von Eiff, C., Schrenzel, J., Peters, G. & Herrmann, M. (2001). Identification and characterization of a novel 38.5-kilodalton cell surface protein of *Staphylococcus aureus* with extended-spectrum binding activity for extracellular matrix and plasma proteins. *J Bacteriol* **183**, 6778-6786.

Hwang, P. K. & Greer, J. (1980). Interaction between hemoglobin subunits in the hemoglobin . haptoglobin complex. *J Biol Chem* **255**, 3038-3041.

Ilangovan, U., Ton-That, H., Iwahara, J., Schneewind, O. & Clubb, R. T. (2001). Structure of sortase, the transpeptidase that anchors proteins to the cell wall of *Staphylococcus aureus*. *Proc Natl Acad Sci U S A* **98**, 6056-6061.

Imamura, T., Tanase, S., Szmyd, G., Kozik, A., Travis, J. & Potempa, J. (2005). Induction of vascular leakage through release of bradykinin and a novel kinin by cysteine proteinases from *Staphylococcus aureus*. *J Exp Med* **201**, 1669-1676.

Inoshima, I., Inoshima, N., Wilke, G. A., Powers, M. E., Frank, K. M., Wang, Y. & Bubeck Wardenburg, J. (2011). A *Staphylococcus aureus* pore-forming toxin subverts the activity of ADAM10 to cause lethal infection in mice. *Nat Med* **17**, 1310-1314.

Janscak, P., MacWilliams, M. P., Sandmeier, U., Nagaraja, V. & Bickle, T. A. (1999). DNA translocation blockage, a general mechanism of cleavage site selection by type I restriction enzymes. *EMBO J* **18**, 2638-2647.

Janscak, P., Sandmeier, U., Szczelkun, M. D. & Bickle, T. A. (2001). Subunit assembly and mode of DNA cleavage of the type III restriction endonucleases EcoP1I and EcoP15I. *J Mol Biol* **306**, 417-431.

Jarraud, S., Peyrat, M. A., Lim, A., Tristan, A., Bes, M., Mougel, C., Etienne, J., Vandenesch, F., Bonneville, M. & Lina, G. (2001). *egc*, a highly prevalent operon of enterotoxin gene, forms a putative nursery of superantigens in *Staphylococcus aureus*. *J Immunol* **166**, 669-677.

Jevons, M. P., Coe, A. W. & Parker, M. T. (1963). Methicillin resistance in staphylococci. *The Lancet* **281**, 904–907.

Ji, Y., Zhang, B., Van, S. F., Horn, Warren, P., Woodnutt, G., Burnham, M. K. & Rosenberg, M. (2001). Identification of critical staphylococcal genes using conditional phenotypes generated by antisense RNA. *Science* **293**, 2266-2269.

Johansson, M. U., de Chateau, M., Wikstrom, M., Forsen, S., Drakenberg, T. & Bjorck, L. (1997). Solution structure of the albumin-binding GA module: a versatile bacterial protein domain. *J Mol Biol* **266**, 859-865.

Johnson, M., Cockayne, A. & Morrissey, J. A. (2008). Iron-regulated biofilm formation in *Staphylococcus aureus* Newman requires *ica* and the secreted protein Emp. *Infect Immun* **76**, 1756-1765.

Jonsson, I. M., Mazmanian, S. K., Schneewind, O., Verdrengh, M., Bremell, T. & Tarkowski, A. (2002). On the role of *Staphylococcus aureus* sortase and sortase-catalyzed surface protein anchoring in murine septic arthritis. *J Infect Dis* **185**, 1417-1424.

Jonsson, I. M., Mazmanian, S. K., Schneewind, O., Bremell, T. & Tarkowski, A. (2003). The role of *Staphylococcus aureus* sortase A and sortase B in murine arthritis. *Microbes Infect* **5**, 775-780.

Kang, M., Ko, Y. P., Liang, X., Ross, C. L., Liu, Q., Murray, B. E. & Hook, M. (2013). Collagen-binding Microbial Surface Components Recognizing Adhesive Matrix Molecule (MSCRAMM) of Gram-positive Bacteria Inhibit Complement Activation via the Classical Pathway. *J Biol Chem* **288**, 20520-20531.

Kantyka, T., Shaw, L. N. & Potempa, J. (2011). Papain-like proteases of *Staphylococcus aureus*. *Adv Exp Med Biol* **712**, 1-14.

Kaplan, J. B., Velliyagounder, K., Ragunath, C., Rohde, H., Mack, D., Knobloch, J. K. & Ramasubbu, N. (2004). Genes involved in the synthesis and degradation of matrix polysaccharide in Actinobacillus actinomycetemcomitans and *Actinobacillus pleuropneumoniae* biofilms. *J Bacteriol* **186**, 8213-8220.

Karavolos, M. H., Horsburgh, M. J., Ingham, E. & Foster, S. J. (2003). Role and regulation of the superoxide dismutases of *Staphylococcus aureus*. *Microbiology* **149**, 2749-2758.

Katayama, Y., Ito, T. & Hiramatsu, K. (2000). A new class of genetic element, staphylococcus cassette chromosome *mec*, encodes methicillin resistance in *Staphylococcus aureus*. *Antimicrob Agents Chemother* **44**, 1549-1555.

Keane, F. M., Clarke, A. W., Foster, T. J. & Weiss, A. S. (2007). The N-terminal A domain of *Staphylococcus aureus* fibronectin-binding protein A binds to tropoelastin. *Biochemistry* **46**, 7226-7232.

Kiedrowski, M. R., Kavanaugh, J. S., Malone, C. L., Mootz, J. M., Voyich, J. M., Smeltzer, M. S., Bayles, K. W. & Horswill, A. R. (2011). Nuclease modulates biofilm formation in community-associated methicillin-resistant *Staphylococcus aureus*. *PLoS One* **6**, e26714.

Kim, H. K., Kim, H. Y., Schneewind, O. & Missiakas, D. (2011). Identifying protective antigens of *Staphylococcus aureus*, a pathogen that suppresses host immune responses. *FASEB J* **25**, 3605-3612.

King, N. P., Sakinc, T., Ben Zakour, N. L., Totsika, M., Heras, B., Simerska, P., Shepherd, M., Gatermann, S. G., Beatson, S. A. & Schembri, M. A. (2012). Characterisation of a cell wall-anchored protein of *Staphylococcus saprophyticus* associated with linoleic acid resistance. *BMC Microbiol* **12**, 8.

Klappenbach, J. A., Saxman, P. R., Cole, J. R. & Schmidt, T. M. (2001). rrndb: the Ribosomal RNA Operon Copy Number Database. *Nucleic Acids Res* **29**, 181-184.

Kluytmans, J., van Belkum, A. & Verbrugh, H. (1997). Nasal carriage of *Staphylococcus aureus*: epidemiology, underlying mechanisms, and associated risks. *Clin Microbiol Rev* **10**, 505-520.

Koch, A. L. (1987). Escherichia coli and Sallmonella: *Cellular and Molecular Biology*, pp. 1611. Edited by F. C. *e. a.* Neidhardt. Washington: American Society of Microbiology, Washington DC.

Kocianova, S., Vuong, C., Yao, Y., Voyich, J. M., Fischer, E. R., DeLeo, F. R. & Otto, M. (2005). Key role of poly-gamma-DL-glutamic acid in immune evasion and virulence of *Staphylococcus epidermidis*. *J Clin Invest* **115**, 688-694.

Kogan, G., Sadovskaya, I., Chaignon, P., Chokr, A. & Jabbouri, S. (2006). Biofilms of clinical strains of Staphylococcus that do not contain polysaccharide intercellular adhesin. *FEMS Microbiol Lett* **255**, 11-16.

Kohler, T., Weidenmaier, C. & Peschel, A. (2009). Wall teichoic acid protects *Staphylococcus aureus* against antimicrobial fatty acids from human skin. *J Bacteriol* **191**, 4482-4484.

Kreiswirth, B. N., Lofdahl, S., Betley, M. J., O'Reilly, M., Schlievert, P. M., Bergdoll, M. S. & Novick, R. P. (1983). The toxic shock syndrome exotoxin structural gene is not detectably transmitted by a prophage. *Nature* **305**, 709-712.

Kretschmer, D., Gleske, A. K., Rautenberg, M., Wang, R., Koberle, M., Bohn, E., Schoneberg, T., Rabiet, M. J., Boulay, F., Klebanoff, S. J., van Kessel, K. A., van Strijp, J. A., Otto, M. & Peschel, A. (2010). Human formyl peptide receptor 2 senses highly pathogenic *Staphylococcus aureus*. *Cell Host Microbe* **7**, 463-473.

Kroll, J. S., Loynds, B. M. & Moxon, E. R. (1991). The *Haemophilus influenzae* capsulation gene cluster: a compound transposon. *Mol Microbiol* **5**, 1549-1560.

Kugelberg, E., Kofoid, E., Reams, A. B., Andersson, D. I. & Roth, J. R. (2006). Multiple pathways of selected gene amplification during adaptive mutation. *Proc Natl Acad Sci U S A* **103**, 17319-17324.

Kuroda, M., Ohta, T., Uchiyama, I., Baba, T., Yuzawa, H., Kobayashi, I., Cui, L., Oguchi, A., Aoki, K., Nagai, Y., Lian, J., Ito, T., Kanamori, M., Matsumaru, H., Maruyama, A., Murakami, H., Hosoyama, A., Mizutani-Ui, Y., Takahashi, N. K., Sawano, T., Inoue, R., Kaito, C., Sekimizu, K., Hirakawa, H., Kuhara, S., Goto, S., Yabuzaki, J., Kanehisa, M., Yamashita, A., Oshima, K., Furuya, K., Yoshino, C., Shiba, T., Hattori, M., Ogasawara, N., Hayashi, H. & Hiramatsu, K. (2001). Whole genome sequencing of meticillin-resistant *Staphylococcus aureus*. *Lancet* **357**, 1225-1240.

Kuroda, M., Yamashita, A., Hirakawa, H., Kumano, M., Morikawa, K., Higashide, M., Maruyama, A., Inose, Y., Matoba, K., Toh, H., Kuhara, S., Hattori, M. & Ohta, T. (2005). Whole genome sequence of *Staphylococcus saprophyticus* reveals the pathogenesis of uncomplicated urinary tract infection. *Proc Natl Acad Sci U S A* **102**, 13272-13277.

Labrie, S. J., Samson, J. E. & Moineau, S. (2010). Bacteriophage resistance mechanisms. *Nat Rev Microbiol* **8**, 317-327.

Lambe, D. W., Jr., Ferguson, K. P., Keplinger, J. L., Gemmell, C. G. & Kalbfleisch, J. H. (1990). Pathogenicity of *Staphylococcus lugdunensis*, *Staphylococcus schleiferi*, and three other coagulase-negative staphylococci in a mouse model and possible virulence factors. *Can J Microbiol* **36**, 455-463.

Lee, L. Y., Hook, M., Haviland, D., Wetsel, R. A., Yonter, E. O., Syribeys, P., Vernachio, J. & Brown, E. L. (2004a). Inhibition of complement activation by a secreted *Staphylococcus aureus* protein. *J Infect Dis* **190**, 571-579.

Lee, L. Y., Liang, X., Hook, M. & Brown, E. L. (2004b). Identification and characterization of the C3 binding domain of the *Staphylococcus aureus* extracellular fibrinogen-binding protein (Efb). *J Biol Chem* **279**, 50710-50716.

Lee, S. W., Mitchell, D. A., Markley, A. L., Hensler, M. E., Gonzalez, D., Wohlrab, A., Dorrestein, P. C., Nizet, V. & Dixon, J. E. (2008). Discovery of a widely distributed toxin biosynthetic gene cluster. *Proc Natl Acad Sci U S A* **105**, 5879-5884.

Lei, M. G., Cue, D., Alba, J., Junecko, J., Graham, J. W. & Lee, C. Y. (2012). A single copy integration vector that integrates at an engineered site on the *Staphylococcus aureus* chromosome. *BMC Res Notes* **5**, 5.

Li, M. Z. & Elledge, S. J. (2007). Harnessing homologous recombination *in vitro* to generate recombinant DNA via SLIC. *Nat Methods* **4**, 251-256.

Li, M. Z. & Elledge, S. J. (2012). SLIC: a method for sequence- and ligation-independent cloning. *Methods Mol Biol* **852**, 51-59.

Lindsay, J. A. & Holden, M. T. (2004). *Staphylococcus aureus*: superbug, super genome? *Trends Microbiol* **12**, 378-385.

Liu, G. Y., Essex, A., Buchanan, J. T., Datta, V., Hoffman, H. M., Bastian, J. F., Fierer, J. & Nizet, V. (2005). *Staphylococcus aureus* golden pigment impairs neutrophil killing and promotes virulence through its antioxidant activity. *J Exp Med* **202**, 209-215.

Liu, L., Li, Y., Li, S., Hu, N., He, Y., Pong, R., Lin, D., Lu, L. & Law, M. (2012). Comparison of next-generation sequencing systems. *J Biomed Biotechnol* **2012**, 251364.

Liu, M., Tanaka, W. N., Zhu, H., Xie, G., Dooley, D. M. & Lei, B. (2008). Direct hemin transfer from IsdA to IsdC in the iron-regulated surface determinant (Isd) heme acquisition system of *Staphylococcus aureus*. *J Biol Chem* **283**, 6668-6676.

Liu, P. Y., Huang, Y. F., Tang, C. W., Chen, Y. Y., Hsieh, K. S., Ger, L. P., Chen, Y. S. & Liu, Y. C. (2010). *Staphylococcus lugdunensis* infective endocarditis: a literature review and analysis of risk factors. *J Microbiol Immunol Infect* **43**, 478-484.

Llewelyn, M. & Cohen, J. (2002). Superantigens: microbial agents that corrupt immunity. *Lancet Infect Dis* **2**, 156-162.

Löfblom, J., Kronqvist, N., Uhlen, M., Stahl, S. & Wernerus, H. (2007). Optimization of electroporation-mediated transformation: *Staphylococcus carnosus* as model organism. *J Appl Microbiol* **102**, 736-747.

Loman, N. J., Constantinidou, C., Chan, J. Z., Halachev, M., Sergeant, M., Penn, C. W., Robinson, E. R. & Pallen, M. J. (2012). High-throughput bacterial genome sequencing: an embarrassment of choice, a world of opportunity. *Nat Rev Microbiol* **10**, 599-606.

Lowy, F. D. (1998). *Staphylococcus aureus* infections. *N Engl J Med* **339**, 520-532.

Ludlam, H. & Phillips, I. (1989). *Staphylococcus lugdunensis* peritonitis. *Lancet* **2**, 1394.

Lussow, A. R. & MacDonald, H. R. (1994). Differential effects of superantigen-induced "anergy" on priming and effector stages of a T cell-dependent antibody response. *Eur J Immunol* **24**, 445-449.

Mack, D., Fischer, W., Krokotsch, A., Leopold, K., Hartmann, R., Egge, H. & Laufs, R. (1996). The intercellular adhesin involved in biofilm accumulation of *Staphylococcus epidermidis* is a linear beta-1,6-linked glucosaminoglycan: purification and structural analysis. *J Bacteriol* **178**, 175-183.

Maguin, E., Duwat, P., Hege, T., Ehrlich, D. & Gruss, A. (1992). New thermosensitive plasmid for gram-positive bacteria. *J Bacteriol* **174**, 5633-5638.

Mardis, E. R. (2008). Next-generation DNA sequencing methods. *Annu Rev Genomics Hum Genet* **9**, 387-402.

Marlinghaus, L., Becker, K., Korte, M., Neumann, S., Gatermann, S. G. & Szabados, F. (2012). Construction and characterization of three knockout mutants of the *fbl* gene in *Staphylococcus lugdunensis*. *APMIS* **120**, 108-116.

Marraffini, L. A. & Schneewind, O. (2005). Anchor structure of staphylococcal surface proteins. V. Anchor structure of the sortase B substrate IsdC. *J Biol Chem* **280**, 16263-16271.

Marraffini, L. A., Dedent, A. C. & Schneewind, O. (2006). Sortases and the art of anchoring proteins to the envelopes of gram-positive bacteria. *Microbiol Mol Biol Rev* **70**, 192-221.

Marraffini, L. A. & Sontheimer, E. J. (2008). CRISPR interference limits horizontal gene transfer in staphylococci by targeting DNA. *Science* **322**, 1843-1845.

Mazmanian, S. K., Ton-That, H., Su, K. & Schneewind, O. (2002). An iron-regulated sortase anchors a class of surface protein during *Staphylococcus aureus* pathogenesis. *Proc Natl Acad Sci U S A* **99**, 2293-2298.

Mazmanian, S. K., Skaar, E. P., Gaspar, A. H., Humayun, M., Gornicki, P., Jelenska, J., Joachmiak, A., Missiakas, D. M. & Schneewind, O. (2003). Passage of heme-iron across the envelope of *Staphylococcus aureus*. *Science* **299**, 906-909.

McAdam, P. R., Templeton, K. E., Edwards, G. F., Holden, M. T., Feil, E. J., Aanensen, D. M., Bargawi, H. J., Spratt, B. G., Bentley, S. D., Parkhill, J., Enright, M. C., Holmes, A., Girvan, E. K., Godfrey, P. A., Feldgarden, M., Kearns, A. M., Rambaut, A., Robinson, D. A. & Fitzgerald, J. R. (2012). Molecular tracing of the emergence, adaptation, and transmission of hospital-associated methicillin-resistant *Staphylococcus aureus*. *Proc Natl Acad Sci U S A* **109**, 9107-9112.

McCormack, N., Geoghegan, J. A., Monk, I. R. & Foster, T. J. (2013). Identification of a new region of clumping factor A required for its export and cell wall localization in *Staphylococcus aureus*. *J Bacteriol* **Submitted**.

McDevitt, D., Wann, E. R. & Foster, T. J. (1993). Recombination at the coagulase locus in *Staphylococcus aureus*: plasmid integration and amplification. *J Gen Microbiol* **139**, 695-706.

McDevitt, D., Francois, P., Vaudaux, P. & Foster, T. J. (1994). Molecular characterization of the clumping factor (fibrinogen receptor) of *Staphylococcus aureus*. *Mol Microbiol* **11**, 237-248.

Mehlin, C., Headley, C. M. & Klebanoff, S. J. (1999). An inflammatory polypeptide complex from *Staphylococcus epidermidis*: isolation and characterization. *J Exp Med* **189**, 907-918.

Mekalanos, J. J. (1983). Duplication and amplification of toxin genes in Vibrio cholerae. *Cell* **35**, 253-263.

Menestrina, G., Dalla Serra, M., Comai, M., Coraiola, M., Viero, G., Werner, S., Colin, D. A., Monteil, H. & Prevost, G. (2003). Ion channels and bacterial infection: the case of beta-barrel pore-forming protein toxins of *Staphylococcus aureus*. *FEBS Lett* **552**, 54-60.

Merino, N., Toledo-Arana, A., Vergara-Irigaray, M., Valle, J., Solano, C., Calvo, E., Lopez, J. A., Foster, T. J., Penades, J. R. & Lasa, I. (2009). Protein A-mediated multicellular behavior in *Staphylococcus aureus*. *J Bacteriol* **191**, 832-843.

Metzker, M. L. (2010). Sequencing technologies - the next generation. *Nat Rev Genet* **11**, 31-46.

Miajlovic, H., Zapotoczna, M., Geoghegan, J. A., Kerrigan, S. W., Speziale, P. & Foster, T. J. (2010). Direct interaction of iron-regulated surface determinant IsdB of *Staphylococcus aureus* with the GPIIb/IIIa receptor on platelets. *Microbiology* **156**, 920-928.

Migeotte, I., Communi, D. & Parmentier, M. (2006). Formyl peptide receptors: a promiscuous subfamily of G protein-coupled receptors controlling immune responses. *Cytokine Growth Factor Rev* **17**, 501-519.

Min, Y. H., Kwon, A. R., Yoon, J. M., Yoon, E. J., Shim, M. J. & Choi, E. C. (2008). Molecular analysis of constitutive mutations in ermB and ermA selected in vitro from inducibly MLSB-resistant enterococci. *Arch Pharm Res* **31**, 377-380.

Mitchell, J., Tristan, A. & Foster, T. J. (2004). Characterization of the fibrinogen-binding surface protein Fbl of *Staphylococcus lugdunensis*. *Microbiology* **150**, 3831-3841.

Moks, T., Abrahmsen, L., Nilsson, B., Hellman, U., Sjoquist, J. & Uhlen, M. (1986). Staphylococcal protein A consists of five IgG-binding domains. *Eur J Biochem* **156**, 637-643.

Molloy, E. M., Cotter, P. D., Hill, C., Mitchell, D. A. & Ross, R. P. (2011). Streptolysin S-like virulence factors: the continuing sagA. *Nat Rev Microbiol* **9**, 670-681.

Monk, I. R., Cook, G. M., Monk, B. C. & Bremer, P. J. (2004). Morphotypic conversion in *Listeria monocytogenes* biofilm formation: biological significance of rough colony isolates. *Appl Environ Microbiol* **70**, 6686-6694.

Monk, I. R., Casey, P. G., Cronin, M., Gahan, C. G. & Hill, C. (2008). Development of multiple strain competitive index assays for *Listeria monocytogenes* using pIMC; a new site-specific integrative vector. *BMC Microbiol* **8**, 96.

Monk, I. R., Casey, P. G., Hill, C. & Gahan, C. G. (2010). Directed evolution and targeted mutagenesis to murinize *Listeria monocytogenes* internalin A for enhanced infectivity in the murine oral infection model. *BMC Microbiol* **10**, 318.

Monk, I. R., Shah, I. M., Xu, M., Tan, M. W. & Foster, T. J. (2012). Transforming the untransformable: application of direct transformation to manipulate genetically *Staphylococcus aureus* and *Staphylococcus epidermidis*. *MBio* **3**.

Moore, F. (2004). *Immunology, Infection, and Immunity*. Washington DC: ASM.

Moreillon, P., Entenza, J. M., Francioli, P., McDevitt, D., Foster, T. J., Francois, P. & Vaudaux, P. (1995). Role of *Staphylococcus aureus* coagulase and clumping factor in pathogenesis of experimental endocarditis. *Infect Immun* **63**, 4738-4743.

Morikawa, K., Takemura, A. J., Inose, Y., Tsai, M., Nguyen Thi le, T., Ohta, T. & Msadek, T. (2012). Expression of a cryptic secondary sigma factor gene unveils natural competence for DNA transformation in *Staphylococcus aureus*. *PLoS Pathog* **8**, e1003003.

Morrissey, J. A., Cockayne, A., Hill, P. J. & Williams, P. (2000). Molecular cloning and analysis of a putative siderophore ABC transporter from *Staphylococcus aureus*. *Infect Immun* **68**, 6281-6288.

Mulcahy, M. E., Geoghegan, J. A., Monk, I. R., O'Keeffe, K. M., Walsh, E. J., Foster, T. J. & McLoughlin, R. M. (2012). Nasal colonisation by *Staphylococcus aureus* depends upon clumping factor B binding to the squamous epithelial cell envelope protein loricrin. *PLoS Pathog* **8**, e1003092.

Murdoch, C. & Finn, A. (2000). Chemokine receptors and their role in inflammation and infectious diseases. *Blood* **95**, 3032-3043.

Muryoi, N., Tiedemann, M. T., Pluym, M., Cheung, J., Heinrichs, D. E. & Stillman, M. J. (2008). Demonstration of the iron-regulated surface determinant (Isd) heme transfer pathway in *Staphylococcus aureus*. *J Biol Chem* **283**, 28125-28136.

Nakamura, R. K., Zimmerman, S. A., Lange, A. J. & Lesser, M. B. (2012). Isolation of methicillin-resistant *Staphylococcus lugdunensis* in a dog with endocarditis. *J Vet Cardiol* **14**, 531-536.

Näsvall, J., Sun, L., Roth, J. R. & Andersson, D. I. (2012). Real-time evolution of new genes by innovation, amplification, and divergence. *Science* **338**, 384-387.

NCBI (2013). Genome project report Staphylococcus aureus: National Center for Biotechnology Information, U.S. National Library of Medicine. http://www.ncbi.nlm.nih.gov/genome/154 accessed 27.08.13.

Nicoloff, H., Perreten, V., McMurry, L. M. & Levy, S. B. (2006). Role for tandem duplication and lon protease in AcrAB-TolC- dependent multiple antibiotic resistance (*Mar*) in an *Escherichia coli* mutant without mutations in *marRAB* or *acrRAB*. *J Bacteriol* **188**, 4413-4423.

Nicoloff, H., Perreten, V. & Levy, S. B. (2007). Increased genome instability in *Escherichia coli* lon mutants: relation to emergence of multiple-antibiotic-resistant (*Mar*) mutants caused by insertion sequence elements and large tandem genomic amplifications. *Antimicrob Agents Chemother* **51**, 1293-1303.

Nilsson, A. I., Zorzet, A., Kanth, A., Dahlstrom, S., Berg, O. G. & Andersson, D. I. (2006). Reducing the fitness cost of antibiotic resistance by amplification of initiator tRNA genes. *Proc Natl Acad Sci U S A* **103**, 6976-6981.

Nilsson, M., Bjerketorp, J., Guss, B. & Frykberg, L. (2004a). A fibrinogen-binding protein of *Staphylococcus lugdunensis*. *FEMS Microbiol Lett* **241**, 87-93.

Nilsson, M., Bjerketorp, J., Wiebensjo, A., Ljungh, A., Frykberg, L. & Guss, B. (2004b). A von Willebrand factor-binding protein from *Staphylococcus lugdunensis*. *FEMS Microbiol Lett* **234**, 155-161.

Nitzan, Y., Wexler, H. M. & Finegold, S. M. (1994). Inactivation of anaerobic bacteria by various photosensitized porphyrins or by hemin. *Curr Microbiol* **29**, 125-131.

Nizet, V. (2007). Understanding how leading bacterial pathogens subvert innate immunity to reveal novel therapeutic targets. *J Allergy Clin Immunol* **120**, 13-22.

Noel, G. J., Brittingham, A., Granato, A. A. & Mosser, D. M. (1996). Effect of amplification of the Cap b locus on complement-mediated bacteriolysis and opsonization of type b *Haemophilus influenzae*. *Infect Immun* **64**, 4769-4775.

O'Connell Motherway, M., O'Driscoll, J., Fitzgerald, G. F. & Van Sinderen, D. (2009). Overcoming the restriction barrier to plasmid transformation and targeted mutagenesis in *Bifidobacterium breve* UCC2003. *Microb Biotechnol* **2**, 321-332.

O'Neill, E., Pozzi, C., Houston, P., Humphreys, H., Robinson, D. A., Loughman, A., Foster, T. J. & O'Gara, J. P. (2008). A novel *Staphylococcus aureus* biofilm phenotype mediated by the fibronectin-binding proteins, FnBPA and FnBPB. *J Bacteriol* **190**, 3835-3850.

O'Riordan, K. & Lee, J. C. (2004). *Staphylococcus aureus* capsular polysaccharides. *Clin Microbiol Rev* **17**, 218-234.

O'Seaghdha, M., van Schooten, C. J., Kerrigan, S. W., Emsley, J., Silverman, G. J., Cox, D., Lenting, P. J. & Foster, T. J. (2006). *Staphylococcus aureus* protein A binding to von Willebrand factor A1 domain is mediated by conserved IgG binding regions. *FEBS J* **273**, 4831-4841.

Oliviero, S., Morrone, G. & Cortese, R. (1987). The human haptoglobin gene: transcriptional regulation during development and acute phase induction. *EMBO J* **6**, 1905-1912.

Otto, M. (2001). *Staphylococcus aureus* and *Staphylococcus epidermidis* peptide pheromones produced by the accessory gene regulator *agr* system. *Peptides* **22**, 1603-1608.

Otto, M. (2006). Bacterial evasion of antimicrobial peptides by biofilm formation. *Curr Top Microbiol Immunol* **306**, 251-258.

Otto, M. (2012). MRSA virulence and spread. *Cell Microbiol* **14**, 1513-1521.

Otto, M. (2013). Staphylococcal infections: mechanisms of biofilm maturation and detachment as critical determinants of pathogenicity. *Annu Rev Med* **64**, 175-188.

Otto, T. D., Sanders, M., Berriman, M. & Newbold, C. (2010). Iterative Correction of Reference Nucleotides (iCORN) using second generation sequencing technology. *Bioinformatics* **26**, 1704-1707.

Pallen, M. J., Lam, A. C., Antonio, M. & Dunbar, K. (2001). An embarrassment of sortases - a richness of substrates? *Trends Microbiol* **9**, 97-102.

Palmqvist, N., Foster, T., Tarkowski, A. & Josefsson, E. (2002). Protein A is a virulence factor in *Staphylococcus aureus* arthritis and septic death. *Microb Pathog* **33**, 239-249.

Panizzi, P., Friedrich, R., Fuentes-Prior, P., Richter, K., Bock, P. E. & Bode, W. (2006). Fibrinogen substrate recognition by staphylocoagulase.(pro)thrombin complexes. *J Biol Chem* **281**, 1179-1187.

Papapetropoulos, N., Papapetropoulou, M. & Vantarakis, A. (2013). Abscesses and wound infections due to *Staphylococcus lugdunensis*: report of 16 cases. *Infection* **41**, 525-528.

Paulsson, M., Petersson, A. C. & Ljungh, A. (1993). Serum and tissue protein binding and cell surface properties of *Staphylococcus lugdunensis*. *J Med Microbiol* **38**, 96-102.

Pearson, W. R. & Lipman, D. J. (1988). Improved tools for biological sequence comparison. *Proc Natl Acad Sci U S A* **85**, 2444-2448.

Pelz, A., Wieland, K. P., Putzbach, K., Hentschel, P., Albert, K. & Götz, F. (2005). Structure and biosynthesis of staphyloxanthin from *Staphylococcus aureus*. *J Biol Chem* **280**, 32493-32498.

Pereira, E. M., Oliveira, F. L., Schuenck, R. P., Zoletti, G. O. & Dos Santos, K. R. (2010). Detection of *Staphylococcus lugdunensis* by a new species-specific PCR based on the fbl gene. *FEMS Immunol Med Microbiol* **58**, 295-298.

Periasamy, S., Joo, H. S., Duong, A. C., Bach, T. H., Tan, V. Y., Chatterjee, S. S., Cheung, G. Y. & Otto, M. (2012). How *Staphylococcus aureus* biofilms develop their characteristic structure. *Proc Natl Acad Sci U S A* **109**, 1281-1286.

Peschel, A., Otto, M., Jack, R. W., Kalbacher, H., Jung, G. & Götz, F. (1999). Inactivation of the dlt operon in *Staphylococcus aureus* confers sensitivity to defensins, protegrins, and other antimicrobial peptides. *J Biol Chem* **274**, 8405-8410.

Peschel, A., Jack, R. W., Otto, M., Collins, L. V., Staubitz, P., Nicholson, G., Kalbacher, H., Nieuwenhuizen, W. F., Jung, G., Tarkowski, A., van Kessel, K. P. & van Strijp, J. A. (2001).*Staphylococcus aureus* resistance to human defensins and evasion of neutrophil killing via the novel virulence factor MprF is based on modification of membrane lipids with l-lysine. *J Exp Med* **193**, 1067-1076.

Peschel, A. (2002). How do bacteria resist human antimicrobial peptides? *Trends Microbiol* **10**, 179-186.

Petersen, K. V., Martinussen, J., Jensen, P. R. & Solem, C. (2013). Repetitive marker-free site-specific integration - a novel tool for multiple chromosomal integration of DNA. *Appl Environ Microbiol*.

Petit, M. A., Mesas, J. M., Noirot, P., Morel-Deville, F. & Ehrlich, S. D. (1992). Induction of DNA amplification in the *Bacillus subtilis* chromosome. *EMBO J* **11**, 1317-1326.

Pettersson, M. E., Sun, S., Andersson, D. I. & Berg, O. G. (2009). Evolution of new gene functions: simulation and analysis of the amplification model. *Genetica* **135**, 309-324.

Pilpa, R. M., Robson, S. A., Villareal, V. A., Wong, M. L., Phillips, M. & Clubb, R. T. (2009). Functionally distinct NEAT (NEAr Transporter) domains within the *Staphylococcus aureus* IsdH/HarA protein extract heme from methemoglobin. *J Biol Chem* **284**, 1166-1176.

Pinna, A., Zanetti, S., Sotgiu, M., Sechi, L. A., Fadda, G. & Carta, F. (1999). Identification and antibiotic susceptibility of coagulase negative staphylococci isolated in corneal/external infections. *Br J Ophthalmol* **83**, 771-773.

Pishchany, G., Dickey, S. E. & Skaar, E. P. (2009). Subcellular localization of the *Staphylococcus aureus* heme iron transport components IsdA and IsdB. *Infect Immun* **77**, 2624-2634.

Pishchany, G., McCoy, A. L., Torres, V. J., Krause, J. C., Crowe, J. E., Jr., Fabry, M. E. & Skaar, E. P. (2010). Specificity for human hemoglobin enhances *Staphylococcus aureus* infection. *Cell Host Microbe* **8**, 544-550.

Pohl, E., Haller, J. C., Mijovilovich, A., Meyer-Klaucke, W., Garman, E. & Vasil, M. L. (2003). Architecture of a protein central to iron homeostasis: crystal structure and spectroscopic analysis of the ferric uptake regulator. *Mol Microbiol* **47**, 903-915.

Ponnuraj, K., Bowden, M. G., Davis, S., Gurusiddappa, S., Moore, D., Choe, D., Xu, Y., Hook, M. & Narayana, S. V. (2003). A "dock, lock, and latch" structural model for a staphylococcal adhesin binding to fibrinogen. *Cell* **115**, 217-228.

Proft, T. & Fraser, J. D. (2003). Bacterial superantigens. *Clin Exp Immunol* **133**, 299-306.

Prokesova, L., Porwit-Bobr, Z., Baran, K., Potempa, J. & John, C. (1988). Effect of serine proteinase from *Staphylococcus aureus* on *in vitro* stimulation of human lymphocytes. *Immunol Lett* **19**, 127-132.

Que, Y. A., Francois, P., Haefliger, J. A., Entenza, J. M., Vaudaux, P. & Moreillon, P. (2001). Reassessing the role of *Staphylococcus aureus* clumping factor and fibronectin-binding protein by expression in *Lactococcus lactis*. *Infect Immun* **69**, 6296-6302.

Que, Y. A., Haefliger, J. A., Piroth, L., Francois, P., Widmer, E., Entenza, J. M., Sinha, B., Herrmann, M., Francioli, P., Vaudaux, P. & Moreillon, P. (2005). Fibrinogen and fibronectin binding cooperate for valve infection and invasion in *Staphylococcus aureus* experimental endocarditis. *J Exp Med* **201**, 1627-1635.

Queck, S. Y., Khan, B. A., Wang, R., Bach, T. H., Kretschmer, D., Chen, L., Kreiswirth, B. N., Peschel, A., Deleo, F. R. & Otto, M. (2009). Mobile genetic element-encoded cytolysin connects virulence to methicillin resistance in MRSA. *PLoS Pathog* **5**, e1000533.

Rautenberg, M., Joo, H. S., Otto, M. & Peschel, A. (2010). Neutrophil responses to staphylococcal pathogens and commensals via the formyl peptide receptor 2 relates to phenol-soluble modulin release and virulence. *FASEB J.*

Rice, K. C., Mann, E. E., Endres, J. L., Weiss, E. C., Cassat, J. E., Smeltzer, M. S. & Bayles, K. W. (2007). The cidA murein hydrolase regulator contributes to DNA release and biofilm development in *Staphylococcus aureus*. *Proc Natl Acad Sci U S A* **104**, 8113-8118.

Richter, C., Chang, J. T. & Fineran, P. C. (2012). Function and regulation of clustered regularly interspaced short palindromic repeats (CRISPR) / CRISPR associated (Cas) systems. *Viruses* **4**, 2291-2311.

Roberts, G. A., Houston, P. J., White, J. H., Chen, K., Stephanou, A. S., Cooper, L. P., Dryden, D. T. & Lindsay, J. A. (2013). Impact of target site distribution for Type I restriction enzymes on the evolution of methicillin-resistant *Staphylococcus aureus* (MRSA) populations. *Nucleic Acids Res.*

Roche, F. M., Downer, R., Keane, F., Speziale, P., Park, P. W. & Foster, T. J. (2004). The N-terminal A domain of fibronectin-binding proteins A and B promotes adhesion of *Staphylococcus aureus* to elastin. *J Biol Chem* **279**, 38433-38440.

Roghmann, M., Taylor, K. L., Gupte, A., Zhan, M., Johnson, J. A., Cross, A., Edelman, R. & Fattom, A. I. (2005). Epidemiology of capsular and surface polysaccharide in *Staphylococcus aureus* infections complicated by bacteraemia. *J Hosp Infect* **59**, 27-32.

Rohde, H., Burdelski, C., Bartscht, K., Hussain, M., Buck, F., Horstkotte, M. A., Knobloch, J. K., Heilmann, C., Herrmann, M. & Mack, D. (2005). Induction of *Staphylococcus epidermidis* biofilm formation via proteolytic processing of the accumulation-associated protein by staphylococcal and host proteases. *Mol Microbiol* **55**, 1883-1895.

Rohde, H., Burandt, E. C., Siemssen, N., Frommelt, L., Burdelski, C., Wurster, S., Scherpe, S., Davies, A. P., Harris, L. G., Horstkotte, M. A., Knobloch, J. K., Ragunath, C., Kaplan, J. B. & Mack, D. (2007). Polysaccharide intercellular adhesin or protein factors in biofilm accumulation of *Staphylococcus epidermidis* and *Staphylococcus aureus* isolated from prosthetic hip and knee joint infections. *Biomaterials* **28**, 1711-1720.

Romero, D. & Palacios, R. (1997). Gene amplification and genomic plasticity in prokaryotes. *Annu Rev Genet* **31**, 91-111.

Rooijakkers, S. H., Ruyken, M., Roos, A., Daha, M. R., Presanis, J. S., Sim, R. B., van Wamel, W. J., van Kessel, K. P. & van Strijp, J. A. (2005). Immune evasion by a staphylococcal complement inhibitor that acts on C3 convertases. *Nat Immunol* **6**, 920-927.

Rosenberg, S. M., Thulin, C. & Harris, R. S. (1998). Transient and heritable mutators in adaptive evolution in the lab and in nature. *Genetics* **148**, 1559-1566.

Rosenstein, R., Nerz, C., Biswas, L., Resch, A., Raddatz, G., Schuster, S. C. & Götz, F. (2009). Genome analysis of the meat starter culture bacterium *Staphylococcus carnosus* TM300. *Appl Environ Microbiol* **75**, 811-822.

Rosenstein, R. & Götz, F. (2010). Genomic differences between the food-grade *Staphylococcus carnosus* and pathogenic staphylococcal species. *Int J Med Microbiol* **300**, 104-108.

Rozalska, B. & Ljungh, A. (1995). Biomaterial-associated staphylococcal peritoneal infections in a neutropaenic mouse model. *FEMS Immunol Med Microbiol* **11**, 307-319.

Ruggiero, A., Tizzano, B., Pedone, E., Pedone, C., Wilmanns, M. & Berisio, R. (2009). Crystal structure of the resuscitation-promoting factor (DeltaDUF)RpfB from M. tuberculosis. *J Mol Biol* **385**, 153-162.

Ruoslahti, E. & Pierschbacher, M. D. (1986). Arg-Gly-Asp: a versatile cell recognition signal. *Cell* **44**, 517-518.

Ruoslahti, E. (1996). RGD and other recognition sequences for integrins. *Annu Rev Cell Dev Biol* **12**, 697-715.

Sakinc, T., Kleine, B. & Gatermann, S. G. (2006). SdrI, a serine-aspartate repeat protein identified in *Staphylococcus saprophyticus* strain 7108, is a collagen-binding protein. *Infect Immun* **74**, 4615-4623.

Sammut, S. J., Finn, R. D. & Bateman, A. (2008). Pfam 10 years on: 10,000 families and still growing. *Brief Bioinform* **9**, 210-219.

Sandegren, L. & Andersson, D. I. (2009). Bacterial gene amplification: implications for the evolution of antibiotic resistance. *Nat Rev Microbiol* **7**, 578-588.

Schaible, U. E. & Kaufmann, S. H. (2004). Iron and microbial infection. *Nat Rev Microbiol* **2**, 946-953.

Schito, G. C., Naber, K. G., Botto, H., Palou, J., Mazzei, T., Gualco, L. & Marchese, A. (2009). The ARESC study: an international survey on the antimicrobial resistance of pathogens involved in uncomplicated urinary tract infections. *Int J Antimicrob Agents* **34**, 407-413.

Schlag, M., Biswas, R., Krismer, B., Kohler, T., Zoll, S., Yu, W., Schwarz, H., Peschel, A. & Götz, F. (2010). Role of staphylococcal wall teichoic acid in targeting the major autolysin Atl. *Mol Microbiol* **75**, 864-873.

Schneewind, O., Model, P. & Fischetti, V. A. (1992). Sorting of protein A to the staphylococcal cell wall. *Cell* **70**, 267-281.

Schnitzler, N., Meilicke, R., Conrads, G., Frank, D. & Haase, G. (1998). *Staphylococcus lugdunensis*: report of a case of peritonitis and an easy-to-perform screening strategy. *J Clin Microbiol* **36**, 812-813.

Schwarz-Linek, U., Werner, J. M., Pickford, A. R., Gurusiddappa, S., Kim, J. H., Pilka, E. S., Briggs, J. A., Gough, T. S., Hook, M., Campbell, I. D. & Potts, J. R. (2003). Pathogenic bacteria attach to human fibronectin through a tandem beta-zipper. *Nature* **423**, 177-181.

Sebulsky, M. T., Hohnstein, D., Hunter, M. D. & Heinrichs, D. E. (2000). Identification and characterization of a membrane permease involved in iron-hydroxamate transport in *Staphylococcus aureus*. *J Bacteriol* **182**, 4394-4400.

Shah, M. M., Iihara, H., Noda, M., Song, S. X., Nhung, P. H., Ohkusu, K., Kawamura, Y. & Ezaki, T. (2007). dnaJ gene sequence-based assay for species identification and phylogenetic grouping in the genus Staphylococcus. *Int J Syst Evol Microbiol* **57**, 25-30.

Sharp, J. A., Echague, C. G., Hair, P. S., Ward, M. D., Nyalwidhe, J. O., Geoghegan, J. A., Foster, T. J. & Cunnion, K. M. (2012). *Staphylococcus aureus* surface protein SdrE binds complement regulator factor H as an immune evasion tactic. *PLoS One* **7**, e38407.

Shorr, A. F. (2007). Epidemiology of staphylococcal resistance. *Clin Infect Dis* **45 Suppl 3**, S171-176.

Sibal, A. K., Lin, Z. & Jogia, D. (2011). Coagulase-negative Staphylococcus endocarditis: *Staphylococcus lugdunensis*. *Asian Cardiovasc Thorac Ann* **19**, 414-415.

Sieprawska-Lupa, M., Mydel, P., Krawczyk, K., Wojcik, K., Puklo, M., Lupa, B., Suder, P., Silberring, J., Reed, M., Pohl, J., Shafer, W., McAleese, F., Foster, T., Travis, J. & Potempa, J. (2004). Degradation of human antimicrobial peptide LL-37 by *Staphylococcus aureus*-derived proteinases. *Antimicrob Agents Chemother* **48**, 4673-4679.

Siezen, R. J., Kuipers, O. P. & de Vos, W. M. (1996). Comparison of lantibiotic gene clusters and encoded proteins. *Antonie Van Leeuwenhoek* **69**, 171-184.

Silverman, G. J. & Goodyear, C. S. (2006). Confounding B-cell defences: lessons from a staphylococcal superantigen. *Nat Rev Immunol* **6**, 465-475.

Singh, N. & Sun, H. Y. (2008). Iron overload and unique susceptibility of liver transplant recipients to disseminated disease due to opportunistic pathogens. *Liver Transpl* **14**, 1249-1255.

Skaar, E. P., Humayun, M., Bae, T., DeBord, K. L. & Schneewind, O. (2004). Iron-source preference of *Staphylococcus aureus* infections. *Science* **305**, 1626-1628.

Soukup, S. W. (1974). Evolution by gene duplication. S. Ohno. Springer-Verlag, New York. 1970. 160 pp. *Teratology* **9**, 250-251.

Spaan, A. N., Henry, T., van Rooijen, W. J., Perret, M., Badiou, C., Aerts, P. C., Kemmink, J., de Haas, C. J., van Kessel, K. P., Vandenesch, F., Lina, G. & van Strijp, J. A. (2013). The staphylococcal toxin Panton-Valentine Leukocidin targets human C5a receptors. *Cell Host Microbe* **13**, 584-594.

Speziale, P., Pietrocola, G., Rindi, S., Provenzano, M., Provenza, G., Di Poto, A., Visai, L. & Arciola, C. R. (2009). Structural and functional role of *Staphylococcus aureus* surface components recognizing adhesive matrix molecules of the host. *Future Microbiol* **4**, 1337-1352.

Speziali, C. D., Dale, S. E., Henderson, J. A., Vines, E. D. & Heinrichs, D. E. (2006). Requirement of *Staphylococcus aureus* ATP-binding cassette-ATPase FhuC for iron-restricted growth and evidence that it functions with more than one iron transporter. *J Bacteriol* **188**, 2048-2055.

Stair, B., Vessels, B., Overholser, E., Zogleman, B., Wall, B. M. & Corbett, C. (2012). Successful daptomycin treatment for *Staphylococcus lugdunensis* endocarditis. *Am J Med Sci* **344**, 64-66.

Stauff, D. L., Torres, V. J. & Skaar, E. P. (2007). Signaling and DNA-binding activities of the *Staphylococcus aureus* HssR-HssS two-component system required for heme sensing. *J Biol Chem* **282**, 26111-26121.

Strauss, A. & Götz, F. (1996). In vivo immobilization of enzymatically active polypeptides on the cell surface of *Staphylococcus carnosus*. *Mol Microbiol* **21**, 491-500.

Sun, F., Cho, H., Jeong, D. W., Li, C., He, C. & Bae, T. (2010). Aureusimines in *Staphylococcus aureus* are not involved in virulence. *PLoS One* **5**, e15703.

Suzuki, H., Lefebure, T., Bitar, P. P. & Stanhope, M. J. (2012). Comparative genomic analysis of the genus Staphylococcus including *Staphylococcus aureus* and its newly described sister species *Staphylococcus simiae*. *BMC Genomics* **13**, 38.

Takahashi, T., Satoh, I. & Kikuchi, N. (1999). Phylogenetic relationships of 38 taxa of the genus Staphylococcus based on 16S rRNA gene sequence analysis. *Int J Syst Bacteriol* **49 Pt 2**, 725-728.

Takeuchi, F., Watanabe, S., Baba, T., Yuzawa, H., Ito, T., Morimoto, Y., Kuroda, M., Cui, L., Takahashi, M., Ankai, A., Baba, S., Fukui, S., Lee, J. C. & Hiramatsu, K. (2005). Whole-genome sequencing of *Staphylococcus haemolyticus* uncovers the extreme plasticity of its genome and the evolution of human-colonizing staphylococcal species. *J Bacteriol* **187**, 7292-7308.

Tan, T. Y., Ng, S. Y. & He, J. (2008). Microbiological characteristics, presumptive identification, and antibiotic susceptibilities of *Staphylococcus lugdunensis*. *J Clin Microbiol* **46**, 2393-2395.

Tee, W. S., Soh, S. Y., Lin, R. & Loo, L. H. (2003). *Staphylococcus lugdunensis* carrying the *mecA* gene causes catheter-associated bloodstream infection in premature neonate. *J Clin Microbiol* **41**, 519-520.

Thakker, M., Park, J. S., Carey, V. & Lee, J. C. (1998). *Staphylococcus aureus* serotype 5 capsular polysaccharide is antiphagocytic and enhances bacterial virulence in a murine bacteremia model. *Infect Immun* **66**, 5183-5189.

Tock, M. R. & Dryden, D. T. (2005). The biology of restriction and anti-restriction. *Curr Opin Microbiol* **8**, 466-472.

Tolosano, E. & Altruda, F. (2002). Hemopexin: structure, function, and regulation. *DNA Cell Biol* **21**, 297-306.

Ton-That, H., Liu, G., Mazmanian, S. K., Faull, K. F. & Schneewind, O. (1999). Purification and characterization of sortase, the transpeptidase that cleaves surface proteins of *Staphylococcus aureus* at the LPXTG motif. *Proc Natl Acad Sci U S A* **96**, 12424-12429.

Ton-That, H., Mazmanian, S. K., Faull, K. F. & Schneewind, O. (2000). Anchoring of surface proteins to the cell wall of *Staphylococcus aureus*. Sortase catalyzed in vitro transpeptidation reaction using LPXTG peptide and NH(2)-Gly(3) substrates. *J Biol Chem* **275**, 9876-9881.

Ton-That, H., Marraffini, L. A. & Schneewind, O. (2004). Protein sorting to the cell wall envelope of Gram-positive bacteria. *Biochim Biophys Acta* **1694**, 269-278.

Torkelson, J., Harris, R. S., Lombardo, M. J., Nagendran, J., Thulin, C. & Rosenberg, S. M. (1997). Genome-wide hypermutation in a subpopulation of stationary-phase cells underlies recombination-dependent adaptive mutation. *EMBO J* **16**, 3303-3311.

Torres, V. J., Pishchany, G., Humayun, M., Schneewind, O. & Skaar, E. P. (2006). *Staphylococcus aureus* IsdB is a hemoglobin receptor required for heme iron utilization. *J Bacteriol* **188**, 8421-8429.

Torres, V. J., Stauff, D. L., Pishchany, G., Bezbradica, J. S., Gordy, L. E., Iturregui, J., Anderson, K. L., Dunman, P. M., Joyce, S. & Skaar, E. P. (2007). A *Staphylococcus aureus* regulatory system that responds to host heme and modulates virulence. *Cell Host Microbe* **1**, 109-119.

Torres, V. J., Attia, A. S., Mason, W. J., Hood, M. I., Corbin, B. D., Beasley, F. C., Anderson, K. L., Stauff, D. L., McDonald, W. H., Zimmerman, L. J., Friedman, D. B., Heinrichs, D. E., Dunman, P. M. & Skaar, E. P. (2010). *Staphylococcus aureus* fur regulates the expression of virulence factors that contribute to the pathogenesis of pneumonia. *Infect Immun* **78**, 1618-1628.

Treangen, T. J. & Salzberg, S. L. (2012). Repetitive DNA and next-generation sequencing: computational challenges and solutions. *Nat Rev Genet* **13**, 36-46.

Tsai, I. J., Otto, T. D. & Berriman, M. (2010). Improving draft assemblies by iterative mapping and assembly of short reads to eliminate gaps. *Genome Biol* **11**, R41.

Tse, H., Tsoi, H. W., Leung, S. P., Lau, S. K., Woo, P. C. & Yuen, K. Y. (2010). Complete genome sequence of *Staphylococcus lugdunensis* strain HKU09-01. *J Bacteriol* **192**, 1471-1472.

Vandenesch, F., Projan, S. J., Kreiswirth, B., Etienne, J. & Novick, R. P. (1993). Agr-related sequences in *Staphylococcus lugdunensis*. *FEMS Microbiol Lett* **111**, 115-122.

Vaudaux, P. E., Francois, P., Proctor, R. A., McDevitt, D., Foster, T. J., Albrecht, R. M., Lew, D. P., Wabers, H. & Cooper, S. L. (1995). Use of adhesion-defective mutants of *Staphylococcus aureus* to define the role of specific plasma proteins in promoting bacterial adhesion to canine arteriovenous shunts. *Infect Immun* **63**, 585-590.

Veiga, H. & Pinho, M. G. (2009). Inactivation of the SauI type I restriction-modification system is not sufficient to generate *Staphylococcus aureus* strains capable of efficiently accepting foreign DNA. *Appl Environ Microbiol* **75**, 3034-3038.

Vigna, F., Stracher, M., Auerbach, A., Suss, A., Majid, K. & Spero, C. (2007). *Staphylococcus lugdunensis* osteomyelitis: a case report. *Am J Orthop (Belle Mead NJ)* **36**, E3-4.

von Eiff, C., Becker, K., Machka, K., Stammer, H. & Peters, G. (2001). Nasal carriage as a source of *Staphylococcus aureus* bacteremia. Study Group. *N Engl J Med* **344**, 11-16.

Vovis, G. F., Horiuchi, K. & Zinder, N. D. (1974). Kinetics of methylation of DNA by a restriction endonuclease from *Escherichia coli* B. *Proc Natl Acad Sci U S A* **71**, 3810-3813.

Vuong, C., Durr, M., Carmody, A. B., Peschel, A., Klebanoff, S. J. & Otto, M. (2004a). Regulated expression of pathogen-associated molecular pattern molecules in *Staphylococcus epidermidis*: quorum-sensing determines pro-inflammatory capacity and production of phenol-soluble modulins. *Cell Microbiol* **6**, 753-759.

Vuong, C., Kocianova, S., Voyich, J. M., Yao, Y., Fischer, E. R., DeLeo, F. R. & Otto, M. (2004b). A crucial role for exopolysaccharide modification in bacterial biofilm formation, immune evasion, and virulence. *J Biol Chem* **279**, 54881-54886.

Waldron, D. E. & Lindsay, J. A. (2006). Sau1: a novel lineage-specific type I restriction-modification system that blocks horizontal gene transfer into *Staphylococcus aureus* and between *S. aureus* isolates of different lineages. *J Bacteriol* **188**, 5578-5585.

Walev, I., Weller, U., Strauch, S., Foster, T. & Bhakdi, S. (1996). Selective killing of human monocytes and cytokine release provoked by sphingomyelinase (beta-toxin) of *Staphylococcus aureus*. *Infect Immun* **64**, 2974-2979.

Walsh, E. J., O'Brien, L. M., Liang, X., Hook, M. & Foster, T. J. (2004). Clumping factor B, a fibrinogen-binding MSCRAMM (microbial surface components recognizing adhesive matrix molecules) adhesin of *Staphylococcus aureus*, also binds to the tail region of type I cytokeratin 10. *J Biol Chem* **279**, 50691-50699.

Walsh, E. J., Miajlovic, H., Gorkun, O. V. & Foster, T. J. (2008). Identification of the *Staphylococcus aureus* MSCRAMM clumping factor B (ClfB) binding site in the alphaC-domain of human fibrinogen. *Microbiology* **154**, 550-558.

Wang, R., Braughton, K. R., Kretschmer, D., Bach, T. H., Queck, S. Y., Li, M., Kennedy, A. D., Dorward, D. W., Klebanoff, S. J., Peschel, A., DeLeo, F. R. & Otto, M. (2007). Identification of novel cytolytic peptides as key virulence determinants for community-associated MRSA. *Nat Med* **13**, 1510-1514.

Wang, R., Khan, B. A., Cheung, G. Y., Bach, T. H., Jameson-Lee, M., Kong, K. F., Queck, S. Y. & Otto, M. (2011). *Staphylococcus epidermidis* surfactant peptides promote biofilm maturation and dissemination of biofilm-associated infection in mice. *J Clin Invest* **121**, 238-248.

Wann, E. R., Gurusiddappa, S. & Hook, M. (2000). The fibronectin-binding MSCRAMM FnbpA of *Staphylococcus aureus* is a bifunctional protein that also binds to fibrinogen. *J Biol Chem* **275**, 13863-13871.

Wastfelt, M., Stalhammar-Carlemalm, M., Delisse, A. M., Cabezon, T. & Lindahl, G. (1996). Identification of a family of streptococcal surface proteins with extremely repetitive structure. *J Biol Chem* **271**, 18892-18897.

Watt, V. M., Ingles, C. J., Urdea, M. S. & Rutter, W. J. (1985). Homology requirements for recombination in *Escherichia coli*. *Proc Natl Acad Sci U S A* **82**, 4768-4772.

Weidenmaier, C., Kokai-Kun, J. F., Kristian, S. A., Chanturiya, T., Kalbacher, H., Gross, M., Nicholson, G., Neumeister, B., Mond, J. J. & Peschel, A. (2004). Role of teichoic acids in *Staphylococcus aureus* nasal colonization, a major risk factor in nosocomial infections. *Nat Med* **10**, 243-245.

Weinberg, E. D. (2000). Microbial pathogens with impaired ability to acquire host iron. *Biometals* **13**, 85-89.

Weiss, W. J., Lenoy, E., Murphy, T., Tardio, L., Burgio, P., Projan, S. J., Schneewind, O. & Alksne, L. (2004). Effect of srtA and srtB gene expression on the virulence of *Staphylococcus aureus* in animal models of infection. *J Antimicrob Chemother* **53**, 480-486.

Wertheim, H. F., Vos, M. C., Ott, A., van Belkum, A., Voss, A., Kluytmans, J. A., van Keulen, P. H., Vandenbroucke-Grauls, C. M., Meester, M. H. & Verbrugh, H. A. (2004). Risk and outcome of nosocomial *Staphylococcus aureus* bacteraemia in nasal carriers versus non-carriers. *Lancet* **364**, 703-705.

Wilke, G. A. & Bubeck Wardenburg, J. (2010). Role of a disintegrin and metalloprotease 10 in *Staphylococcus aureus* alpha-hemolysin-mediated cellular injury. *Proc Natl Acad Sci U S A* **107**, 13473-13478.

Wyatt, M. A., Wang, W., Roux, C. M., Beasley, F. C., Heinrichs, D. E., Dunman, P. M. & Magarvey, N. A. (2010). *Staphylococcus aureus* nonribosomal peptide secondary metabolites regulate virulence. *Science* **329**, 294-296.

Xia, G., Corrigan, R. M., Winstel, V., Goerke, C., Grundling, A. & Peschel, A. (2011). Wall teichoic Acid-dependent adsorption of staphylococcal siphovirus and myovirus. *J Bacteriol* **193**, 4006-4009.

Xiang, H., Feng, Y., Wang, J., Liu, B., Chen, Y., Liu, L., Deng, X. & Yang, M. (2012). Crystal structures reveal the multi-ligand binding mechanism of *Staphylococcus aureus* ClfB. *PLoS Pathog* **8**, e1002751.

Xu, S. Y., Corvaglia, A. R., Chan, S. H., Zheng, Y. & Linder, P. (2011). A type IV modification-dependent restriction enzyme SauUSI from *Staphylococcus aureus* subsp. aureus USA300. *Nucleic Acids Res* **39**, 5597-5610.

Yagi, Y. & Clewell, D. B. (1976). Plasmid-determined tetracycline resistance in *Streptococcus faecalis*: tandemly repeated resistance determinants in amplified forms of pAMalpha1 DNA. *J Mol Biol* **102**, 583-600.

Yao, J., Zhong, J., Fang, Y., Geisinger, E., Novick, R. P. & Lambowitz, A. M. (2006). Use of targetrons to disrupt essential and nonessential genes in *Staphylococcus aureus* reveals temperature sensitivity of LI.LtrB group II intron splicing. *RNA* **12**, 1271-1281.

Yasui, K., Kano, Y., Tanaka, K., Watanabe, K., Shimizu-Kadota, M., Yoshikawa, H. & Suzuki, T. (2009). Improvement of bacterial transformation efficiency using plasmid artificial modification. *Nucleic Acids Res* **37**, e3.

Yoon, E. J., Kwon, A. R., Min, Y. H. & Choi, E. C. (2008). Foggy D-shaped zone of inhibition in *Staphylococcus aureus* owing to a dual character of both inducible and constitutive resistance to macrolide-lincosamide-streptogramin B. *J Antimicrob Chemother* **61**, 533-540.

Zapotoczna, M., Heilbronner, S., Speziale, P. & Foster, T. J. (2012a). Iron-Regulated Surface Determinant (Isd) Proteins of *Staphylococcus lugdunensis*. *J Bacteriol* **194**, 6453-6467.

Zapotoczna, M., Jevnikar, Z., Miajlovic, H., Kos, J. & Foster, T. J. (2012b). Iron-regulated surface determinant B (IsdB) promotes *Staphylococcus aureus* adherence to and internalization by non-phagocytic human cells. *Cell Microbiol*.

Zbinden, R., Müller, F., Brun, F. & von Graevenitz, A. (1997). Detection of clumping factor-positive *Staphylococcus lugdunensis* by Staphaurex Plus®. *Journal of Microbiological Methods* **31**, 95-98.

Zhang, Y. Q., Ren, S. X., Li, H. L., Wang, Y. X., Fu, G., Yang, J., Qin, Z. Q., Miao, Y. G., Wang, W. Y., Chen, R. S., Shen, Y., Chen, Z., Yuan, Z. H., Zhao, G. P., Qu, D., Danchin, A. & Wen, Y. M. (2003). Genome-based analysis of virulence genes in a non-biofilm-forming *Staphylococcus epidermidis* strain (ATCC 12228). *Mol Microbiol* **49**, 1577-1593.

Zong, Y., Mazmanian, S. K., Schneewind, O. & Narayana, S. V. (2004). The structure of sortase B, a cysteine transpeptidase that tethers surface protein to the *Staphylococcus aureus* cell wall. *Structure* **12**, 105-112.

Zong, Y., Xu, Y., Liang, X., Keene, D. R., Hook, A., Gurusiddappa, S., Hook, M. & Narayana, S. V. (2005). A 'Collagen Hug' model for *Staphylococcus aureus* CNA binding to collagen. *EMBO J* **24**, 4224-4236.